UNIVERSITY OF SOUTHAMPTON

EFFECTS OF LIPID ON MEMBRANE PROTEIN FUNCTION

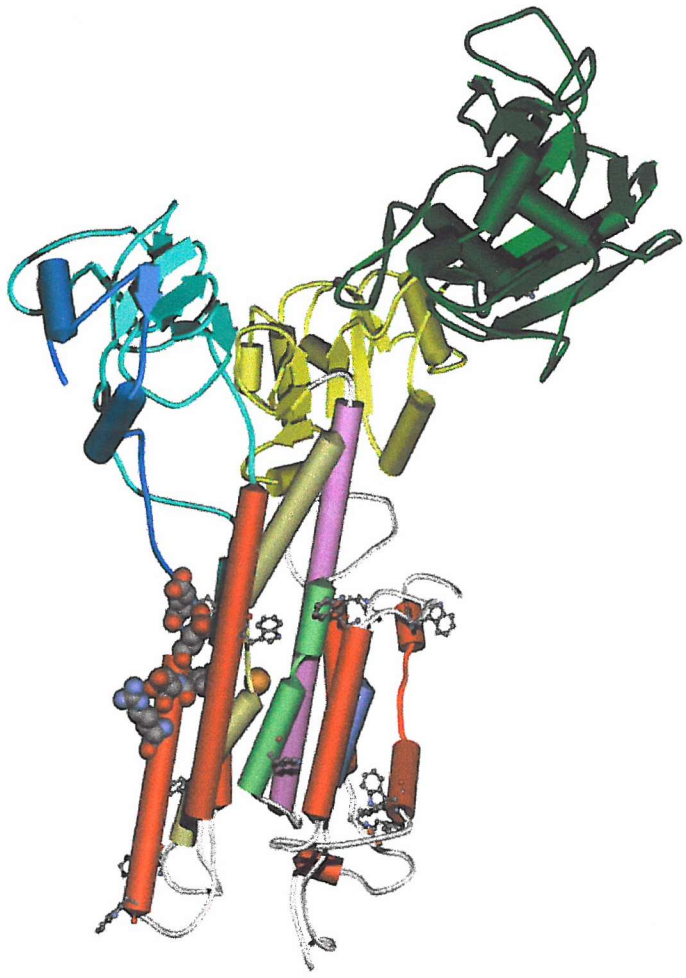

by Jeffrey David Pilot

A thesis presented for the degree of

Doctor of Philosophy

Division of biochemistry and Molecular Biology

University of Southampton

United Kingdom

UNIVERSITY OF SOUTHAMPTON

ABSTRACT

FACULTY OF SCIENCE

DIVISION OF BIOCHEMISTRY AND MOLECULAR BIOLOGY

Doctor of Philosophy

EFFECTS OF LIPID ON MEMBRANE PROTEIN FUNCTION

by Jeffrey David Pilot

The effects of phospholipids on the functioning of the membrane proteins diacylglycerol kinase (DGK) of *Escherichea coli* and Ca^{2+}-ATPase of sarcoplasmic reticulum have been investigated. A procedure has been developed for the reconstitution of DGK into phospholipid bilayers containing dihexanoylglycerol (DHG) as substrate. DGK activity was found to be dependent on fatty acyl chain length, with highest activity in dioleoylphosphatidylcholine (di(C18:1)PC). Low activities in di(C14:1)PC followed from an increase in K_m values for DHG and ATP with no effect on v_{max}, whilst low activity in di(C24:1)PC followed from a decrease in v_{max} with no effect on K_m. In mixtures of two phosphatidylcholines with different chain lengths, the activity corresponded to that expected for the average chain length of the mixture. Cholesterol increased activity in di(C14:1)PC by possibly changing the bilayer thickness. In mixtures of di(C18:1)PC and anionic phospholipids, the presence of cardiolipin, dioleoylphosphatidic acid (di(C18:1)PA), or dioleoylphosphatidylserine (di(C18:1)PS) all resulted in lower activities for DGK than in di(C18:1)PC, whilst the presence of dioleoylphosphatidylglycerol (di(C18:1)PG had little effect on activity. In some cases low kinase activity in the presence of anionic phospholipids followed from a decrease in v_{max}, in some cases it followed from an increase in K_m for DHG, and for di(C18:1)PA, from both.The presence of anionic phospholipids had little effect on Ca^{2+}-ATPase activity. However, inclusion of 10 mol % anionic phospholipid (di(C18:1)PA or di(C18:1)PS) led to higher levels of accumulation of Ca^{2+} by the Ca^{2+}-ATPase reconstituted into sealed vesicles, 10 mol % being the optimum concentration. Cardiolipin or phosphatidylinositol 4-phosphate were more effective than di(C18:1)PA or di(C18:1)PS in increasing accumulation of Ca^{2+}. The experimental data fitted to a slippage model, with anionic phospholipids decreasing the rate of slippage. DGK activities in the presence of phosphatidylethanolamines are lower than in di(C18:1)PC, suggesting that the presence of lipids preferring a hexagonal H_{II} phase leads to low activities. Activities of DGK are low in gel phase lipid.

ACKNOWLEDGEMENTS

I thank my supervisor Professor Lee for his help and guidance, which was at times above and beyond the call of duty, and the past and present members of the group. I would particularly like to thank Malcolm and Barbara for easing the transition from biochemist to molecular biologist, if this is possible. A special mention to Chris Anthony for help with the conference, it meant a lot. Raj Gill, without you I would not be here. Paul and Pete, even if the lab work was bad the pool was good; seriously though, it really meant a lot to have you guys to moan at.

Thanks Garrath for being there when I needed a friend and for providing an alternative view to life. Mark, thanks for being yourself, you know what I mean by that. Alistair, what can I say than you're larger than life.

Mum and Dad, thank you for your unconditional and continuous support - I will pay you back someday. I remember when I visited for a weekend and we went to Dons for a barbecue. It put things back in perspective and I really cannot thank you enough for that.

Gran and Grandpa, what can I say but thanks for the support and for being a great source of good advice.

Finally Pia, without your love and huge support I would not be here writing this, thankfully you are still here while I am writing this. I love you.

For anyone out there completing a PhD just remember to relax once in a while and appreciate what you have got rather than what you could have, as what you have got is usually a whole lot more. One more thing, always wear sunscreen.

ABBREVIATIONS

AEBSF	4-(2-Aminoethyl)-benzenesulfonyl fluoride
ATP	Adenosine triphosphate
BCA	Bichoninic acid
Ca^{2+}-ATPase	Ca^{2+} and Mg^{2+} activated ATPase
CL	Cardiolipin
cmc	Critical micelle concentration
DAG	Diacylglycerol
DHG	Dihexanoylglycerol
DOG	Dioleoylglycerol
DGK	Diacylglycerol kinase
DM	Dodecylmaltoside
di(Br_2C18:0)PC	1,2-di(9,10-dibromostearoyl) phosphatidylcholine
di(C18:1)PA	Dioleoylphosphatidic acid
di(C14:1)PC	Dimyristoylphosphatidylcholine
di(C16:1)PC	Dipalmitoylphosphatidylcholine
di(C18:1)PC	Dioleoylphosphatidylcholine
di(C20:1)PC	Dieicosenoylphosphatidylcholine
di(C22:1)PC	Dieurcylphosphatidylcholine
di(C24:1)PC	Dinervonylphosphatidylcholine
di(C18:1)PE	Dioleoylphosphatidyylethanolamine
di(C18:1)PG	Dioleoylphosphatidylglycerol
di(C18:1)PI	Dioleoylphosphatidylinositol
di(C18:1)PI(4)*P*	Dioleoylphosphatidylinositol-4-monophosphate
di(C18:1)PS	Dioleoylphosphatidylserine

EDTA	Ethylenediamine tetraacetic acid
EGTA	Ethyleneglycol-bis(β-aminothylether)-N,N,N',N'-tetraacetic acid
FCCP	Carbonyl cyanide p-(trifluoromethoxy) phenylhydrazone
HEPES	N-(2-hydroxyethyl)piperazine-N'-(2-ethanesulphonic acid)
LDH	Lactate dehydrogenase
MES	2-(N-morpholino)ethanesulphonic acid
MOPS	3-(N-morpholino)propanesulphonic acid
NADH	β-Nicotinamide adenine dinucleotide [reduced form]
OG	Octylglucopyranoside
PA	Phosphatidic acid
PE	Phosphatidylethanolamine
PG	Phosphatidylglycerol
PEP	Phospho-enol-pyruvate
PIPES	Piperazine-N, N'-bis(2-ethanesulfonic acid)
PK	Pyruvate kinase
SDS	Sodium dodecyl sulphate
SR	Sarcoplasmic reticulum
TRIS	Tris(hydroxymethyl)aminomethane

CONTENTS

CHAPTER 2: MATERIALS AND METHODS

CHAPTER 3: THE EFFECTS OF ANIONIC PHOSPHOLIPIDS ON THE FUNCTION OF THE Ca^{2+}-ATPase OF SARCOPLASMIC RETICULUM

CHAPTER 5: EFFECTS OF BILAYER THICKNESS ON THE ACTIVITY OF DIACYLGLYCEROL KINASE OF *ESCHERICHEA COLI*

CHAPTER 1: GENERAL INTRODUCTION

1.1 Biological membranes

Biological membranes are an essential part of a cell, separating the cell from its environment, giving it individuality by maintaining essential differences between the cell and its environment. Membranes are highly selective permeability barriers that allow communication between the inside and outside of the cell. In eukaryotic cells evolution has led to the formation of compartments or organelles each with its own membrane and function, such as mitochondria, chloroplasts and lysosomes. Despite their differing functions, all biological membranes have a common general structure; each is a very thin film of lipid and protein molecules held together mainly by noncovalent interactions. Membrane structure is however very diverse, owing to the fact that the membrane serves as a suitable environment for specific proteins to insert and mediate distinctive membrane functions. Proteins operate as pumps, gates, receptors, energy transducers, and enzymes; specific lipids may be required to interact specifically with these proteins for functioning. Membrane lipids can be described as relatively small molecules that contain both a hydrophilic and a hydrophobic moiety. In aqueous media these lipids spontaneously arrange to form a continuous double layer approximately 60 to 100 Å in thickness. In 1972, S. Jonathan Singer and Garth Nicolson proposed a fluid mosaic model for the overall organisation of biological membranes (Singer & Nicholson, 1972). The essence of the model is that membranes are two-dimensional solutions of oriented lipids and proteins (Figure 1.1). Membranes are structurally and functionally asymmetric; the outer and inner surfaces of all biological membranes have different components and enzymatic activities. Membranes are fluid structures in which lipid molecules can diffuse rapidly in the

plane of the membrane; conversely, transverse movement is very slow unless mediated by a specific membrane protein. In contrast, proteins cannot transverse across the membrane, they can only move laterally (Devaux, 1991).

1.2 Membrane proteins

Membrane proteins are responsible for most of the dynamic processes carried out by membranes. Protein content varies from membrane to membrane; the plasma membranes of most cells have a protein content of typically 50 % by weight. Membrane proteins can be classified as either integral or peripheral on the basis of their interaction with the membrane. Peripheral, or extrinsic, membrane proteins are easily dissociated from the membrane; they are bound to the membrane by electrostatic and hydrogen bond interactions, which can be disrupted by the addition of salts or changing the pH. Some are modified with hydrophobic chains, which increase the strength of binding to the membrane. Many peripheral proteins are bound to the surfaces of integral membrane proteins. Integral, or intrinsic, membrane proteins contain hydrophobic regions, enabling them to interact extensively with the hydrocarbon chains of membrane lipids. Agents that compete for these nonpolar interactions can release integral membrane proteins, resulting in complete physical disruption of the membrane. Nearly all known integral membrane proteins span the lipid bilayer and interact with both sides of the membrane; some proteins only span the membrane once, whilst others have several transmembrane regions.

1.3 Membrane lipids

The definition of a lipid is a water-insoluble molecule that is highly soluble in an organic solvent such as chloroform. Lipids have a variety of biological roles including serving as fuel molecules, energy stores, signal molecules, and components of membranes (Stryer, 1995). The four classes of membrane lipids are phospholipids, sphingolipids, glycolipids, and sterols. Phospholipids are abundant in all biological membranes. They are either derived from glycerol, a three-carbon alcohol, or a more complex alcohol called sphingosine. Phospholipids derived from glycerol are the more common and called phosphoglycerides. A phosphoglyceride consists of two hydrophobic fatty acyl chains and a phosphorylated alcohol that are attached by ester links to the glycerol backbone (Figure 1.2). The fatty acyl chains usually contain an even number of carbon atoms, ranging between 14 and 24, with C16, C18, and C20 being the most common (Stryer, 1995). Many phospholipids contain one saturated and one unsaturated fatty acyl chain. The configuaration of the double bonds in the unsaturated chains is nearly always *cis*, resulting in a kink in the chain and a disruption of the packing order of the bilayer. All of the phosphoglycerides are derivatives of phosphatidate; the phosphate group of phosphatidate becomes esterified to the hydroxyl group of one of several alcohol moieties, including choline, ethanolamine, serine, glycerol and inositol (Figure 1.3). Sphingolipids are derived from the backbone of sphingosine, which is an amino alcohol containing a long unsaturated hydrocarbon chain. This class of lipids includes sphingomyelins, cerebrosides and gangliosides. In sphingomyelins the amino group of the sphingosine backbone is attached to a fatty acid by an amide bond and the primary hydroxyl group is esterified to either phosphocholine or phosphoethanolamine (Figure 1.4). Cerebrosides and gangliosides both contain sugar residues linked to the primary

hydroxyl of sphingosine. Cerebrosides contain only one sugar residue, either glucose or galactose, whilst gangliosides are more complex containing a branched chain of up to seven sugar residues attached to this group (Stryer, 1995). Cerebrosides and gangliosides are often classified as glycolipids due to the presence of the sugar group. In addition to sphingosine based glycolipids there are glycerol-based glycolipids where diacylglycerol (Figure 1.5) is attached to sugar residues. The most important sterol lipid is cholesterol (Figure 1.6), found in the plasma membrane of many eukaryotic cells.

Phospholipid headgroups can adopt a number of different conformations depending on the headgroup structure, the pH and ionic composition of the aqueous phase and other external factors. Interaction between headgroups is via a network of hydrogen and ionic bonds (Stryer, 1995). Inter- or intra-molecular hydrogen bonds can exist between the hydroxyl, phosphate, amino, ester C=O and carboxylic acid groups, without the need for water to mediate the interaction (Stryer, 1995). Phosphatidylethanolamine (PE) has an especially strong tendency to form intermolecular hydrogen bonds. The amine group forms two hydrogen bonds with neighbouring phosphates, allowing a tighter molecular packing of PE in the bilayer (Hauser et al., 1981). Phosphatidylcholine (PC) does not form intermolecular hydrogen bonds, but charge interactions exist between the PO_4^- of one PC, and the NMe_3^+ group of an adjacent PC (Stryer, 1995). The charge on the surface of the membrane is determined by the ionisation state of the lipid and the ionic strength of the surrounding aqueous environment. The surface charge can be altered by changing the pH, which alters the ionisation state of the polar headgroup, or by the binding of ions to the surface of the membrane (Stryer, 1995). PC and PE are zwitterionic lipids; they have no net charge at neutral pH and form neutral membranes. Phosphatidic acid

(PA), phosphatidylserine (PS), phosphatidylinositol (PI), and cardiolipin (CL) are charged lipids having a net negative charge at neutral pH, producing a negatively charged membrane surface attracting positively charged ions. In addition to the polar headgroup, the phosphate group of all phospholipids is ionised by changes in pH; other groups including the amino groups of PE and PS can become protonated as a result of a pH change. The charge carried is dependent upon the pK of the group and the environmental pH (Figure 1.7).

1.3.1 Phospholipid phases

It is evident that the polar head groups of phospholipids will have an affinity for water, whilst the hydrocarbon tails will have an aversion for water. The contradicting requirements of the two parts of the phospholipid molecule can be met by forming an aggregated structure in water. A number of different structures, or phases, can be formed in water. Important structures adopted by phospholipids in aqueous medium include lamellar, cubic, and hexagonal phases (Figure 1.8). The phase adopted depends on the temperature and the structure and degree of hydration of the lipid. The two most important structures adopted by phospholipids are lamellar, or bilayer, and inverted hexagonal (H_{II}) phases (Lee, 1983). The lamellar phase is composed of an alternating sequence of planar lipid bilayers and layers of water. The packing of rod-like aggregates into a hexagonal array forms the hexagonal phase, of which there are two types, the normal (H_I) and the inverted (H_{II}). In the H_I phase lipids form hydrocarbon chain cored tubes; in the H_{II} phase the lipids form water cored rods with their headgroups facing the inside surface of the cylinder and the fatty acyl chains pointing outwards. Additionally, lipids can form cubic phases that are

structurally complex and not very energetically favourable. In this phase the lipid aggregates into a complex three-dimensional lattice, of which there are many types. Membrane lipids mostly form bicontinuous cubic phases that have regions that are continuous with respect to both polar and non-polar components (Lindblom & Rilfors, 1989).

The lamellar phase can only be adopted by phospholipids that have an overall cylindrical shape (Cullis et al., 1986). Phosphatidylcholine is an example of a cylindrical lipid since the area occupied at the membrane surface by the headgroup is approximately equal to the area occupied by the two fatty acyl chains. In contrast, hexagonal phases are formed by conically shaped phospholipids where the areas occupied by the headgroup and the fatty acyl chains are different. Phospholipids with a smaller headgroup than tail area form H_{II} structures and phospholipids with a larger headgroup than tail area form H_I structures. Due to its relatively small headgroup phosphatidylethanolamine is a conically shaped lipid that adopts an inverted hexagonal H_{II} phase. Additionally, PE with *cis*-unsaturated fatty acyl chains is more likely to adopt the H_{II} phase than PE with saturated fatty acyl chains, as illustrated by a lower transition temperature from the bilayer to hexagonal H_{II} phase. This is because unsaturated chains produce a more conical shape than saturated chains. Phosphatidic acid (PA) could also be expected to readily adopt the H_{II} phase as its headgroup is relatively small, but charge repulsion between the negatively charged headgroups results in PA adopting a larger than expected area at the membrane surface, so that the 'effective' size of PA is larger than expected, thus favouring the bilayer phase.

Under physiological conditions the majority of lipids will adopt a lamellar, crystalline phase. In the liquid-crystalline phase, the phospholipid fatty acyl chains are

relatively disordered and are able to undergo intra- and inter-molecular motions (Lee, 1983). In contrast, the fatty acyl chains are relatively ordered in the gel phase and exist in a rigid conformation (Lee, 1983). Temperature, hydration, and ionic strength or pH changes can induce a gel to liquid-crystalline phase transition; a lateral expansion and decrease in the thickness of the bilayer accompanies this transition (Lee, 1983). The temperature at which this transition occurs is governed by the structure of the lipid molecule. In the gel phase PC fatty acyl chains pack into many different temperature dependent arrangements because they occupy a smaller area than the headgroup. To overcome this problem the hydrocarbon chains can be tilted in relation to the bilayer surface or the headgroups can be alternately displaced perpendicular to the bilayer surface, giving a rippled structure (Hauser et al., 1981). PC undergoes a pretransition below the gel to liquid-crystalline phase transition that corresponds to the transition from the tilted structure to the rippled structure (Lee, 1983). This pretransition stage enables the fatty acyl chains to be positioned perpendicular to the bilayer prior to the gel to liquid-crystalline phase transition. PE and other similar lipids possess a smaller headgroup which allows the fatty acyl chains to pack closer together, perpendicular to the bilayer surface; they do not exist in a tilted phase and consequently do not exhibit a pretransition stage (Hauser et al., 1981).

The gel to liquid-crystalline phase transition temperature can be altered in many ways. Increasing the length of the fatty acyl chains increases the gel to liquid-crystalline phase transition temperature, whilst introducing *cis* double bonds to the fatty acyl chains decreases the transition temperature (Lee, 1983). The positioning of the *cis* double bond is important. Fatty acyl chains with a double bond at either end of the chain have a higher transition temperature than chains with a double bond

positioned in the middle (Barton & Gunstone, 1975). pH variation and the addition of mono- or divalent cations can also influence the transition temperature (Hauser, 1991); the ionizable groups on lipids are susceptible to pH changes around their pK values. If bilayers are composed entirely of PC, the transition temperature is independent of pH over the range 3-10 (Hauser, 1991). Bilayers composed entirely of PE, or anionic lipids such as PA undergo a decrease in transition temperature when the pH is raised from 7 to 13. This is due to the deprotonation of the amino and ionizable groups of PE and PA respectively (Hauser, 1991). However, the effect of increasing the pH on negatively charged bilayers can be negated by the addition of divalent cations, which neutralise the negative charge and raise the transition temperature as a consequence (Trauble & Eibl, 1974). Monovalent cations can slightly raise the transition temperature by interacting weakly with anionic lipids; the transition temperature of PC bilayers is hardly affected by cations, due to weak interaction between the two (Hauser, 1991).

A second phase transition is observed for lipids that form non-lamellar phases. These lipids undergo a transition from the liquid-crystalline phase to the non-bilayer H_{II} phase. In the case of PE this occurs approximately 10°C above the gel to liquid-crystalline phase transition (Lee, 1983). Temperature, headgroup size, unsaturation of the acyl chains and ionisation and water content are all factors that can influence this secondary phase transition (Cullis et al., 1986). Non-bilayer preferring lipids can be stabilised to maintain a bilayer structure if the bilayer contains approximately more than 20 % of a bilayer preferring lipid (Cullis et al., 1986). The ability of bilayer preferring lipids to stabilise the bilayer depends on the unsaturation and quantity of the non-bilayer-preferring lipid present and the temperature. Increasing the unsaturation of PE in a PC: PE bilayer favours the formation of non-bilayer structures

(Cullis et al., 1986). The negatively charged lipid PS will stabilise PE in a bilayer in the absence of divalent cations. The subsequent addition of a divalent cation would result in the separation of PE and PS, allowing PE to form the favoured H_{II} phase (Tilcock, 1986).

1.3.2 Non-bilayer lipids in membranes

Non-bilayer structures are not permitted in biological membranes, but non-bilayer preferring lipids are allowed and they have an important role to play (Gruner, 1985). The presence of PE, a H_{II} phase lipid, has a significant effect on the physical properties of a lipid bilayer. This effect is termed bilayer 'frustration', as the PE is forced to adopt a bilayer structure (Gruner, 1985). A number of stresses are exerted upon a lipid monolayer at the air-water interface. A repulsive lateral surface pressure arises from the thermal motions of the headgroup and fatty acyl chains, whilst an attractive force called the surface tension arises from contact of the fatty acyl chains with water (Seddon, 1990). The surface tension can be minimised by tight packing in the chain region, which reduces the exposure of the hydrocarbon interior of the membrane to water. The surface pressures and tension, for a phospholipid such as PC, must be in balance across the monolayer for it to remain flat. If the lateral pressure existing between the headgroups increases over that existing between the chains, the monolayer will curve towards the chain region. Conversely, if the lateral pressure existing in the chain region increases, the monolayer will curve towards the aqueous region; this would occur by increasing the PE content of a PC monolayer. In a symmetrical bilayer two monolayers would want to curve in the same direction. This is impossible, for it would create free volume in the interior of the bilayer. In reality,

the curvature of the two monolayers cancel each other out and the bilayer remains flat, albeit in a state of physical frustration. It has been suggested that these effects could be important for the proper function of the intrinsic membrane proteins in the membrane (Seddon, 1990). Non-bilayer preferring lipids may also play a significant role in other membrane functions; having the ability to form non-bilayer structures could be advantageous when performing functions such as membrane fusion (Cullis et al., 1986; Lindblom & Rilfors, 1989). Changes to the environment of some cells results in the alteration of the composition of their membranes to maintain a balance between bilayer and non-bilayer preferring lipids. This shows the importance of non-bilayer preferring lipids in biological membranes and has been demonstrated in the bacteria Pseudomonas fluorescens (Cullen et al., 1971).

1.4 Structure and function of membrane proteins

The complexity of the lipid composition of the biological membrane means that the effects of lipid structure on membrane protein function is best studied using simple model systems in which a membrane protein is reconstituted into a lipid bilayer of defined composition. This approach is only possible if the membrane protein can be purified in a large quantity (greater than 1 mg). In this thesis, we study two such membrane proteins, the Ca^{2+}-ATPase and diacylglycerol kinase (DGK).

1.4.1 The Ca^{2+}ATPase

The Ca^{2+}ATPase is an integral membrane protein whose interaction with phospholipids has been well documented, in particular the effects of phospholipid

structure on ATPase activity (Lee et al., 1995). The Ca^{2+}ATPase belongs to a family of cation transporters, the P-type ATPases, so called because a phosphorylated intermediate involving an Asp residue is formed during the catalytic cycle. It is located in the membrane of the sarcoplasmic reticulum (SR) of skeletal muscle and consists of a single polypeptide chain of approximately 115 kDa. The SR is an intricate membrane network found within skeletal muscles that controls muscle contraction by regulating the calcium ion concentration surrounding muscle fibres (Stryer, 1995). The SR can be divided into two regions, the network and terminal cisternae. Terminal cisternae are enlarged portions of the SR that form junctions with transverse or T-tubules, which are invaginations of the sarcolemma, the plasma membrane surrounding skeletal muscle cells. The increase in cytoplasmic Ca^{2+} necessary for muscle contraction is triggered by a nerve impulse, which induces depolarisation of the sarcolemma (Figure 1.9). Sarcoplasmic reticulum consists of one third lipid and two thirds protein by weight. The Ca^{2+}ATPase accounts for 80 % of the total protein present in the SR and its function is to pump Ca^{2+} into the lumen of the SR, where the Ca^{2+} is bound to the protein calsequestrin whose function is probably to reduce either the concentration gradient opposing Ca^{2+} transport or Ca^{2+} leak (Campbell & MacLennan, 1983). The SR membrane consists of 90 % phospholipid and 10 % neutral lipids such as cholesterol and free fatty acids (MacLennan et al., 1971). The major phospholipids are phosphatidylcholine (PC) and phosphatidylethanolamine accounting for about 70% and 23% respectively of the total lipid. The remainder includes phosphatidylinositol (PI) and phosphatidylserine (PS). The fatty acyl chains range in length from 16 to 22 carbons, with 18 carbons being the preferred length (Lee, 1998). Approximately 50% of the chains in PCs are unsaturated.

The function of the Ca^{2+}ATPase is the vectorial transport of two Ca^{2+} ions from the cytoplasm across the SR membrane into the lumen via the hydrolysis of one molecule of ATP. This transport is brought about by a cycle of conformational changes, driven by phosphorylation and dephosphorylation, in which the Ca^{2+}-ATPase alternates between two conformational states, E1and E2, as shown in Figure 1.10 (Stahl & Jencks, 1987; Myung & Jencks, 1995). The E1 form binds two Ca^{2+} ions from the cytoplasm with high affinity initiating each cycle. Following ATP binding, either before or after Ca^{2+} binding, phosphorylation of the Ca^{2+}-ATPase at Asp351 by the γ-phosphate of ATP occurs, bringing about a change to the low affinity E2 conformation. This conformational change is linked to a realignment of the trans-membrane helices, and the two Ca^{2+} ions are released into the lumen of the SR. The phosphoenzyme (E2P) is then hydrolysed and undergoes a conformational change back to E1 and the cycle continues.

1.4.1.1 Structure of the Ca^{2+}ATPase

The X-ray structure of the Ca^{2+}-ATPase with two Ca^{2+} ions bound in the transmembrane binding sites has been resolved to 2.6Å (Toyoshima et al., 2000). The overall architecture of the Ca^{2+}-ATPase can be seen in Figure 1.11 and consists of three main regions, the cytoplasmic, transmembrane and lumenal. The cytoplasmic region consists of three well-separated domains (designated as A, N and P). The P (phosphorylation) and N (nucleotide binding) domains are located between transmembrane helices M4 and M5. The central domain P contains the residue of phosphorylation (Asp 351) and is composed of two parts, the N-terminal part (Asn 330 – Asn 359), connected to M4, and the C-terminal part (Lys 605 – Asp 737). The

two parts are assembled into a seven-stranded parallel β-sheet with eight short associated helices, forming a typical Rossman fold. Asp 351 is situated in the C-terminal end of the central β-strand (Toyoshima et al., 2000). Clustered around Asp 351 are the residues critical for ATP hydrolysis, producing a negatively charged surface. Domain N is the largest of the three cytoplasmic domains and is formed by the residues (Gln 360 – Arg 604) inserted between the two parts of the P domain. It consists of a seven-stranded β-sheet with two helix bundles sandwiching it. This domain is involved in ATP binding. By soaking crystals with the ATP analogue TNP-AMP it was possible to locate the nucleotide-binding pocket in the N domain (Toyoshima et al., 2000). Phe 487 is a critical residue for ATP binding. Clustered around Phe 487 are the residues Lys 515 and Lys 492 necessary for ATP binding, producing a positively charged pocket, which is in contrast to the region surrounding the phosphorylation site. The A (actuator) domain is the smallest domain comprising the 110 residues between transmembrane helices M2 and M3. The function of the A domain is unclear, though the finding that mutations and the proteolytic cleavage of residues in this domain uncouple ATP hydrolysis from Ca^{2+} transport indicate its involvement in transferring energy from the P and N domains through to the calcium binding sites (Andersen, 1995, Møller et al., 1996).

Fitting the X-ray structural data onto the 8 Å model of the proposed E2 conformation (Zhang et al., 1998) it was clear that the A domain undergoes a significant shift in its position relative to the P-domain following the conversion of E1 to E2 (Toyoshima et al., 2000). In order to fit the high-resolution structure of the E1 structure to the 8 Å model of the E2 conformation it was necessary to rotate the A domain through 90° parallel to the bilayer surface and to tilt the N-domain towards the P domain by 22°. To accommodate large domain motions the sequences linking

the domains must be flexible, which they are. Domain N can be isolated by several proteases, suggesting that the region around Ser 350 and Gly 609 is indeed flexible. The connecting strands between domains N and P and domains A and P have no regular secondary structure. Shifting the domains in this way has inevitable consequences for the organisation of the transmembrane helices since, for example, moving domain A will require adjustments in the alignment of transmembrane helices M1, M2 and M3 to which this domain is attached. As pointed out by Toyoshima et al. (2000) there are hydrogen bonds between helices M1-M3 and M4 in the calcium-binding domain and between M3 and the loop between M6 and M7 (L67 on Figure 1.11), which is thought to be important for concerted domain motions. They postulate that calcium binding causes a reorganisation of M1-M3 in the E1 conformation releasing the A domain; the release of domain A then facilitates the reorganisation of the N domain relative to the P domain. This results in the open structure that can then bind ATP. In the presence of calcium and ATP, Asp 351 will be phosphorylated. This requires that the P and N domains come into close proximity. However, in the X-ray crystal structure domains N and P are quite separate. This may be the result of using TNP-AMP. The presence of ATP and certain analogues is known to prevent the crystallisation of the Ca^{2+}-ATPase in the presence of Ca^{2+} (Martonosi, 1995) whereas TNP-AMP demonstrably does not. It is thought that TNP-AMP prevents the necessary conformational changes brought about by ATP binding to bring the N domain close to the P domain, so that phosphate transfer can take place.

The transmembrane domain (M) consists of ten α-helices embedded in the lipid bilayer (MacLennan et al., 1985). The lengths of the helices and the inclination to the membrane vary substantially. Helices M2, M3 and M5 are very long (~60 Å) and fairly straight. Helix M5 is located centrally within the transmembrane domain

and extends from the lumenal surface of the membrane to the centre of the cytosolic domain P, looking like the centre mast of the enzyme. Helix M10 has a kink located towards the centre of the bilayer. Helices M4 and M6 are partially unwound around the centre of the membrane and a number of helices are tilted, such as M4 and M7. The transmembrane helices M4-M6 and M8 each contain one negatively charged residue and make up the two calcium-binding sites (Andersen, 1995; Møller et al., 1996; MacLennan et al., 1997). Calcium binding site I is located in the space between helices M5 and M6 with contribution from M8, whilst site II is formed almost 'on' helix M4. Mutagenesis revealed the key groups involved in calcium binding, Asn 768 and Glu 771 in M5, Thr 799 and Asp 800 in M6 and Glu 908, in M8 for site I and Glu 309, in M4 with involvement of Asn 796 and Asp 800 in M6 for site II (Toyoshima et al., 2000). Additionally, a number of the residues involved in Ca^{2+} binding are involved in H-bonding with each other and with residues on other helices. These hydrogen-bond networks must be important for the cooperative binding of two Ca^{2+} ions (Toyoshima et al., 2000). A possible route for Ca^{2+} entry to the transmembrane binding sites is the area surrounded by M2, M4 and M6. It is a cavity with a rather wide opening and is clearly water accessible. The rows of exposed oxygen atoms formed by the unwound part of M4 (Pro 312 and Glu 309) and of M6 (Gly 801 and Asp 800) are orientated towards the cytoplasm providing a hydrophilic pathway leading to the Ca^{2+} binding sites. The outlet of Ca^{2+} is likely to be located in an area surrounded by M3-M5 near the lumenal side of the membrane, where a ring of oxygen atoms with bound water molecules is formed. The lumenal domain is the smallest domain consisting of small loops except for the one connecting M7 and M8 that can be seen on Figure 1.11 as L78 (Toyoshima et al., 2000).

1.4.1.2 Effects of phospholipid chain length on Ca^{2+}-ATPase activity

The activity of the Ca^{2+}-ATPase when reconstituted into lipid bilayers of phosphatidylcholine (PC) is sensitive to fatty acyl chain length (Lee et al., 1995a). Highest ATPase activity is found in dioleoylphosphatidylcholine (di(C18:1)PC), whilst PCs with longer or shorter monounsaturated fatty acyl chains support lower activities (East & Lee, 1982; Froud et al., 1986). Ca^{2+}-ATPase activity in PC bilayers with C16 and C20 monounsaturated chains is only slightly less than that in di(C18:1)PC (Lee, 1983; Starling et al., 1993). Reconstitution of the Ca^{2+}-ATPase into bilayers of either dimyristoylphosphatidylcholine (di(C14:1)PC) or dinervonylphosphatidylcholine di(C24:1)PC results in a change in the stoichiometry of Ca^{2+} binding from the usual two Ca^{2+} ions bound per Ca^{2+}-ATPase molecule as in di(C18:1)PC, to 1 Ca^{2+} ion bound. (Michelangeli et al., 1990a; Starling et al., 1993, 1994). The change in stoichiometry of Ca^{2+} binding follows from a cooperative effect of all the 30 phospholipid molecules that surround the ATPase in the membrane, rather than the binding of one phospholipid molecule to a unique site on the ATPase (Starling et al., 1994). The change in bilayer thickness appears to result in a realignment of the transmembrane helices, effectively destroying one of the Ca^{2+} binding sites. The effects exhibited by reconstituting the Ca^{2+}-ATPase into di(C14:1)PC and di(C24:1)PC are not identical. Firstly, a Mg^{2+} sensitive gating site controls access to the Ca^{2+} binding sites; in di(C24:1)PC the effect of Mg^{2+} on the gating site is normal, whereas no response is observed in di(C14:1)PC (Starling et al., 1994). Secondly, the Ca^{2+}-ATPase exists as a mixture of two conformations, E1 and E2, and only the E1 conformation can bind Ca^{2+} ions at the cytoplasmic sites (de Meis, 1981; Wictome et al., 1995; Henderson et al., 1994). Reconstitution of the Ca^{2+}-ATPase into di(C14:1)PC results in a shift in the E1/E2 equilibrium, towards E1; this

shift is not seen in di(C24:1)PC (Starling et al., 1994). Thirdly, the addition of cholesterol and other hydrophobic molecules to the Ca^{2+}-ATPase reconstituted in di(C14:1)PC restores activity levels to normal; this effect is not observed upon the addition of hydrophobic molecules to the Ca^{2+}-ATPase reconstituted into di(C24:1)PC (Michelangeli et al., 1991; Starling et al., 1993, 1994; Lee et al., 1994; Starling et al., 1994).

Low steady state Ca^{2+}-ATPase activities in long and short chain reconstituted systems are due to decreases in the rates of phosphorylation and dephosphorylation, not alterations in Ca^{2+} binding (Michelangeli et al., 1991; Starling et al., 1995a). In di(C14:1)PC the rates of both phosphorylation and dephosphorylation of the Ca^{2+}-ATPase are reduced. There was no significant phosphorylation of the Ca^{2+}-ATPase by P_i in di(C14:1)PC, unlike in di(C18:1)PC (Michelangeli et al., 1991; Starling et al., 1995a). Long chain lipids, such as di(C24:1)PC, also reduce the rate of dephosphorylation of the Ca^{2+}-ATPase, they do not however have any effect on the rate of phosphorylation by ATP (Starling et al., 1994,1995a). The rate and level of phosphorylation of the Ca^{2+}-ATPase by P_i is identical in di(C24:1)PC and di(C18:1)PC. This observation is consistent with the theory of a smaller conformational change for the Ca^{2+}-ATPase in di(C24:1)PC than di(C14:1)PC. However, for the Ca^{2+}-ATPase in di(C24:1)PC the rate of dephosphorylation is reduced sufficiently for it to become the rate limiting step in ATP hydrolysis (Starling et al., 1995). The rate of the Ca^{2+} transport step is identical for the Ca^{2+}-ATPase in di(C24:1)PC and di(C18:1)PC, even though only one Ca^{2+} ion is transported in di(C24:1)PC (Starling et al., 1995a). In summary, the conformational changes enforced on the Ca^{2+}-ATPase as a result of fatty acyl chain length variation, are greater for the Ca^{2+}-ATPase in di(C14:1)PC than di(C24:1)PC. Although the effects

of fatty acyl chain length presumably follow from changes in bilayer thickness, the bilayer thickness as experienced by the ATPase is not given by the average fatty acyl chain length in the membrane. For example in mixtures of di(C14:1)PC and di(C18:1)PC the average chain length corresponds to a PC which would bind two Ca^{2+} ions, the mixture of lipids binds only one Ca^{2+} ion (Lee, 1998).

The strength of interactions of different chain lengths PCs with the ATPase have been investigated using fluorescence quenching techniques with brominated or spin-labelled lipids (Caffrey & Feigenson, 1981; East & Lee, 1982; Froud et al., 1986a). Binding of these phospholipids to the ATPase results in a quenching of fluorescence from a specific interaction between the fluorophore (tryptophan) and the quencher (brominated or spin-labelled phospholipids). The rate of exchange of phospholipids between the surface of the Ca^{2+}-ATPase and the bulk phospholipid phase is slow when compared to the fluorescence lifetime for tryptophan (Simmonds et al., 1982). Thus, the degree of fluorescence quenching is proportional to the fractional occupation of the lipid-protein interface by the bromine-containing lipid. Experiments using these techniques have shown that the ATPase has little specificity for phospholipid binding at the annular sites of the protein-lipid interface (Caffrey & Feigenson, 1981; East & Lee, 1982; Froud et al., 1986a). Therefore the effects of short and long chain phospholipids follow from changes in the proportions of the bulk phospholipid bilayer and not from some changes in specific protein-lipid interactions. (Caffrey & Feigenson, 1981; East & Lee, 1982; Froud et al., 1986a). Cholesterol, however, is thought to exhibit its effects on the Ca^{2+}-ATPase in di(C14:1)PC by binding to a small number of non-annular sites that are possibly located between the trans-membrane α-helices (Simmonds et al., 1982, 1984; Ding et al., 1994). When the Ca^{2+}-ATPase is reconstituted with brominated phospholipids the addition of

cholesterol has little effect on the fluorescence quenching, indicating that cholesterol is essentially excluded from the annular shell (Simmonds et al., 1982). However, the addition of brominated cholesterol to the Ca^{2+}-ATPase reconstituted into di(C18:1)PC results in fluorescence quenching, suggesting that cholesterol can bind at sites inaccessible to phospholipids (Simmonds et al., 1982).

The Ca^{2+}-ATPase aggregates in di(C14:1)PC and di(C24:1)PC (Cornea & Thomas, 1994). It has been suggested that this aggregation could be the explanation for low Ca^{2+}-ATPase activities in di(C14:1)PC and di(C24:1)PC. This suggestion has been proven incorrect by experiments involving the reconstitution of the Ca^{2+}-ATPase into sealed vesicles of di(C14:1)PC and di(C24:1)PC (Starling et al., 1995b). The vesicles had very high molar ratios of lipid to protein, so that each individual vesicle contained only one or two isolated Ca^{2+}-ATPase molecules; aggregation was not possible under these conditions (Starling et al., 1995b). Isolation of the Ca^{2+}-ATPase molecules in the vesicles was proven by a lack of cross-linking with high concentrations of cross-linkers, such as glutaraldehyde. The Ca^{2+}-ATPase in di(C14:1)PC and di(C24:1)PC vesicles exhibits the same low activity that it shows in membrane fragments of di(C14:1)PC and di(C24:1)PC, once the addition of the detergent, $C_{12}E_8$, has made the vesicles leaky to ATP. Therefore, aggregation of the Ca^{2+}-ATPase in short and long chain lipids is not the explanation for low activity (Starling et al., 1995b).

1.4.1.3 Effects of phospholipid phase on the Ca^{2+}-ATPase

There are two possible bilayer phases for phospholipids depending on the temperature; these are gel phase or liquid-crystalline phase (Lee, 1983). The fatty acyl

chain lengths and degree of unsaturation of the phospholipids determine the temperature of transition between these two phases. For PEs a further phase transition can occur at high temperature from the liquid crystalline phase to the hexagonal H_{II} phase. In the gel phase the phospholipids are packed closely together, whereas phospholipids in the liquid-crystalline phase have considerable freedom of movement. Lipids must be in the liquid-crystalline state to support ATPase activity; the ATPase is essentially inactive in the gel phase, a fact attributable to a slow rate of phosphorylation (Starling et al., 1995c). The gel phase has little effect on Ca^{2+} binding, however, the affinity of the ATPase for Ca^{2+} in di(C16:0)PC is slightly higher in the gel phase than in the liquid-crystalline phase. This is in agreement with the observed shift in the E1/E2 equilibrium towards E1 in the gel phase (Starling et al., 1995c). However, the major effects of the gel phase are the reduction of the rates of phosphorylation and dephosphorylation of the Ca^{2+}-ATPase (Starling et al., 1995c).

1.4.1.4 Effects of phospholipid headgroup on the Ca^{2+}-ATPase

Phospholipid headgroups have two different effects on the functioning of the Ca^{2+}-ATPase. Firstly, they affect the activity of the Ca^{2+}-ATPase when it is reconstituted into unsealed membrane fragments; secondly, they affect the ability of the Ca^{2+}-ATPase to accumulate Ca^{2+} when reconstituted into sealed vesicles. When the Ca^{2+}-ATPase is reconstituted into membrane fragments consisting of one type of phospholipid, it is the PC headgroup that supports the greatest Ca^{2+}-ATPase activity, whilst the activity of the Ca^{2+}-ATPase reconstituted into di(C18:1)PE is about half that in PC (Bennett et al., 1978; Warren et al., 1975). The effects of PE on the activity of the Ca^{2+}-ATPase have been shown to be very temperature dependent, suggesting

that the tendency to form hexagonal H_{II} phases rather than a bilayer phase governs ATPase activity and headgroup structure is unimportant. Ca^{2+}-ATPase activities in di(C18:1)PC and di(C18:1)PE are identical below 15°C (Cullis & de Kruijff, 1978), where both di(C18:1)PC and di(C18:1)PE exist in the bilayer phase (Cullis & de Kruijff, 1978). Above 15°C di(C18:1)PE transforms into the hexagonal H_{II} phase and Ca^{2+}-ATPase activities are lower in di(C18:1)PE than di(C18:1)PC (Starling et al., 1996). Egg yolk PE also undergoes a transformation to the hexagonal phase at 28°C (Cullis & de Kruijff, 1978); Ca^{2+}-ATPase activities are identical in di(C18:1)PC and egg yolk PE below 28°C, but lower in egg yolk PE than di(C18:1)PC above 28°C (Starling et al., 1996).

The Ca^{2+}-ATPase activity in di(C18:1)PA is very similar to that in PC at neutral pH and low free Mg^{2+} concentrations (Warren et al., 1975). However, the activity of the Ca^{2+}-ATPase in di(C18:1)PA decreases very rapidly at higher concentrations of Mg^{2+}, typically to around 5% of the activity seen in di(C18:1)PC; this inhibition can be relieved by the addition of the Mg^{2+} chelator EDTA (Warren et al., 1975). Mg^{2+} also affects the temperature dependence of Ca^{2+}-ATPase activity in di(C18:1)PA. The Ca^{2+}-ATPase is only active at temperatures above 17°C at high Mg^{2+} levels, whereas the Ca^{2+}-ATPase is active above 10°C at low Mg^{2+} levels (Warren et al., 1975). This is consistent with Mg^{2+} raising the phase transition temperature of di(C18:1)PA. In mixtures of di(C18:1)PC and di(C18:1)PA Ca^{2+}-ATPase activity decreases with increasing di(C18:1)PA content. This suggests that while the di(C18:1)PA headgroup reduces Ca^{2+}-ATPase activity on its own, the addition of free Mg^{2+} complexes with the di(C18:1)PA headgroup further reducing activity with the formation of altered lipid phases (Warren et al., 1975). Therefore, Ca^{2+}-ATPase activity generally decreases as the level of negative charge increases.

The activity of the Ca^{2+}-ATPase in mixtures of di(C18:1)PC and phosphatidylinositol 4-phosphate (PtdIns-4P) is very different (Starling et al., 1995d). Ca^{2+}-ATPase activity increases with increasing PtdIns-4P content, with maximal activity being observed with a PtdIns-4P content of approximately 10%; no further increase in activity is observed with a higher PtdIns-4P content. PtdIns-4P achieves its effects by increasing the rate of dephosphorylation of the phosphorylated Ca^{2+}-ATPase by a factor of 2 (Starling et al., 1995d). Reconstitution with low concentrations of phosphatidylinositol (PtdIns) has no significant effect on Ca^{2+}-ATPase activity (Starling et al., 1995d). These results suggest PtdIns-4P binds to a small number of sites on the Ca^{2+}-ATPase, which are distinct from the regions of the Ca^{2+}-ATPase that interact with boundary lipids; the location of these sites is not known.

The structure of the phospholipids can also influence Ca^{2+} accumulation by the Ca^{2+}-ATPase when reconstituted into sealed vesicles. Although membranes composed of di(C18:1)PC support the highest activity of the Ca^{2+}-ATPase, sealed vesicles composed entirely of di(C18:1)PC accumulate relatively low levels of Ca^{2+} (Navarro et al., 1984; Gould et al., 1987a). Using the method for reconstitution used to reconstitute the Ca^{2+}-ATPase into vesicles of di(C18:1)PC, no Ca^{2+} accumulation is observed for the Ca^{2+}-ATPase in vesicles composed entirely of di(C18:1)PE (Bennett et al., 1978). This is because di(C18:1)PE does not form vesicles, but a H_{II} structure that is devoid of a membrane enclosed interior (Bennett et al., 1978). However, vesicles containing mixtures of di(C18:1)PC and di(C18:1)PE are able to accumulate more Ca^{2+} than di(C18:1)PC vesicles alone as Ca^{2+} accumulation was found to increase with increasing di(C18:1)PE content (Navarro et al., 1984; Cheng et al., 1986 Gould et al., 1987a). It was suggested that the presence of di(C18:1)PE decreases the rate of passive leak of Ca^{2+} out of the sealed vesicles (Gould et al., 1987).

di(C18:1)PE has a cone shape as a result of its relatively small headgroup, whereas di(C18:1)PC has a cylindrical shape. The addition of methyl groups to the di(C18:1)PE headgroup results in an increase in size for the headgroup. The addition of methyl groups to the headgroup results in a decrease in Ca^{2+} accumulation (Navarro et al., 1984). Raising the temperature from 25 °C to 37 °C results in vesicles with a high di(C18:1)PE content becoming leaky, probably a result of the formation of H_{II} structures (Navarro et al., 1984). Increasing the protein to lipid ratio reduces the temperature effect, due to the higher percentage of Ca^{2+}-ATPase molecules stabilising the bilayer structure (Navarro et al., 1984). Experiments incorporating a small percentage of the anionic lipids di(C18:1)PS and PtdIns-4P into di(C18:1)PC vesicles suggest that they increase Ca^{2+} accumulation (Szymanska et al., 1991). Maximal Ca^{2+} accumulation was observed in vesicles composed of 50% di(C18:1)PC and 50% di(C18:1)PS, further increases in the percentage of di(C18:1)PS resulting in reduced Ca^{2+} accumulation. Ca^{2+} accumulation was 2.5 fold greater in di(C18:1)PC vesicles containing 50% di(C18:1)PS than in vesicles containing solely di(C18:1)PC. Maximal Ca^{2+} accumulation in di(C18:1)PC vesicles containing PtdIns-4P was found using a 10-25 mole % fraction of PtdIns-4P; the increase observed was 1.6 fold greater than the Ca^{2+} accumulation seen for di(C18:1)PC vesicles (Szymanska et al., 1991).

1.4.2 Diacylglycerol kinase (DGK)

The diacylglycerol kinases (DGKs) are a group of enzymes that catalyse the transfer of the γ-phosphate of ATP to *sn*-1,2,-diacylglycerol (DAG), producing phosphatidic acid (PA) and ADP. The DGK of *E. coli* is the best studied of the prokaryotic DGKs; it has little resemblance to the eukaryotic DGKs. *E. coli* DGK is

an intrinsic cytoplasmic membrane protein, whilst the eukaryotic DGKs are extrinsic membrane proteins that bind to the membrane surface through domains such as the C1 domain found in protein kinase C (Topham & Prescott, 1999). In mammalian systems, DAG is a second messenger regulating various cellular responses, including the activation protein kinase C (PKC). Thus, DGK is an important enzyme for inactivating PKC by attenuation of the DAG level, contributing to the regulation of the cellular response (Shirai et al., 2000). There is no evidence of a signalling function for DAG in bacteria. Therefore, the essential metabolic role for *E. coli* DGK is the conversion of DAG produced during membrane-derived oligosaccharides (MDO) biosynthesis to yield phosphatidic acid (PA) (Cronan & Rock, 1996). One step of the MDO pathway is the transfer of the phosphoglycerol head group of PG in the outer leaflet of the cytoplasmic membrane to the nascent MDO, generating DAG as a by-product. The conversion of DAG to PA is necessary both so that PG can be readily replenished and to detoxify the cytoplasmic membrane of DAG (Neidhart et al., 1996), a lipid known for its ability to promote formation of nonbilayer lipid phases (Schorn & Marsh, 1996a). Once produced, PA re-enters the phospholipid biosynthetic pathway and undergoes a series of reactions to synthesise the three major membrane phospholipid species of *E. coli* (Neidhart et al., 1996), as shown in Figure 1.12. The three phospholipids are phosphatidylethanolamine (PE), phosphatidylglycerol (PG) and cardiolipin (CL), which are present in the following molar proportions respectively, 75 %, 15-20 % and 5-10 % (Neidhart et al., 1996).

The DGK of *E. coli* has been cloned and over-expressed from the *dgk*A structural gene (Loomis et al., 1985). It has been solubilized from *E. coli* in acidic butan-1-ol and purified in organic solvent (Russ et al., 1988), suggesting that the enzyme must be unusually hydrophobic. This is also consistent with the unusual stability of the

enzyme. In both its membrane-bound form and dissolved in butan-1-ol DGK remains active after heating to 100°C (Russ et al., 1988). These observations are in accordance with correlations between protein hydrophobicity and thermal stability (Bigelow, 1967). More recent DGK purification protocols involve solubilization of the membrane in detergents such as Triton X-100, dodecylmaltoside or octylglucoside, followed, in the case of DGK incorporating an N-terminal His_6 sequence, by purification using Ni-NTA affinity chromatography (Lau & Bowie, 1997). The poly-His affinity tag facilitates binding to Ni-NTA. NTA is a tetradentate chelating adsorbent, which occupies four of the six ligand binding sites in the coordination sphere of the nickel ion, leaving two sites free to interact with the 6 x His tag (The QIAexpressionist, 1998). Sanders et al. (1996) showed that the activity of the His-tagged enzyme was very similar to that of the native enzyme. The poly-His tag has been shown to be mobile in NMR spectroscopy, suggesting that it does not interact with the rest of the protein (Vinogradova et al., 1997). Therefore, the His-tag did not need to be cleaved from the enzyme in studies of enzyme structure or function.

1.4.2.1 Structure of DGK

With a molecular mass of just 13 kDa, *E. coli* DGK is the smallest known kinase. Studies using circular dichroism (CD) and infrared spectroscopy (IR) of DGK in PC multilayers have shown that DGK is highly α-helical, with an α-helical content of about 74% (Sanders et al., 1996). This is consistent with hydropathy plots, which predict three transmembrane α-helices per DGK molecule. β-lactamase and β-galactosidase fusion experiments also suggest the presence of three transmembrane α-helices, with the N-terminus on the cytoplasmic side and the C-terminus on the

periplasmic side of the membrane (Smith et al., 1994). The suggested topology fits the inside-positive rule with most of the Lys and Arg residues on the cytoplasmic side of the membrane (Von Heijne, 1992). DGK is also suggested to contain two amphipathic helices on the cytoplasmic side of the membrane (Figure 1.13). Transmembrane α-helix TM3 contains two tryptophan (Trp) residues at the C-terminal end on the periplasmic side of the membrane, whilst TM1 contains one Trp on the periplasmic side of the membrane; aromatic resides are often found at the ends of the transmembrane α-helices in membrane proteins, showing that aromatic residues have a preference for the lipid-water interface (Wimley & White, 1996). These aromatic residues possibly act as 'floats', stabilising the helices in the lipid bilayer environment (Mall et al., 2001).

Wen et al. (1996) have suggested that transmembrane α-helix M1 is relatively short containing just 15 residues, running from Glu-34 to Asp-48, compared to a more normal figure of around 20, whereas M2 running from Asp-51 to Glu-68 contains 17 residues and M3, from Met 96 to Trp-117, contains 22 residues. In the family of bacterial DGKs (Figure 1.14), the residue equivalent to Glu-34 in *E. coli* DGK is not conserved, whereas Glu-28 is conserved in all but the DGK from the cyanobacterium *Synechocystis sp.* (Kaneko et al., 1995) where a Gln replaces it. If it is assumed that M1 starts at Glu-28 rather than Glu-34, the length of M1 becomes 21 residues. This would imply that Glu-34 is embedded within the lipid bilayer. There are precedents for suggesting that an acidic residue might be located within the hydrocarbon core of the bilayer. For example, in the Ca^{2+}-ATPase Asp-59 is buried within the bilayer and faces out into the bilayer, forming an ion pair with Arg-63 (Toyoshima et al., 2000). It is possible that in *E. coli* DGK Glu-34 forms an ion pair with Arg-32. The presence of amphipathic helix 2 between TM2 and TM3 makes it almost impossible to derive a

tertiary structural model for a monomeric DGK in which all three TM helices are packed with one another (regardless of the orientation of amphipathic helix 2). Additionally, the now apparent shortness of TM2 suggests that rather than being in contact with the lipid bilayer it could be in contact with other helices at the centre of some oligometric structure within the membrane. In fact cross-linking studies with glutaraldehyde in dodecylmaltoside (DM) and DM-cardiolipin micelles have established that catalytically functional DGK exists as a trimer with three complete active sites (Vinogradova et al., 1997). Cross-linking to trimers is also seen with Cu (II)-phenanthroline, which forms disulphide bonds between Cys residues; DGK contains two Cys residues (Cys-46 and Cys-113) near the periplasmic ends of TM1 and TM3. The observation of trimers suggests that these Cys residues on adjacent subunits may be close together. The same trimeric structure is suggested in either the presence or absence of cardiolipin (Vinogradova et al., 1997). Cross-linking experiments have suggested that M2 is at the trimer interface of DGK (Nagy et al., 2000), suggesting that M1 and M3 will be exposed to lipid in the membrane.

Using a random mutagenesis approach, Wen et al. (1996) showed that the vast majority of residues in DGK tolerated a variety of neutral amino acid substitutions, but that 8 positions tolerated no change. It is likely that some of these residues are located at the active site; six were predicted to be on the cytoplasmic side of the membrane, one on the periplasmic side and one in TM2 (Figure 1.13). Subsequent studies showed that the residue in TM2 thought to be essential was in fact not so (Lau et al., 1999). The essential residue on the periplasmic side was Asp-51, located in a small loop between TM1 and TM2. Asp-51 could be replaced with Pro and still form an active enzyme, suggesting that the role of Asp-51 could be a structural one in forming the turn, rather than being an active site residue (Lau et al., 1999). The

remaining 6 residues, A14, E69, N72, E76, K94 and D95, located on the cytoplasmic side of the membrane are assumed to be part of the active site.

The discovery that DGK is a trimer with three complete active sites raised the question of whether the active sites are contained within each monomer or whether they are composed of residues from different subunits. Lau et al. (1999) adopted a subunit mixing approach in which inactive enzyme variants were prepared by engineering mutations in each potential half-site. According to a shared site model, subunits bearing deleterious mutations on the opposite halves of a shared active site should be able to complement one another when mixed. Those on the same half-site, however, will not complement. Having identified the six potential active-site residues, Lau et al., (1999) created the following mutants, A14Q, E69C, N72S, E76L, K94L, and D95N and tested for restoration of activity upon subunit mixing. CD spectra of the mutants showed no significant differences from that of the wild type, indicating that the gross secondary structure of the protein is unaltered by the mutations (Lau et al., 1999). The study of complementation showed that A14Q complements E69C, N72S, K94L, and D95N but not E76L. The mutant E76L also complements E69C, N72S, and K94L, albeit less effectively than A14Q. As predicted by a shared site model, DGK activity in mixtures of single mutant subunits with wild type subunits was found to be proportional to the fraction of wild-type subunits. Therefore, residues from different subunits participate in forming each active site of the trimeric DGK (Lau et al., 1999). It is suggested that Ala-14 and Glu-76 are present on one half site and Glu-69, Asn-72 and Lys-94 are present on the other (Lau et al., 1999). However, D95N behaves anomalously, complementing A14Q but not E69C, N72S, or E76L and inhibiting K94L. Mutations in this apparent active site residue can completely inactivate wild type subunits when mixed. It is possible that this mutant has an altered

conformation that is transmitted to the wild type subunit; however, no gross structural alterations were found in the CD spectrum (Lau et al., 1999). It is more likely that D95N behaves like a double mutant and inactivates more than one half-site, suggesting that each Asp 95 may participate in more than one active site (Lau et al., 1999). In summary, catalytically functional DGK is trimeric with three active sites per trimer and consists of subunits that are 121 residues in length. The active sites are located at the subunit-subunit interfaces with residues from different subunits making up the active site.

1.4.2.2 Enzyme kinetics

DGK carries out a two-phase reaction, between the water soluble ATP and the membrane bound DAG. Activity of the enzyme requires the presence of detergent micelles or membranes because of the insoluble nature of the substrate DAG. This creates potential problems because a detergent could, in principle, act both as a solubilizer of DAG and as an activator of the protein. The environment of DGK in a detergent micelle will, in general, be very different to that in a phospholipid bilayer and thus addition of lipids to DGK in detergent micelles might be expected to lead to an increase in activity. For such studies it would be convenient to have a 'background' detergent in which DGK showed no activity, to which activating lipids could then be added. In micelle studies it is also necessary to show that the rate of exchange of DAG between bulk micelles and those containing the enzyme are fast enough to maintain an equilibrium distribution of the substrate between the micelle containing the enzyme and the bulk micelles. In fact exchange has been shown to be fast with β-octyl glucoside micelles (Walsh & Bell, 1986a). A further possible

complication is that concentrations of DAG above 3.4 mol % in the micelles have been found to be inhibitory, possibly due to a change in the structure of the micelle when it contains a large number of DAG molecules (Walsh & Bell, 1986a).

Activity in octylglucoside (OG) micelles was found to be highest at pH 6.5, at an ionic strength of 100 mM (Walsh & Bell, 1986a). Activity exhibits Michaelis-Menten kinetics with respect to MgATP, with an apparent K_m of 300 μM and v_{max} of 10.4 μmol/min/mg of protein (Walsh & Bell, 1986a). The true substrate was shown to be MgATP rather than free ATP and it was also shown that the Mg^{2+} acts as an activator, binding directly to the enzyme, with maximal activity being observed at about 10 mM free Mg^{2+} (Walsh & Bell, 1986a). Other divalent metal ions including Co^{2+}, Cd^{2+}, Zn^{2+}, Fe^{2+}, Ni^{2+} and especially Mn^{2+} are also able to stimulate DGK but Ca^{2+}, Sr^{2+} and Cu^{2+} are not (Walsh & Bell, 1986a). The dependance of activity on DAG concentration in micelles also showed Michaelis-Menten kinetics, with K_m values of 0.92 mol % for dioleoyglycerol, a C18 chain length DAG, and 3.6 % for dioctanoylglycerol, a C8 chain length DAG; these differences probably reflect the greater water solubility of dioctanoylglycerol. The apparent v_{max} for both substrates was 10.5 μmol/min/mg of protein (Walsh & Bell, 1986a).

A very fundamental question with regard to the mechanism of any kinase is whether it catalyses phosphoryl transfer via a direct substrate to acceptor pathway or whether it first catalyses formation of an enzyme-phosphate intermediate followed by a second transfer of the phosphoryl from enzyme to acceptor. The kinetics of DGK are consistent with the formation of a ternary complex MgATP-DAG-Enzyme, suggesting a direct phosphoryl transfer mechanism for DGK, rather than one involving the formation of a phosphorylated enzyme intermediate (Badola & Sanders, 1997). This suggests that ATP must bind to the enzyme with its γ-phosphate close to

the –OH group of the DAG. Kinetic studies suggest random order binding of ATP and DAG, either substrate being able to bind in the presence or absence of the other (Badola & Sanders, 1997). The nucleotide specificity has been studied using a range of MgATP analogues, including GTP and ITP (Badola & Sanders, 1997). Both GTP and ITP have K_m values rather similar to ATP but with a very much reduced v_{max}. It was suggested that the change in v_{max} rather than K_m showed that a conformation change occurs following the binding of one or both substrates prior to phosphate transfer (Badola & Sanders, 1997). As for other kinases, the purpose of the change is to exclude water from the active site so that hydrolysis does not significantly compete with transfer (Badola & Sanders, 1997).

The dependance of DGK activity on the structure of the diacylglycerol substrate has been investigated (Walsh & Bell, 1990). *sn*-1,2-Diacylglycerols varying in chain length from C4 to C18 were all substrates for DGK. Increasing the acyl chain length from C6 to C18 decreased the apparent K_m with no effect on v_{max}. Introduction of bulky substituents into the chains had little effect. This suggests that the primary determinants of DAG recognition are in the glycerol backbone and ester linkages. Conversion of the *sn*-2 ester group to an amide led to a small increase in the K_m but no effect on v_{max}. Changing the *sn*-1 ester group to an amide had a small effect on K_m but resulted in a very large decrease in v_{max}. Modification to the *sn*-3 carbon had a major effect on v_{max}. Analogues in which the –OH group at the *sn*-3 position was removed were not inhibitors of the enzyme, suggesting that the –OH group is also important in binding, functioning as a hydrogen bond donor in its interaction with the enzyme. Thus the key groups are the *sn*-3 -OH group and *sn*-1 ester group.

1.4.2.3 Effects of detergents and lipids

Reports on the effects of lipids on the activity of DGK in detergent micelles are rather confused, largely because of difficulties in choosing the appropriate 'background' detergent. An ideal detergent would solubilise the protein and deliver water-insoluble substrates, whilst not functioning as an activator (cofactor) itself. Walsh and Bell (1986b) reported that completely delipidated DGK showed no activity in OG and that addition of lipid was required for activity, indicating that OG cannot act as a lipid cofactor for DGK and would serve as an ideal detergent. A complication of the analysis was, however, that the substrate dioleoylglycerol (DOG) could, in the absence of any other lipid, act as both a substrate and as an activator lipid. This dual role was confirmed making use of the observation that only *sn*-1,2-diacylglycerols can function as substrates. It was shown that *sn*-1,3-dioleoyglycerol , which is not a substrate, would activate the enzyme in the presence of *sn*-1,2- dioleoylglycerol as substrate (Walsh & Bell, 1986b). The absolute dependence on an added lipid cofactor when *sn*-1,2-dioctanoylglycerol is employed as a substrate both indicates that OG cannot act as a lipid cofactor and that DGK has an absolute requirement for a lipid cofactor (Walsh & Bell, 1986b). However, Russ et al. (1988) studied activity against dipalmitoylglycerol (DPG) in Triton X-100 as detergent and found zero activity in this detergent, but found that addition of either octyl β-glucoside, hexyl β-D-glucoside or lauryl maltoside resulted in activity, suggesting that these detergents could act as activating 'lipids'. It is possible that these differences follow from the use of different diacylglycerols with different mixing properties with the detergent. Dipalmitoylglycerol has a melting point above the temperature of the enzyme assay (25 °C), whereas the melting point of dioleoglycerol is much lower. Thus it could be

that DPG was insoluble in Triton X-100 but soluble in other detergents and that this could explain the detergent activation observed in Triton X-100.

Effects of lipid on the activity of DGK in Triton X-100 are structurally rather non-specific. Enzyme activity was observed in the presence of fatty acids such as oleic acid and in the presence of phospholipids such as phosphatidylethanolamine, egg yolk phosphatidic acid or dipalmitolyphosphatidic acid. These lipids only gave activity when in the presence of Triton X-100 (Bohnenberger & Sandermann, 1983). It is interesting that phosphatidic acid, the product of the reaction, acted like a normal lipid activator and did not lead to inhibition of activity as might have been expected for a reaction product (Bohnenberger & Sandermann, 1983). Other lipids activated DGK in either the presence or absence of Triton X-100; these included phosphatidylglycerol, phosphatidylserine, cardiolipin, and egg yolk phosphatidycholine (Bohnenberger & Sandermann, 1983). The difference between the two groups of lipid appeared to be that only the second group was able to solubilize the DPG substrate. Dipalmitoylphosphatidylcholine (di(C16:0)PC) showed no activation in either the presence or absence of Triton X-100; since the gel to liquid crystalline phase transition temperature of di(C16:0)PC is 42 °C, this suggests that the lipid must be in the liquid crystalline phase to affect activity (Bohnenberger & Sandermann, 1983). Bohnenberger and Sandermann (1983) reported that cardiolipin was especially effective in stimulating the enzyme, cardiolipin being able to increase activity for the kinase in the presence of other lipids such as phosphatidylethanolamine.

Walsh and Bell (1986b) showed that cardiolipin was also the most effective lipid in activating DGK using OG as detergent. They found that cardiolipin, phosphatidycholine and phosphatidylglycerol gave the same maximal activities, but

less cardiolipin was required to give this maximal activity than for the other lipids. Half maximal stimulation by cardiolipin was observed at 1 mol % cardiolipin in octyl glucoside; given this low value it was suggested that cardiolipin bound specifically to a few sites on DGK rather than just binding non-specifically to the lipid-protein interface of the protein (Walsh & Bell, 1986b). Maximal stimulation observed with phosphatidylserine and phophatidic acid were less than that observed with the other phospholipids. Walsh and Bell (1986a) found that di(C18:1)PC and di(C16:0)PC had identical effects on activity, in disagreement with the results of Russ et al. (1988) in Triton X-100 who found, as described above, that di(C16:0)PC had no effect on activity. Walsh and Bell (1986b) also studied stimulation of activity by a series of saturated phosphatidylcholines and showed that effects on activity increased with increasing chain length from C8 to C16. It was found that incubation of the enzyme in OG in the presence of DOG at 25 °C led to loss of activity in several minutes: this was seen only in the presence of DOG, and the effect was prevented by lipids that activated the enzyme (Walsh & Bell, 1986b).

The possible roles of individual transmembrane helices in the interactions with detergents have started to be explored in studies in which residues Gly-35 and Leu-48 in TM1 have been replaced with Ala residues (Zhou et al., 1997). Although not expressed as well as wild type, the enzyme had a 50 % wild type v_{max} with a similar K_m (Zhou et al., 1997). However, detergent sensitivities were very different. For wild type enzyme, highest activity was seen in Triton X-100 in the presence of cardiolipin with DOG as substrate; the activity seen in DM was about 80 % of that in Triton X-100 and the activity in OG was about 60 % of that in Triton X-100. For the Ala-mutant, activity in Triton X-100 was about half that of wild type, but activities in DM and OG were very low (Zhou et al., 1997). It was also seen that thermal inactivation is

faster for the mutant (Zhou et al., 1997). Thus although TM1 is not involved in substrate binding etc. it is important in stabilising interactions with the rest of the protein. A mutant in which Ala replaced all the residues in TM3 expressed at low levels and showed no activity; a mutant in which Ala replaced all the residues in TM2 failed to express (Zhou et al., 1997).

There have as yet been no published studies of the effects of phospholipid structure on the activity of DGK reconstituted into lipid bilayers. However, Sanders et al. (1996) have shown that reconstitution is possible by mixing DGK in 1 % DM, a non-denaturing detergent, with lipid in octylglucosde followed by dialysis to remove detergent or by dilution followed by centrifugation and washing. Gorzelle et al. (1999) have reported that some DGK mutants can be misfolded and have devised a method in which DGK undergoes a procedure known as 'reconstitutive refolding'. The method involved purifying the kinase in a range of detergents including DM, Triton X-100, CHAPSO, BOG, and dodecylphosphocholine (DPC), followed by the addition of (1-palmitoyl-2-oleoyl-phosphatidylcholine) POPC in the relative detergent; this was followed by detergent removal using dialysis or Bio-Beads. DGK vesicular solutions were then subjected to both micellar and vesicular activity assays. DGK activity was low in every assay bar the one relating to the DGK purified into dodecylphosphocholine (DPC), thus this method for simultaneously reconstituting and refolding DGK is referred to as 'reconstitutive refolding' (Gorzelle et al., 1999). Refolding of DGK is proposed to occur unevenly and at a late stage of detergent removal (dialysis), typically 30 hours and after several buffer changes (Gorzelle et al., 1999).

1.4.2.4 Interactions of DAGs with phospholipids

In studies of the activity of DGK in phospholipid bilayers it will be necessary to consider the two possible roles of the phospholipid bilayer, as activator of the protein and as solvent for the substrate DAG. Mixing properties of DAG with phopholipid bilayers have been shown to be rather complex. The phase diagrams for mixtures of dimyristolphosphatidylcholine (DMPC) and dimyristoylglycerol (DMG) (Schorn & Marsh, 1996a) and of dipalmitoylphosphatidylcholine (DPPC) and dipalmitoylglycerol (DPG) (Lopez-Garcia et al., 1994a) have been established from differential scanning calorimetric (DSC) studies. In the region up to about 45 mol % DMG, the DSC scans broaden with increasing content of DMG, with the onset temperature for the transition remaining fairly constant: this is indicative of immiscibility in the gel phase. However, at about 45 mol % DMG, the character of the DSC scans changes abruptly to give a single sharp peak. This is typical of 'compound' formation- the formation of a complex between DMPC and DMG, melting sharply at 54 °C, with a stoichiometry of about 1 DMPC molecule per DMG molecule. The single sharp peak remains up to 65 mol % DMG but at higher concentrations a new peak appears which is different in heating and cooling scans, indicating a metastable transition. This transition is likely to correspond to that of pure DMG since DMG is known to show such metastable transitions, from isotropic liquid at high temperatures to one of two crystalline forms, a metastable α or a stable β form (Schorn & Marsh, 1996a). The metastable transition of DMG appears only above about 65 mol % DMG suggesting that a second 'compound' can be formed between DMG and DMPC, with a stoichiometry of 2 molecules of DMG per 1 molecule of DMPC. The phase diagram is therefore divided into three parts, corresponding to the formation of stoichiometric compounds with approximate DMPC: DMG

stoichiometries of 1:1 and 1:2 (Figure 1.15). In region I the fluid phase is a normal lamellar L_α phase. In region II the fluid phase is the hexagonal H_{II} phase. Finally, in region III, the fluid phase is isotropic (I). Region I shows a normal eutectic type of phase diagram with gel phase immiscibility between gel phase DMPC and compound C1, with the eutectic point lying close to 0 mol % DMG. This region of the phase diagram is consistent with complete miscibility of DMPC and the compound C1 in the liquid crystalline phase and essentially complete immiscibility of DMPC and C1 in the gel phase.

Formation of the compound C1 could be stabilized by hydrogen bonding between the –OH group of the DAG and the ester carbonyls of the phosphatidylcholine (Heimburg et al., 1992). This would be consistent with infrared studies which suggest that the addition of DPG reduces the degree of hydration of the fatty acyl carbonyl groups of DPPC (Lopez-Garcia et al., 1994a). In region I chain packing is increased by addition of DMG, resulting in increased chain order for the DMPC (Schorn & Marsh, 1996b). Interestingly, the unique conformational features found for the *sn*-2 chain of a phospholipid in a bilayer are also found for the *sn*-2 chain of DMG when incorporated into a bilayer of DMPC. The conformation and orientation of the glycerol backbone adopted by DMG in the bilayer must be similar to that adopted by DMPC; this conformation for DMG is different to that adopted in the crystal structure (Schorn & Marsh, 1996b; Sanders, 1994; Pascher, 1996).

1:1 compound formation between 1,2-dioleoylglycerol (DOG) and DMPC has also been suggested (Dibble et al., 1996). However, in this case the 1:1 complex of DOG with DMPC is largely immiscible with DMPC in the liquid crystalline phase as well as in the gel phase (Dibble et al., 1996). The importance of this observation is that DOG-rich and DOG-poor domains will coexist in the liquid crystalline phase.

Similar immiscibility was observed in the liquid crystalline phase for mixtures of DOG and DPPC (Ortiz et al., 1988). The different effects of the saturated and unsaturated DAGs are presumably a result of the effects of the bulky *cis* double bond. DOG and dimyristoylphosphatidylserine (DMPS) also form a 1:1 complex that again is largely immiscible with DMPS in both the liquid crystalline and gel phases (Dibble et al., 1996). In ternary mixtures of DMPS, 1-palmitoyl-2-myristoyl-phosphatidylcholine (PMPC) and DOG, DOG has been reported to interact preferentially with DMPS (Dibble et al., 1996). This could be because the headgroup of phosphatidylserine can only participate in intermolecular hydrogen bonding as a hydrogen bond acceptor (Dibble et al., 1996). Addition of Ca^{2+} to bilayers containing phophatidylserine in mixtures with zwitterionic lipids leads to formation of rigid domains of a phosphatidylserine-Ca^{2+} complex (Lopez-Garcia et al., 1994b). The formation of such rigid domains would be expected to lead to reduced miscibility with DAG, and this has indeed been observed in mixtures of DPG with dipalmitoylphosphatidylserine (DPPS); DPG is less miscible with DPPS in the presence of Ca^{2+} than in the absence of Ca^{2+} (Lopez-Garcia et al., 1994b).

In mixtures with phosphatidylethanolamines, the major effect of DAGs is on the temperature of the bilayer-hexagonal phase transition, which is decreased markedly by the presence of just a few mol % of DAG (Epand, 1985). For example, addition of 9 mol % of the DAG derived from egg yolk phosphatidylcholine (which will be predominantly 1-palmitoyl, 2-oleoylglycerol) to egg yolk phosphatidylethanolamine results in the formation of hexagonal phase at 25 °C, a temperature at which egg yolk phosphatidylethanolamine alone is purely lamellar (Das & Rand, 1986). The effect has been attributed to a reduction in the spontaneous

radius of curvature of the lipid-water interface, due to both headgroup size and hydration effects.

The activity of DGK has usually been determined in the presence of detergent micelles, necessary to solubilise the hydrophobic diacylglycerol substrate (Sanders et al., 1996; Walsh & Bell, 1986a, 1986b). The activity of DGK in micelles of a detergent such as OG in the absence of phospholipid is very low when the substrate is a short-chain diacylglycerol such as dioctanoylglycerol (Walsh & Bell, 1986b). Addition of phospholipids leads to increased activity, cardiolipin being the most efficient phospholipid in restoring activity (Walsh & Bell, 1986b). Higher activities are seen with dioleoylglycerol (DOG) as substrate but the situation is complex since long-chain diacylglycerols can act as both substrate and activating lipid (Walsh & Bell, 1986b). Walsh et al. (1990) have shown that, in the presence of activating phospholipids, the lower activities observed for short chain diacylglycerols follow from higher K_m values for the diacylglycerol with v_{max} values being independent of chain length.

In this thesis we establish a reconstitution protocol for DGK, allowing us to measure enzyme activity in a lipid bilayer. We show that, in the bilayer system, the activity of DGK is sensitive to phospholipid chain length, headgroup and phase.

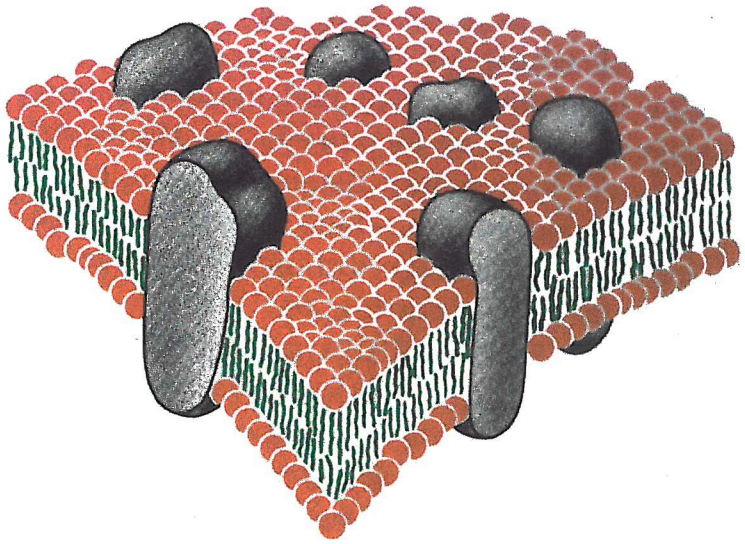

Figure 1.1 Fluid mosaic model

Model showing the overall organisation of biological membranes. Membranes are two-dimensional solutions of oriented lipids and globular proteins (Singer & Nicholson, 1972).

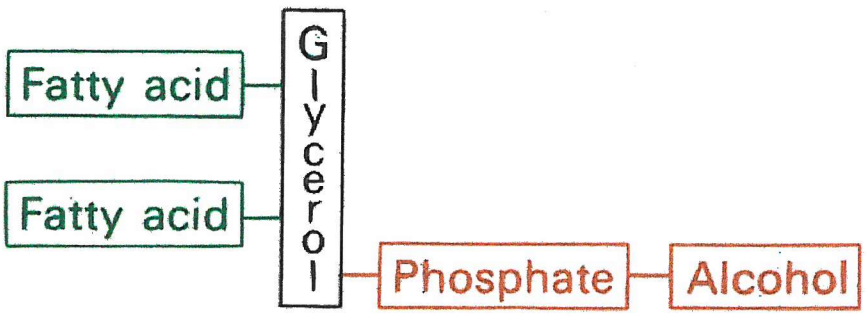

Figure 1.2 Components of a phosphoglyceride

Two fatty acid chains and a phosphorylated alcohol are attached to a glycerol backbone by ester links.

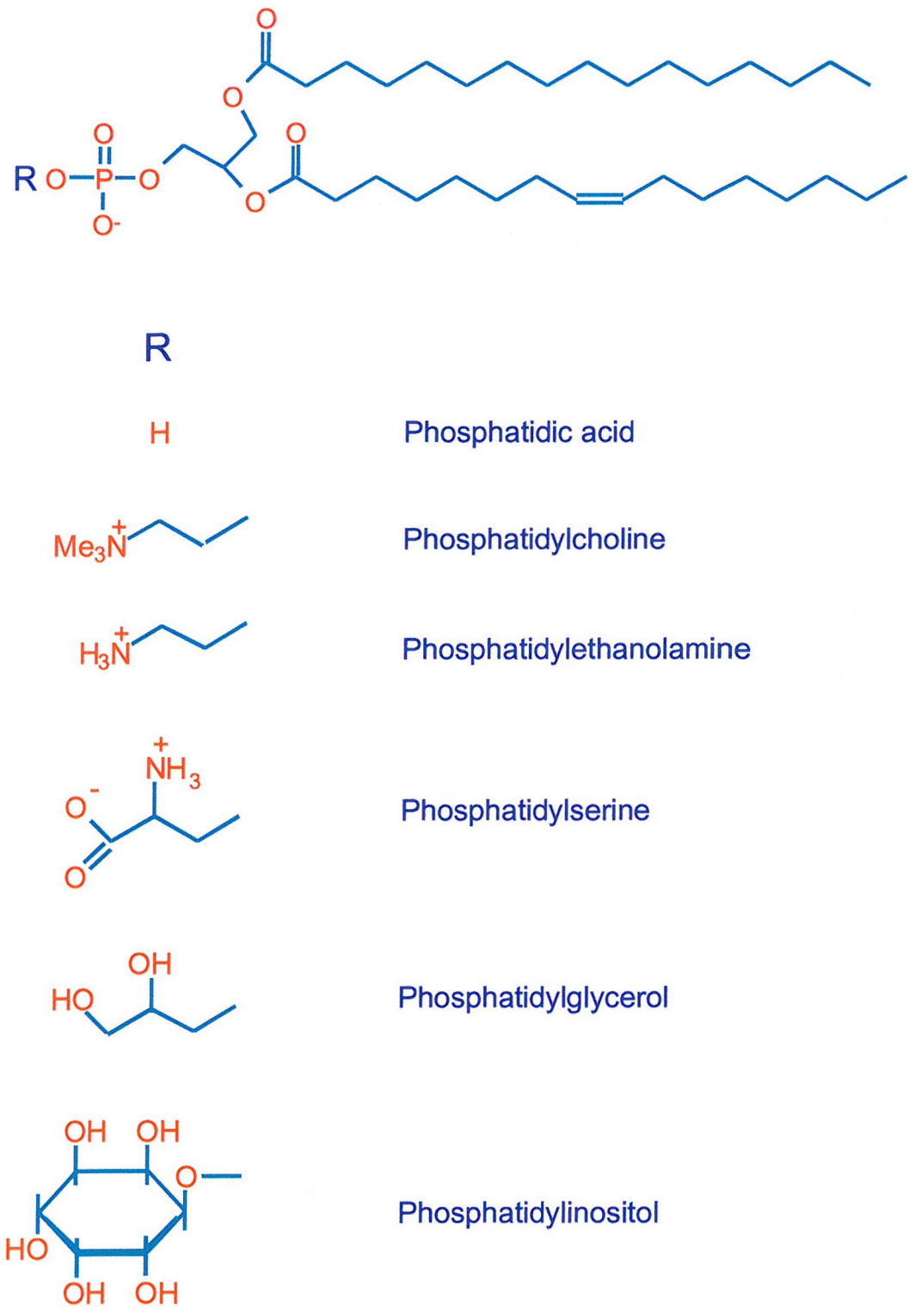

Figure 1.3 Structures of lipids commonly found in biological membranes

Shown are the alcohol moieties (R) that become esterified to the phosphate group of phospahatidate to form the appropriate phospholipids.

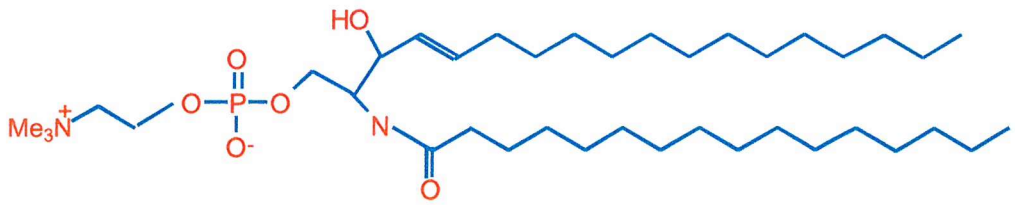

Figure 1.4 The structure of sphingomyellin

Diagram showing that the amino group of the sphingosine backbone is attached to a fatty acid by an amide bond, and that the primary hydroxyl group of sphingosine is esterified to phosphocholine.

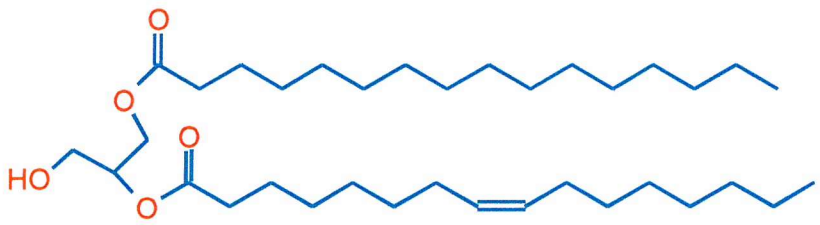

Figure 1.5 The structure of a diacylglycerol

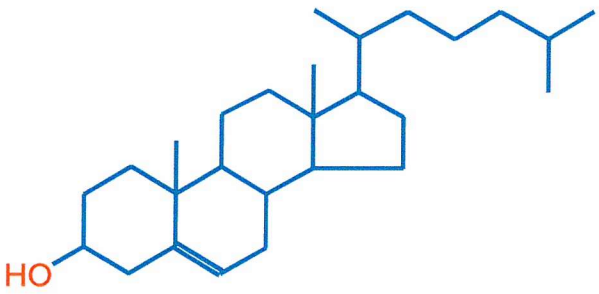

Figure 1.6 The structure of cholesterol

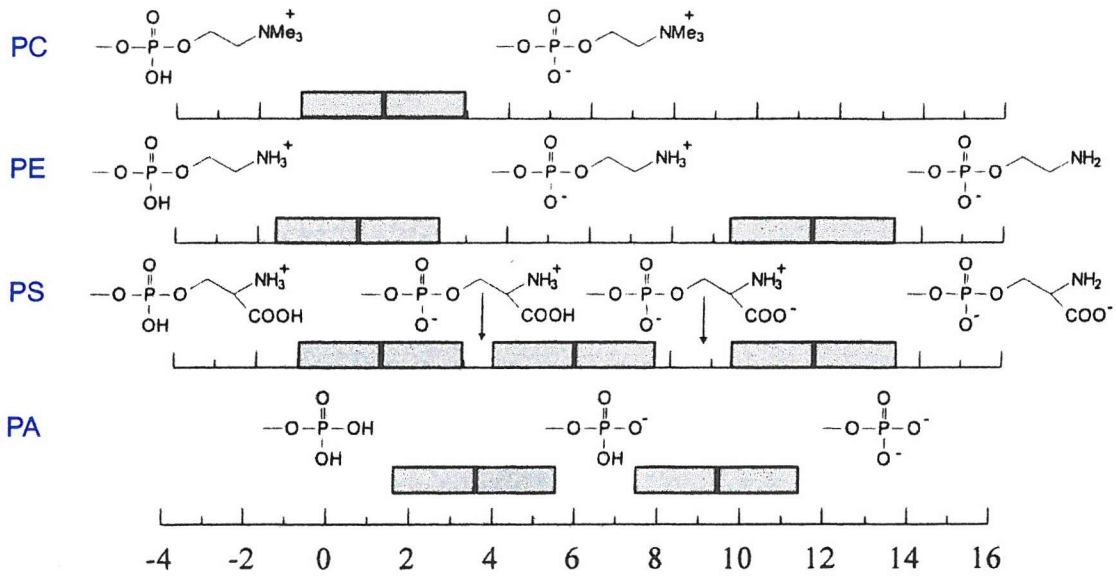

Figure 1.7 Ionisation states of phospholipids (Stryer, 1995)

Diagram showing the ionisation states of various phospholipids as a function of the bulk pH in a medium of 100 mM salt. The shaded areas illustrate where partial ionisation occurs, assuming that ionisation occurs over a range of two pH units either side of the apparent pK value.

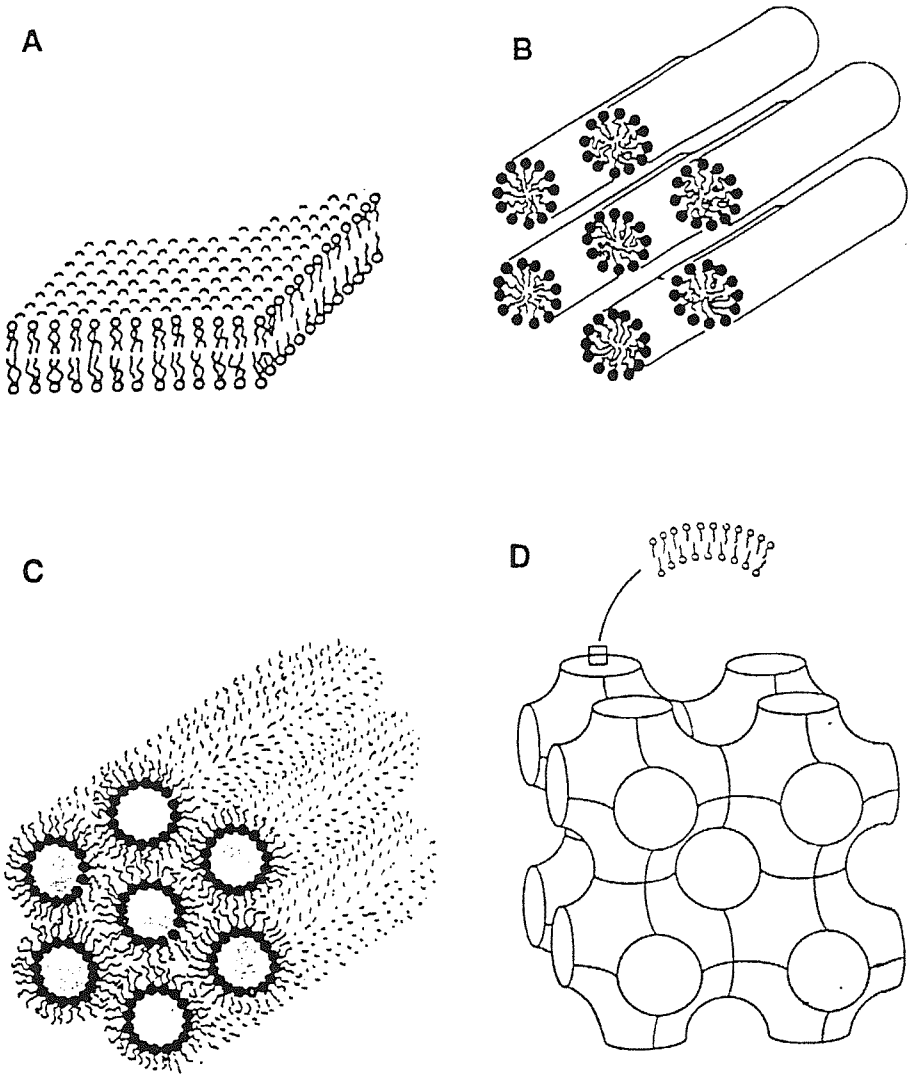

Figure 1.8 Structures adopted by phospholipids in aqueous media

The phospholipid phases: lamellar or bilayer (A) , normal hexagonal (B) , inverted hexagonal (C) , and cubic (D).

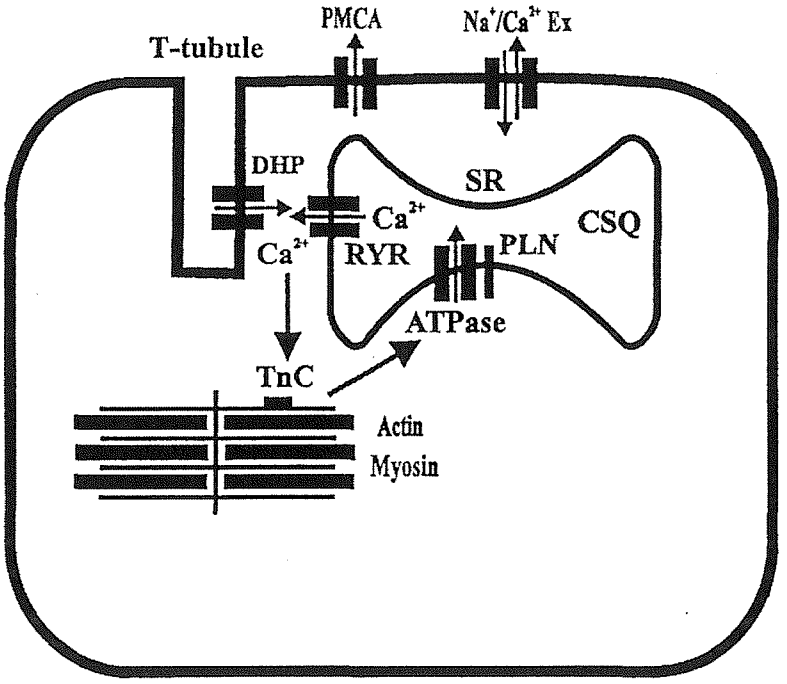

Figure 1.9 Schematic diagram of the regulation of muscle contraction

The increase in cytoplasmic Ca^{2+} necessary for muscle contraction is triggered by a nerve impulse, which induces depolarisation of the sarcolemma. This wave of depolarisation is conveyed down the T-tubules to reach the terminal cisternae, where it causes a conformational change in the dihydropyridine receptor (DHP) (Catterall, 1991). This activates the ryanodine receptor (RYR) in the sarcoplasmic reticulum (SR), which allows Ca^{2+} to be released into the cytoplasm (McPherson & Campbell, 1993). The Ca^{2+} released into the cytoplasm binds to specific sites on the troponin C (TnC) complex inducing a conformational change that is transmitted to tropomyosin allowing the interaction of actin and myosin. Utilising ATP hydrolysis the thin filaments slide over the thick, the sarcomere shortens and muscle contraction takes place. Muscle relaxation is generally the reverse except for the actions of the Ca^{2+}-ATPase (ATPase) that pumps two Ca^{2+} ions back into the SR where they are bound by the protein calsequestrin (CSQ) (McPherson & Campbell, 1993).

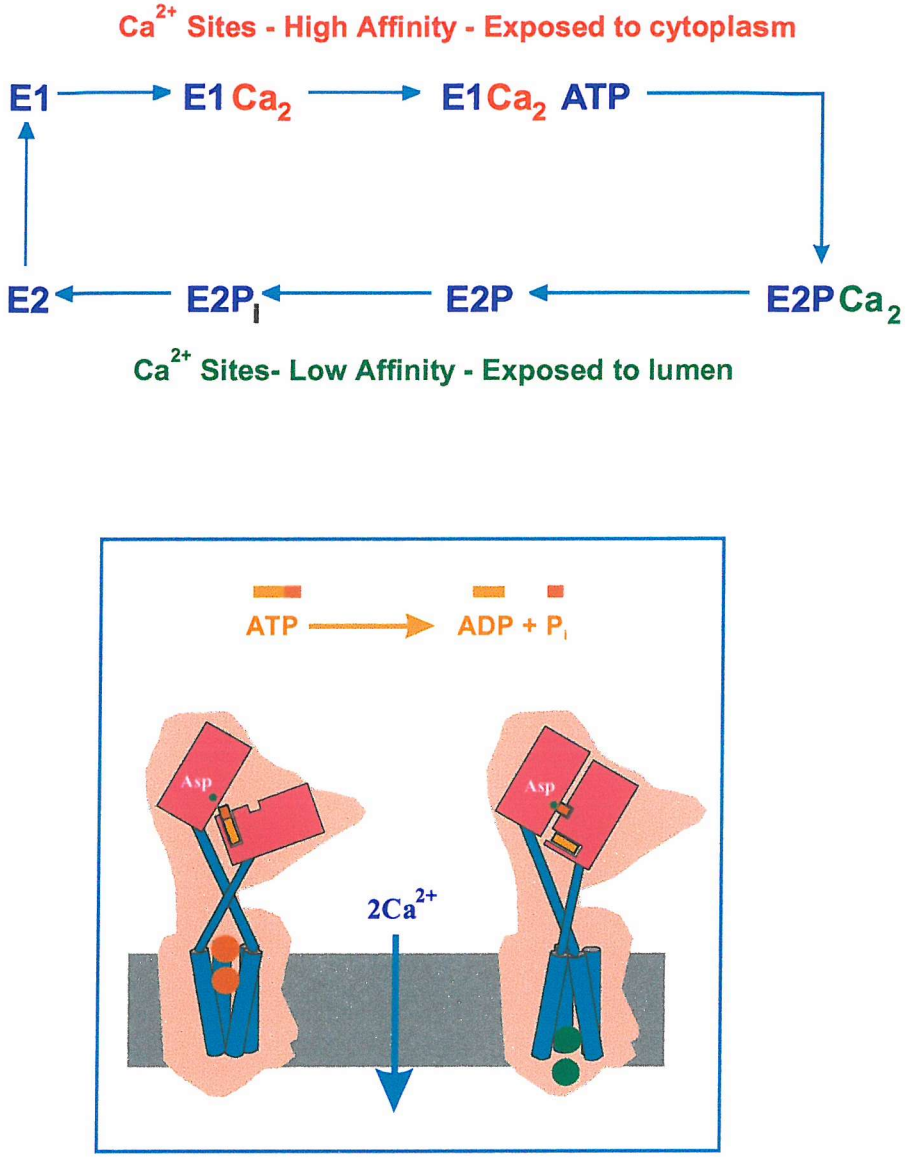

Figure 1.10 The E1-E2 reaction cycle of the Ca^{2+}-ATPase

Diagram showing how the E1-E2 reaction scheme (top) and how it is linked to the vectorial transport of two Ca^{2+} ions.

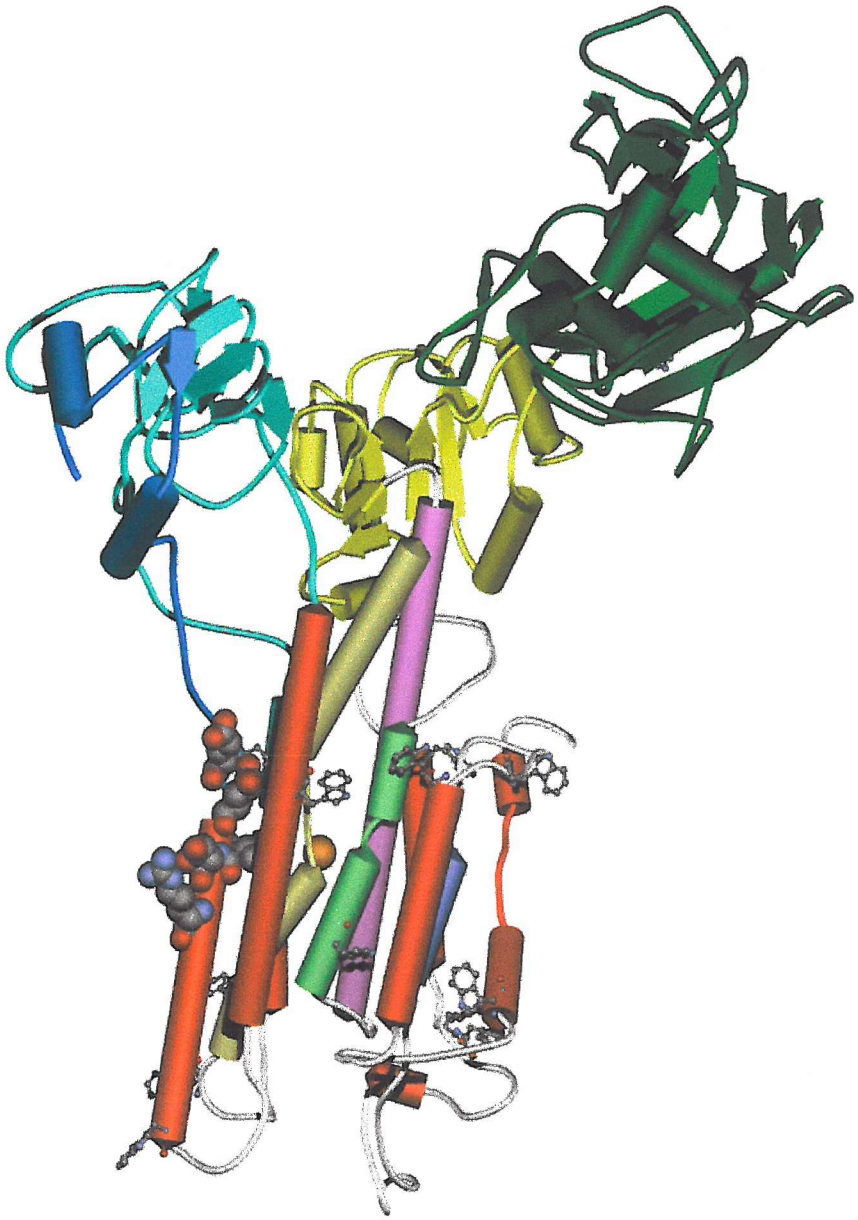

Figure 1.11 Overall architecture of the Ca^{2+}-ATPase (Lee & East, 2001)

The three cytoplasmic domains A, P, and N are coloured blue, yellow and green respectively. The N-terminal region is coloured dark blue. The four transmembrane α-helices involved in binding Ca^{2+} at the high affinity pair of sites are coloured as follows: M4, yellow; M5, lilac; M6, green; M8, blue; the other transmembrane α-helices are coloured red. Of the two bound Ca^{2+} ions (orange) only one is visible in this view. Trp residues are shown in ball-and-stick representation. Charged residues in helix M1 are shown in space-fill representation.

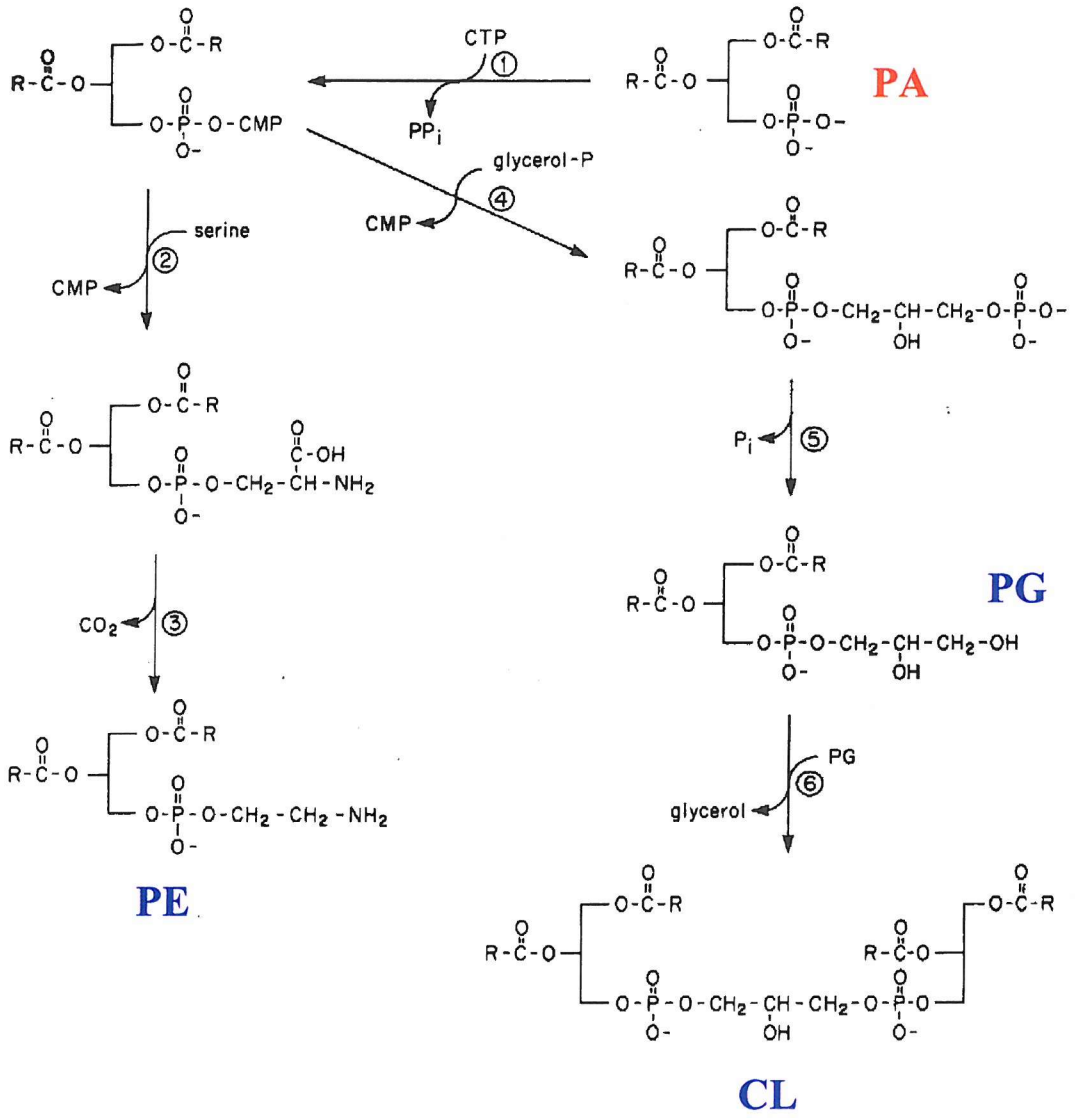

Figure 1.12 Phospholipid Biosynthetic Pathway of *E. coli* (Neidhart et al., 1996)

Phosphatidic acid (PA) is produced by the phosphorylation of diacylglycerol (DAG) by diacylglycerol kinase (DGK). PA can the re-enter the phospholipid biosynthetic pathway and undergo a series of reactions to synthesise the three major phospholipid species of *E. coli*: phosphatidylethanolamine (PE), phosphatidylglycerol (PG) and cardiolipin (CL), which are present in the following molar proportions respectively, 75%, 15-20% and 5-10%.

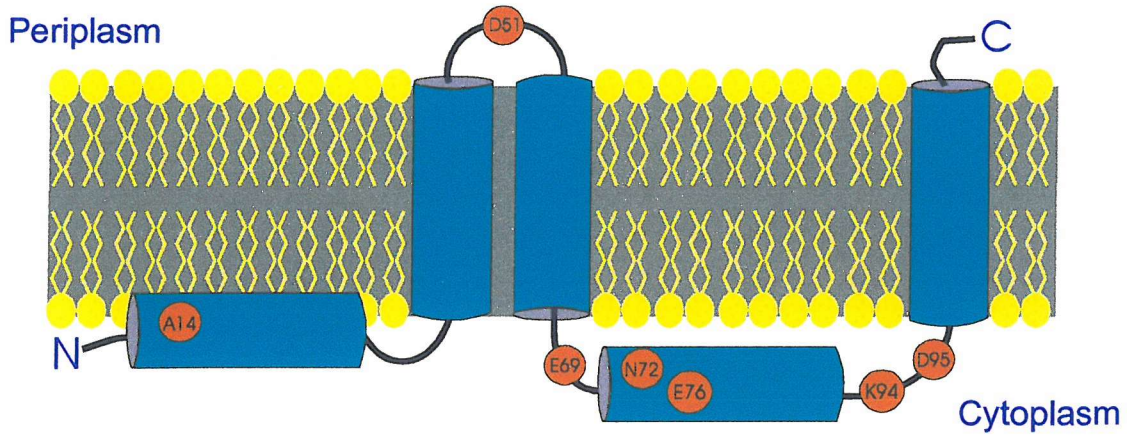

Figure 1.13 Topological model of DGK

The topology of DGK derived from β-lactamase and β-galactosidase fusion experiments (Smith et al., 1994). The three transmembrane α-helices and two amphipathic helices are depicted as rods. TM1 is relatively short and located at residues 35-48, whereas TM2 and TM3 are located at residues 52-68 and 96-117 respectively. The two cytoplasmic domains are located at residues 1-34 and 69-95. Red circles indicate the residues in DGK that tolerate no substitution.

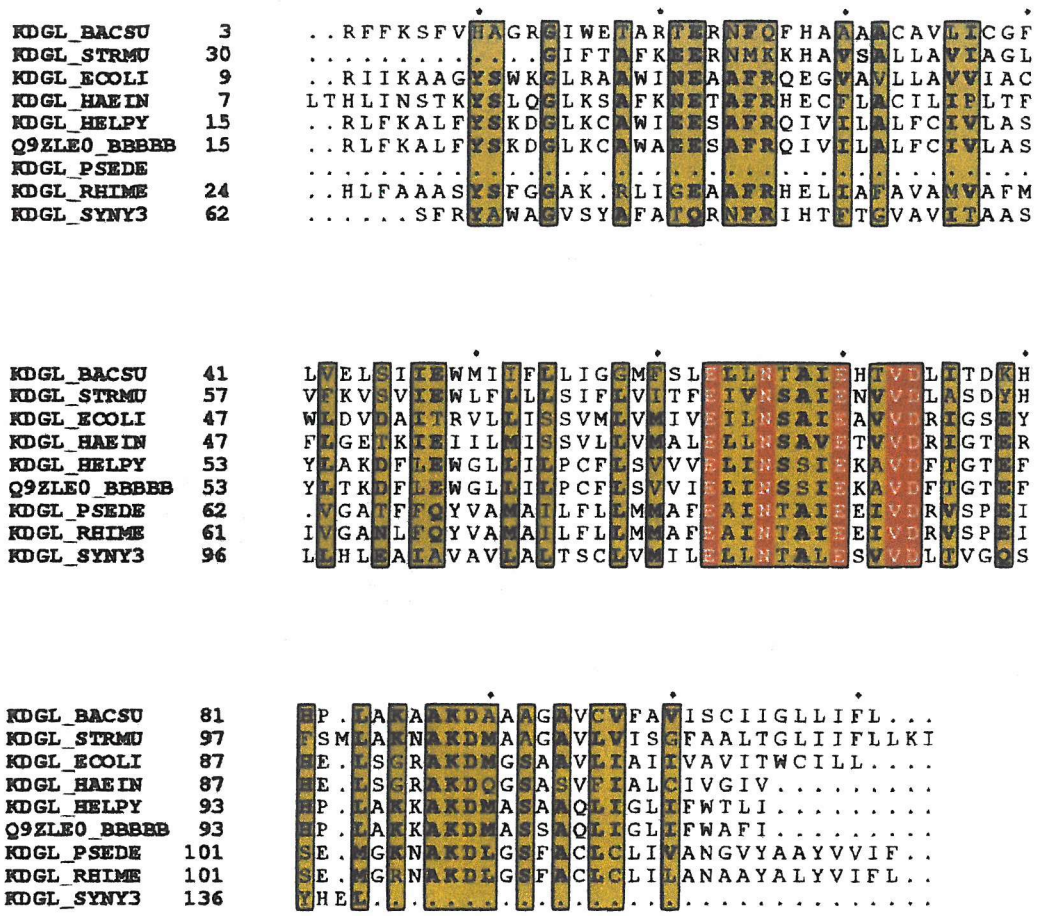

Figure 1.14 Sequence data of the diacylglycerol kinases

The figure shows the sequence comparison of the family of bacterial diacylglycerol kinases, as taken from the SWISS-PROT database. There is little sequence homology between the bacterial diacylglycerol kinases. The names to the left hand side refer to the SWISS-PROT entry name for the sequences. For example, KDGL_BACSU refers to the diacylglycerol kinase from *Bacillus subtilis*. In ascending order the others are diacylglycerol kinases from: *Streptococcus mutans* (KDGL_STRMU), *Escherichea coli* (KDGL_ECOLI), *Haemophilus influenzae* (KDGL_HAEIN), *Helicobacter pylori* (KDGL_HELPY), *Helicobacter pylori J99* (Q9ZLE0_BBBBB), *Pseudomonas denitrificans* (KDGL_PSEDE), *Rhizobium meliloti* (KDGL_RHIME), and *Synechocystis sp.* (KDGL_SYNY3).

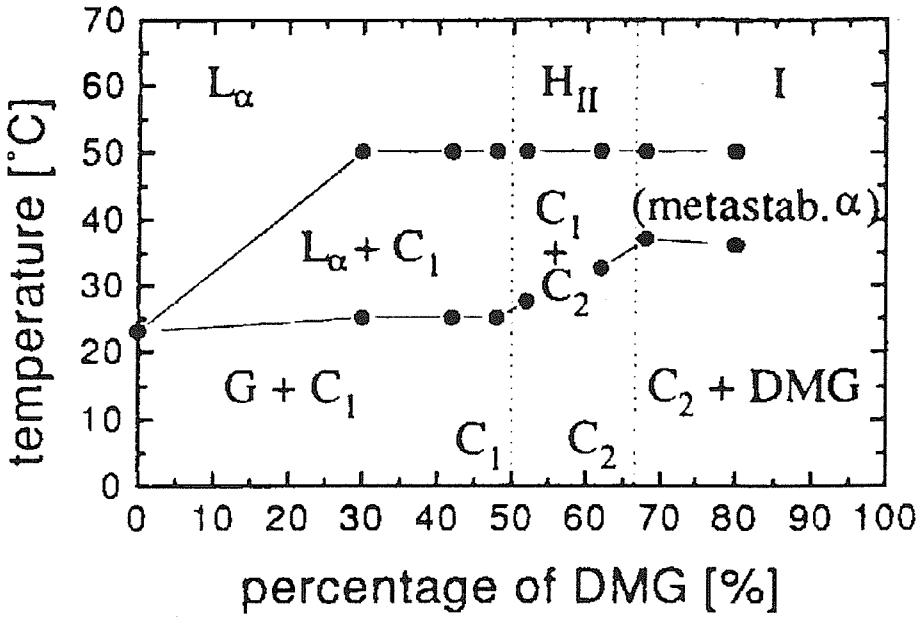

Figure 1.15 Phase diagram of hydrated mixtures of DMG and DMPC (Schorn & Marsh, 1996a)

The phase diagram is divided into three parts corresponding to the formation of stoichiometric compounds with approximate dimyristoylphosphatidylcholine (DMPC): dimyristoylglycerol (DMG) stoichiometries of 1: 1 (C_1) and 1: 2 (C_2). The three regions characterised by the stoichiometric complexes, C1 and C2, in the gel phase are: region I (0-50 mol % DMG), region II (50-67 mol % DMG), and region III (67-100 mol % DMG).

CHAPTER 2: MATERIALS AND METHODS

2.1 Materials and reagents

Materials

The following specialist materials were used:

Molecular weight markers, 1Kb DNA ladder (Gibco. BRL) & protein markers (Sigma)

Wizard^{TM} miniprep DNA purification systems (Promega)

Muslin

Nucleopore polycarbonate membranes (Costar)

Dialysis tubing, 7 kDa cutoff (Medicell)

Reagents

The following specialist reagents were used:

A23187, free acid (Calbiochem)

Agarose (Pharmacia)

Amberlite XAD-2 (BDH)

Antipyrylazo III (Fluka)

ATP, disodium salt (Boehringer Mannmeim)

Bicinchonic acid (Sigma)

Bio-Beads SM-2, mesh size 20-50 (Bio-Rad)

$C_{12}E_8$, dodecyloctaethyleneglycol monoether (Calbiochem)

Carbonyl cyanide p-(trifluoromethoxy)phenylhydrazone (FCCP)

Cardiolipin (Avanti Polar Lipids)

Coomassie Blue (Sigma)

1,2-dihexanoyl-sn-glycerol (Sigma)

1,2-dioleoyl-sn-glycerol (Lipid Products)

Dimethyl Sulfoxide (DMSO)

Dodecylmaltoside (Calbiochem)

Lacatate dehydrogenase (Boehringer Mannheim)

β-mercaptoethanol (Sigma)

NADH (Boehringer Mannheim)

Ni-NTA-agarose resin (Qiagen)

Octylglucoside (Sigma)

PEP, tricyclohexylammonium salt (Boehringer Mannheim)

Phenylmethylsulphonylfluoride (Sigma)

Phosphatidic acid (Avanti Polar Lipids)

Phosphatidylcholines (Avanti Polar Lipids)

Phosphatidylethanolamine (Avanti Polar Lipids)

Phosphatidylinositol (Avanti Polar Lipids)

Phosphatidylinositol-4-monophosphate (Avanti Polar Lipids)

Phosphatidylserine (Avanti Polar Lipids)

Pipes (Sigma)

Pyruvate Kinase (Sigma)

Restriction endonucleases (New England Biolabs)

Sagatal^{TM} (May and Baker)

All other reagents were of analytical grade and obtained from Sigma unless stated otherwise.

2.2 Methods

2.2.1 Introduction to molecular biology

Plasmids psD004 and psD005, containing a synthetic gene that codes for the DGK enzyme, were constructed as described by James U. Bowie and kindly supplied to us. These synthetic gene plasmids are derivatives of pTrcHisB (Invitrogen); the genes are expressed under the control of the isopropyl-β-D-thiogalactosidase (IPTG) inducible promoter Ptrc. A polyhistidine tag used in purification was incorporated into both proteins. While the sequence encoded by psD005 is identical to the natural *E. coli* sequence, the sequence encoded by psD004 differs at two positions. The psD004 synthetic gene encodes an Arg at position 117 instead of a Trp and a Thr at position 118 rather than a Ser. Both enzymes encoded by the synthetic genes are active. All experiments were performed using the protein encoded by the plasmid psD005.

2.2.2 DNA Preparation

2.2.2.1 Promega Wizard™ miniprep of plasmid DNA

The materials and reagents used in this preparation are listed in the Promega Wizard™ miniprep of plasmid DNA handbook and Table 2.1. A single colony was transferred into 10 ml LB medium containing the antibiotic ampicillin and incubated overnight at 37 °C with shaking. The culture was then spun to collect the cells, which were resuspended in 300 µl resuspension buffer. The resuspended cells were transferred to a 1.5 ml microcentrifuge tube, where they were mixed by inversion with

300 µl cell lysis buffer until the suspension became clear. 300 µl of neutralising buffer were added followed by inversion mixing. The sample was spun at 13 000 g for 3 minutes, the supernatant was transferred to a fresh tube and spun for a further 3 minutes. The cleared supernatant was transferred to two microcentrifuge tubes; 500 µl of DNA purification resin was added to each one, mixed and left for 5 minutes at room temperature. The resin/DNA mix was transferred from both tubes into a 5 ml syringe barrel connected to a vacuum manifold via a minicolumn. The resin/DNA mix was then drawn into the minicolumn by applying the vacuum. Adding 3-4 ml of column wash by breaking and reapplying the vacuum washed the resin in the minicolumn. The minicolumn was transferred to a minicentrifuge tube and spun at 13 000 g for 1 minute. Once completed, the minicolumn was placed in a fresh microcentrifuge tube ready for DNA elution. 100 µl sterile water was added, heated to 70°C and left for 1 minute at room temperature. The column was then spun at 13 000 g for 1 minute; the DNA concentration was then assessed by measuring the optical density on a spectrophotometer. The DNA solution was diluted 100 fold in water and the absorbance at 260 and 280 nm was measured. At 260 nm ~50 µg/ml of double stranded DNA has an absorbance of 1. The ratio of A_{260} / A_{280} provides an estimate of the purity of DNA. This value is ~1.8 for pure DNA.

Table 2.1 Reagents used in the Promega Wizard™ miniprep of plasmid DNA

Resuspension buffer	**Cell lysis buffer**
50 mM Tris – HCl, pH 7.5	0.2 M NaOH
10 mM EDTA	1 % SDS
100 µg/ml Rnase A	

Column wash

80 mM potassium acetate

8.3 mM Tris – HCl

40 μM EDTA

55 % ethanol (prior to use)

Neutralising buffer

1.32 M potassium acetate

pH 4.8

2.2.2.2 Restriction digests

Following production of the isolated plasmid by the DNA mini-prep, a double digest with the restriction endonucleases NCoI and HindIII was carried out; this enabled the DNA to be identified on an agarose gel. The appropriate volume (depending on DNA concentration) was placed into an Eppendorf tube containing 14 μl sterile water and 2 μl enzyme buffer 2 (10 mM Tris – HCl, 10 mM $MgCl_2$, 50 mM NaCl, 1 mM DTT, pH 7.9). The chosen enzyme buffer was one in which both the restriction endonucleases had an optimum activity. An equal amount (10 units) of the restriction enzyme solutions NcoI and Hind III were added to the Eppendorf tube, the sample was mixed, spun for 5 seconds and incubated for 1 hour at 37 °C.

2.2.2.3 Agarose gel analysis

Agarose gels (10% concentration) were run in 1 x Tris acetate EDTA (TAE) buffer (diluted from a 50 X stock) containing ethidium bromide of a final concentration 0.6 μg/ml. The DNA samples were mixed with gel loading buffer (GLB) in the ratio of 1:4, GLB: DNA, and run alongside a 1Kb DNA ladder (Gibco. BRL) at 100 volts until the expected bands were produced.

Table 2.2 Reagents used in agarose gel analysis

50 x TAE	**Gel loading buffer**
242 g Tris	3 ml glycerol
57.1 ml glacial acetic acid	30 mg bromophend blue
1.9 g NaEDTA	1 ml 10 x TE buffer
Sterile water to 1 L	Sterile water up to 10 ml
pH to 8.0	
Stock ethidium bromide	**Agarose NA**
100 mg ethidium bromide	100 g from Pharmacia
10 ml sterile water	

2.2.3 Diacylglycerol Kinase (DGK)

2.2.3.1 Purification of DGK

Tagged DGK was overproduced in *E. coli* strain WH1061 harbouring the inducible plasmid psD005. Plasmids were harvested according to the method of Maniatis et al. (1989). A single colony was transferred into 50 ml LB media containing 100 μg/ml ampicillin and incubated at 37 °C with shaking to prepare an overnight culture. 500 ml of the same media were inoculated with this culture and incubated at 37 °C until the absorbance at 600 nm reached 1.0 in a 1 cm cuvette. Expression of DGK was then induced by the addition of isopropyl thiogalactoside (IPTG) to a final concentration of 200 μg/ml. Following incubation for an additional 4 hours, the cells were harvested by centrifugation and stored at –20 °C until required.

All purification steps were carried out at 4 °C. In a standard purification approximately 6 g of wet cells were resuspended in 60 ml of buffer A (50 mM sodium phosphate / 0.3 M NaCl at pH 7.5) containing 1 mM phenylmethylsulphonylfluoride (PMSF). Octylglucopyranoside(OG) was added to a final concentration of 3 % (w/v) and the suspension was stirred gently for 2 hours to solubilise DGK. The suspension was centrifuged at 15,000 rpm in a Sorvall SS-34 rotor for 30 minutes to remove any insoluble material and the supernatant was mixed with 6 ml (bed volume) Ni-NTA-agarose (Qiagen) resin and agitated gently for 2 hours. The resin had been previously equilibrated in buffer A. Resin with bound protein was pelleted by centrifugation at 5,000 rpm for 5 minutes in a bench centrifuge, then resuspended in 60 ml of buffer A containing 1.5% OG and 0.03 M imidazole (the imidazole was added from a 2 M stock solution adjusted to pH 8.0). The resin/protein complex was collected again by centrifugation, resuspended in 2ml of buffer A containing 1.5% OG and 0.03M imidazole (buffer B) before being packed into a small column. The column was washed with buffer B until the absorbance of the effluent at 280 nm dropped below 0.1. The detergent was changed to dodecylmaltoside (DM) by washing the column with approximately five column volume washes of buffer A containing 0.5 % DM without any imidazole (buffer C). The affinity of the protein for the Ni-NTA resin is reduced in DM, so elution can take place in a low imidazole concentration (Lau & Bowie, 1997). The protein was eluted in buffer A containing 0.5 % DM and 0.25 M imidazole (buffer D). The eluted protein was aliquoted out and stored at –70 °C after flash freezing with liquid nitrogen. Full activity was recovered upon thawing of the frozen aliquots. Approximately 30-40 mg of purified protein was obtained from 6 g of wet cells paste (about 2 L of culture).

2.2.3.2 Determination of protein concentration by absorbance (at 280nm)

Protein concentration was estimated by absorbance at 280nm, using an extinction coefficient of 25 200 M^{-1} cm^{-1} for DGK. This figure was calculated from the number of tryptophan and tyrosine residues according to the method described by Copeland (1994).

2.2.3.3 Determination of protein concentration by the Bicinchoninic Acid Assay

Protein concentration was measured exactly by the bicinchoninic acid assay (BCA), as described by Smith et al. (1985). Serial dilutions of BSA were used to obtain a protein standard curve. The protein concentration was determined from this by adding one part of the sample to 20 parts of BCA assay reagent (50:1 BCA: 4% (w/v) $CuSO_4$) and incubating at 37 °C for 30 minutes. Following incubation, the absorbance of 562 nm was measured on a Dynatech MR5000 plate reader.

2.2.3.4 SDS polyacrylamide gel electrophoresis

SDS polyacrylamide gel electrophoresis was carried out according to the method of Laemmli (1970) using 12% acrylamide separating gels. The compositions of the solutions and gel preparation are given in Table 2.3. Gels were set and run on a BioRad mini-gel system. Electrophoresis was carried out at a constant current of 20 mAmps. Bromophenol blue was used as a dye front marker. Coomasie blue was used to stain the gels followed by destaining in destain solution. Once the protein bands were readily visible, the gels were scanned using a Joyce-Loebl gel scanner. Resolving gels were produced by the relative dilutions of acrylamide solution and Tris

buffer (pH 8.8) to give final concentrations of 12 % w/v acrylamide, 0.375 M Tris and 0.1 % w/v SDS. To begin polymerisation 0.3 ml of 10 % ammonium persulphate and 5 µl TEMED were added to 10 ml of the above mixture. Stacking gels were produced with final concentrations of 4.5 % acrylamide, 0.125 M Tris (pH 6.8) and 0.1 % SDS. The additions of APD and TEMED were as for resolving gels.

Table 2.3 Solutions and reagents used in SDS-PAGE

30 % (w/v) acrylamide / 0.27 % (w/v) bisacrylamide

10 % sodium dodecyl sulphate (SDS)

2.25 M Tris-HCl pH 8.8

0.5 M Tris-HCl pH 6.8

10 % ammonium persulphate

Loading buffer

62.5 mM Tris-HCl pH 6.8

10 % (w/v) glycerol

2 % (w/v) SDS

1 % (w/v) β-mercaptoethanol

0.04 % (w/v) bromophenol blue

Coomassie Blue stain

1.25 g Coomassie Brilliant Blue

227 ml methanol

46 ml glacial acetic acid

227 ml analar water

Running buffer

0.025 M Tris

0.192 M glycine

0.1 % (w/v) SDS

Destain

200 ml methanol

625 ml water

75 ml glacial acetic acid

2.2.4 Sarcoplasmic reticulum (SR) and the Ca^{2+}-ATPase

2.2.4.1 Preparation of SR

Sarcoplasmic reticulum was prepared as described by East & Lee (1982) from rabbit fast-twitch skeletal muscle. All steps were performed at 4 °C. A female New Zealand White rabbit was given a lethal injection of Sagatal anaesthetic (5 ml pentabarbitone, 60 mg/ml) and drained of blood from the carotid artery. The fast-twitch skeletal muscle from the back and hind legs was removed and finely chopped before being homogenised (Waring blender, full speed) for approximately 30 seconds in 500 ml buffer 1 (Table 2.4). The homogenate was centrifuged at 8,300 g for 35 minutes in a Sorvall RC3B centrifuge. The supernatant was filtered through a single layer of muslin, and centrifuged at 12,000 g for 30 minutes to remove the mitochondrial fraction; the supernatant was then centrifuged at 53,000 g for 40 minutes. The resulting supernatant was discarded and the pellets were resuspended by homogenisation in buffer 2 (Table 2.4); the homogenate was left to stir gently for 40 minutes to allow the actinomyosin contractile proteins to precipitate, before centrifugation at 125,000 g for 45 minutes. The supernatant was discarded and the pellet resuspended in a minimal volume of Buffer 3. The SR vesicles obtained were stored on ice and the protein concentration determined before being aliquoted, snap frozen in liquid nitrogen, and stored at –70 °C.

2.2.4.2 Preparation of Ca^{2+}-ATPase

Ca^{2+}-ATPase was prepared from freshly prepared SR by solubilising SR in buffer C (Table 2.4) containing potassium cholate at a ratio of 1 mg protein to 0.4 mg

cholate. The solubilised SR was quickly loaded onto a discontinuous sucrose gradient consisting of 3 ml of 60 %, 19 ml of 30 %, and 13.5 ml of 20 % sucrose (w/v) in buffer D (Table 2.4). The gradients were spun overnight at 95,000 g in a swing out rotor. The purified Ca^{2+}-ATPase band at the 30-60 % interface was collected, resuspended in buffer D and then centrifuged at 37,000 g for 1 hr. The supernatant was discarded and the pellet resuspended in a small volume (1-2 ml) of buffer C; the sample was then dialysed for 3.5 hr in 1 litre of buffer C containing 10 g of washed amberlite resin to remove the cholate. The pure Ca^{2+}-ATPase was aliquoted, snap frozen in liquid nitrogen and stored at –70 °C

Table 2.4 Buffers used in the purification of SR and Ca^{2+}-ATPase

Buffer 1	**Buffer 2**	**Buffer 3**
0.1 M NaCl	0.6 M KCl	0.1 M sucrose
10 mM MOPS	5 mM Tris	30 mM MOPS
pH 7	pH 6.5	pH 7

Buffer C	**Buffer D**
0.25 M sucrose	50 mM K_2HPO_4
1 M KCl / 50 mM K_2HPO_4	1 M KCl
pH 8.0	pH 8.0

2.2.4.3 Measurement of Ca^{2+}-ATPase protein concentration

Protein concentration was measured according to the method of Hardwicke & Green (1974). Dilutions of SR or Ca^{2+}-ATPase protein solutions were made in 1 %

SDS, and the absorption spectrum of each sample was recorded from 340-260 nm. The absorption at 280 nm was used to calculate the protein concentration, assuming the optical density of 1 mg/ml solution of SR and Ca^{2+}-ATPase to be 1.0 and 1.2 respectively.

2.2.4.4 Measurement of Ca^{2+}-ATPase activity

The steady state activity of the SR Ca^{2+}-ATPase was measured using a coupled enzyme assay (Froud et al., 1986a). The assay links the hydrolysis of ATP by the Ca^{2+}-ATPase to the oxidation of NADH by pyruvate kinase (PK) and lactate dehydrogenase (LDH). Phosphoenolpyruvate (PEP) serves as a phosphate donor, leading to the regeneration of ATP (Figure 2.1). Each assay was initiated by the addition of an aliquot of 25 mM $CaCl_2$ to a pre-equilibrated mixture of 40 mM Hepes/KOH, pH 7.2, 100 mM KCl, 5.1 mM $MgSO_4$, 1.01 mM EGTA, 2.1 mM ATP, 0.53 mM PEP, 0.15 mM NADH, 7.5 IU pyruvate kinase, 18 IU lactate dehydrogenase, and 10 μg SR or Ca^{2+}-ATPase in a final volume of 2.5 ml at 25°C. The oxidation of NADH was monitored by the decrease in absorbance at 340 nm, and related to the Ca^{2+}-ATPase activity by the following equation:

$$\text{Activity (IU/mg)} = (\Delta OD_{340}\ min^{-1}.\ vol) / (Ca^{2+}\text{-ATPase}.\ \varepsilon_{340})$$

$\Delta OD_{340}\ min^{-1}$ = change in optical density at 340 nm per min

vol = volume in cuvette (ml)

Ca^{2+}-ATPase = amount of Ca^{2+}-ATPase (or SR) protein in cuvette (mg)

ε_{340} = extinction coefficient of NADH at 340 nm ($M^{-1}\ cm^{-1}$)

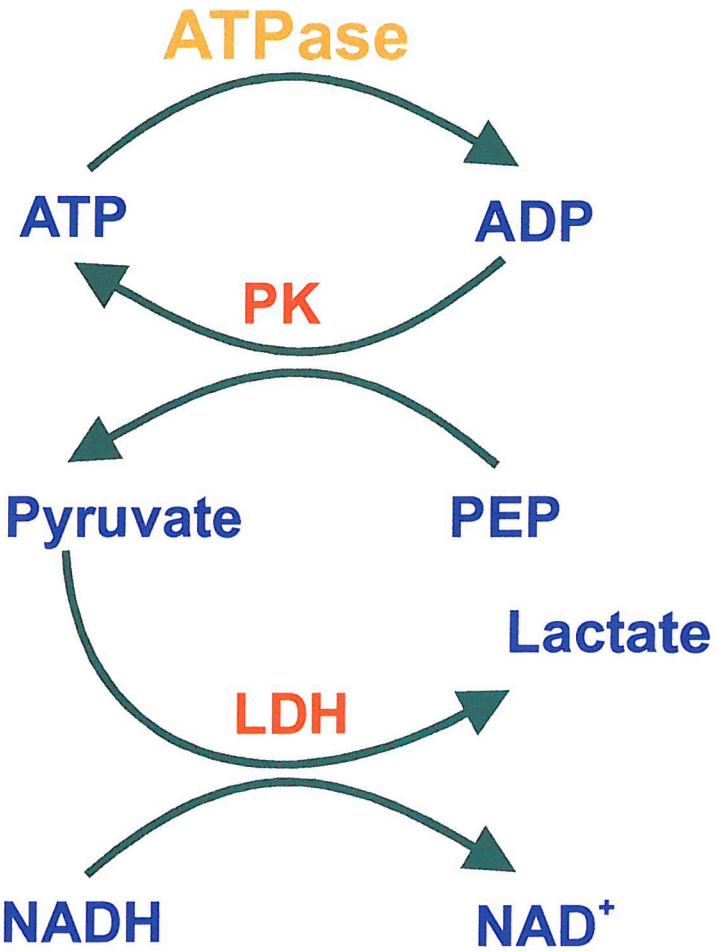

Figure 2.1 Reaction scheme of the coupled enzyme assay

Reaction scheme of the coupled enzyme assay linking the hydrolysis of ATP by the Ca^{2+}-ATPase to the oxidation of NADH by the coupling enzymes pyruvate kinase (PK) and lactate dehydrogenase (LDH).

CHAPTER 3: THE EFFECTS OF ANIONIC PHOSPHOLIPIDS ON THE FUNCTION OF THE Ca^{2+}-ATPase OF SARCOPLASMIC RETICULUM

3.1 Introduction

3.1.1 Reconstitution

It is difficult to establish the lipid requirements for a properly functioning membrane from studies of intact biological membranes because of the shear complexity of the composition of such membranes. Reconstitution enables us to remove a particular protein from its native membrane and place it in a membrane of defined lipid composition to study its properties. For efficient reconstitution, the protein must be removed from its native membrane with minimal disruption. The detergent must not denature the protein in any way, as its characteristics will be changed and it may not reconstitute. This is why each protein has a unique purification and reconstitution procedure.

3.1.2 Lipid vesicles

Vesicles are often used as model membrane systems in reconstitution studies. A vesicle is a membrane of lipid molecules in the form of a bilayer enclosing an aqueous volume. Vesicles are characterized by size and the number of lipid bilayers they contain. There are three types of vesicles that can be formed depending upon the method of preparation (Figure 3.1). Small unilamellar vesicles (SUV) only contain one lipid bilayer

and range in diameter from 20 to 50 nm. Large unilamellar vesicles (LUV) also contain one lipid bilayer but they are much larger, their diameters ranging from 50 to 10,000 nm. Multilamellar vesicles (MLV) are composed of many concentric lamellae and can be very large, their diameters can be anything up to 10,000 nm. MLV are spontaneously formed when water is added to a dried film of lipid and the system is shaken, at a temperature above the gel to liquid-crystalline phase transition temperature. Using ultrasonic radiation to break up suspensions of MLV can form SUV. Sonication can be performed using either a probe or bath sonicator depending upon the concentration of the lipid; a bath sonicator is more suitable for large volumes of dilute lipids.

Ethanol injection, ether injection and reverse-phase evaporation are other methods used for the preparation of vesicles. Ethanol injection involves the solubilisation of lipids in ethanol followed by injection into a buffer solution where they spontaneously form LUVs (Szoka & Papahadjopoulos, 1980). Ether injection involves dissolving lipids in diethylether and injecting the mixture into an aqueous solution at a temperature at which the ether is vapourised. As the solvent is removed LUV are formed (Szoka & Papahadjopoulos, 1980). Reverse-phase evaporation involves mixing lipids that are dissolved in organic solvent with an aqueous phase followed by sonicating the mixture to produce small water droplets stabilized by a lipid monolayer. The organic phase is removed by evaporation causing the droplets to collapse into a viscous gel-like state, resulting in some droplets disintegrating and releasing their contents. The excess lipid is used to complete the bilayers of other droplets thereby forming LUVs, although some vesicles are produced that contain a few bilayers they are not MLVs (Szoka & Papahadjopoulos, 1978).

All of these methods usually produce vesicles of different sizes. However, vesicles can be sized by extruding them through polycarbonate filters. Extrusion can also be used directly to obtain unilamellar vesicles from MLV, the advantage being that no solvent or detergent is required. Additionally, these vesicles are quick and easy to prepare and a population of vesicles with homogenous size and structure is produced (Hope et al., 1985; MacDonald et al., 1991). Vesicle size once extruded through polycarbonate filters depends upon the pore size of the filter and the lipid composition of the original vesicles. When extruded through a 100 nm pore polycarbonate filter egg PC produced vesicles with an average diameter of 75 nm over a range from 30 to 150 nm, whilst PA produced vesicles with an average diameter of 100 nm over a range from 60 to 220 nm (MacDonald et al., 1991).

3.1.3 Detergents

Detergents are used to solubilise lipid bilayers. Detergents are amphiphilic molecules consisting of a hydrophobic part, usually one or two alkyl chains, and a hydrophilic polar headgroup (Figure 3.2). At a certain concentration detergent molecules aggregate to form micelles; this is known as the critical micelle concentration (CMC) (Lichtenberg et al., 1983). Below the CMC value the detergent is present in monomeric form only in aqueous medium; above the CMC all the additional detergent forms micelles. A micelle has a hydrophobic core and a polar surface, and is normally spherical or disk-shaped. The aggregation number refers to the number of detergent molecules per micelle and varies from 10 to over 100. The CMC value of a detergent is determined by

the chemistry of the detergent and the composition and temperature of the solvent. The more hydrophobic the detergent the greater its tendency to form micelles and the lower the CMC, thus the CMC of a detergent is partially determined by the hydrophobic-hydrophilic balance. In addition, short chain length phospholipids can also function as detergents as they have reasonable CMC values such as 14.6 mM for di(C6:0)PC. The CMC decreases with increasing chain length and this is why longer chain phospholipids will never be seen in the monomer form. Above the CMC the predominant structure adopted by the short-chain phospholipids is the micelle and for the longer chain phospholipids is the lamellar form (Lichtenberg et al., 1983). The CMC of a detergent gives an indication of its ability to penetrate the bilayer. A detergent with a low CMC will be more hydrophobic and therefore have a greater tendency to penetrate the bilayer at low concentration.

3.1.4 Solubilisation of phospholipid vesicles

Solubilisation involves the transformation of lamellar phospholipid structures into mixed micelles composed of phospholipid and detergent. The solubilisation process is proposed to occur in three stages involving the interaction of detergents with lipid bilayers and depends upon the nature and concentration of the detergent present (Lichtenberg et al., 1983; Rigaud et al., 1995). Stage 1 begins with little detergent and whole vesicles. As the total detergent concentration is raised both the concentration of monomeric detergent in the aqueous phase and the mole fraction of detergent in the bilayer is increased. At these sub-solubilising detergent concentrations there is an

increase in membrane permeability, which is indicative of structural perturbations. This stage ends when the bilayer becomes saturated with detergent, and the concentration of detergent monomers in the aqueous phase is approximately equal to the CMC. Stage 2 involves a structural transition in which the saturated lipid bilayers in the form of vesicles become phospholipid–detergent micelles. In this stage both the structures exist and as the total detergent concentration is raised the phospholipid-detergent micelle structure becomes predominant. Stage 3 signals that the bilayer is completely solubilised into mixed micelles. The further addition of detergent results in an increase in the mole fraction of detergent in the mixed micelles and a reduction in their size. The concentration of free detergent in aqueous media has to be at or above the CMC for solubilisation to occur (Lichtenberg et al., 1983; Rigaud et al., 1995). By observing the optical density of the system we can assess the stage of the solubilisation process. The turbidity of the system in stage 1 yields a high optical density that is only marginally affected by detergent. The turbidity of the system decreases in stage 2 as more detergent is added and the vesicles are gradually solubilised. The system becomes optically transparent in stage 3, as all the phospholipid is solubilised. The optical density test is generally applicable although ideal behaviour is not always observed for all detergents (Patternostre et al., 1988).

3.1.5 Solubilisation of biological membranes

The addition of detergent to biological membranes results in the membrane becoming permeable and the contents of the cell leaking out. The membrane will

eventually lyse and mixed micelles will form consisting of detergent and lipid or detergent, lipid and protein. In the mixed micelle the hydrophobic part of the protein that is normally located within the membrane is covered by either or both the hydrophobic part of the detergent and lipid molecules present in the micelle. As the detergent concentration is further increased lipid will be removed from the mixed micelles to leave detergent-protein micelles and detergent-lipid micelles. The degree to which lipid is removed is dependent upon the relative affinities of the lipid and detergent for the protein.

3.1.6 Reconstitution of membrane proteins into vesicles

There are many methods used for the reconstitution of membrane proteins into vesicles, the most successful methods involving the use of detergents. Of the methods that use organic solvents only reverse phase has proved suitable and then only for very hydrophobic proteins (Rigaud et al., 1983). In general, organic solvents denature the majority of membrane proteins. The sonication of lipids and proteins in a mixed suspension has been investigated but protein inactivation is seen in many cases due to the long sonication times. Additionally, the vesicles produced tend to be relatively small, which is a problem if the protein being reconstituted is a transporter of some kind as the transported substance could quickly build up to inhibitory levels inside the small vesicle. The freeze-thaw technique where protein is added to sonicated vesicles before the rapid freezing step has been used successfully for some proteins (Kasahara & Hinkle, 1977). The downside of this procedure is of possible alterations to protein structure during the

freeze-thaw steps. Under certain conditions direct incorporation of proteins into preformed vesicles is possible (Jain & Zakim, 1987). The conditions include the vesicles being SUVs and containing some sort of impurity like cholesterol. This process involves two-stages, firstly the proteins are incorporated into a small number of vesicles followed by fusion of the protein containing vesicles with the remaining vesicles. This produces vesicles with a wide size range and a heterogenous population of vesicles.

As stated before the most successful methods involve the use of detergents. The principle is that the lipids and proteins are solubilised together forming mixed micelles, before the detergent is removed resulting in the formation of bilayer vesicles containing the proteins inserted in the bilayer in the native conformation. The choice of detergent is critical as it must both solubilise the protein without denaturing it and be easily removed. The method for removal of detergent depends on the particular properties of the detergent used. Detergents with high CMC's are easily removed by dialysis and are also suitable for gel-filtration techniques where the smaller detergent micelles formed by these detergents are retained in the column as the vesicles containing protein elute first. However, detergents with low CMC's are better removed by absorption using hydrophobic resins (Rigaud et al., 1988). Triton X-100 is a detergent with a low CMC and is effectively removed with no loss of protein activity by Bio-Beads SM-2 (Holloway, 1973). In addition, Bio-Beads absorb low amounts of phospholipids ensuring that, if a high enough concentration of lipid is used, an insignificant level of phospholipid is lost and can be ignored in any calculations. The rate of Triton X-100 removal was dependent on the Bio-Bead to detergent ratio and the availability of free bead surface (Levy et al., 1990b). Bio-Beads are thought to absorb both the monomer and micellar

forms of the detergent. Resins can be used for a variety of different detergents and not just those with low CMC's, producing a great variety of vesicles depending on the precise conditions and components of the reconstitution system in question.

Detergent removal from detergent-lipid micelles is thought to be the reverse of solubilisation (Levy et al., 1990c). At high detergent concentrations only mixed micelles are present, when the level of detergent decreases vesicles begin to form and their numbers increase at the expense of mixed micelles; eventually the detergent drops to a level where only vesicles exist. Ideally all the detergent would be removed, but in reality a few detergent molecules will remain in the system. However, the presence of protein in the mixed micelle complicates matters as the rate of detergent removal from the lipid-detergent and lipid-detergent-protein micelles plays an important role in the efficiency of the reconstitution of the protein and the size of the vesicle. Rapid removal of detergent results in the formation of SUV whilst slow detergent removal yields LUV (Levy et al., 1990b).

There are two mechanisms for the removal of detergent. The first method involves both types of micelles, lipid-detergent and lipid-protein-detergent, being disrupted simultaneously, their contents mix and they form homogenous vesicles as the detergent is further removed. The second method involves protein-rich structures forming by the initial reduction of detergent, followed by the formation of detergent saturated vesicles from the lipid-detergent micelles as the detergent concentration is further decreased. Further detergent removal leads to the insertion of proteins into the preformed detergent saturated vesicles (Rigaud et al., 1995). The mechanism used depends upon the protein to be reconstituted and its propensity for self-aggregation, in addition to the

detergent used and its rate of removal. The Ca^{2+}-ATPase is a membrane protein with a propensity to self-aggregate and fast removal of detergent is thought to proceed via mechanism 1 whilst slow detergent removal proceeds via mechanism 2. The type of detergent used in slow detergent removal with this type of protein results in different populations of vesicles forming. Some detergents, such as Triton X-100 and $C_{12}E_8$, appear unable to transfer the protein from the protein-rich structures to the preformed detergent saturated vesicles either totally or partially, whilst others, such as OG have no problems and produce homogenous vesicles (Levy et al., 1992; Rigaud et al., 1995). When reconstituting with cholate the rate of detergent removal is unimportant, as mechanism 1 is always followed. Membrane proteins that do not aggregate easily follow mechanism 1 independent of the rate of detergent removal. The orientation of the protein within the membrane of the vesicle is also important. In the biological membrane, protein orientation is asymmetric, whereas reconstituted proteins can insert into the bilayer in a symmetrical manner. This can give the appearance that only a proportion of the protein is active as only the 'correctly' orientated proteins can show activity. Symmetrical orientation of proteins results from methods involving simultaneous incorporation of protein and vesicle formation. Asymmetric protein orientation can be obtained if the protein is incorporated into preformed vesicles (Eytan, 1982). It is thought that the most hydrophobic portion of the protein inserts first into the bilayer (Rigaud et al., 1988).

3.1.7 Reconstitution of the Ca^{2+}-ATPase

The Ca^{2+}-ATPase has been reconstituted into sealed vesicles using a number of different techniques. The first reconstitution of the Ca^{2+}-ATPase into sealed vesicles able

to accumulate Ca^{2+} was performed by Racker (1972) and used the cholate dialysis method. This method involved mixing excess soybean phospholipids and purified Ca^{2+}-ATPase in the detergent cholate, followed by dialysis to remove the cholate and form sealed vesicles containing the Ca^{2+}-ATPase. A variation of this method again involved mixing the Ca^{2+}-ATPase with excess lipid in cholate or deoxycholate, but detergent removal was performed by the passage through a column of Sephadex G-50 (Gould et al., 1987a). Using either procedure Ca^{2+} accumulation was only possible in the presence of oxalate or phosphate ions that are trapped in the lumen of the vesicles where they precipitate the Ca^{2+} pumped into the lumen by the Ca^{2+}-ATPase and thus reduce the free Ca^{2+} concentration in the lumen. This suggests that the vesicles produced are leaky to Ca^{2+}. The addition of the ionophore FCCP had no effect on the rate of Ca^{2+} transport, whilst the addition of the ionophore valinomycin led to a slight stimulation. This suggests that no pH gradient was established during transport but that a small membrane potential was present opposing further transport of Ca^{2+} into the vesicles (Racker, 1972).

The effect of varying the lipid composition of the vesicles has led to the publication of contrasting results. Initial reconstitution studies with purified soy phospholipids showed that Ca^{2+} transport was not possible by vesicles containing PC alone, whilst vesicles composed entirely of PE supported a significant amount of Ca^{2+} transport; vesicles containing a mixture of PC and PE in the ratio of 1:4 were able to transport slightly more Ca^{2+} than vesicles containing purely PE (Knowles & Racker, 1975; Knowles et al., 1976). Further studies using more defined phospholipids showed very low levels of Ca^{2+} accumulation with vesicles composed entirely of di(C18:1)PC , however, a large initial rate of Ca^{2+} transport for vesicles composed entirely of

di(C18:1)PE was observed, which decreased with time (Navarro et al., 1984). In addition, vesicles composed of high levels di(C18:1)PE and a little di(C18:1)PC once again exhibited high and stable levels of Ca^{2+} accumulation. In contrast to the previous studies, Andersen et al. (1983) and Heegaard et al. (1990) have shown that significant levels of Ca^{2+} accumulation are attainable using vesicles composed entirely of di(C18:1)PC and egg PC. In conclusion, it is evident that vesicles composed of mixtures of PC and PE containing up to 80-mol % PE show higher levels of Ca^{2+} accumulation than those composed of entirely PC (Gould et al., 1987a). The effects of PE on Ca^{2+} accumulation have been suggested to follow from its ability to adopt a hexagonal H_{II} phase (Navarro et al., 1984), resulting in a reduction on the rate of leak of Ca^{2+} from the vesicles (Gould et al., 1987b).

The Ca^{2+}-ATPase has been reconstituted using the freeze thaw sonication technique in which preformed sonicated lipid vesicles are mixed with protein and rapidly frozen in liquid nitrogen (Zimniak & Racker, 1978). Upon thawing, large liposomes are formed that can be broken up by a short sonication to produce unilamellar liposomes. Using this technique the Ca^{2+}-ATPase has been reconstituted into vesicles composed of entirely egg PC and soy PE and both preparations were able to accumulate Ca^{2+}. Other studies using this technique have shown that it is possible to produce vesicles capable of accumulating Ca^{2+} using PCs varying in fatty acyl chain length, soybean phospholipids and mixtures of PC and PS (Caffrey & Feignson, 1981; Ueno & Sekine, 1986; Szymanska, 1991). Both the levels of Ca^{2+} accumulation and the rates of Ca^{2+} transport were comparable to those of vesicles produced by the dialysis method. Oxalate or phosphate was included in the reconstitution medium to act as a Ca^{2+} precipitating agent

inside the vesicle; low levels of Ca^{2+} accumulation were seen in their absence (Ueno & Sekine, 1986).

Vesicles produced by the freeze thaw sonication method are heterogenous (Navarro & Essig, 1984), consisting of some vesicles rich in protein that accumulate very low levels of Ca^{2+}/mg protein due to the extremely low lumenal volume available to each Ca^{2+} pump and other vesicles containing only a few protein molecules that are able to accumulate high levels of Ca^{2+}/mg protein due to the high lumenal volume available to each Ca^{2+} pump. Vesicles composed of PC and PS show increased Ca^{2+} transport rates when compared to vesicles composed solely of PC (Szymanska et al., 1991). Compared to vesicles composed of entirely PC, vesicles composed of equal amounts of PC and PS exhibited the greatest Ca^{2+} transport rates whereas vesicles composed of 90% or more PS transported Ca^{2+} at a greatly reduced rate, with vesicles composed of entirely PS accumulating tiny amounts of Ca^{2+} (Warren et al., 1974a). This suggests that the freeze thaw sonication procedure is inefficient and that this inefficiency is responsible for the differences in Ca^{2+} accumulation levels observed with different lipids.

Reconstitution of the Ca^{2+}-ATPase by mixing solubilised protein and lipid and then removing the detergent with Bio-Beads produces vesicles with the highest reported levels of Ca^{2+} accumulation without Ca^{2+} precipitating anions in the lumen and vesicles with a very low rate of Ca^{2+} leak (Levy et al., 1990a). The procedure developed by Levy et al. (1990a) involves solubilising the Ca^{2+}-ATPase in the detergent $C_{12}E_8$ before mixing with liposomes that have been prepared by reverse phase evaporation and partially solubilised with OG. The detergent is removed by the addition of aliquots of Bio-Beads. These vesicles, which are composed of egg PC: egg PA (9:1), are able to accumulate high

levels of Ca^{2+} in the absence of any precipitating anions due to their low ionic permeability. The highest levels of Ca^{2+} accumulation were achieved in the presence of the ionophores FCCP and valinomycin. Approximately 80% of the protein inserted right side out. The internal volume of the vesicles was large compared to SR vesicles, allowing greater Ca^{2+} accumulation before inhibition by internal Ca^{2+} prevents further uptake (Levy et al., 1990a).

The effects of detergent structure on the efficiency of reconstitution by this procedure have been studied (Levy et al., 1992). The Ca^{2+}-ATPase was always solubilised in $C_{12}E_8$, but the liposomes were treated with OG, Triton X-100, $C_{12}E_8$ or cholate. Vesicles reconstituted with OG showed the greatest initial rate of Ca^{2+} transport, whilst overall Ca^{2+} accumulation decreased in the order of Triton X-100, OG, $C_{12}E_8$, cholate. In each case the decrease in Ca^{2+} accumulation was due to the decreasing size of the vesicles produced by each detergent. Reconstituting with Triton X-100 produced vesicles with a diameter of 150 nm and an internal volume of 225 µl/mg protein; OG produces vesicles with a diameter of 100 nm and an internal volume of 135 µl/mg protein, whilst cholate produces the smallest vesicles with a diameter of 60 nm and an internal volume of 68 µl/mg protein. The conditions producing the highest levels of Ca^{2+} accumulation have been defined for each detergent (Levy et al., 1992). This was achieved by varying the amount of detergent and the rate of detergent removal. For OG, maximal Ca^{2+} accumulation was obtained at the OG concentration required for the onset of solubilisation of the liposomes; the onset of solubilisation was defined by a reduction in the level of light scatter. This suggests that OG needs to destabilize the preformed lipid vesicles to allow the incorporation of the Ca^{2+}-ATPase into the bilayer. The rate at which

detergent was removed had little effect on the Ca^{2+} transport activities of vesicles reconstituted using OG. However, slow detergent removal best facilitates the incorporation of the Ca^{2+}-ATPase into partially solubilised preformed liposomes. When reconstituting vesicles using cholate, Ca^{2+} transport only occurred once the concentration of cholate was greater than that required for the onset of liposome solubilisation. This is because increasing the cholate concentration increases the number of ternary mixed micelles and therefore Ca^{2+} accumulation, as Ca^{2+}-ATPase containing vesicles are formed from ternary micelles (Levy et al., 1992). Reconstitution using cholate is independent of the rate of detergent removal. Vesicles reconstituted using Triton X-100 or $C_{12}E_8$ only transported Ca^{2+} once the concentration of detergent was greater than that required for the onset of liposome solubilisation. For both detergents the initial rate and total extent of Ca^{2+} accumulation increased with increasing detergent concentration; in both cases reconstitution is also affected by the rate of detergent removal. Both the rate and total extent of Ca^{2+} accumulation increased with increasing the rate of detergent removal when reconstituting with $C_{12}E_8$. Only the total extent of Ca^{2+} accumulation significantly increases when the rate of Triton X-100 removal is increased.

Levy et al. (1992) reported that vesicles composed of egg PC alone had a reduced rate of Ca^{2+} transport when compared to vesicles containing 10% egg PA, as in this study. Levy et al. (1992) proposed that the effect of PA could be to increase the level of protein incorporation or correct orientation into the vesicles or exert some effect on the function of the Ca^{2+}-ATPase specific to negatively charged lipids.

The aim of this chapter is to investigate the effect of anionic phospholipids on the ability of the Ca^{2+}-ATPase to accumulate Ca^{2+} into sealed vesicles.

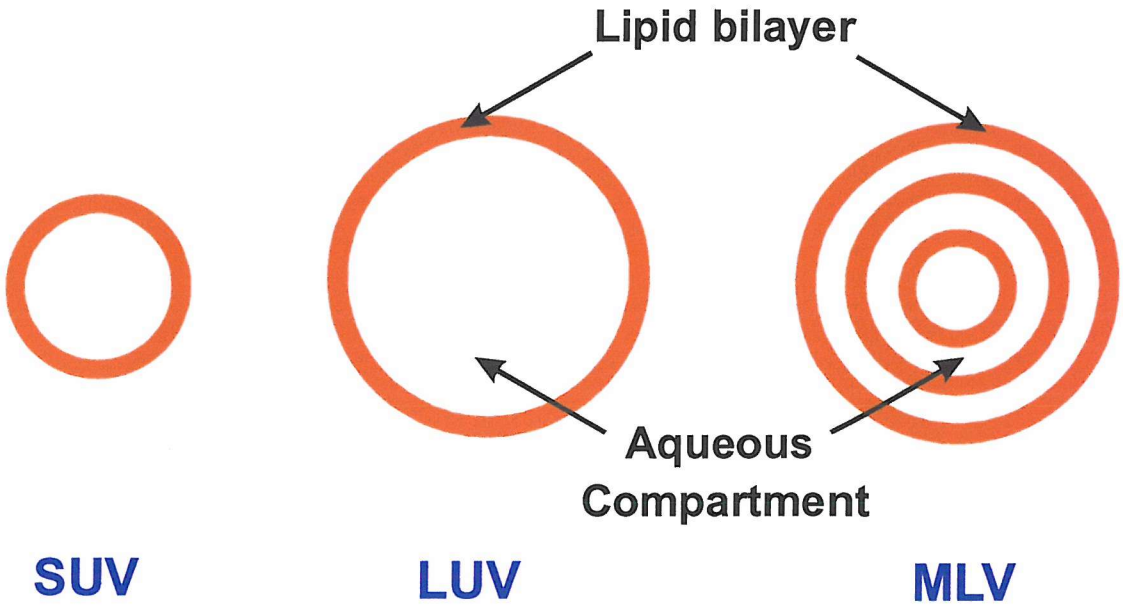

Figure 3.1 Types of lipid vesicles

Small unilamellar vesicles (SUV) contain one lipid bilayer and range in diameter from 20 to 50 nm. Large unilamellar vesicles (LUV) also contain one lipid bilayer, their diameters ranging from 50 to 10,000 nm. Multilamellar vesicles (MLV) are composed of many concentric lamellae and can be very large, with diameters anything up to 10,000 nm.

A

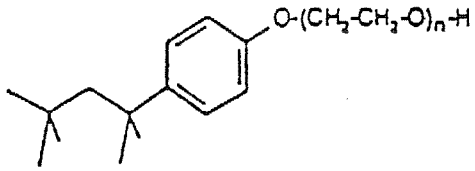

B

C

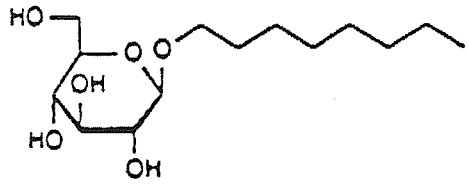

D

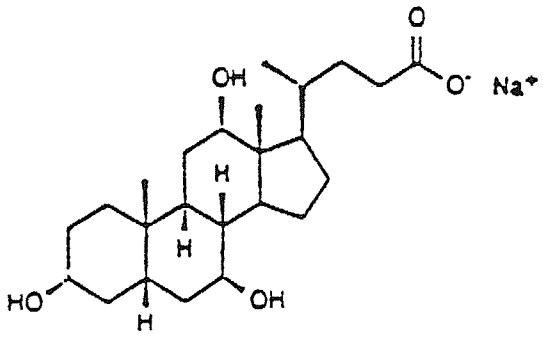

E

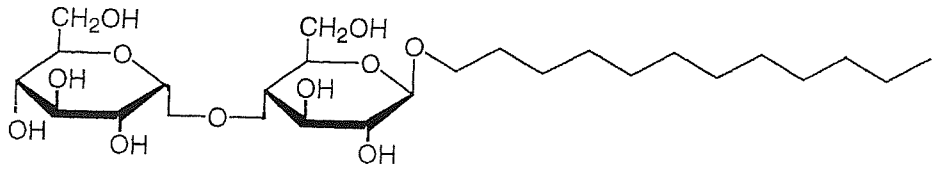

Figure 3.2 The structures of several detergents

Triton X-100 (**A**), $C_{12}E_8$ (**B**), octylglucoside (**C**), sodium cholate (**D**), dodecylmaltoside (**E**).

3.2 Methods

3.2.1 Preparation of SM_2 Bio-Beads

Washed Bio-Beads were prepared by adding 5 g of SM_2 Bio-Beads to 50 ml of methanol and stirring gently for 15 min. The Bio-beads were collected on a sintered glass funnel and washed thoroughly with methanol (100 ml). The Bio-Beads were then immediately washed with 200 ml buffer A (10 mM Pipes/100 mM K_2SO_4, pH 7.1) before being loaded into a column where they were slowly washed (2 hrs) with 400 ml of buffer A. After completion of this wash the Bio-Beads were immersed in buffer A and stored at 4°C until required.

3.2.2 Reconstitution into sealed vesicles

Reconstituted vesicles were prepared by a modification of the method described by Levy et al. (1992). The required composition of phospholipid (30 μmol) was aliquoted into a scintillation vial and placed in a vacuum dessicator for approximately 3 hrs to dry down from organic solvent. The lipid was resuspended in 1.4 ml of buffer A (10 mM Pipes/100 mM K_2SO_4, pH 7.1) to give a lipid concentration of 16 mg/ml. The vial was flushed with nitrogen, sealed with parafilm and warmed under a hot tap before being vortex-mixed for 10-20 secs to dislodge the lipid from the walls of the vial. The lipid suspension was sonicated in a bath sonicator (Ultrawave Model U100) for approximately 5 mins or until the sample had an almost transparent appearance. The lipid sample was transferred to a 10 ml glass vial and diluted to 4 mg lipid/ml using buffer A. Octyl-β-D-glucoside (OG) was added dropwise with mixing to the lipid sample to give a final concentration of 40 mM, resulting in the lipid suspension

becoming clear. SR (1 mg of protein) was solubilised in 0.5 ml of buffer B (10 mM Pipes/100 mM K_2SO_4, 0.1 mM $CaCl_2$, pH 7.1) containing 3 mg $C_{12}E_8$. The solubilised SR was added to the solubilised liposomes to give a 1:40 ratio of protein:lipid (w/w) and the sample was swirled gently for 1 min to ensure mixing. Within 1-2 minutes of mixing an aliquot of washed SM_2 Bio-Beads (80 mg/ml of proteoliposome solution) was added to remove the detergent and the vial was sealed under nitrogen. After an hour of occasional swirling another aliquot of Bio-Beads was added; this was repeated twice more sealing the sample under nitrogen each time. The fourth aliquot of Bio-Beads was only allowed to settle for 5 min before the cloudy proteoliposome suspension was removed. The sample was then kept on ice and used for experimentation within 6 hr.

3.2.3 Ca^{2+} accumulation by sealed vesicles

Accumulation of Ca^{2+} by the reconstituted vesicles was measured at 25 °C using 80 μM of the indicator Antipyralazo III to monitor the drop in external Ca^{2+} concentration as Ca^{2+} is pumped into the vesicles, measuring the absorbance difference 720-790 nm in an Amino-Bowman DW 2000 dual wavelength spectrophotometer. The absorption change was calibrated by the incremental addition of Ca^{2+} prior to the addition of ATP to initiate uptake. The assay buffer was 10 mM Pipes, 100 mM K_2SO_4, 5 mM $MgSO_4$, pH 7.1, containing 120 μM Ca^{2+}, 80 μM Antipyralazo III, 0.8 mM ATP and a protein concentration of 0.04 mg/ml. Carbonyl cyanide p-trifluoromethoxy)phenylhydrazone (FCCP) in DMSO (Dimethyl Sulfoxide) was added to a concentration of 0.25 μM before the addition of Ca^{2+} to

make the vesicles permeable to H^+. Simulations of Ca^{2+} accumulation were performed using the program FACSIMILE (UKEA).

3.3 Results

3.3.1 Ca^{2+} accumulation

The mixing of SR vesicles solubilised in $C_{12}E_8$ with dioleoylphosphatidylcholine (di(C18:1)PC) solubilised in OG, followed by detergent removal with SM_2 Bio-Beads, produced a preparation of sealed vesicles capable of accumulating Ca^{2+}. Ca^{2+} accumulation can be calculated from the change in absorbance over a period of time, in respect to the calibrated signal from the incremental addition of Ca^{2+} prior to the commencement of uptake. The raw data obtained from the spectrophotometer showing Ca^{2+} accumulation into vesicles composed of di(C18:1)PC can be seen in Figure 3.3. The following calculations describe how to convert this data into the amount of Ca^{2+} accumulated to produce a graph as shown in Figure 3.4. To obtain the calibration signal the aliquots of a concentrated stock of Ca^{2+} were added to yield total Ca^{2+} concentrations of 40, 80 and 120 μM. Since 40 μM Ca^{2+} corresponds to 40 nmoles Ca^{2+}/ml and the assay volume is 3 ml, then an addition of 40 μM Ca^{2+} corresponds to the addition of 120 nmoles Ca^{2+}, this resulting in an increase of Antipyrylazo III absorbance of 1.66×10^{-2}. The addition of ATP initiates Ca^{2+}ATPase activity resulting in Ca^{2+} being pumped into the vesicle and a reduction in external Ca^{2+} concentration shown by a decrease in Antipyrylazo III absorbance. A small increase in absorbance immediately after the addition of ATP occurs, as shown on Figure 3.3, and is due to a small change in pH. The expected drop in absorbance corresponding to the uptake of Ca^{2+} follows the addition of ATP. To calculate the amount of Ca^{2+} accumulated the absorbance difference between two time points following ATP is measured. Time zero is taken as the point with the highest absorbance. The amount of Ca^{2+} accumulated is calculated by comparing this change

in absorbance with the Ca^{2+} calibration signal. The total protein in this assay is 120 μg, uptake corresponding to 337.5 nmoles Ca^{2+} accumulated/mg protein after one minute. A spreadsheet is used to convert absorbance values recorded at one-second intervals into Ca^{2+} accumulated in nmoles Ca^{2+}/mg protein, which is then plotted as a function of time (Figure 3.4).

It was observed that the level of Ca^{2+} accumulation was identical with that observed for vesicles reconstituted by adding the solubilised SR to a preparation of pre-formed large unilamellar vesicles, using the method of Levy et al. (1992) (Figure 3.5). In addition we found that good retention of activity was achieved without any mixing or swirling of the Bio-Bead containing sample.

As reported by Levy et al. (1992) we found that the addition of 0.25 μM FCCP led to increased levels of Ca^{2+} accumulation, as the Ca^{2+}-ATPase acts as a Ca^{2+}/H^{+}-ATPase (Figure 3.6). FCCP makes the reconstituted vesicles permeable to H^{+} ions, equilibrating H^{+} across the membrane. The addition of the K^{+} ionophore valinomycin had no significant effect on Ca^{2+} accumulation in the presence of FCCP (data not shown), illustrating that no significant membrane potential built up in the presence of FCCP. Therefore, all experiments were performed in the presence of 0.25 μM FCCP. This concentration of FCCP was found to produce maximal levels of Ca^{2+} accumulation, independent of the lipid composition of the vesicles.

As shown in Figure 3.7 the rate of Ca^{2+} accumulation by the Ca^{2+}-ATPase reconstituted into vesicles of di(C18:1)PC at a lipid: Ca^{2+}-ATPase ratio (w/w) of 40:1 decreased significantly with time following the addition of 0.8 mM ATP, reaching a final steady-state level of Ca^{2+} accumulation of approximately 1000 nmoles of Ca^{2+}/mg protein after 15 minutes. The incorporation of a small percentage of negatively charged lipid into di(C18:1)PC vesicles resulted in increased Ca^{2+}

accumulation levels. The incorporation of 10 mol % dioloeoylphosphatidic acid (di(C18:1)PA) into vesicles composed of di(C18:1)PC increased the level of Ca^{2+} accumulation to approximately 2000 nmoles Ca^{2+}/mg protein after 15 minutes (Figure 3.7). As shown in Figure 3.7 the effect of incorporating 10 mol % dioleoylphosphatidylserine (di(C18:1)PS) into di(C18:1)PC vesicles resulted in Ca^{2+} accumulation levels identical to those seen in the presence 10 mol % di(C18:1)PA. The effect of 10 mol % cardiolipin on Ca^{2+} accumulation was considerably more marked than that of di(C18:1)PA or di(C18:1)PS (Figure 3.7). 10 mol % cardiolipin increased the level of Ca^{2+} accumulation to approximately 4200 nmoles of Ca^{2+}/mg protein after 15 minutes.

Figure 3.8 shows the effect of di(C18:1)PA on Ca^{2+} accumulation as a function of the concentration of di(C18:1)PA in the lipid mixture. 10 mol % di(C18:1)PA was the optimal concentration for Ca^{2+} accumulation. Lower levels of Ca^{2+} accumulation were observed at 5 mol % di(C18:1)PA, and 15 and 20 mol % di(C18:1)PA resulted in slightly lower levels of Ca^{2+} accumulation than 10 mol % di(C18:1)PA (Figure 3.8). An identical pattern was observed when using di(C18:1)PS in place of di(C18:1)PA (data not shown). This suggests that 10 mol % of anionic phospholipid is the optimal concentration.

As shown in Figure 3.9, 10 mol % cardiolipin was again found to be the optimal concentration of anionic lipid required for accumulation, with lower levels of Ca^{2+} accumulation being observed at either 5 or 20 mol % cardiolipin. The presence of either 5 or 20 mol % cardiolipin results in approximately identical levels of Ca^{2+} accumulation of about 2100 nmoles of Ca^{2+} / mg protein after 15 mins (Figure 3.9). The effect of 5 mol % cardiolipin was comparable with that of 10 mol % di(C18:1)PA.

Figure 3.10 illustrates the effects of di(C18:1)PE on Ca^{2+} accumulation by comparing vesicles composed of di(C18:1)PC:di(C18:1)PE and di(C18:1)PC (7:3) and vesicles composed of di(C18:1)PC:di(C18:1)PE:di(C18:1)PA (6:3:1) and di(C18:1)PC:di(C18:1)PA (9:1). The presence of di(C18:1)PE resulted in little, if any, increase in Ca^{2+} accumulation levels in the presence of solely di(C18:1)PC or both di(C18:1)PC and di(C18:1)PA. Ca^{2+} accumulation levels were identical for vesicles composed of di(C18:1)PC and 10 to 40 mol % di(C18:1)PE. It was not possible to reconstitute vesicles containing more than 50 mol % di(C18:1)PE using this method. At higher percentages there was a difficulty in hydrating the lipid mixtures that came off the walls of the scintillation vials as turbid aggregates. Prolonged sonication had no visible effect on the sample and in addition solubilisation of the lipid mixture was also a problem. This is in contrast to the work of Gould et al. (1987b) who found that levels of Ca^{2+} accumulation were significantly increased by the addition of di(C18:1)PE up to 80%, when using an alternative method for reconstitution.

As shown in Figure 3.11 the presence of 10 mol % phosphatidylinositol (di(C18:1)PI) had an effect on accumulation of Ca^{2+} very similar to that of 10 mol % di(C18:1)PA. However, the effect of phosphatidylinositol-4-monophosphate (di(C18:1)PI(4)*P*) was more marked, the presence of 10 mol % di(C18:1)PI(4)*P* increasing Ca^{2+} accumulation levels to approximately 2800 nmoles/mg protein, whilst the presence of 5 mol % di(C18:1)PI(4)*P* had an effect on accumulation very similar to that of 10 mol % di(C18:1)PI (Figure 3.11). Although high, these levels of Ca^{2+} accumulation were not as high as those recorded in the presence of cardiolipin.

To assess whether the decrease in the rate of Ca^{2+} accumulation with time was due to the depletion of ATP or build up of ADP, as a result of ATP hydrolysis of ATP by the Ca^{2+}-ATPase, the effect of an ATP-regenerating system, consisting of 7.5 IU

pyruvate kinase, 0.53 mM phosphoenolpyruvate, 0.15 mM NADH and 18 IU lactate dehydrogenase was observed (Figure 3.12). This resulted in slightly increased levels of Ca^{2+} accumulation at longer times in vesicles composed of 100% di(C18:1)PC. However, in the presence of the regenerating system the rate of Ca^{2+} accumulation still decreased with time (Figure 3.12). In contrast, the rate of hydrolysis of ATP by the Ca^{2+}-ATPase reconstituted into vesicles composed of 100% di(C18:1)PC, measured in the presence of an ATP regenerating system, was unaltered with time, remaining constant until all the ATP and phosphoenolpyruvate in the system had been consumed (data not shown). Therefore the stoichiometry of net Ca^{2+} accumulation to ATP hydrolysed decreases with time. A similar observation has been made for native SR vesicles in the absence of any Ca^{2+}-precipitating agent in the lumen of the vesicles (Yu & Inesi, 1995).

A problem usually encountered in Ca^{2+} accumulation studies is that the level of Ca^{2+} accumulated varies between preparations of SR. Variations in both activity and the maximum level of phosphorylation of the Ca^{2+}-ATPase have been previously reported (Gould et al., 1986a; Michelangeli et al., 1990b). This was overcome by performing all of the experiments in this chapter with the same SR preparation, thus making all the results comparable.

3.3.2 Ca^{2+}-ATPase activities of reconstituted vesicles

The rate of ATP hydrolysis, the Ca^{2+}-ATPase activity, in the reconstituted vesicles was found to be about one-half of that in the native SR vesicles that were used for the reconstitution. This suggests that the incorporation of the Ca^{2+}-ATPase molecules across the membrane was approximately random, with approximately 50 %

of the Ca^{2+}-ATPase molecules having a right side out orientation (Table 3.1). This was confirmed by the addition of the detergent $C_{12}E_8$ at low concentrations (0.8 mg/ml) to the reconstituted vesicles, which made them leaky to ATP and led to a doubling of Ca^{2+}-ATPase activity (Table 3.1). The addition of $C_{12}E_8$ at this same concentration to purified Ca^{2+}-ATPase had no effect on ATPase activity (de Foresta et al., 1989); similarly, $C_{12}E_8$ had no effect on the Ca^{2+}-ATPase activity of SR vesicles when measured in the presence of the Ca^{2+} ionophore A23187 (Table 3.1). The rate of ATP hydrolysis of the reconstituted vesicles was unaffected by the addition of either the proton ionophore FCCP or the Ca^{2+} ionophore A23187. The rate of ATP hydrolysis of the vesicles reconstituted by the Bio-Beads method was not generally affected by the presence of 10 mol % anionic lipids (Table 3.1). The reason for the higher activity in the presence of 10 mol % cardiolipin and $C_{12}E_8$ is unclear.

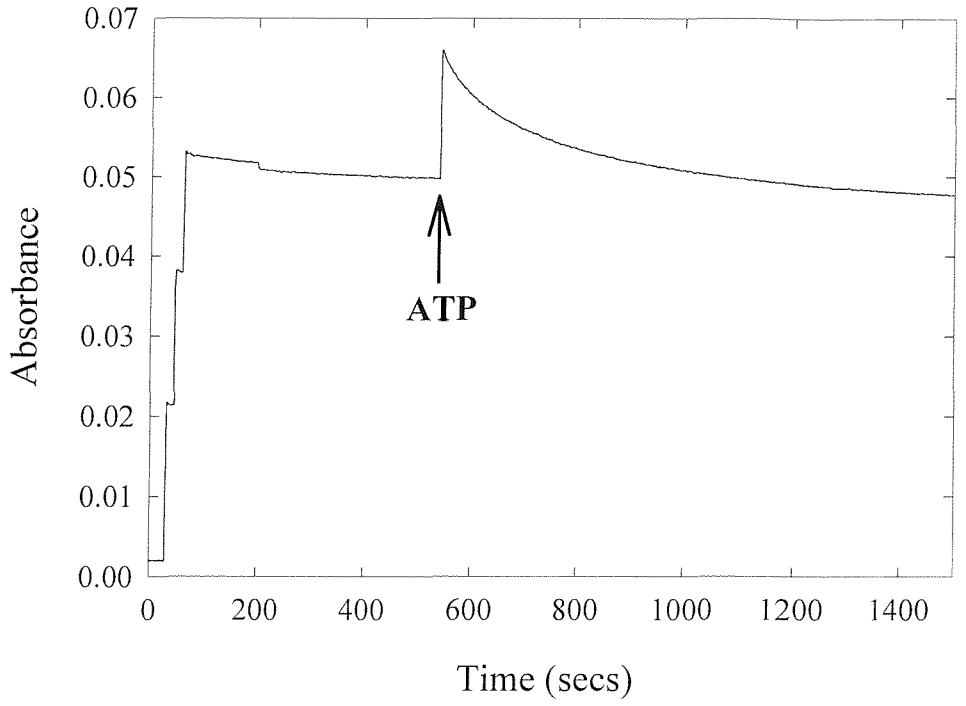

Figure 3.3 Ca^{2+} accumulation trace illustrating absorbance changes

The figure illustrates the changes in absorbance during ATP dependent Ca^{2+} accumulation by reconstituted vesicles composed of di(C18:1)PC. Accumulation of Ca^{2+} was initiated by the addition of 0.8 mM ATP. The sample contained 0.02 mg of protein/ml at a lipid: protein ratio (w/w) of 40: 1 in 10 mM Pipes, pH 7.1, 100 mM K_2SO_4, 5 mM Mg^{2+}, 80 μM Antipyrylazo III, 0.25 μM FCCP and an initial Ca^{2+} concentration of 120 μM. Shown at the start of the trace are the three calibration steps produced by the incremental addition of three steps of 40 μM Ca^{2+}. The reaction was initiated by the addition of 0.8 mM ATP.

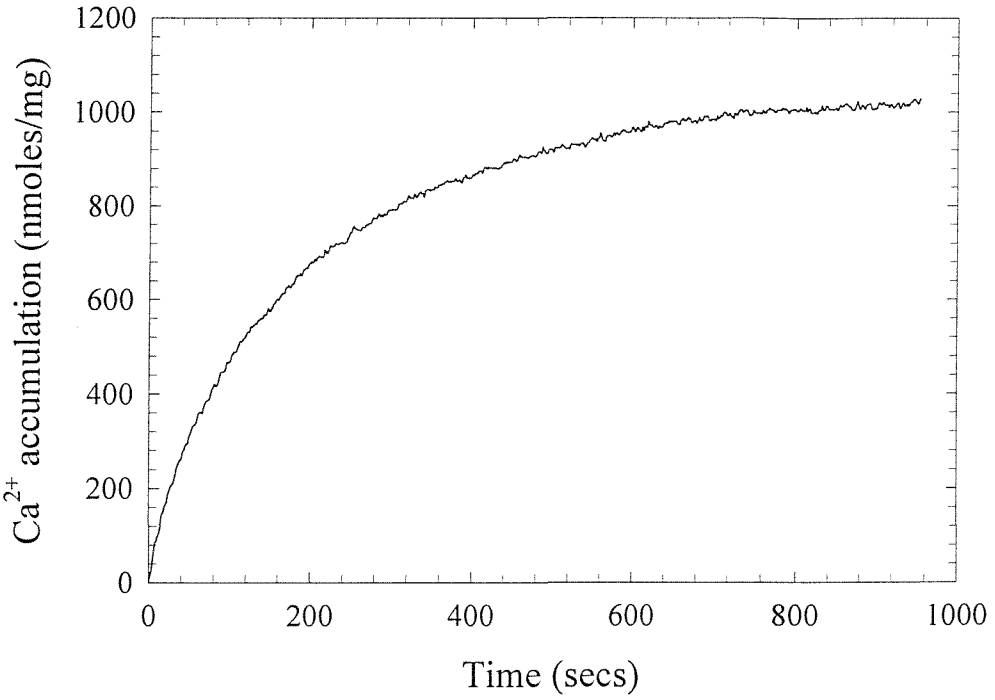

Figure 3.4 ATP-dependent Ca^{2+} accumulation into sealed vesicles

The figure shows ATP dependent Ca^{2+} accumulation by the Ca^{2+}-ATPase reconstituted with di(C18:1)PC. Accumulation of Ca^{2+} was initiated by the addition of 0.8 mM ATP. The sample contained 0.02 mg of protein/ml at a lipid: protein ratio (w/w) of 40: 1 in 10 mM Pipes, pH 7.1, 100 mM K_2SO_4, 5 mM Mg^{2+}, 80 μM Antipyrylazo III, 0.25 μM FCCP and an initial Ca^{2+} concentration of 120 μM.

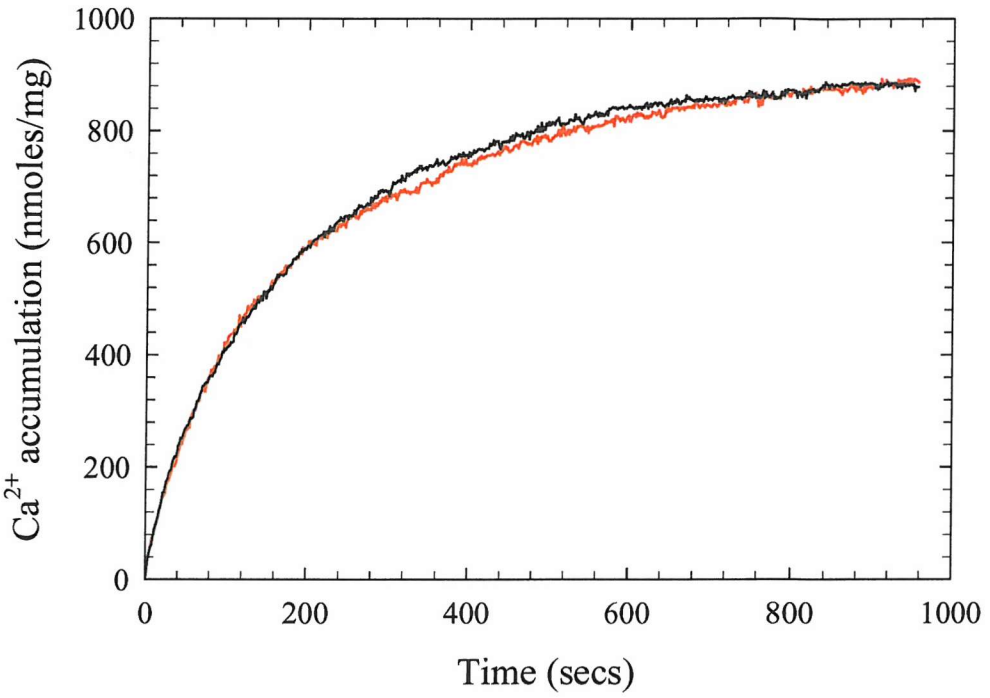

Figure 3.5 ATP-dependent Ca^{2+} accumulation into sealed vesicles

The figure shows identical levels of ATP dependent Ca^{2+} accumulation by sealed vesicles, both composed of di(C18:1)PC, when reconstituted by the modified method described in the methods section (black trace) or by adding the solubilised SR to a preparation of pre-formed large unilamellar vesicles (red trace), using the method of Levy et al. (1992). Accumulation of Ca^{2+} was initiated by the addition of 0.8 mM ATP. Samples contained 0.02 mg of protein/ml at a lipid: protein ratio (w/w) of 40: 1 in 10 mM Pipes, pH 7.1, 100 mM K_2SO_4, 5 mM Mg^{2+}, 80 μM Antipyrylazo III, 0.25 μM FCCP and an initial Ca^{2+} concentration of 120 μM.

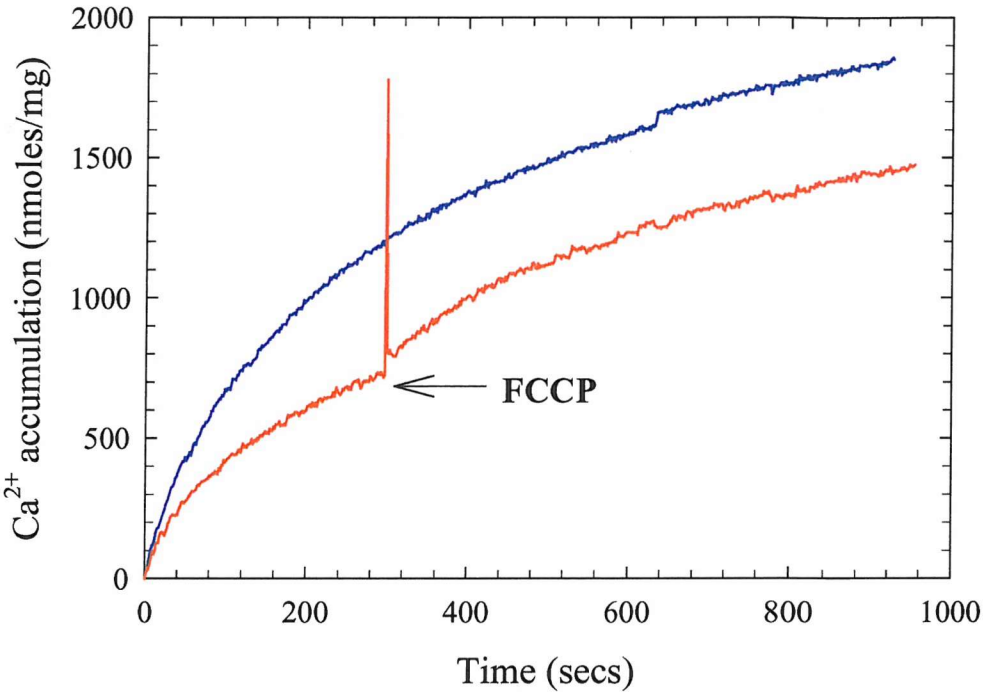

Figure 3.6 The effect of the H^+ ionophore FCCP on Ca^{2+} accumulation

The figure shows levels of ATP dependent Ca^{2+} accumulation by reconstituted vesicles composed of 90 % di(C18:1)PC / 10 % di(C18:1)PA are greater in the presence of FCCP (blue trace) than in its absence (red trace). For the experiment in the absence of FCCP, FCCP was added after 5 min resulting in an increase in the rate of accumulation of Ca^{2+}. Accumulation of Ca^{2+} was initiated by the addition of 0.8 mM ATP. Samples contained 0.02 mg of protein/ml at a lipid: protein ratio (w/w) of 40: 1 in 10 mM Pipes, pH 7.1, 100 mM K_2SO_4, 5 mM Mg^{2+}, 80 µM Antipyrylazo III, 0.25 µM FCCP (if present) and an initial Ca^{2+} concentration of 120 µM.

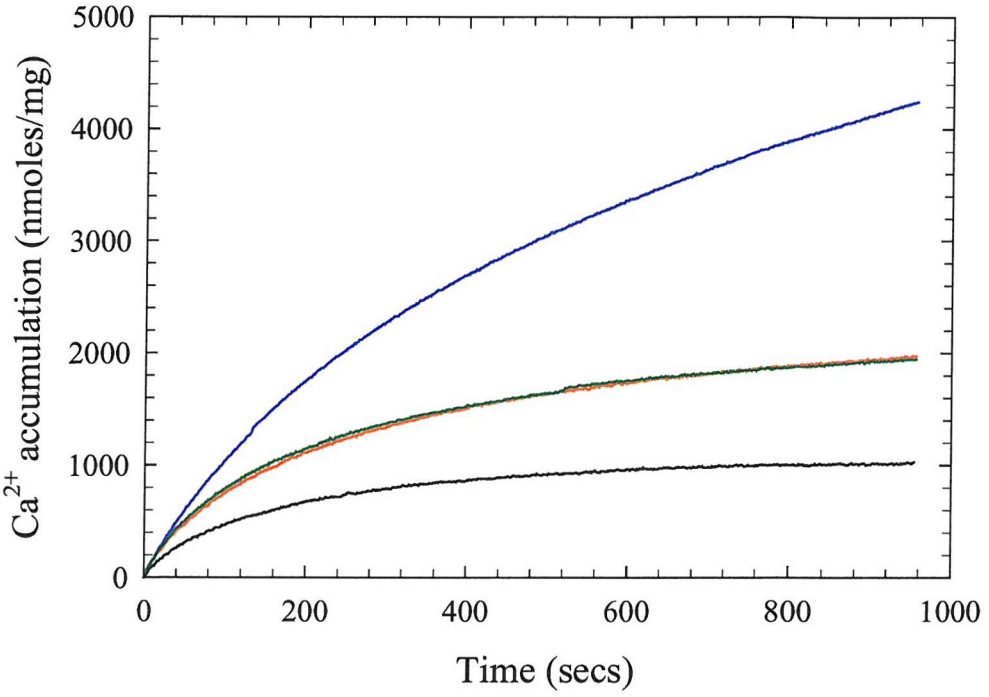

Figure 3.7 The effect of negatively charged lipids on Ca^{2+} accumulation

The figure shows ATP dependent Ca^{2+} accumulation by reconstituted vesicles in the presence of 10 mol % anionic lipid. In ascending order, levels of Ca^{2+} accumulation are shown in the presence of 100 % di(C18:1)PC (black trace), 90 % di(C18:1)PC / 10 % di(C18:1)PS (green trace), 90 % di(C18:1)PC / 10 % di(C18:1)PA (red trace), 90% di(C18:1)PC / 10% cardiolipin (blue trace). Accumulation of Ca^{2+} was initiated by the addition of 0.8 mM ATP. Samples contained 0.02 mg of protein/ml at a lipid: protein ratio (w/w) of 40: 1 in 10 mM Pipes, pH 7.1, 100 mM K_2SO_4, 5 mM Mg^{2+}, 80 μM Antipyrylazo III, 0.25 μM FCCP and an initial Ca^{2+} concentration of 120 μM.

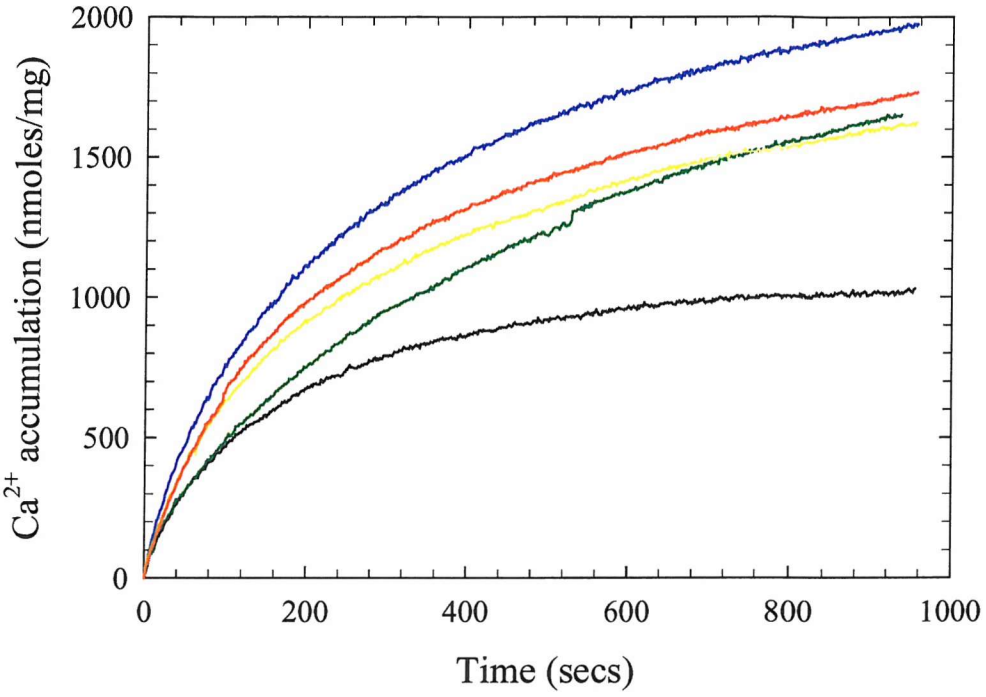

Figure 3.8 The effect of di(C18:1)PA on Ca^{2+} accumulation

The figure shows ATP dependent Ca^{2+} accumulation by reconstituted vesicles containing different concentrations of the anionic phospholipid di(C18:1)PA. In ascending order, levels of Ca^{2+} accumulation are shown in the presence of 100 % di(C18:1)PC (black trace), 85 % di(C18:1)PC / 15 % di(C18:1)PA (yellow trace), 95 % di(C18:1)PC / 5 % di(C18:1)PA (green trace), 80 % di(C18:1)PC / 20 % di(C18:1)PA (red trace), 90 % di(C18:1)PC / 10 % di(C18:1)PA (blue trace). Accumulation of Ca^{2+} was initiated by the addition of 0.8 mM ATP. Samples contained 0.02 mg of protein/ml at a lipid: protein ratio (w/w) of 40: 1 in 10 mM Pipes, pH 7.1, 100 mM K_2SO_4, 5 mM Mg^{2+}, 80 μM Antipyrylazo III, 0.25 μM FCCP and an initial Ca^{2+} concentration of 120 μM.

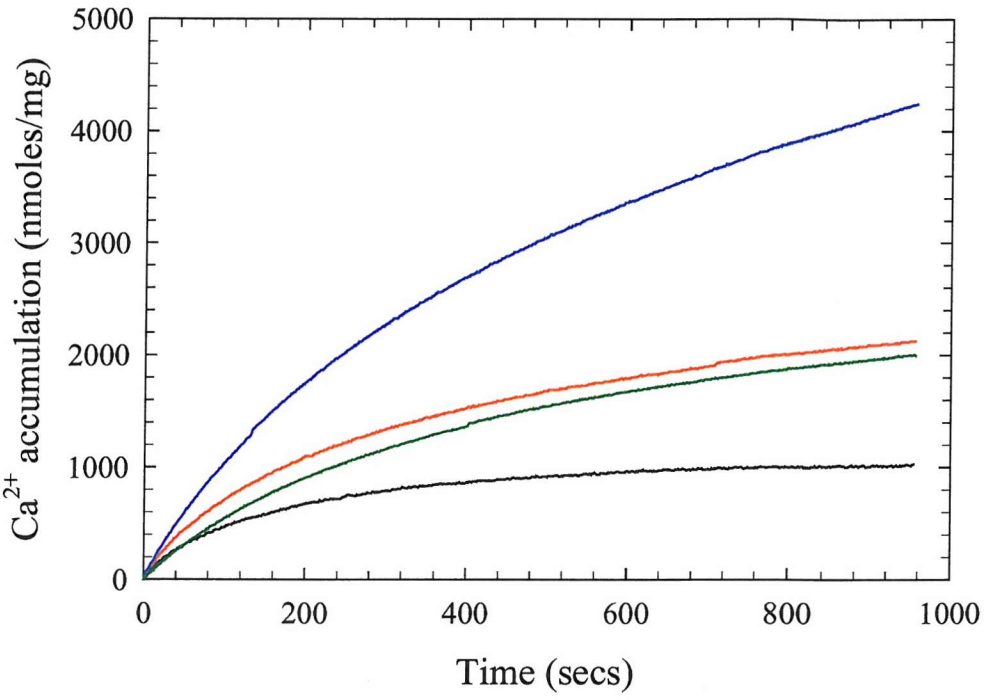

Figure 3.9 The effect of cardiolipin on Ca^{2+} accumulation

The figure shows ATP dependent Ca^{2+} accumulation by reconstituted vesicles containing, in ascending order, 100 % di(C18:1)PC (black trace), 80 % di(C18:1)PC / 20 % cardiolipin (green trace), 95 % di(C18:1)PC / 5 % cardiolipin (red trace), 90 % di(C18:1)PC / 10 % cardiolipin (blue trace). Accumulation of Ca^{2+} was initiated by the addition of 0.8 mM ATP. Samples contained 0.02 mg of protein/ml at a lipid: protein ratio (w/w) of 40: 1 in 10 mM Pipes, pH 7.1, 100 mM K_2SO_4, 5 mM Mg^{2+}, 80 μM Antipyrylazo III, 0.25 μM FCCP and an initial Ca^{2+} concentration of 120 μM.

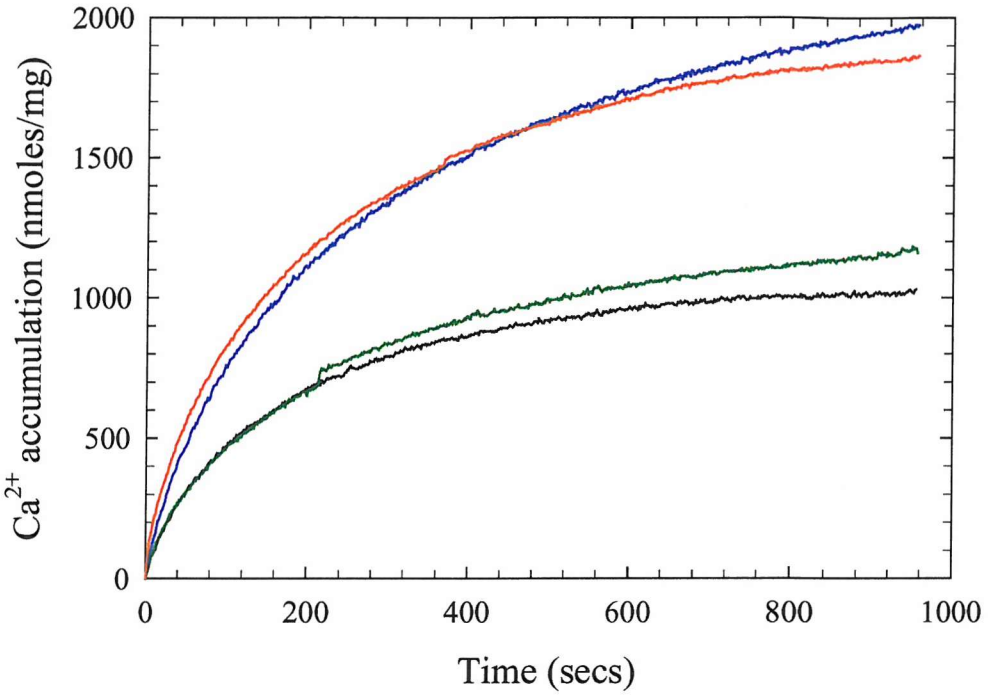

Figure 3.10 The effect of di(C18:1)PE on Ca^{2+} accumulation

The figure shows ATP dependent Ca^{2+} accumulation by reconstituted vesicles containing, in ascending order, 100 % di(C18:1)PC (black trace), 70 % di(C18:1)PC / 30 % di(C18:1)PE (green trace), 60 % di(C18:1)PC / 30 % di(C18:1)PE / 10 % di(C18:1)PA (red trace), 90 % di(C18:1)PC / 10 % di(C18:1)PA (blue trace). Accumulation of Ca^{2+} was initiated by the addition of 0.8 mM ATP. Samples contained 0.02 mg of protein/ml at a lipid: protein ratio (w/w) of 40: 1 in 10 mM Pipes, pH 7.1, 100 mM K_2SO_4, 5 mM Mg^{2+}, 80 μM Antipyrylazo III, 0.25 μM FCCP and an initial Ca^{2+} concentration of 120 μM.

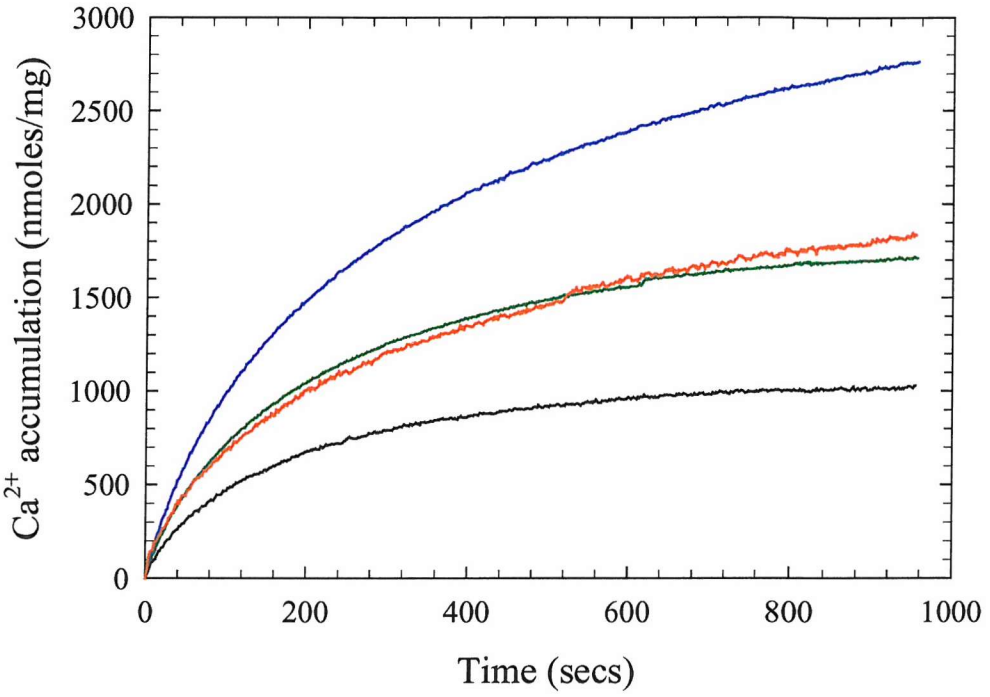

Figure 3.11 The effect of phosphatidylinositols on Ca^{2+} accumulation

The figure shows ATP dependent Ca^{2+} accumulation by reconstituted vesicles containing, in ascending order, 100 % di(C18:1)PC (black trace), 90 % di(C18:1)PC / 10 % di(C18:1)PI (green trace), 95 % di(C18:1)PC / 5 % di(C18:1)PI(4)*P* (red trace) 90 % di(C18:1)PC / 10 % di(C18:1)PI(4)*P* (blue trace). Accumulation of Ca^{2+} was initiated by the addition of 0.8 mM ATP. Samples contained 0.02 mg of protein/ml at a lipid: protein ratio (w/w) of 40: 1 in 10 mM Pipes, pH 7.1, 100 mM K_2SO_4, 5 mM Mg^{2+}, 80 μM Antipyrylazo III, 0.25 μM FCCP and an initial Ca^{2+} concentration of 120 μM.

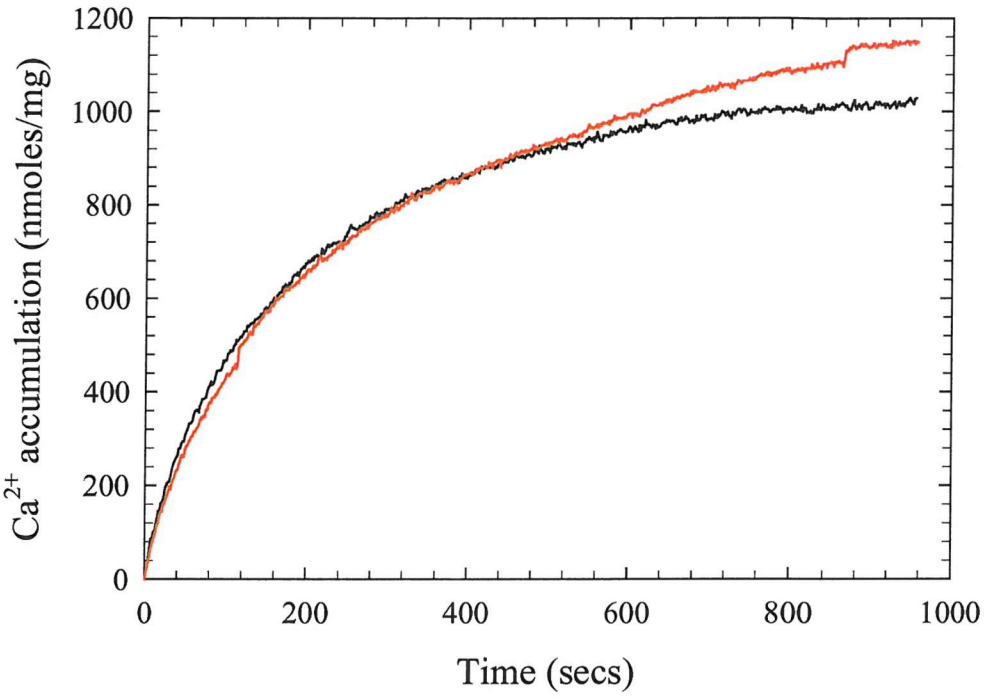

Figure 3.12 Accumulation of Ca^{2+} in the presence of an ATP-regenerating system

The figure shows ATP dependent Ca^{2+} accumulation by reconstituted vesicles containing 100 % DOPC measured in the absence (black trace) or presence (red trace) of an ATP-regenerating system. Accumulation of Ca^{2+} was initiated by the addition of 0.8 mM ATP. Samples contained 0.02 mg of protein/ml at a lipid: protein ratio (w/w) of 40: 1 in 10 mM Pipes, pH 7.1, 100 mM K_2SO_4, 5 mM Mg^{2+}, 80 μM Antipyrylazo III, 0.25 μM FCCP and an initial Ca^{2+} concentration of 120 μM.

Lipid	Ca^{2+}-ATPase activity (units/mg protein)	
	$-C_{12}E_8$	$+C_{12}E_8$
SR vesicles	**3.4 ± 0.3**	**3.3 ± 0.3**
100% DOPC	**1.5 ± 0.2**	**3.3 ± 0.3**
90% DOPC/10% DOPA	**1.9 ± 0.2**	**3.2 ± 0.3**
90% DOPC/10% DOPE	**1.5 ± 0.2**	**3.3 ± 0.3**
90% DOPC/10% DOPI	**1.3 ± 0.1**	**3.5 ± 0.4**
90% DOPC/10% PtdIns(4)*P*	**1.7 ± 0.2**	**3.3 ± 0.3**
95% DOPC/5% PtdIns(4)*P*	**1.7 ± 0.2**	**3.4 ± 0.3**
90% DOPC/10% Cardiolipin	**1.5 ± 0.2**	**4.4 ± 0.4**

Table 3.1 Steady-state Ca^{2+}-ATPase activities for reconstituted vesicles

Ca^{2+}-ATPase activities of the reconstituted vesicles were measured using the experimental conditions described in the Materials and methods section in 40 mM Hepes, 10 mM KCl, 2.1 mM ATP, 5 mM Mg^{2+}, 0.53 mM PEP, 7.5 IU pyruvate kinase, 0.15 mM NADH, 7.5 IU lactate dehydrogenase.. $C_{12}E_8$ was used at a concentration of 0.8 mg/ml in the presence of A23187 at a concentration of 5 μg/ml.

3.4 Discussion

3.4.1 Reconstitution into sealed vesicles

In the past a number of methods have been used for the reconstitution of the Ca^{2+}-ATPase into sealed vesicles, such as cholate dialysis, freeze thaw sonication and detergent removal using hydrophobic resins (Racker, 1972; Zimniak & Racker, 1978; Levy et al., 1990a). The method that produced vesicles able to accumulate the highest levels of Ca^{2+} involved detergent removal by hydrophobic resin called Bio-Beads (Levy et al., 1990a). This published method had been slightly modified to produce vesicles also exhibiting a high level of Ca^{2+} accumulation (Dalton et al., 1998). The preparation of liposomes by reverse phase evaporation was replaced by extrusion of multilamellar vesicles to produce large unilamellar vesicles. The vesicles are then solubilised before the addition of the Ca^{2+}-ATPase as in the report by Yu et al. (1993). This method has been used, in a modified form, to produce vesicles exhibiting a very low ionic permeability that are able to accumulate identical levels of Ca^{2+}. In the modification, the freeze-thaw step that precedes sonication has been removed, as it was deemed not necessary. This has eliminated the possibility of alterations to protein structure, which can occur during the freeze-thaw steps. The extrusion step was also eliminated. In addition, maximum Ca^{2+}-ATPase activity was obtained without regular mixing or swirling of the Bio-Bead containing sample. Our results have shown that Ca^{2+} accumulation was independent of whether the vesicles were unilamellar or multilamellar before solubilisation in detergent (Figure 3.5). Vesicle diameters were very large, as determined by using a Coulter N4 Plus particle sizer that measures particle size by light scattering (Dalton et al., 1998). The large size and hence large lumenal volume of the vesicles meant that Ca^{2+} accumulation was a

relatively slow process (Figure 3.4), allowing the time course of accumulation to be monitored easily.

3.4.2 Accumulation of Ca^{2+} into sealed vesicles

The lipid composition of all biological membranes is very diverse and it is unclear why this diversity is required for the proper functioning of the membrane and the proteins embedded in it. As described in the introduction, a relatively wide range of phospholipid structures will sustain a high rate of ATP hydrolysis by the Ca^{2+}-ATPase; the optimal bilayer thickness requires phospholipid acyl chains of between C16 and C20 in length; the phospholipids have to form bilayers and be in the liquid-crystalline phase and the optimal headgroup is zwitterionic, either phosphatidylcholine or phosphatidylethanolamine (Lee et al., 1995a; Lee, 1998). Previous studies have shown, in contradiction to our results (Table 3.1), that the only exception to this general pattern is the presence of small quantities of di(C18:1)PI(4)*P* in the bilayer. Di(C18:1)PI(4)*P* increases the ATPase activity of the Ca^{2+}-ATPase when reconstituted in small quantities into membrane fragments (Starling et al., 1995a). The effect of di(C18:1)PI(4)*P* is specific; the presence of di(C18:1)PA and di(C18:1)PI at low mole fractions had no effect on ATPase activity, and at higher quantities led to inhibition (Dalton et al., 1998). The native SR membrane contains about 10 mol % anionic phospholipid, consisting of approximately 2 mol % phosphatidylserine and 8 mol % phosphatidylinositol (PtdIns) and PtdIns(4)*P*, but no PtdIns(4,5)P_2 (Lau et al., 1979; Milting et al., 1994). The absence of PtdIns(4,5)P_2 in the SR membrane means that SR lacks the capacity for the generation of Ins(1,4,5)P_3 (Milting et al., 1994).

The aim here was to investigate the possibility that the role of anionic phospholipids in the SR membrane is to increase Ca^{2+} accumulation levels, rather than maximise the rate of ATP hydrolysis. Previous published studies on the effects of lipid composition on accumulation of Ca^{2+} are difficult to compare as they have used a variety of different methods. Another problem when comparing Ca^{2+} accumulation is whether the reported differences in accumulation of Ca^{2+} follow from direct effects of the phospholipid on the Ca^{2+}-ATPase or whether they reflect differences in the efficiency of Ca^{2+}-ATPase incorporation into the vesicles.

Many reports have suggested that accumulation of Ca^{2+} by the Ca^{2+}-ATPase into reconstituted vesicles composed of phosphatidylcholine is relatively low and that the incorporation of up to 80 mol % phosphatidylethanolamine into these vesicles results in increasing levels of Ca^{2+} accumulation (Navarro et al., 1984; Gould et al., 1987a). The ability to form vesicles composed of entirely di(C18:1)PE that are able to accumulate Ca^{2+} depends on the method of reconstitution (Bennett et al., 1978; Knowles et al., 1976). Vesicles that are composed entirely of negatively charged lipids support low levels of Ca^{2+} accumulation, comparable to or lower than levels observed for vesicles composed of 100% di(C18:1)PC (Bennett et al., 1978; Navarro et al., 1984). However, vesicles composed of mixtures of negatively charged lipids and di(C18:1)PC have been shown to support higher levels of Ca^{2+} accumulation than vesicles composed of di(C18:1)PC alone (Szymanska et al., 1991). Highest levels of Ca^{2+} accumulation have been observed in vesicles composed of di(C18:1)PC and either 50 mol % phosphatidylserine or 25 mol % phosphatidylinositol-4-phosphate (Szymanska et al., 1991). However, the method used was the freeze-thaw sonication technique, which could be responsible for the high levels of Ca^{2+} accumulation due to the efficiency of reconstitution. All published studies using the reconstitution

procedure of Levy et al. (1990) have reported higher levels of Ca^{2+} accumulation in vesicles composed of mixtures of egg phosphatidylcholine and egg phosphatidic acid than in vesicles composed of egg phosphatidylcholine alone (Levy et al., 1992).

Accumulation of Ca^{2+} by the reconstituted vesicles was measured in the presence of FCCP (Figure 3.6) to prevent H^+ gradients or membrane potentials building up and inhibiting Ca^{2+} accumulation (Levy et al., 1990a). It is shown in Figure 3.7 that the presence of small quantities of negatively charged lipid in the reconstituted vesicle led to higher levels of Ca^{2+} accumulation than in purely DOPC vesicles, the effect of cardiolipin being greater than that of DOPA or DOPS. The effect of the negatively charged lipid reaches a maximum at about 10 mol %, higher concentrations leading to lower levels of Ca^{2+} accumulation (Figures 3.8 and 3.9). This is in contrast with the previously described study in which vesicles composed of di(C18:1)PC and either 50 mol % phosphatidylserine or 25 mol % phosphatidylinositol-4-phosphate supported the highest levels of Ca^{2+} accumulation (Szymanska et al., 1991).

As shown in Figure 3.10, the presence of di(C18:1)PE has no effect on the level of Ca^{2+} accumulation in the presence of di(C18:1)PC or both di(C18:1)PC and negatively charged lipid. When reconstituting using the Bio-Beads method it was only possible to incorporate up to 50 mol % di(C18:1)PE into di(C18:1)PC vesicles. This is in contrast to the work of Gould et al. (1987b) who found that levels of Ca^{2+} accumulation were significantly increased by the addition of up to 80 mol % di(C18:1)PE , when using an alternative method for reconstitution. Navarro et al. (1984) suggested that the effect of phosphatidylethanolamine on Ca^{2+} accumulation is related to its ability to adopt a hexagonal H_{II} phase rather than a bilayer phase. The bilayer to hexagonal H_{II} phase transition temperature is 15°C (Cullis & Kruijff, 1978).

The effect of di(C18:1)PI on accumulation of Ca^{2+} is very similar to that of di(C18:1)PA and di(C18:1)PS; however, the effect of di(C18:1)PI(4)*P* is more marked. The fact that the largest effects with the negatively charged phospholipids on Ca^{2+} accumulation are seen with di(C18:1)PI(4)*P* and cardiolipin suggests that the negative charge borne by the phospholipid is important. However, the total negative charge on the membrane is not important since 20 mol % di(C18:1)PA does not have the same effect on Ca^{2+} accumulation as 10 mol % cardiolipin (Figures 3.8 and 3.9).

One possible mechanism for the effects of anionic phospholipids could be the formation of an anionic phospholipid-Ca^{2+} complex in the lumen of the reconstituted vesicles. The formation of such a complex would reduce the free lumenal concentration of Ca^{2+}, thus reducing the level of the phosphorylated intermediate $E2PCa_2$, leading to a reduction in the inhibition of the Ca^{2+}-ATPase (Scheme 3.1). Effective concentrations of anionic phospholipids in the lumenal volume are high. Vesicle diameters have been calculated using light scattering experiments to be approximately 120 nm (Dalton et al., 1999). Vesicles of this diameter give a calculated internal volume of 174 μl/mg protein, in agreement with the value of 175 μl/mg of protein estimated by Levy et al. (1990a). If 10 mol % of anionic lipid is present and distributed randomly across the membrane, the concentration of anionic lipid on the inner surface, expressed in terms of lumenal volume is 15 mM. If this anionic phospholipid were to complex with significant amounts of Ca^{2+} in the lumen and this were to be an important factor in the accumulation of Ca^{2+}, levels of Ca^{2+} accumulation would be expected to increase linearly with increasing levels of anionic phospholipid. However, this is not the case, as the effect of anionic phospholipid seems to saturate at 10 mol % (Figure 3.8). Furthermore, the effect of lumenal phosphate on Ca^{2+} accumulation levels is more pronounced in the presence of anionic

phospholipid than in vesicles of PC alone (Dalton et al., 1999). The presence of lumenal phosphate reduces the level of free lumenal Ca^{2+}, thus increasing Ca^{2+} accumulation levels. If anionic phospholipids did indeed increase Ca^{2+} accumulation levels from the reduction in the level of free lumenal Ca^{2+}, then the effects of lumenal phosphate would be less in the presence of anionic phospholipid. We therefore conclude that complexing of lumenal Ca^{2+} by anionic phospholipids is not the explanation for the observed effects of anionic phospholipids on the accumulation of Ca^{2+}.

An alternative theory for the effects of anionic lipids could be that they reduce the rate of a leak pathway of Ca^{2+} across the membrane of the reconstituted vesicles. Two types of leak pathway can be distinguished. Firstly, there is simple passive leak of Ca^{2+} down its concentration gradient by the mediation of the Ca^{2+}-ATPase or some other protein in the SR membrane. Secondly, Ca^{2+} can leak as a result of slippage on the Ca^{2+}-ATPase. Here the phosphorylated intermediate of the Ca^{2+}-ATPase releases Ca^{2+} on the cytoplasmic side of the SR membrane, rather than the lumenal side (Scheme 3.1). The presence of a passive leak pathway has been shown in experiments measuring the rate of Ca^{2+} release from Ca^{2+}-loaded SR vesicles lacking Ca^{2+} channels (Inesi & de Meis, 1989). Here Ca^{2+} leak is inhibited by μM concentrations of Ca^{2+} in the cytoplasm, unlike Ca^{2+} release through the Ca^{2+} channel, which is stimulated by μM concentrations of Ca^{2+} in the cytoplasm, suggesting that the passive leak pathway could involve the Ca^{2+}-ATPase (Inesi & de Meis, 1989). The passive leak of Ca^{2+} has also been demonstrated in vesicles reconstituted from phospholipids and purified Ca^{2+}-ATPase, again suggesting that Ca^{2+} leak occurs through the Ca^{2+}-ATPase (Inesi et al., 1983; Gould et al., 1987b, 1987c). Experimental evidence also exists for a slippage pathway (Inesi & de Mesi, 1989, Nayer et al., 1982). Here the

uptake of Ca^{2+} by SR vesicles, on the addition of ATP, is followed by the release of some of the accumulated Ca^{2+} even in the continued presence of ATP and external Ca^{2+}, conditions under which passive leak is inhibited (McWhirter et al., 1987). The release of Ca^{2+} is also observed in the presence of acetyl phosphate instead of ATP, illustrating that Ca^{2+} release does not correspond to the back-reaction (de Meis, 1981) in which Ca^{2+} efflux is linked to the conversion of ADP to ATP (McWhirter et al., 1987). The rate of passive leak of Ca^{2+} across the membrane is slow as has been shown by the addition of hexokinase in the presence of glucose to rapidly remove ATP from the reconstituted system (Dalton et al., 1999). This suggests that slippage is the important factor regarding Ca^{2+} leak out of the vesicle.

Using a simulation of the reaction scheme shown in Scheme 3.1 it is possible to show that passive leak and slippage result in very different time dependencies of accumulation of Ca^{2+} (Figure 3.13). The simulations of Scheme 3.1 used the package FACSIMILE (UKEA) running on a PC system and were performed by Professor Anthony G. Lee. FACSIMILE handles all the mathematical calculations once the definition of the steps of the reaction sequence to be simulated and the values for the rate constants of these steps are entered into the program. This information is provided in the form of a sub-routine and is shown in full in Appendix 1. Rate constants for the uptake pathway, steps 1-8 under 'COMPILE EQUATIONS', in Scheme 3.1 are listed under 'COMPILE INITIAL' and can be assigned on the basis of experimental data. The rate constants k1f and k1b define the rates of the E2→ E1 and E1→ E2 steps respectively and were taken from Lee et al. (1995b). The rates k2f, k2b, k3f and k3b define the affinity of the Ca^{2+}-ATPase for Ca^{2+}. For simplicity the dissociation constants for the first and second Ca^{2+} sites, k2b/k2f and k3b/k3f respectively, were both set at 1 μM since the dissociation constant of the Ca^{2+}-

ATPase for Ca^{2+} is in the μM range. The rates of these steps were set to be so fast that the exact values of the rates had no influence on the simulations. The dissociation constant for ATP, k4b/k4f, was set at the experimentally determined value of 10 μM (Lacapere et al., 1990). Once again rates were set so fast that they did not influence the simulations. The rates of phosphorylation (k5f) and dephosphorylation (k5b) of the phosphorylated intermediate E2P were set at 100 s^{-1} (Dalton et al., 1998) and 10^{-6} s^{-1} (Froud & Lee, 1986) respectively, ensuring that phosphorylation was effectively irreversible. Ca^{2+} binding has been simplified to a two-step binding process, since this was found to give the same result as the full binding model described by Henderson et al. (1994). The rate of dissociation of the first Ca^{2+} from the phosphorylated intermediate $E2PCa_2$ has been set at twice that of the second Ca^{2+} with rate constants 60 s^{-1} and 30 s^{-1} respectively (Orlowski & Champeil, 1991), to give a single exponential decay for the Ca^{2+}-dissociation process. The affinity of the two lumenal Ca^{2+} binding sites on E2P for Ca^{2+} has been estimated to be 2-3.5 mM (Myung & Jencks, 1994) and has been set here at 3.3 mM. The internal volume of the vesicles has been set at 174 μl/mg protein (Dalton et al., 1999). Therefore the only variables in the simulation are the rates of passive leak and slippage.

In the programme, step 9 is the slippage step and step 10 is passive leak. The rates of steps 9 and 10 are varied to observe their effects on the accumulation of Ca^{2+}. For the simulations shown in Figure 3.13 it was assumed that the total concentration of Ca^{2+}-ATPase was 0.175 μM and the concentration of correctly-orientated active Ca^{2+}-ATPase molecules was 0.045 μM, assuming that 50 % of the Ca^{2+}-ATPase is functional and with a random distribution of Ca^{2+}-ATPase molecules across the membrane. Before the addition of ATP the Ca^{2+}-ATPase will be present in its Ca^{2+}-bound form, the initial concentration of $E1Ca_2$ being 0.045 μM. The initial

concentrations of ATP and Ca^{2+} in the external medium are set at 0.8 and 0.12 mM respectively. The remaining factor that needs to be accounted for is the relationship between the internal volume of the vesicles and the external volume of the sample. The Ca^{2+}-sensitive dye antipyrylazo III monitors the change in external Ca^{2+} concentration as Ca^{2+} is pumped into the lumen of the vesicles by the Ca^{2+}-ATPase. The increase in concentration of Ca^{2+} in the lumen of the vesicles will be much greater than the corresponding drop in concentration of Ca^{2+} in the external medium, due to the relatively small lumenal volume. With an external vesicle radius (r_o) of 47 nm, a lipid concentration of 0.8 mg/ml and a lipid: protein ratio of 40:1 (w/w), the internal to external volume ratio is 382.6. This represents the factor by which the concentration of Ca^{2+} changes on moving from the external medium into the vesicle lumen and is included as the factor v in steps 6,7 and 10 of the reaction sequence.

The simulation results are shown in Figure 3.13. In the presence of passive leak, the level of accumulation of Ca^{2+} increases almost linearly with time until the rate of transport of Ca^{2+} into the vesicles is equal to the rate of leak out, at which time the maximal level of accumulation is achieved; this maximal level decreases with increasing leak rate (Figure 3.13A). In contrast, in the presence of slippage the accumulation of Ca^{2+} increases non-linearly with time and the effects of slippage are seen at very short times; the level of accumulation of Ca^{2+} decreases with increasing rate of slippage (Figure 3.13B). These very different patterns of effect mean that passive leak and slippage can easily be distinguished. As shown in Figure 3.14 the experimental data shown in the results section are matched by the slippage model rather than by passive leak. The presence of anionic phospholipid results in increased levels of accumulation of Ca^{2+} as the rate of slippage decreases. The exact shapes of the accumulation curves in the slippage model depend on a number of parameters in

the simulation, but as shown in figure 3.14 good agreement can be obtained between the experimental data and the expectations of the slippage model.

In the simulations, an internal volume of 174 μl/mg protein was assumed (Dalton et al., 1998) with a random orientation of the Ca^{2+}-ATPase across the membrane, in agreement with the experimental data shown in Table 3.1. The proportion of active Ca^{2+}-ATPase in the SR preparations can be determined by measuring the maximal level of phosphorylation observed with ATP in the presence of high concentrations of Ca^{2+}; maximal levels of phosphorylation have been shown to vary between preparations, but are typically about 3.2 nmol/mg protein (Starling et al., 1993), corresponding to 35 % of the Ca^{2+}-ATPase being active. With these parameters, the simulations match the experimental data with slippage rates of 250 s^{-1}, 65 s^{-1} and 0 in the absence of anionic phospholipid and in the presence of 10 mol % di(C18:1)PA and cardiolipin respectively, and with a slippage rate of 45 s^{-1} in the presence of 5 mol % cardiolipin (Table 3.2). Rates of slippage in the presence of di(C18:1)PI are the same as in the presence of di(C18:1)PS or di(C18:1)PA, with the rate of slippage in the presence of di(C18:1)PI(4)*P* being lower (Table 3.2).

We can conclude that in the absence of negatively charged phospholipids the rate of slippage on the Ca^{2+}-ATPase is relatively high. The optimal concentration of negatively charged phospholipid to reduce Ca^{2+} slippage was found to be 10 mol %, approximately the same as the mole fraction of negatively charged phospholipid in the native SR membrane (Lau et al., 1979; Milting et al., 1994). This suggests that reducing the slippage may be important for the physiological function of the Ca^{2+}-ATPase. SR may be able to control levels of Ca^{2+} accumulation through the actions of di(C18:1)PI(4)*P*. Di(C18:1)PI(4)*P* decreases the rate of slippage much more than the equivalent percentage of di(C18:1)PI. The presence in SR of phosphatidylinositol-4-

Kinase and a Ca^{2+}-dependent phosphomonoesterase capable of catalysing the breakdown of di(C18:1)PI(4)P (Varsanyl et al., 1989; Schafer et al., 1987) reinforce the theory regarding control of Ca^{2+} accumulation.

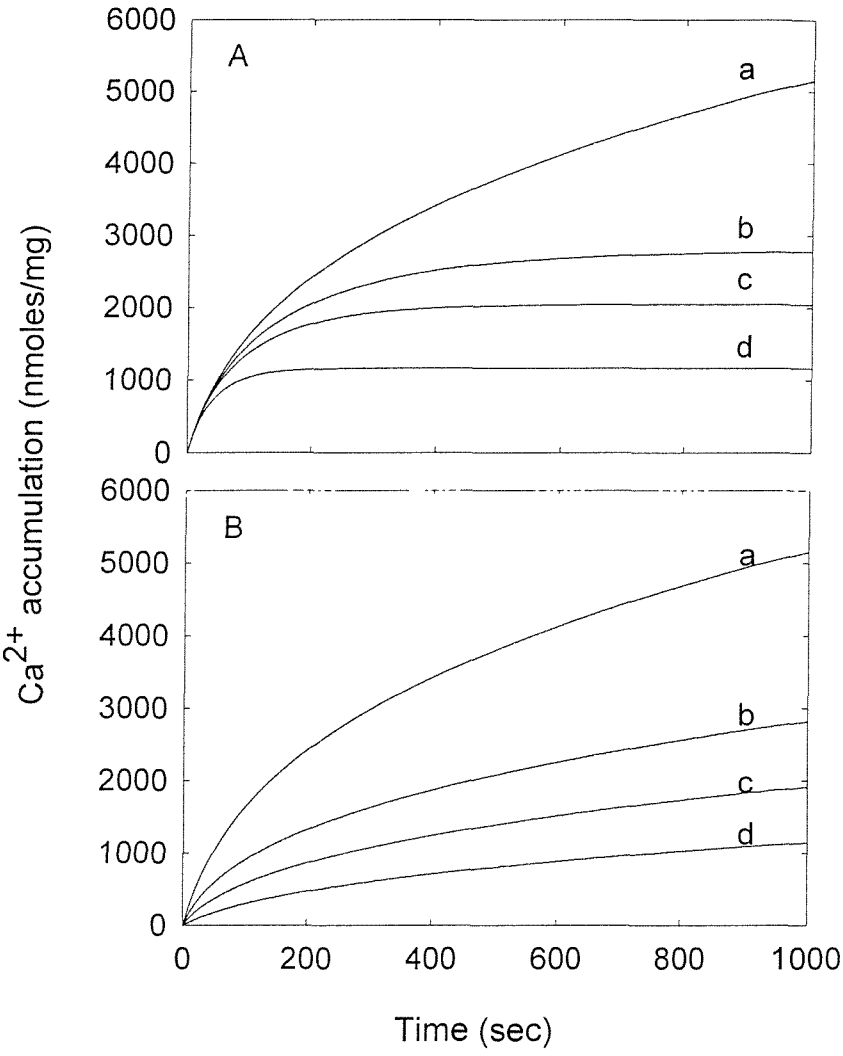

Figure 3.13 Simulations of Ca^{2+} accumulation

Simulations were performed using the parameters described in the text with a concentration of active, outwardly oriented Ca^{2+}-ATPase of 0.045 μM, a lumenal volume of 174 μl/mg protein, and initial Ca^{2+} and ATP concentrations of 120 μM and 0.8 mM respectively. (**A**) shows the effect of simple passive leak, with rates (s^{-1}) for the leak step ($Ca^{2+}{}_i \rightarrow Ca^{2+}{}_o$) of : (a) 0; (b) 5×10^{-6}; (c) 1×10^{-5}; (d) 3×10^{-5}. (**B**) shows the effect of slippage, with rates (s^{-1}) for the slippage step ($E2PCa_2 \rightarrow E2 + Ca^{2+}{}_o + Ca^{2+}{}_o$) of (a) 0; (b) 50; (c) 150; (d) 500.

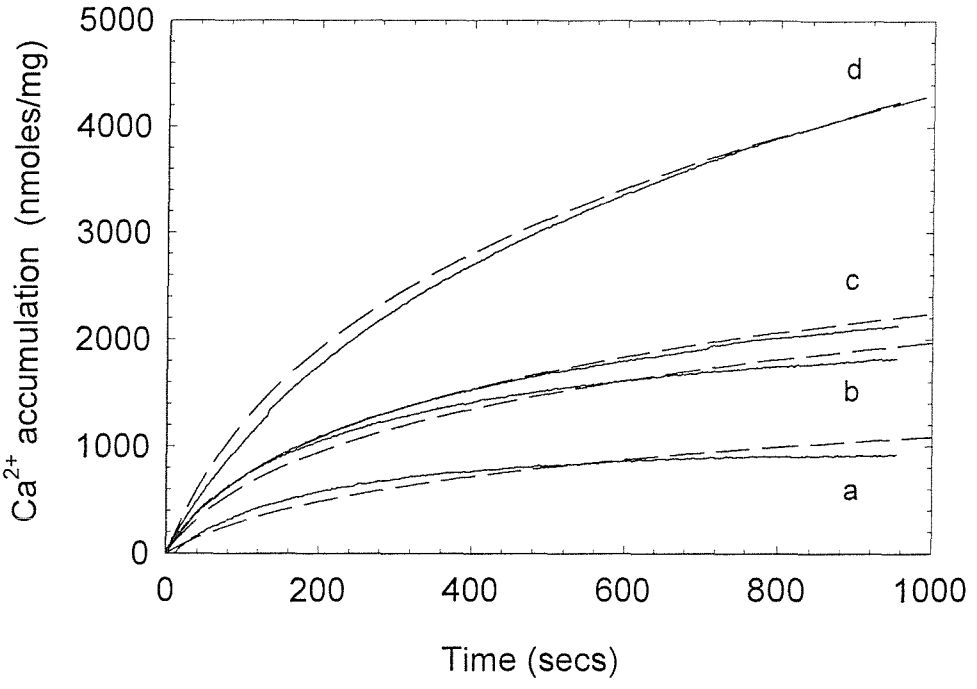

Figure 3.14 ATP-dependent accumulation of Ca^{2+} by reconstituted vesicles and slippage simulations

The solid lines show ATP dependent Ca^{2+} accumulation by reconstituted vesicles containing: (a) di(C18:1)PC; (b) 90 % di(C18:1)PC / 10 % di(C18:1)PA; (c) 95 % di(C18:1)PC / 5 % cardiolipin; (d) 90 % di(C18:1)PC / 10 % cardiolipin. Accumulation of Ca^{2+} was initiated by the addition of 0.8 mM ATP. Samples contained 0.02 mg of protein/ml at a lipid: protein ratio (w/w) of 40: 1 in 10 mM Pipes, pH 7.1, 100 mM K_2SO_4, 5 mM Mg^{2+}, 80 μM Antipyrylazo III, 0.25 μM FCCP and an initial Ca^{2+} concentration of 120 μM. The continuous lines show experimental data and the broken lines show simulations for the slippage model with the parameters given in the text, assuming an internal volume of 174 μl/mg protein, a concentration of active, outwardly oriented Ca^{2+}-ATPase of 0.03 μM and rates for the slippage step (s^{-1}) of: (a) 250; (b) 65; (c) 45; and (d) 0.

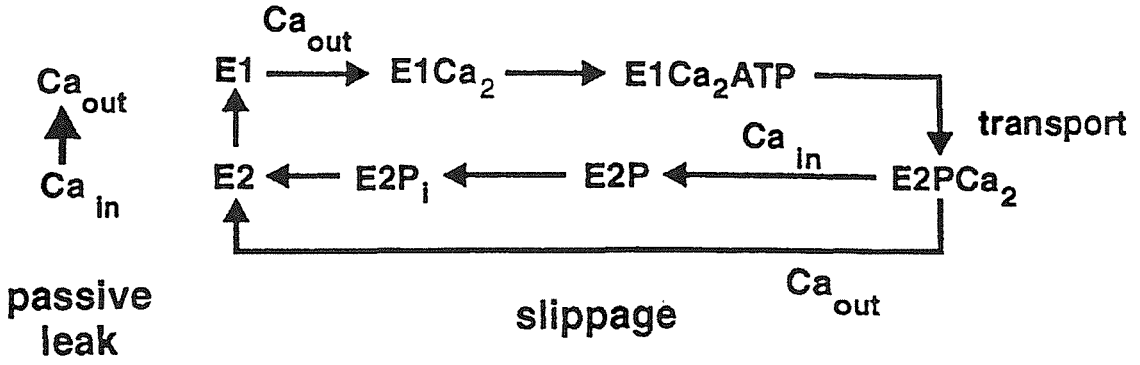

Scheme 3.1 Simplified reaction scheme for the Ca^{2+}-ATPase showing leak and slippage pathways

Lipid	Slippage rate (s^{-1})
Di(C18:1)PC	250
Di(C18:1)PC/10 % di(C18:1)PA	65
Di(C18:1)PC/10 % di(C18:1)PS	65
Di(C18:1)PC/10 % di(C18:1)PI	65
Di(C18:1)PC/10 % di(C18:1)PI(4)*P*	15
Di(C18:1)PC/5 % cardiolipin	45
Di(C18:1)PC/10 % cardiolipin	0

Table 3.2 Rates of slippage ($E2PCa_2 \rightarrow E2P + 2Ca^{2+}$) for the Ca^{2+}-ATPase in reconstituted lipid vesicles

CHAPTER 4: The activity of DGK in mixed micelles and the establishment of a reconstitution system for measuring DGK activity in the bilayer

4.1 Introduction

Functional and structural studies of individual membrane components are very difficult due to the complexity of biological membranes. The enzyme DGK simplifies the task of assessing membrane protein function as it carries out a simple reaction catalysing the direct transfer of the γ-phosphate of ATP to *sn*-1,2,-diacylglycerol (DAG), producing phosphatidic acid (PA) and ADP. This is in contrast to the Ca^{2+}-ATPase, whose mechanism is relatively complex involving at least one phosphorylated intermediate with many steps contributing to the observed overall rate (de Meis, 1981). A further simplification in the characterisation of protein function is the ability to isolate a protein from its native membrane and place it in a membrane of defined lipid composition to study its properties. This is a process known as reconstitution. For efficient reconstitution, the protein must be removed from its native membrane with minimal disruption. The detergent must not denature the protein in any way, as its characteristics will be changed and it may not reconstitute. This is why each protein has a unique purification and reconstitution procedure. DGK activity has usually been determined in the presence of detergent micelles, necessary to solubilise the hydrophobic diacylglycerol substrate (Walsh & Bell, 1986a,b).

4.1.1 Detergents and solubilisation

Detergents are amphiphilic molecules, having both a hydrophilic and a hydrophobic region. The hydrophobic regions are usually one or two alkyl chains in

length and have poor solubility in water, whilst the hydrophilic region is polar and may be charged or uncharged (Lichtenberg et al., 1983). The structures of detergents used for the solubilsation of DGK can be seen in Figure 4.1. Detergents can be classified both on the basis of their charge and/or the nature of the polar and hydrophobic portions (Yanagita & Kagawa, 1986); there are two main categories. The ionic detergents consist of a nonpolar hydrocarbon chain and a charged headgroup region; examples include the anionic detergents SDS and cholate (Yanagita & Kagawa, 1986). The non-ionic detergents consist of a nonpolar hydrocarbon chain and a polar headgroup; examples include octylglucoside (OG) and dodecylmaltoside (DM) in which the headgroup consists of the sugar residues glucose and maltose respectively (Yanagita & Kagawa, 1986). As described in Chapter 3, at a certain concentration detergent molecules aggregate to form micelles. This is known as the critical micelle concentration (CMC) and is defined as the minimum concentration of detergent at which micelles are formed (Lichtenberg et al., 1983). The conditions dictating the CMC value of a detergent can be found in Chapter 3. As a general rule the ionic detergents have high CMC values and form relatively small micelles but can denature proteins at concentrations below their CMCs, whilst the non-ionic detergents usually have low CMC values thus forming larger micelles and are normally milder in action (Yanagita & Kagawa, 1986).

The solubilisation of membrane components by detergent involves the transformation of lamellar phospholipid structures into mixed micelles composed of phospholipid and detergent. The process is detailed in chapter 3 and, as shown in Figure 4.2, is proposed to occur in three stages (Rigaud et al., 1995). In summary, stage 1 involves saturating the bilayer with detergent and the bilayer structure

becomes unstable. Stage 2 involves a structural transition from the bilayer to micellar phase. Stage 3 signals that the bilayer is completely solubilised into mixed micelles.

4.1.2 Detergents as micelles

Previous studies on the activities of membrane-bound enzymes of lipid biosynthesis in artificial membranes have produced little in-depth kinetic data. This is mainly a result of difficulties in delivering hydrophobic and/or amphipathic substrates to the enzymes (Walsh & Bell, 1986a). Complications, including a loss of enzymatic activity resulting from solubilisation with detergents, either by denaturation or by removal of phospholipid cofactors, were frequent. In addition, enzyme activity could be limited by the slow exchange of hydrophobic molecules between vesicles when enzyme and substrate are reconstituted into vesicles (Roseman & Thompson, 1980). In addition, enzyme molecules with active sites facing the inside of a vesicle may be inaccessible to soluble substrates.

The use of mixed micelles can circumvent these problems by providing a precisely defined environment containing enzyme, substrates, and phospholipid (Lichtenberg et al., 1983). In essence an artificial bilayer environment is provided in which the hydrophobic portions of membrane proteins, and lipids, can insert and function (Walsh & Bell, 1986a). However, several criteria must be satisfied before the kinetic data derived from a mixed micellar assay can be appropriately interpreted. Firstly, the enzyme must be completely solubilised by the detergent to ensure the homogeneity of the enzyme microenvironment in the assay. Secondly, the rate of exchange of hydrophobic substrates between the mixed micelles must be sufficiently rapid to maintain the steady state substrate concentration in mixed micelles that

contain enzyme in equilibrium with the bulk solution. Proving that the latter criterion has been met is very important; otherwise the kinetics of substrate transfer between mixed micelles may become confused with the kinetics of the enzyme reaction. Finally, enzyme activities in detergent micelles may be very different to those in a lipid bilayer environment.

4.1.3 DGK and detergent micelles

A mixed micellar assay for DGK has been established with the aim of facilitating studies on the mechanism of DGK and its phospholipid cofactor requirements (Walsh & Bell, 1986a; Lau & Bowie, 1997). In the mixed micelle the hydrophobic region of the protein that is normally located within the membrane is covered by either or both the hydrophobic part of the detergent and the lipid molecules present in the micelle. The findings of the studies of Walsh and Bell (1986a) can be found in detail in chapter 1. In summary, OG was found to be an ideal detergent as DGK was completely solubilised and showed no activity in the absence of an activating lipid, thus allowing studies of activating lipids (Walsh & Bell, 1986a). In addition, no evidence was found for a limitation of the reaction velocity by the rate of diacylglycerol exchange. The activity of DGK in OG micelles in the absence of phospholipid is very low when the substrate is a short-chain diacylglycerol such as dioctanoylglycerol (Walsh & Bell, 1986b). Addition of phospholipids leads to increased activity, cardiolipin being the most efficient phospholipid in restoring activity (Walsh & Bell, 1986b). Higher activities are seen with dioleoylglycerol (DOG) as substrate, but the situation is complex since long-chain diacylglycerols can act as both substrate and activating lipid (Walsh & Bell, 1986b). Walsh et al. (1990)

have shown that, in the presence of activating phospholipids, the lower activities observed for short-chain diacylglycerols follow from higher K_m values for the diacylglycerol with v_{max} values being independent of chain length.

4.1.4 Reconstitution

The most successful methods for the reconstitution of membrane proteins involve the use of detergents. Reconstitution using detergent is generally the reverse of the solubilisation process, whereby bilayer fragments or vesicles form upon the removal or reduction of detergent (Levy et al., 1990b; Rigaud et al., 1995). When the concentration of detergent decreases the number of detergent molecules in the mixed micelles decrease such that micelle-micelle interactions become energetically favourable, and the total number of micelles begins to decrease (Rigaud et al., 1995). As the concentration of detergent is further decreased the number of micelles also decrease and a transformation from the micellar phase will occur; the lipid bilayer will now reform to minimise exposure of hydrophobic regions to the aqueous environment (Rigaud et al., 1995). The method for removal of detergent depends on the particular properties of the detergent used and is detailed Chapter 3.

4.1.5 Developing a reconstitution

To develop a detergent-mediated reconstitution for a membrane protein it is necessary to find a detergent that will solubilise both the protein of interest and the lipid into which it is to be reconstituted, without denaturing the protein. The solubilisation process can be tested by measuring the turbidity of the protein

suspension as a function of detergent concentration. The addition of detergent to a membrane suspension results in the formation of small micelles that scatter light less than the original suspension. Therefore it is possible to measure the extent of solubilisation of a membrane suspension by a detergent and hence gain both an indication of the effectiveness of that detergent under a certain set of conditions and the concentration of detergent needed to form micelles (Hirata, 1986).

Once a suitable detergent has been found and a reconstitution procedure established, the suitability of both the detergent and reconstituting procedure needs to be determined. Sucrose density gradient centrifugation allows separation of macromolecules on the basis of density, and lipid, being less dense, will remain at the top of the gradient, whilst protein will be found in the low dense layers. Reconstituted protein and lipid preparations should be located at an intermediate density. Therefore, if the reconstitution procedure is working properly a band at an intermediate density level should be found (Levy et al., 1992). Protein stability in the detergent of choice is also a very important factor and is easily assessed for DGK by measuring enzyme activity over a fixed period of time.

Here we measure DGK activity in the micelle to facilitate studies on the mechanism and phospholipid cofactor requirements and establishing a reconstitution protocol for DGK, allowing us to measure enzyme activity in a lipid bilayer.

A

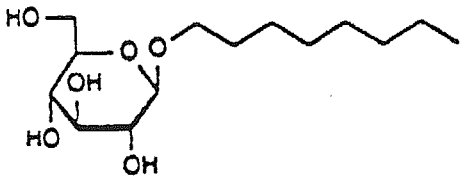

B

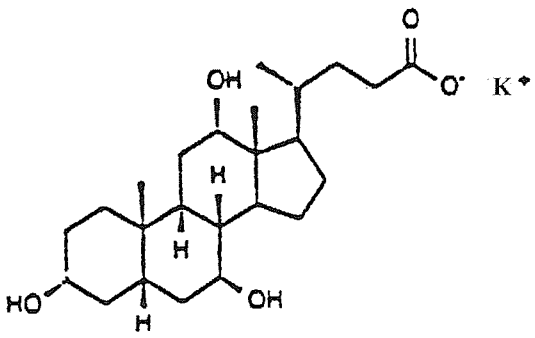

C

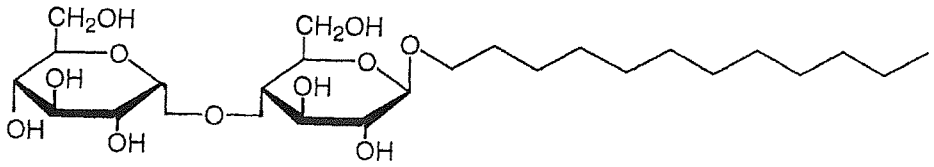

Figure 4.1 Detergents used to solubilise DGK

Octylglucoside (**A**), potassium cholate (**B**), dodecylmaltoside (**C**).

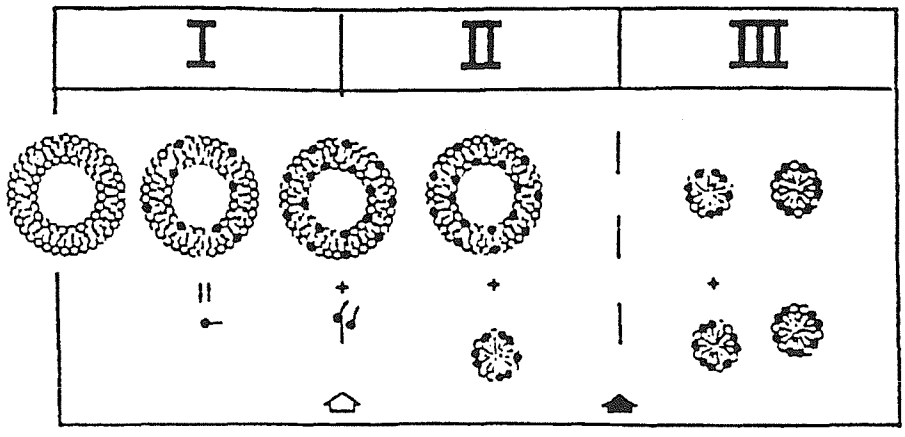

Figure 4.2 The three-stage model of solubilisation of lipid vesicles (Rigaud et al., 1995)

Stage 1 involves saturating the bilayer with detergent and the bilayer structure becomes unstable. Stage 2 involves a structural transition from the bilayer to micellar phase. Stage 3 signals that the bilayer is completely solubilised into mixed micelles.

4.2 Methods

4.2.1 Purification of DGK

A plasmid expressing His-tagged DGK was generously provided by Professor James Bowie of UCLA (California). The plasmid was expressed in *E. coli* strain WH1061 in which the chromosomal DGK gene was disrupted (Lau & Bowie, 1997). DGK was purified as described by Lau and Bowie (1997) and the full procedure is in the methods section. In brief, cells were treated with 3 % (w/v) OG and the solubilised material was adsorbed onto Ni-NTA-agarose resin (Qiagen). Following washing and packing into a column, the detergent was changed to 0.5 % dodecylmaltoside (DM) and the protein was eluted with buffer (50 mM sodium phosphate, 0.3 M NaCl, pH 7.5) containing 0.5 % DM and 0.25 M imidazole. The eluted protein gave a single band on SDS polyacrylamide gel electrophoresis and was flash frozen in liquid nitrogen and stored at –80 °C. Protein concentrations were estimated using an extinction coefficient of 25,200 $M^{-1}cm._1$ at 280 nm.

4.2.2 Mixed micellar assay of DGK activity

DGK activity in the micelle was measured using a coupled enzyme assay based on the one developed by Lau and Bowie (1997). The concentrations of the components were adjusted so that the DGK-catalysed reaction was rate limiting, and the optical density (OD) of NADH was not compromising the sensitivity of the assay. 2.5 μmol of the diacylglycerol and 1.34 μmol of the required phospholipid (if needed) were dried from choloroform solution onto the walls of a thin glass vial. Buffer (6.4 ml; 60 mM Pipes, pH 6.85) containing 64 mM OG was added and the sample

sonicated to clarity in a bath sonicator (Ultrawave). 0.8 ml of this sample was used to make up each assay cuvette. The assay was initiated by the addition of 4 μg DGK into 1 ml of the assay buffer described below.

4.2.3 Reconstitution of DGK

4.2.3.1 Preparation of potassium cholate

Potassium cholate was prepared by dissolving equimolar quantities of cholic acid and potassium hydroxide in methanol, followed by precipitation of potassium cholate from the methanol solution by addition of an excess of diethyl ether and leaving overnight at 4 °C. The solvent was then filtered off and the solid potassium cholate remaining was dried under vacuum for about 12 hrs. The potassium cholate was then stored at room temperature, away from direct light, until required.

4.2.3.2 Light scatter measurements

The solubility of DGK and phospholipids in a number of detergents was determined by plotting graphs of detergent concentration against degree of light scatter. An SLM 8000C fluorimeter was used to measure light scatter at an excitation and emission wavelength of 500 nm. Slit widths of 2 nm were used for excitation and emission. All solutions were made in 60 mM Pipes, pH 6.85. The detergents tested were OG, DM and potassium cholate. Final concentrations of 5 μM protein and 0.56 mM phospholipid were used in 3 ml 60 mM Pipes, pH 6.85. A control sample containing detergent minus protein and lipid was measured, and the values subtracted to correct the results.

4.2.3.3 Preparation of SM_2 Bio-Beads

Washed Bio-Beads were prepared by adding 5 g of SM_2 Bio-Beads (mesh size 20-50) to 50 ml of methanol and stirring gently for 15 min. The Bio-beads were collected on a sintered glass funnel and washed thoroughly with methanol (100 ml). The Bio-Beads were then immediately washed with 200 ml buffer A (10 mM Pipes/100 mM K_2SO_4, pH 7.1) before being loaded into a column where they were slowly washed (2 hrs) with 400 ml of buffer A. After completion of this wash the Bio-Beads were immersed in buffer A and stored at 4°C until required.

4.2.3.4 Reconstitution into lipid bilayers using the dialysis method

Purified DGK was reconstituted into lipid bilayers by mixing lipid and DGK in cholate followed by detergent removal by dialysis. Phosphatidylcholine (24 μmol) and 6 μmol 1,2-dihexanoylglycerol (DHG) were dried from choloroform solution onto the walls of a thin glass vial. Buffer (1200 μl; 60mM Pipes, pH 6.85) containing 28 mM cholate was added and the sample was sonicated to clarity in a bath sonicator (Ultrawave). DGK (66 μg) was added to obtain a lipid to protein molar ratio of 6000:1 and the suspension left at room temperature for 15 min, followed by dialysis against 1 litre of 60 mM Pipes, pH 6.85 for 2 x 3 hr periods at 4 °C with one change of buffer. The buffer contained 10 g of washed amberlite resin to remove the cholate. Fractions were assayed for protein content by using a modified Lowry assay from Sigma. The assay was initiated by the addition of 200 μl of the reconstituted sample into 1 ml of the assay buffer described below.

4.2.3.5 Reconstitution into lipid bilayers using the Bio-Bead method

Purified DGK was reconstituted into lipid bilayers by mixing lipid and DGK in OG followed by detergent removal using Bio-Beads. Reconstituted vesicles were prepared by a modification of the method described by Levy et al. (1992). Phosphatidylcholine (24 μmol) and 6 μmol 1,2-dihexanoylglycerol (DHG) were dried from choloroform solution onto the walls of a thin glass vial. The lipid was resuspended in 1.4 ml of buffer (60 mM Pipes, pH 6.85) and sonicated in a bath sonicator (Ultrawave Model U100) for approximately 5 mins. The lipid sample was diluted to 4 mg lipid/ml using buffer A. OG was added with mixing to a final concentration of 40 mM. DGK (66 μg) solubilised in 0.5 % (w/v) DM was added with mixing to give a lipid to protein ratio of 6000:1. Detergent was removed by addition of four aliquots of washed SM_2 Bio-Beads, as described by Levy et al. (1992), to give the final preparation of vesicles. The sample was kept on ice and used for experimentation within 6 hr. Fractions were assayed for protein content by using a modified Lowry assay from Sigma. The assay was initiated by the addition of 200 μl of the reconstituted sample into 1 ml of the assay buffer described below.

4.2.3.6 Reconstitution into lipid bilayers using the dilution method

Purified DGK was reconstituted into lipid bilayers by mixing lipid and DGK in OG or cholate followed by dilution to decrease the concentration of detergent below its critical micelle concentration. Phospholipid (8 μmol) and the required concentration of diacylglycerol (usually 2 μmol 1,2-dihexanoylglycerol) were dried from choloroform solution onto the walls of a thin glass vial. Buffer (400 μl; 60mM

Pipes, pH 6.85) containing 94 μM OG or 28 mM cholate was added and the sample was sonicated to clarity in a bath sonicator (Ultrawave). DGK (22 μg) was added to obtain a lipid to protein molar ratio of 6000:1 and the suspension left at room temperature for 15 min, followed by incubation on ice until use. The assay was initiated by the addition of 20 μl, representing a 50-fold dilution, of the reconstitution mixture into 1 ml of the assay buffer described below.

4.2.3.7 Assay of DGK activity

DGK activity was measured using a coupled enzyme assay based on that developed for studies of the Ca^{2+}-ATPase (Warren et al., 1974b) and modified according to the one developed by Lau & Bowie (1997). The production of ADP by the action of DGK on ATP was coupled to the oxidation of NADH through pyruvate kinase and lactate dehydrogenase. The assay medium consisted of buffer (60 mM Pipes, pH 6.85) containing phosphoenolpyruvate (2 mM), NADH (0.2 mM), ATP (5 mM), Mg^{2+} (20 mM), pyruvate kinase (18 units), and lactate dehyrogenase (22 units). The mixture was incubated at 25 °C for 10 min to ensure that any residual ADP in the ATP sample was consumed. For studies in which DGK activity was measured in micelles of OG, the assay medium also contained 5.1 mol% 1,2-dioleoyl-sn-glycerol or 5.1 mol % 1,2-dihexanoyl-sn-glycerol with 2.4 mol% of the required phospholipid, and 92.5 mol % OG, as described above. The assay was initiated by addition of 4 μg DGK to 1 ml of the assay medium. For studies of DGK reconstituted into phospholipid bilayers, the reaction was initiated by addition of 1.5 μg DGK dissolved in cholate with phospholipid and DHG to 1 ml of the assay medium. The oxidation of

NADH was monitored by the decrease in absorbance at 340 nm, which was related to DGK activity by the following equation:

$$\text{Activity } (\mu\text{moles/min/mg}) = (\Delta OD_{340}\ \text{min}^{-1}.\ \text{vol}) / (\text{DGK}.\ \varepsilon_{340})$$

$\Delta OD_{340}\ \text{min}^{-1}$ = change in optical density at 340 nm per min

vol = volume in cuvette (ml)

DGK = amount of DGK protein in cuvette (mg)

ε_{340} = extinction coefficient of NADH at 340 nm ($M^{-1}\ cm^{-1}$)

4.2.3.8 Sucrose density centrifugation

Gradient centrifugation was used to characterise the reconstituted preparation. Di(C18:1)PC (20 μmol) was mixed with [^{3}H]dipalmitoylphosphatidylcholine (0.2 nmol) in chloroform and dried onto the walls of a glass vial. The mixture was resuspended in 0.8 ml buffer (10 mM Pipes, 100 mM K_2SO_4, pH 7.1) containing 28 mM cholate. The sample was sonicated to clarity in a sonication bath (Ultrawave). DGK (150 μg) was added and the mixture left at room temperature for 15 minutes. The sample was then dialysed at 4 °C against two lots of buffer (500 ml; 10 mM Pipes, 100 mM K_2SO_4, pH 7.1) for a total of 5 hours. Samples of dialysate (0.4 ml) were then loaded onto sucrose gradients containing the following solutions of sucrose (w/w) in 10 mM Pipes, 100 mM K_2SO_4, pH 7.1: 2.5, 5.0, 10.0, 20.0, and 30 %. The 30 % sucrose solution also contained 0.05 % (w/v) Triton X-100. Samples were spun at 80,000 g for 18 h at 4 °C and then 1 ml fractions were collected from the gradients

and analysed for lipid and protein content by, respectively, liquid scintillation counting and a modified Lowry protein assay (Sigma Diagnostics).

4.3 Results

4.3.1 DGK purification and solubilisation

DGK was purified according to the method of Lau & Bowie (1997). The typical yield of purified protein was in the range of 50-70 mg of pure enzyme from 12 g of wet cell paste (approximately 4 litres of culture). The solubility of both DGK and DGK with lipid was tested in the non-ionic detergents OG and DM and the ionic detergent cholate, by measuring light scatter as a function of detergent concentration. As can be seen in Figure 4.3, for complete solubilisation of DGK a DM concentration of approximately 5-9 mM is required. This figure corresponds with the DM concentration of 10.34 mM that is used to both elute and store DGK (Lau & Bowie, 1997). An OG concentration of approximately 30 mM was required for complete solubilisation of DGK (Figure 4.4) and corresponds well to the CMC of OG, which is 25 mM. For the mixed micellar and reconstitution assays of DGK we also needed to know what concentration of detergent was required to solubilise the phospholipid and diacylglycerol lipid present. The effect of OG on the turbidity of phosphatidylcholine and a mixture of phosphatidylcholine and 1,2-dihexanoylglycerol (DHG) can be seen in Figures 4.5 and 4.6 respectively. In both, an OG concentration of approximately 25 mM was required for complete solubilisation. The turbidity of DGK, phospholipid and DHG as a function of OG and potassium cholate concentration can be seen in Figures 4.7 and 4.8, respectively. These two light scattering experiments were performed at a ratio of lipid to protein the same as that we were planning to use in the reconstitution of DGK. As can be seen, OG and cholate concentrations of approximately 25 mM and 11 mM respectively were required for complete solubilisation of DGK in a lipid mixture of di(C18:1)PC and DHG. The concentration

of cholate required for solubilisation corresponds well with the CMC of potassium cholate of 13-15 mM.

4.3.2 Mixed micellar assay of DGK

The development of a mixed micellar assay for DGK provided an initial system for the analysis of the possible cofactor requirements and the reaction mechanism. As described in the methods section, our mixed micellar assay was based on the one developed by Lau and Bowie (1997). Initially, DGK activity was assayed in 1.5 % (w/v) OG, corresponding to an OG concentration of 51 mM, with 1,2-dioleoyl-sn-glycerol (DOG) as substrate and cardiolipin as the lipid activator. DOG and cardiolipin were present at 5.1 mol % and 2.4 mol % respectively, expressed relative to the total amount of detergent and lipid present. The light scatter results show that an OG concentration of 51 mM is more than sufficient to solubilise DGK and the contents of the assay.

DGK has an absolute requirement for a phospholipid cofactor in OG micelles and cardiolipin has been reported to be the best activator (Walsh & Bell, 1986a). We investigated, using DOG as substrate, whether other phospholipids behaved as lipid activators and stimulated DGK activity (Table 4.1). The chosen phospholipids were di(C18:1)PC, di(C14:1)PC, di(C22:1)PC, di(C18:1)PA, di(C18:1)PS, and di(C18:1)PE. We found that DGK activity was identical with each phospholipid when using DOG as substrate. However, when a control experiment was performed in the absence of any phospholipid, DGK activity remained at the same level. This is consistent with published reports that long chain diacylglycerols can act both as substrate and as activating lipid (Walsh & Bell, 1986b). In contrast, the activity of

DGK against the short chain diacylglycerol 1,2-dihexanoylglycerol (DHG) in OG micelles is very low in the absence of added phospholipid (Table 4.1). Addition of di(C18:1)PC, di(C18:1)PE or di(C18:1)PS had little effect on activity but addition of di(C18:1)PA led to a small increase in activity and addition of cardiolipin led to a large increase in activity. This is consistent with published reports stating that, in the presence of short-chain diacylglycerols, DGK has an absolute requirement for an added lipid cofactor, with cardiolipin being the best (Walsh & Bell, 1986a).

4.3.3 Reconstitution of DGK into lipid bilayers

Because it was shown that DOG acted both as substrate and as lipid activator, for studies of lipid effects on the activity of DGK we have used DHG as substrate. The light scatter results have shown that both octylglucoside and cholate are suitable detergents for reconstitution studies of DGK. The first step in the reconstitution of DGK involved mixing DGK in 0.5 % DM with a phospholipid/DHG mixture, normally containing 20 mol % DHG, solubilised in 28 mM cholate to give a molar ratio of phospholipid to DGK of 6000:1. This ratio was chosen to ensure the appropriate DHG: DGK ratio, as described below. The mixture was incubated for 15 min at room temperature, and was stored on ice until use. The reconstitution mixture was diluted 50 fold into buffer, decreasing the concentration of cholate below its critical micelle concentration (10 mM; (Lee, 2000)), reforming membrane fragments; dilution factors between 20 and 200 fold were found to be equally effective (Table 4.2).

An important requirement for the success of the reconstitution procedure is that DGK has to be reconstituted into a bilayer already containing the diacylglycerol

substrate. Further, the amount of diacylglycerol in the bilayer has to be sufficient for steady state kinetics to be measurable over a time period of several minutes. Figure 4.9 shows ATP hydrolysis recorded as a function of time for DGK reconstituted into bilayers of di(C18:1)PC containing DHG at mol % DHG values of 20 % and 7.5 %, at a molar ratio of di(C18:1)PC:DGK of 4000:1. As shown for bilayers containing 20 mol % DHG, linear kinetics are observed for 100 secs (Red curve) whereas for bilayers containing 7.5 mol % DHG, linear kinetics are observed for about 15 secs (Blue curve).

The rate measured with 20 mol % DHG as substrate in bilayers of di(C18:1)PC is ca 65 μmoles/min/mg (Table 4.2), when reconstituted using cholate as detergent followed by detergent removal by either dilution or dialysis. This is comparable to the activity with DOG as substrate observed in the OG micelles (Table 4.1). Walsh et al. (1990) have shown that changing the chain length of the diacylglycerol substrate affects only K_m ands not v_{max}. The similar v_{max} values for DHG in reconstituted bilayers and for DOG in micelles therefore shows that the cholate dilution procedure forms unsealed membrane fragments, as observed when the Ca^{2+}-ATPase was reconstituted in this way (Warren et al., 1974a). If sealed vesicles had been formed with a random distribution of DGK across the bilayer, a maximum activity 50 % of v_{max} would have been observed because lipid bilayers are impermeable to ATP. The fact that sealed vesicles were not formed was confirmed by the addition of $C_{12}E_8$ to the sample did not bring about an increase in activity (Table 4.3). If sealed vesicles had been formed then the detergent $C_{12}E_8$ would have 'punched' holes in the vesicles, making them permeable to ATP, which would have led to a doubling of activity as the inwardly facing DGK became accessible to ATP. DGK was also reconstituted using OG as detergent instead of cholate. In this case

activities observed following detergent removal by dilution into buffer or by using Bio-Beads were half those observed in detergent micelles and when reconstituted using cholate, suggesting the formation of sealed vesicles (Table 4.3). This was confirmed when the addition of $C_{12}E_8$ led to approximately a doubling of activity when DGK was reconstituted into di(C18:1)PC using OG as detergent, followed by detergent removal by either dilution or Bio-Beads (Table 4.3).

The observed maximum decrease in NADH absorption agreed closely with the expected decrease if all the diacylglycerol in the membrane had been converted to phosphatidic acid. For example, total conversion of the 20 mol % DHG in Figure 4.9 would lead to the production of 98 nmoles of ADP and to a decrease in NADH absorption of 0.61, in good agreement with the measured value of 0.53. This shows that DGK mixes properly with diacylglycerol and phospholipid on reconstitution; a mixed system in which significant amounts of membrane lack DGK does not form.

The dilution experiments detailed in Table 4.2 confirm that the majority of the added DHG partitions into the phospholipid bilayer. The partition coefficient K_p for DHG between the lipid bilayer and the aqueous phase is defined as

$$K_p = [DHG]_L / [DHG]_w \qquad (1)$$

where $[DHG]_L$ and $[DHG]_w$ are the concentrations of DHG in the phospholipid bilayer and the aqueous phase, respectively, in units of moles/litre. This can be written more conveniently as

$$K_p = (n_{DHG})_L / (n_{DHG})_w \beta[L] \qquad (2)$$

where (n_{DHG})L and (n_{DHG})w are the number of moles of DHG in the phospholipid and aqueous phases respectively, [L] is the concentration of phospholipid (moles/litre of the aqueous medium) and β is the volume of a mole of lipid in litre/mole. The fraction of the added DHG that is bound to the phospholipid bilayer is thus given by

$$fraction\ bound = (n_{DHG})_L / [(n_{DHG})_L + (n_{DHG})_w] = 1/ [1 + 1/ K\beta[L]] \qquad (3)$$

If $K\beta[L] > 1$ then essentially all the added DHG will be bound to the bilayer. However, for smaller values of $K\beta[L]$ the added DHG will be only partly bound, the fraction bound decreasing with decreasing concentration of phospholipid. For example, if 50 % of the added DHG is bound at one particular phospholipid concentration, at a ten fold lower concentration of phospholipid the fraction of DHG that is bound will be only 5 %. As described later, DGK activity is dependent on the concentration of DHG and a large change in the bound concentration of DHG would result in a significant change in measured activity. As shown in Table 4.2, a ten fold change in the concentration of phospholipid at a fixed molar ratio of DHG to phospholipid had no effect on the measured activity of DGK, consistent with all the added DHG being membrane bound.

The reconstituted DGK was also characterised by centrifugation on a discontinuous sucrose gradient (Figure 4.10). When DGK and lipid were run separately on the gradient, all the DGK was found at the bottom of the gradient and all the lipid at the top. In contrast, when DGK was mixed with di(C18:1)PC in cholate followed by dialysis to remove the detergent, DGK was found at the 10 % sucrose interface, together with the lipid (Figure 4.10). The molar ratio of lipid:protein for the DGK-containing fraction was 2250:1, compared to 1750:1 in the original mixture. This molar ratio gives an average density for the sample of 1.033,

corresponding to a density between that of a 6 % sucrose solution (density 1.0219) and a 10 % sucrose solution (density 1.0381), agreeing with the location of the sample at the interface between the 6 and 10 % sucrose solutions (Figure 4.10). The experiment shows that reconstitution has resulted in a homogeneous sample.

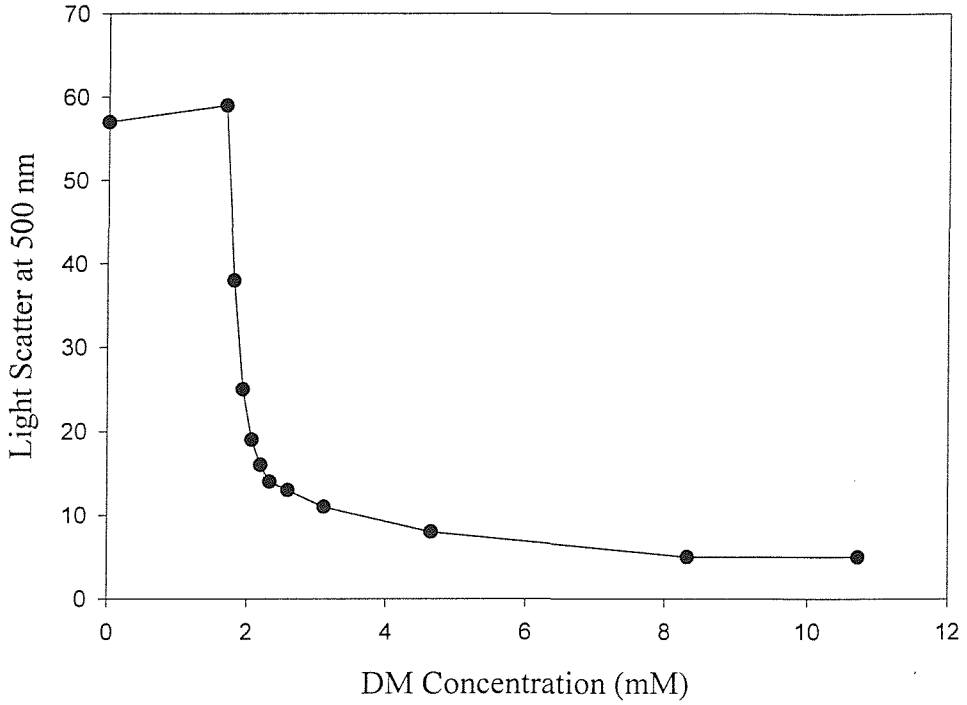

Figure 4.3 Effect of the detergent DM on the turbidity of DGK

The turbidity of DGK at a concentration of 5 μM was monitored as a function of increasing DM concentration. The buffer used was 60 mM Pipes, pH 6.85 at 25 °C. The light scatter was recorded on a fluorimeter using excitation and emission wavelengths of 500 nm.

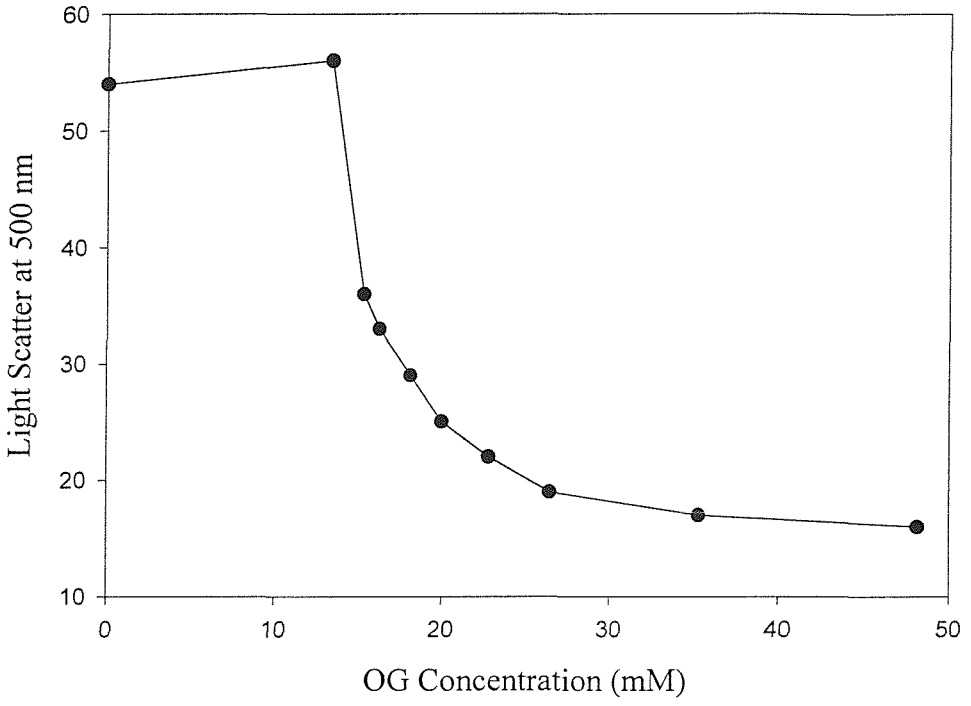

Figure 4.4 Effect of the detergent OG on the turbidity of DGK

The turbidity of DGK at a concentration of 5 μM was monitored as a function of increasing OG concentration. The buffer used was 60 mM Pipes, pH 6.85 at 25 °C. The light scatter was recorded on a fluorimeter using excitation and emission wavelengths of 500 nm.

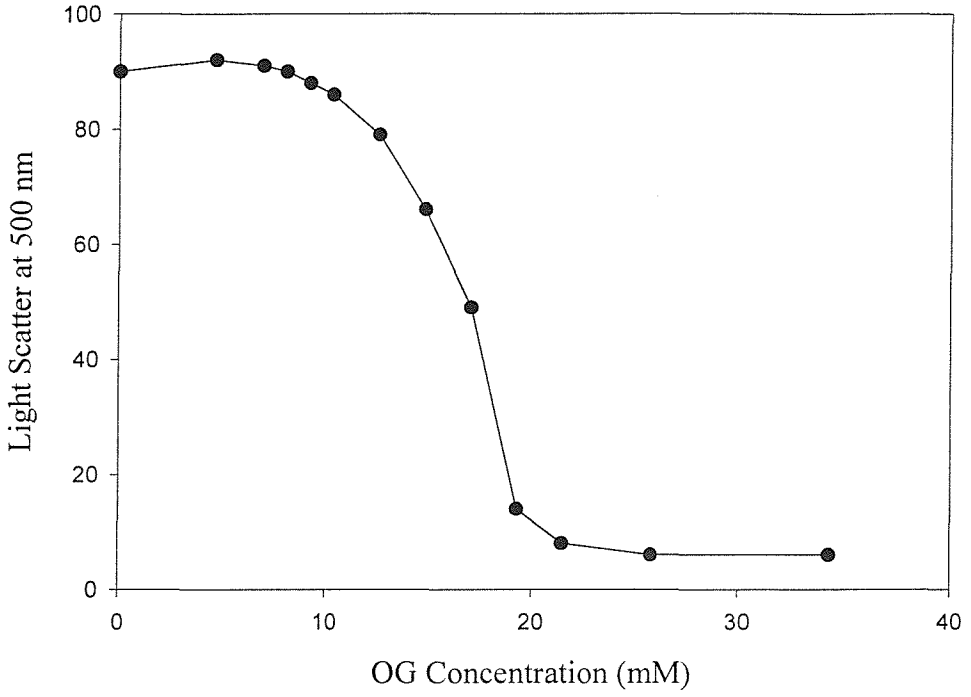

Figure 4.5 Effect of the detergent OG on the turbidity of di(C18:1)PC

The turbidity of dioleoylphosphatidylcholine (di(C18:1)PC) at a concentration of 0.56 mM was monitored as a function of increasing OG concentration. The buffer used was 60 mM Pipes, pH 6.85 at 25 °C. The light scatter was recorded on a fluorimeter using excitation and emission wavelengths of 500 nm.

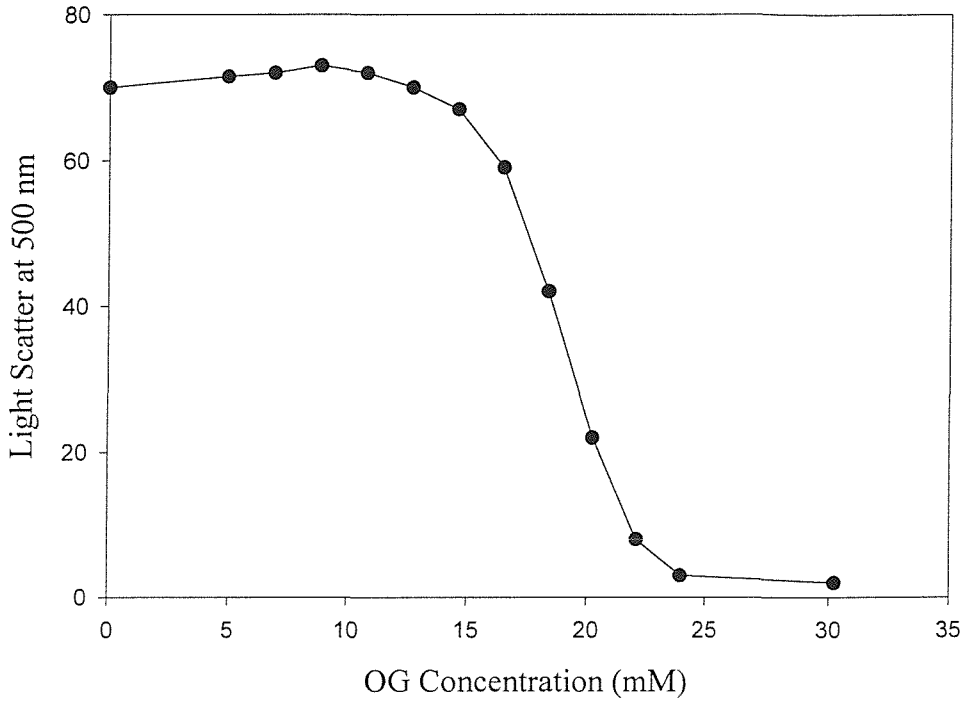

Figure 4.6 Effect of the detergent OG on the turbidity of a mixture of di(C18:1)PC and DHG

The turbidity of a dioleoylphosphatidylcholine (di(C18:1)PC) and 1,2-dihexanoylglycerol (DHG) mixture, at a molar ratio of di(C18:1)PC to DHG of 8:1, was monitored as a function of increasing OG concentration. The buffer used was 60 mM Pipes, pH 6.85 at 25 °C. The light scatter was recorded on a fluorimeter using excitation and emission wavelengths of 500 nm.

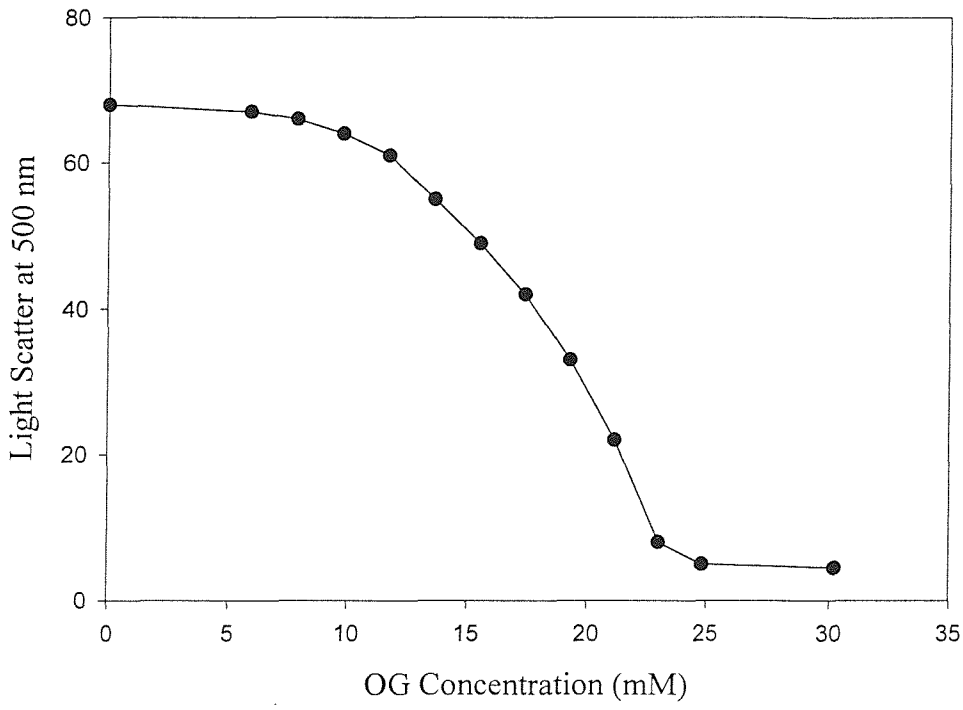

Figure 4.7 Effect of the detergent OG on the turbidity of a mixture of di(C18:1)PC, DHG and DGK

The turbidity of a dioleoylphosphatidylcholine (di(C18:1)PC) and 1,2-dihexanoylglycerol (DHG) mixture, at a molar ratio of di(C18:1)PC to DHG of 8:1, containing DGK at a molar ratio of total lipid to DGK of 6000:1 was monitored as a function of increasing OG concentration. The buffer used was 60 mM Pipes, pH 6.85 at 25 °C. The light scatter was recorded on a fluorimeter using excitation and emission wavelengths of 500 nm.

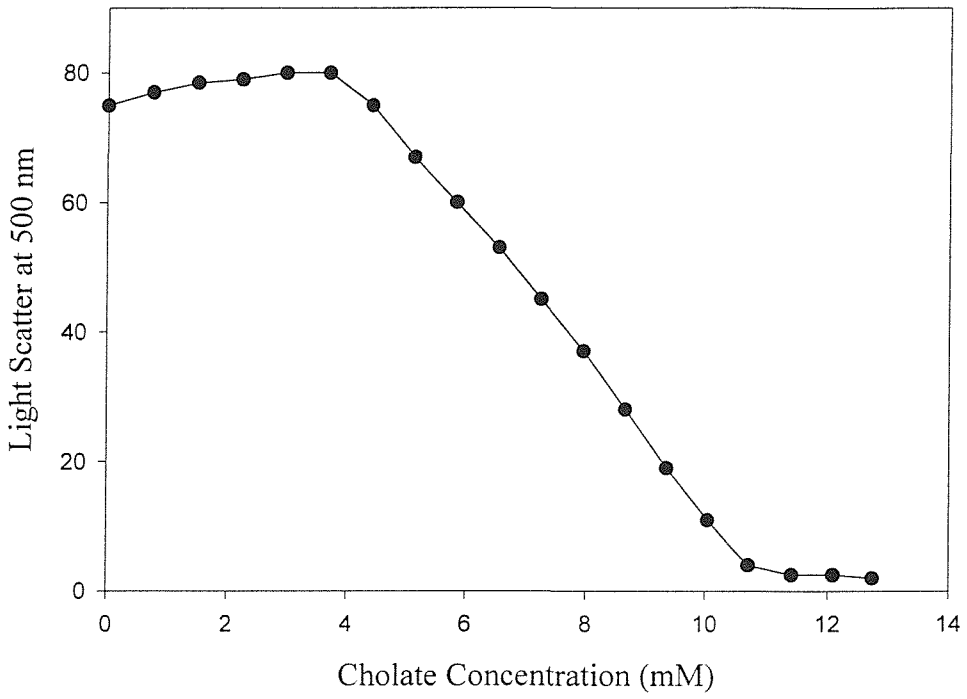

Figure 4.8 Effect of the detergent potassium cholate on the turbidity of a mixture of di(C18:1)PC, DHG and DGK

The turbidity of a dioleoylphosphatidylcholine (di(C18:1)PC) and 1,2-dihexanoylglycerol (DHG) mixture, at a molar ratio of di(C18:1)PC to DHG of 8:1, containing DGK at a molar ratio of total lipid to DGK of 6000:1 was monitored as a function of increasing cholate concentration. The buffer used was 60 mM Pipes, pH 6.85 at 25 °C. The light scatter was recorded on a fluorimeter using excitation and emission wavelengths of 500 nm.

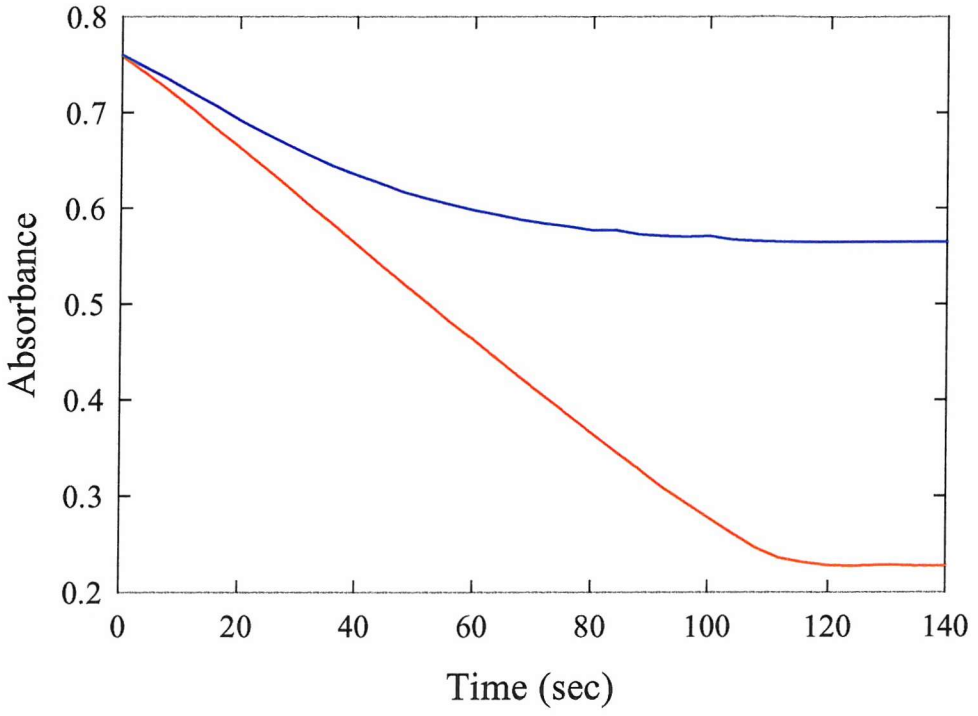

Figure 4.9 Kinetics of ATP hydrolysis for reconstituted DGK

ATP hydrolysis was coupled to the oxidation of NADH and followed by the decrease in absorbance at 340 nm. DGK was reconstituted at a molar ratio of di(C18:1)PC:DGK of 4000:1 into bilayers of di(C18:1)PC containing a mol % of DHG of 20 % (red trace) or 7.5 % (blue trace). The concentration of DGK was 5 μg/ml.

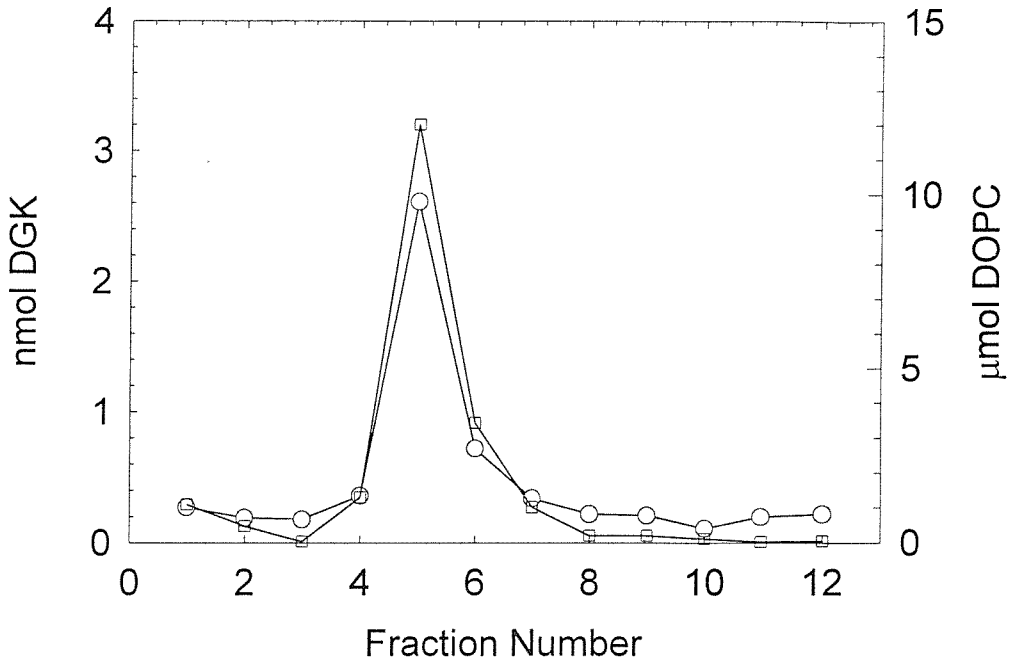

Figure 4.10 Sucrose density gradient analysis of the reconstituted DGK

A sample of DGK reconstituted with di(C18:1)PC at a lipid:protein molar ratio of 1750:1 was separated on a discontinuous sucrose gradient from 30 to 2.5 % sucrose. 1 ml fractions were taken and analysed for lipid (□; right hand axis) and DGK (O; left hand axis).

Phospholipid	Activity against DOG (μmoles/min/mg protein)	Activity against DHG (μmoles/min/mg protein)
Di(C18:1)PC	63.3	1.5
Di(C14:1)PC	58.3	-
Di(C22:1)PC	66.2	-
Di(C18:1)PE	65.1	1.8
Di(C18:1)PS	67.1	1.2
Di(C18:1)PA	70.3	6.8
Cardiolipin	72.6	24.2
No added phospholipid	65.3	1.0

Table 4.1 Steady-state activities of DGK in micelles of OG with 1,2-dioleoylglycerol (DOG) or 1,2-dihexanoylglycerol (DHG) as substrate

The activity of DGK was measured according to the experimental conditions described in the methods section, in 1.5 % (w/v) OG at 25 °C. In all assays the concentrations of phospholipid and diacylglycerol were 2.4 and 5 mol %, respectively, except when no phospholipid was present when concentration of diacylglycerol was 4.6 mol %. All concentrations are expressed as a mol % of the mixture of OG, phospholipid and diacylglycerol.

Dilution factor	Final concentration (μM) of di(C18:1)PC	Final concentration (μM) of DHG	Activity against DHG (μmoles/min/mg protein)
20	900	225	58.5
33	540	135	59.3
50	360	90	59.8
200	90	22	60.3

Table 4.2 Effects of dilution on DGK activity

DGK (22 μg) was incubated with di(C18:1)PC (8 μmoles) and DHG (2 μmoles) in cholate and then diluted by the given factor into 1 ml of assay medium and the activity determined.

Reconstitution detergent and method of removal	DGK activity (μmoles/min/mg protein) in the absence of $C_{12}E_8$	DGK activity (μmoles/min/mg protein) in the presence of $C_{12}E_8$
Potassium cholate - dilution	55	47
Potassium cholate - dialysis	53	50
Octylglucoside - dilution	27	54
Octylglucoside – Bio-Beads	26	50

Table 4.3 Steady-state DGK activities under different methods of detergent removal

The activity of DGK was measured according to the experimental conditions described in the methods section, in 60 mM Pipes, pH 6.85 at 25 °C, at a constant molar ratio of 6000:1 phospholipid:DGK and the given mol % DHG. The concentration of 1,2-dihexanoylglycerol (DHG) was 20 mol % in di(C18:1)PC bilayers. When present, $C_{12}E_8$ was used at a concentration of 0.8 mg/ml.

4.4 Discussion

The assay of DGK in mixed micelles has demonstrated that DGK has an absolute requirement for a lipid cofactor. Activity in the presence of OG and 1,2-dioleoyl-sn-glycerol (DOG) was shown to be due to DOG acting as both substrate and activator (Table 4.1; Walsh & Bell, 1986a). The absolute dependence on an added lipid cofactor when 1,2-dihexanoyl-sn-glycerol (DHG) is employed (Table 4.1) indicates that DHG cannot act as a lipid cofactor for DGK, a fact possibly attributable to its short alkyl chain. Detergent is required in the mixed micellar assay to disperse and deliver water-insoluble lipid substrates and cofactors to the enzyme. Here, octylglucoside provides a non-activating inert matrix into which the lipid cofactors and substrates can be added. Since DOG can act as activating lipid, we decided to use DHG as substrate. Walsh & Bell (1990) examined over forty-seven structural analogues of 1,2-diacyl-sn-glycerol as substrates using mixed micellar assay methods. It was shown that 1,2-diacyl-sn-glycerols varying in chain length from diC_6 to $diC_{18:1}$ were all substrates for DGK (Walsh & Bell, 1990), and that the primary determinant of diacylglycerol recognition by DGK is the glycerol backbone and ester linkages. We chose the substrate DHG (diC_6) since the short chain is long enough to ensure bilayer anchoring but short enough not to disrupt the host bilayer; it is also a very poor activator (Walsh & Bell, 1990). The fact that DHG is a poor activator makes it more appealing as it will be a very convenient substrate for the examination of lipid cofactor dependencies.

The fact that DHG is not an activator of DGK has enabled us to study the roles of phospholipids as activators of DGK. As shown in Table 4.1, cardiolipin is the best activator followed by phosphatidic acid. Phosphatidylcholine, phosphatidylserine, and phosphatidylethanolamine were seen to not activate at all. Lipids with anionic

headgroups are generally better activators than similar lipids with neutral head groups (Walsh & Bell, 1986a). This explains the effects of cardiolipin and phosphatidic acid, but not phosphatidylserine. The greater activity observed for cardiolipin could be due to a combination of its double negative charge and the combined length of its acyl chains.

Although a mixed micellar assay is very useful for the assay of DGK activity, it does represent a very artificial environment. That is why a reconstitution procedure for the reconstitution of DGK into phospholipid bilayers was required. We have established a protocol by which the DGK can be reconstituted into lipid bilayers containing DHG as substrate. With 20 mol % of DHG in the lipid bilayer, linear steady-state kinetics can be recorded for up to 100 seconds when the molar ratio of DHG: DGK is 800:1 (Figure 4.9). The normal substrate for DGK is a diacylglycerol with fatty acyl chains of length about C18. These DAGs will be fully membrane bound and thus the binding site for diacylglycerol on DGK is likely to be accessible from the lipid bilayer. An important parameter in any kinetic analysis of DHG as a substrate for DGK will therefore be the proportion of the total DHG that is bound to the membrane. If DHG partitions between water and the lipid bilayer with a significant fraction of the DHG remaining in the aqueous phase then decreasing the concentration of lipid in the sample will decrease the proportion of DHG bound to the bilayer, according to Equation 3. Varying the concentration of phospholipid was, in fact, found to have no effect on DGK activity against DHG (Table 4.2) so that, under the conditions of these experiments, the bulk of the DHG must be membrane bound.

Long chain diacylglycerols have complex effects on the properties of phospholipid bilayers with the formation of high melting complexes between the phospholipids and the diacylglycerol, with the complexing often being immiscible

with uncomplexed phospholipid (Boden et al., 1991). However, 25 mol % DHG has been shown to be miscible with dipalmitoylphosphatidylcholine in the liquid crystalline phase with no evidence for phase separation of the type seen with long chain diacylglycerols (de Boeck & Zidovetski, 1992). The presence of 25 mol % DHG had only a small effect on the order parameter profile for the phospholipid fatty acyl chains and the effect of DHG has been likened to that of benzyl alcohol which binds at the lipid-water interface, hydrogen bonding to the phospholipid phosphate groups with the benzyl group penetrating a small way into the hydrocarbon core of the bilayer (de Boeck & Zidovetski, 1992; Hamilton et al., 1991). NMR studies are consistent with a similar location for the diacylglycerols with the –OH group of the diacylglycerol located close to the lipid-water interface (Heimberg et al., 1992).

The fact that DGK activity is observed in di(C18:1)PC membrane fragments containing DHG as substrate, suggests that di(C18:1)PC can function as an activator of DGK in bilayers but not in mixed micelles. One theory is that in the mixed micelle there is an excess of OG, which has a short alkyl chain length that is probably incapable of binding the substrate and presenting it to the DGK active site. Thus, a lipid activator such as di(C18:1)PC with a longer alkyl chain length able to correctly orientate the DHG substrate would be kept away from the enzyme due to the excess OG. However, the double negative charge of cardiolipin may attract it to the protein in preference to OG, and cardiolipin would then be able to present the substrate to DGK to give activity.

CHAPTER 5: Effects of bilayer thickness on the activity of diacylglycerol kinase of *Escherichea coli*

5.1 Introduction

5.1.1 The lipid bilayer and membrane proteins

The lipid component of the biological membrane provides more than a simple permeability barrier and support for membrane proteins. These additional roles often require the presence of lipids with particular structures and physical properties, helping to explain the many different chemically distinct species of lipid found in an average membrane. In part, the complexity of the lipid composition follows from the wide variety of fatty acyl chains contained in the lipids (Ansell et al., 1973). The length of the fatty acyl chains is a major determinant of the thickness of the hydrophobic core of the membrane. In turn, the thickness of the hydrophobic core can be expected to match the thickness of the transmembrane domains of the intrinsic membrane proteins because the cost of exposing either the fatty acyl chains or hydrophobic amino acids to water is high (Tanford, 1980).

The variety of lipid fatty acyl chain lengths can lead to a non-homogenous distribution of lipids within a single membrane. For example, the plasma membrane in mammalian cells is enriched in sphingolipids that contain longer fatty acyl chains (C24) than the glycerophospholipids that make up the bulk of the phospholipids in mammalian cell membranes. These sphingolipids have a high gel to liquid crystalline phase transition temperature (Koynova & Caffrey, 1995); thus in mixtures of sphingolipids and glycerophospholipids, the sphingolipids tend to separate out as solid domains of gel phase lipid (Simons & Ikonen, 1997). The plasma membrane is

also enriched in cholesterol, which tends to produce a thicker bilayer by reducing the extent of motion of the fatty acyl chains (Ding et al., 1994).

5.1.1.1 Transmembrane regions and hydrophobic matching

Correct matching of the hydrophobic region of a membrane protein to the hydrophobic core of the lipid bilayer is likely to be important for membrane protein function (Figure 5.1). Most membrane proteins span the membrane in the form of one or more hydrophobic right-handed α-helices, the exception being the bacterial outer membrane proteins that form β-sheets and span the membrane as β-barrels. An ideal α-helix has 3.6 residues per turn and a translation per residue of 1.50 Å. With a thickness for the hydrocarbon core of a typical lipid bilayer of 30 Å, about 20 residues will be required to span the core of the bilayer. Analysis of the compositions of a large number of membrane proteins predicted to contain single transmembrane α-helices has shown that hydrophobic residues make up the bulk of the of the residues, the most common being Leu (Landolt-Marticorena et al., 1993; Wallin et al., 1997). Amino acids essentially excluded are the basic (Arg and Gln) and acidic (Asp and Glu) amino acids and their amide counterparts (Asn and Gln). Transmembrane α-helices are relatively rich in bulky residues such as Ile, Val and Thr, whose effects of large residue volume will, in the membrane, be balanced by the favourable hydrophobic interactions of a large side chain with the fatty acyl chains (Mall et al., 2001). The polar regions flanking the transmembrane domain are enriched in Arg and Lys on the C-terminal side; Asn, Ser, and Pro are enriched in the N-terminal flanking region. The presence of a positively charged N-terminus (cytoplasmic) could play a role in the process of insertion into the membrane, according to the inside positive

rule of von Heijne (1996). The observed preference for Trp and Tyr residues for the ends of transmembrane α-helices agrees with the measurements of the binding of small peptides at the lipid-water interface, which show that aromatic residues have a preference for this interface (Wimley & White, 1996). Furthermore, a number of tryptophan analogues have been shown to bind in the glycerol backbone and lipid headgroup region of the bilayer, stabilised partly by the location of the aromatic ring in the electrostatically complex environment provided by this region of the bilayer, and partly by exclusion of the flat, rigid ring system from the hydrocarbon core of the bilayer for entropic reasons (Yau et al., 1998). While it is agreed that aromatic residues at the ends of transmembrane α-helices probably act as 'floats' at the interface, serving to fix the helix within the lipid bilayer, it is at present unclear whether the aromatic rings are located in the hydrocarbon or the headgroup region of the bilayer.

The cost of exposing hydrophobic fatty acyl chains or protein residues to water is such that the hydrophobic thickness of the protein should match that of the bilayer. The question then is how the system responds when these do not match. Studies with model peptides have suggested that the extent to which lipid fatty acyl chains can stretch or compress to match the hydrophobic length of the peptide is rather limited (Webb et al., 1998). However, α-helical membrane proteins are not rigid but, in fact, can distort to match the thickness of the bilayer (Mall et al., 2001). This means that short hydrophobic α-helices are excluded from thick lipid bilayers but that long hydrophobic α-helices can incorporate into thin bilayers by simply tilting to decrease their effective length across the bilayer (Webb et al., 1998; Mall et al., 2000; Ren et al., 1997, 1999). This tilting could result in a change in activity for the protein, particularly if the transmembrane region of the protein is important for the function of

the protein. For example, the Ca^{2+}-ATPase of skeletal muscle sarcoplasmic reticulum contains 10 transmembrane α-helices tilted at about 10^{o} with respect to the bilayer normal (Toyoshima et al., 2000) and bilayer thickness has been shown to be important for the function of the ATPase (Lee, 1998). ATPase activity is highest in bilayers of dioleoylphosphatidylcholine (di(C18:1)PC), with lower activities in bilayers of shorter or longer chain phospholipids (Lee, 1998; Caffrey & Feigenson, 1981; Johannson et al., 1981; Starling et al., 1993). Although changing the bilayer thickness leads to changes in the state of aggregation of the Ca^{2+}-ATPase (Cornea & Thomas, 1994) this has shown not to be the explanation for the effects on activity (Starling et al., 1995b). Rather, changes in helix packing lead to changes in the rates of phosphorylation and dephosphorylation, in the stoichiometry of Ca^{2+} binding, and in the equilibrium between the two major conformation states of the ATPase, E1 and E2 (Lee, 1998).

The effect of reconstituting the Ca^{2+}-ATPase into bilayers of di(C14:1)PC can be reversed by the addition of a variety of sterols, alcohols, and esters (Starling et al., 1993). It would be predicted that if the hydrophobic core of the bilayer is thinner than the hydrophobic region of the membrane spanning protein, then the bilayer could be thickened using decane. Decane has been shown to increase the thickness of black lipid membranes of phosphatidylcholines with chain lengths from 14 to 24 carbons (Haydon et al., 1977; Benz et al., 1975). It is assumed that the decane is mainly located at the centre of the bilayer (Andrews et al., 1970) and that it complements the phospholipid chains by extending the hydrophobic hydrocarbon region and increasing the separation between the polar headgroups on the opposite sides of the bilayer (Johansson et al., 1981). In agreement, decane increases activity for the Ca^{2+}-ATPase in di(C14:1)PC but decreases it in di(C24:1)PC (Starling et al., 1993). Cholesterol

also increases bilayer thickness and addition of cholesterol also increases the activity of the Ca^{2+}-ATPase in di(C14:1)PC. However, in this case the effect was suggested to follow from direct binding to the Ca^{2+}-ATPase (Ding et al., 1994).

5.1.1.2 Studying lipid-protein interactions

A disadvantage of using the Ca^{2+}-ATPase for studies of lipid-protein interactions is that the mechanism of the ATPase is relatively complex, involving at least one phosphorylated intermediate, with more than one step in the reaction sequence that can contribute to the observed overall rate. We have therefore decided to study a kinetically simple intrinsic membrane protein, diacylglycerol kinase (DGK) of *Escherichia coli,* which catalyses the direct transfer of the γ-phosphate of ATP to *sn*-1,2,-diacylglycerol (DAG), producing phosphatidic acid (PA) and ADP. Here we use our reconstitution protocol to measure enzyme activity in a bilayer, using the substrate DHG, and show that, in the bilayer system, the activity of DGK is sensitive to bilayer thickness. In addition, we will be measuring the relative affinities of DGK for phospholipids ranging in fatty acyl chain length from C14 to C24, using fluorescence techniques.

5.1.2 Fluorescence spectroscopy

Fluorescence spectroscopy was used to study the interaction of DGK with a lipid bilayer. Fluorescence is the emission of light when a molecule returns from an excited electronic state to the ground state (Lakowicz, 1983). Compounds containing conjugated double bonds absorb light of an appropriate wavelength to form the short-

lived excited state of the molecule; this absorption occurs in less than 10^{-15} sec and results in the excitation of an electron from the ground state (S_0) to a higher energy level (S_1 and S_2 etc.). After the absorption of light, energy can be lost quickly (about 10^{-12} sec) through non-radioactive processes, such as heat, and the energy of the excited molecules falls to the lowest vibrational energy of the excited state (S_1 V_0). The emission of light that occurs on the return from this excited state is known as fluorescence. The lower energy of the emitted light in relation to the absorbed light is seen as a shift to a longer wavelength, and is known as the Stokes shift (Lakowicz, 1983). Fluorescence is dominated by the Trp residues in proteins that contain these residues (Lakowicz, 1983), partly due to the strong absorbance by the Trp residues and a relatively high quantum yield for Trp (about 0.2). In the absence of Trp residues, Tyr residues dominate fluorescence. However, Tyr fluorescence is uncommon in the presence of Trp residues due to efficient energy transfer between Tyr and Trp residues.

5.1.2.1 Fluorescence quenching

Fluorescence quenching can be used to investigate the environment surrounding Trp residues, by monitoring the quenching of Trp residues (Lakowicz, 1983). Fluorescence quenching is a process of deactivation of the excited state resulting in a diminishing of the fluorescence intensity. One type of fluorescence quenching involves the quenching of Trp fluorescence by brominated phospholipids. Brominated phospholipids are able to quench the fluorescence of these Trp residues when the bromine they contain is in physical contact with them, and can be used to study membrane proteins (East & Lee, 1982; Webb et al., 1998). Brominated

phospholipids are produced by introducing bromines across the C-C double bonds of unsaturated fatty acyl chains (East & Lee, 1982). The presence of bulky bromine groups on the fatty acyl chains have a similar effect on the phase transition temperature as the presence of a cis double bond, thus the properties of brominated and non-brominated phospholipids are essentially identical. The lateral exchange of phospholipids in a bilayer occurs at a rate of about 10^8 per second, which is slower than the fluorescence decay time of Trp residues (East & Lee, 1982). Therefore, fluorescence quenching by phospholipids is considered a static process and can be used to measure the relative affinities of membrane proteins for phospholipids that vary in fatty acyl chain length and head group (East & Lee, 1982).

5.1.2.1 Measuring lipid binding affinity

The observed changes in Trp fluorescence when DGK is reconstituted in a mixture of brominated and non-brominated phospholipids at varying mole ratios can be used to obtain the relative binding constants of a membrane protein for different phospholipids. Because fluorescence quenching is considered a static process, the lattice model (Figure 5.2) of quenching can be used to analyse fluorescence quenching of membrane proteins by brominated lipids. In the lattice model, the degree of Trp fluorescence quenching is proportional to the probability of a brominated phospholipid occupying a lattice site close enough to the Trp residue to cause quenching. For a random distribution of lipids, the probability of a brominated phospholipid not occupying any lattice site is $1 - x_{Br}$ where x_{Br} is the mole fraction of brominated phospholipid in the bilayer. The probability that any Trp will fluoresce is proportional to the probability that none of the lattice sites close enough to the Trp

residue to cause quenching is occupied by a brominated phospholipid. Fluorescence intensity can therefore be described as

$$F = F_{min} + (F_0 - F_{min})(1 - x_{Br})^n \quad (5.1)$$

where F_0 and F_{min} are the fluorescence intensities for the protein in non-brominated and brominated phospholipid, respectively. F is the fluorescence intensity in the phospholipid mixture where the mole fraction of brominated phospholipid is x_{Br}, whilst n is the number of lattice sites from which the fluorescence of a given Trp residue can be quenched.

In a mixture of phospholipids with different affinities for the protein, the lattice model can be used to describe the fluorescence quenching; at each lattice site an equilibrium will exist described by

$$PQ + L \rightleftarrows PL + Q \quad (5.2)$$

where L and Q represent the non-brominated and brominated phospholipids respectively, and PQ and PL are complexes of the protein (P) with these phospholipids. The concentrations of the phospholipids are expressed as mole fractions and therefore for the bulk lipid

$$[L]^{free} + [Q]^{free} = 1 \quad (5.3)$$

and for each lattice site

$$[PQ] + [PL] = 1 \quad (5.4)$$

where $[L]^{free}$ is the concentration of the non-brominated bulk phospholipid and $[Q]^{free}$ is the concentration of brominated bulk phospholipid. [PQ] is the concentration of the protein-brominated phospholipid complex and [PL] is the concentration of the protein-phospholipid complex. If the phospholipid is in large excess, it is possible to replace $[L]^{free}$ and $[Q]^{free}$ by their total concentrations, [L] and [Q], respectively. The

relative binding constant (K) of non-brominated lipid relative to brominated lipid can then be expressed as

$$K = [PL][Q] / [PQ][L] \quad (5.5)$$

If L binds more strongly than Q then fluorescence will be high as the sites around the protein will tend to be occupied by the non-brominated lipid; the opposite is true if Q binds more strongly than L.

The fraction of sites at the lipid-protein interface occupied by the brominated lipid (f_{Br}) can be expressed as

$$f_{Br} = [PQ] / [PQ] + [PL] \quad (5.6)$$

Therefore, rearrangement of equation (5.5) and substitution into equation (5.6) gives

$$f_{Br} = ([PL][Q] / K[L]) / (([PL][Q] / K[L]) + [PL]) \quad (5.7)$$

Further rearrangement gives

$$f_{Br} = [Q] / ([Q] + K[L]) \quad (5.8)$$

The rearrangement of equation (5.3) and substitution into equation (5.8) gives

$$f_{Br} = [Q] / ([Q] + K[1 - [Q]) \quad (5.9)$$

The expression of the terms as mole fractions gives

$$f_{Br} = x_{Br} / (x_{Br} + K(1 - x_{Br})) \quad (5.10)$$

where x_{Br} is the mole fraction of brominated phospholipid in the mixture. Quenching is proportional to the fraction of each site around one Trp residue occupied by the brominated phospholipid or

$$\text{Quenching} \propto (f_{Br})^n \quad (5.11)$$

Therefore, the fluorescence remaining is proportional to $(1 - f_{Br})^n$ and fluorescence quenching can then be fitted to an equation analogous to Equation 5.1, in which

$$F = F_{min} + (F_0 - F_{min})(1-f_{Br})^n \quad (5.12)$$

where F_0 and F_{min} are the fluorescence intensities for the protein in non-brominated and brominated phospholipid, respectively. F is the fluorescence intensity in the phospholipid mixture where the mole fraction of brominated phospholipid is x_{Br}. The fraction of sites occupied by brominated phospholipid is related to x_{Br} by Equation 5.10.

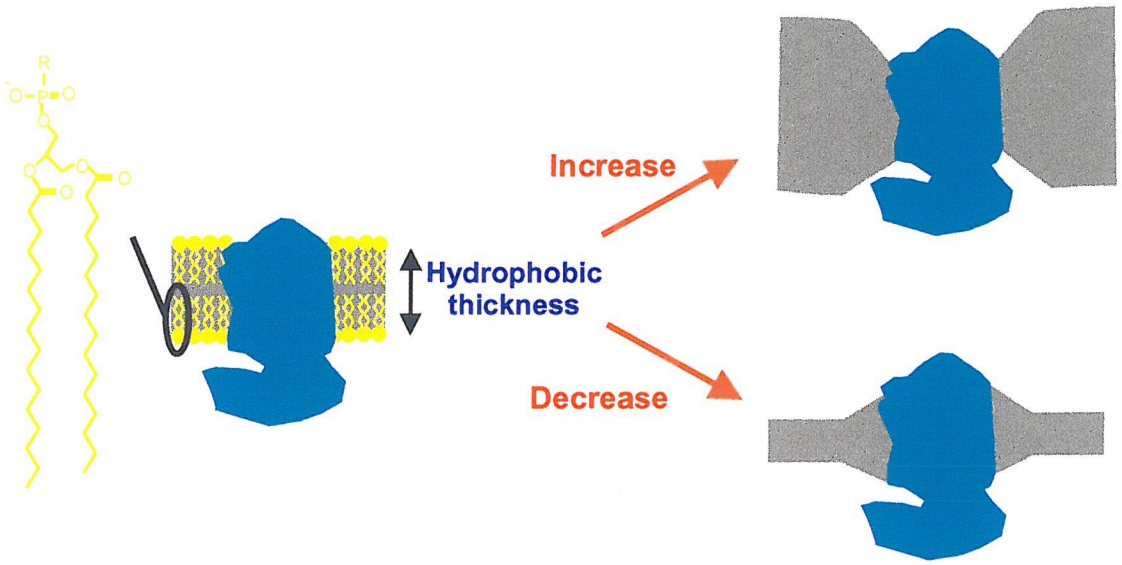

Figure 5.1 Hydrophobic matching between the protein and the bilayer

Diagram illustrating that the thickness of the hydrophobic core of the lipid bilayer must match the hydrophobic membrane-spanning region of a membrane protein (blue), to ensure optimum protein function.

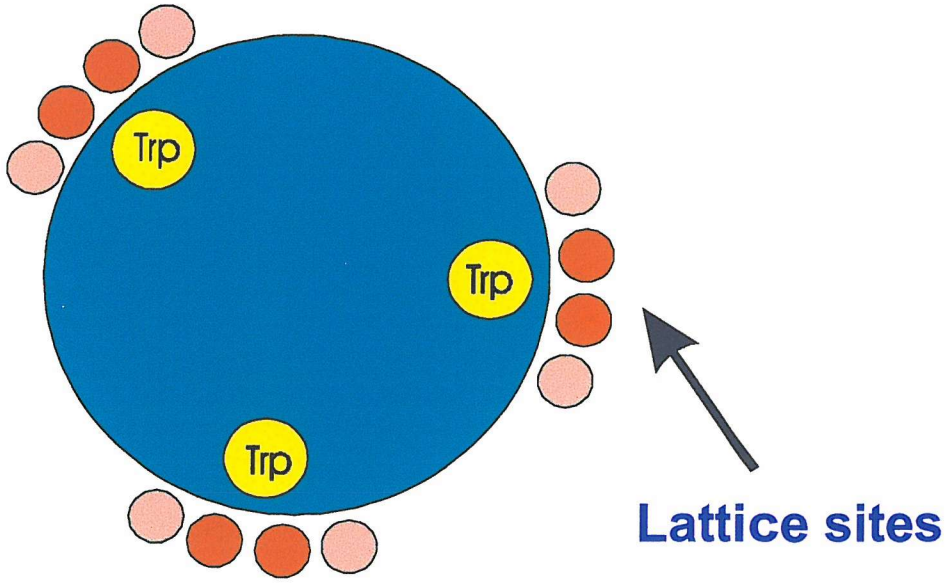

Figure 5.2 Diagram showing the lattice sites around a membrane protein

In this diagram there are two lattice sites (shown in deep red) close enough to the Trp residues of the protein to cause quenching if occupied by brominated phospholipid.

5.2 Methods

5.2.1 Reconstitution of DGK

5.2.1.1 Preparation of potassium cholate

Potassium cholate was prepared by dissolving equimolar quantities of cholic acid and potassium hydroxide in methanol, followed by the precipitation of the potassium cholate from the methanol solution by adding an excess of diethyl ether and leaving overnight at 4 °C. The solvent was then filtered off and the solid potassium cholate remaining was dried in a vaccuum dessicator for about 12 hrs. The potassium cholate was then stored at room temperature, away from direct light, until required.

5.2.1.2 Reconstitution of DGK

Purified DGK was reconstituted into lipid bilayers by mixing lipid and DGK in cholate followed by dilution to decrease the concentration of cholate below its critical micelle concentration, using a protocol previously used for the Ca^{2+}-ATPase (Warren et al., 1974a). Phospholipid (8 μmol) and the required concentration of diacylglycerol (usually 2 μmol DHG) were dried from choloroform solution onto the walls of a thin glass vial. Buffer (400 μl; 60mM Pipes, pH 6.85) containing 28 mM cholate was added and the sample was sonicated to clarity in a bath sonicator (Ultrawave). DGK (22 μg) was added to obtain a lipid to protein molar ratio of 6000:1 and the suspension left at room temperature for 15 min, followed by

incubation on ice until use. 20 μl of the sample was then diluted into 1 ml of the assay buffer described below, representing a 50-fold dilution.

5.2.1.3 Assay of DGK activity

DGK activity was measured using a coupled enzyme assay based on that developed for studies of the Ca^{2+}-ATPase (Warren et al., 1974b) and modified according to the one developed by Lau & Bowie (1997). The production of ADP by the action of DGK on ATP was coupled to the oxidation of NADH through pyruvate kinase and lactate dehydrogenase. The assay medium consisted of buffer (60 mM Pipes, pH 6.85) containing phosphoenolpyruvate (2 mM), NADH (0.2 mM), ATP (5 mM), Mg^{2+} (20 mM), pyruvate kinase (18 units), and lactate dehyrogenase (22 units). The mixture was incubated at 25 °C for 10 min to ensure that any residual ADP in the ATP sample was consumed. The reaction was initiated by addition of DGK (1.5 μg) dissolved in cholate with phospholipid and DHG to 1 ml of the assay medium. The oxidation of NADH was monitored by the decrease in absorbance at 340 nm, which was related to DGK activity by the following equation:

$$\text{Activity } (\mu\text{moles/min/mg}) = (\Delta OD_{340}\ \text{min}^{-1}.\ \text{vol}) / (\text{DGK}.\ \varepsilon_{340})$$

$\Delta OD_{340}\ \text{min}^{-1}$ = change in optical density at 340 nm per min

vol = volume in cuvette (ml)

DGK = amount of DGK protein in cuvette (mg)

ε_{340} = extinction coefficient of NADH at 340 nm ($M^{-1}\ cm^{-1}$)

5.2.2 Fluorescence

5.2.2.1 Preparation of brominated phospholipids

The production of 1,2-bis (9,10-dibromostearoyl)-sn-glycero-3-phosphorylcholine (di(Br_2C18:0)PC) was completed according to the method of Dawidowicz & Rothman (1976). 100 mg of di(C18:1)PC in 5 ml chlororform was reacted with 12 µl of bromine at –4 °C. The reaction was left for 30 minutes, before removing the solvent and excess bromine by rotary evaporation. The di(Br_2C18:0)PC was stored in chloroform (50 mg/ml) under nitrogen at –4 °C.

5.2.2.2 Reconstitution of DGK into brominated lipid mixtures

DGK was reconstituted into mixtures of the brominated lipid, di(Br_2C18:1)PC, and the following non-brominated lipids: di(C14:1)PC, di(C16:1)PC, di(C18:1)PC, di(C20:1)PC, di(C22:1)PC, and di(C24:1)PC to determine the relative binding constant of DGK for phospholipids varying in fatty acyl chain length. Purified DGK was reconstituted into lipid bilayers of brominated and non-brominated lipids using a similar procedure to that described in section 5.2.1.2. The brominated lipid (di(Br_2C18:0)PC) and the required concentration of non-brominated lipid, using a total of 2 µmoles lipid, were dried from choloroform solution onto the walls of a thin glass vial. Buffer (400 µl; 60mM Pipes, pH 6.85) containing 28 mM cholate was added and the sample was sonicated to clarity in a bath sonicator (Ultrawave). DGK (20 nmoles) was added to obtain a lipid to protein molar ratio of 100:1 and the suspension left at room temperature for 15 min, followed by incubation on ice until

use. 100 μl of the sample was then diluted into 2.9 ml of the assay buffer (60mM Pipes, pH 6.85) representing a 30-fold dilution.

5.2.2.3 Fluorescence measurements

Fluorescence measurements were performed on an SLM8000C fluorimeter at 25 °C, using an excitation wavelength of 290 nm. Fluorescence emission spectra were recorded between 300 and 400 nm. Slit widths of 4 nm were used for excitation and emission. Experiments were performed in 60 mM Pipes, pH 6.85. Results were corrected for light scattering by subtracting the emission spectra of reconstituted phospholipid minus DGK.

5.3 Results

5.3.1 Effects of bilayer thickness on DGK activity

DGK was reconstituted into phospholipid bilayers containing DHG at a molar ratio of total lipid to DGK of 6000:1. The value for v_{max}, with DHG as substrate, in bilayers of di(C18:1)PC is ca 75 IU/mg (Figure 5.4), a figure comparable to that observed with DOG as substrate in OG micelles (Table 5.1). Reconstitution using this procedure is complete within 5 mins. If DGK is mixed with di(C14:1)PC in cholate and samples are taken after 5 mins or 3 h, the same activity is recorded (Table 5.2). DGK is stable in bilayers of di(C14:1)PC for at least 3 h (data not shown).

5.3.1.1 Effects of phospholipids on DGK activity are reversible

Reconstitution of DGK into bilayers of di(C14:1)PC gave a lower activity against DHG than for DGK reconstituted into bilayers of di(C18:1)PC (Table 5.2). To demonstrate that the effect of di(C14:1)PC was fully reversible, a sample of the reconstituted DGK was added to micelles of OG containing DOG, conditions under which DOG acts as the activating lipid so giving full activity (Table 5.1). As shown in Table 5.2, when added to micelles of OG, DGK reconstituted into di(C14:1)PC or into di(C18:1)PC gave the same activity, equal to that for unreconstituted enzyme, showing that the effects of reconstitution are reversible.

5.3.1.2 Effects of phospholipid chain length on DGK activity

DGK was reconstituted into bilayers of phosphatidylcholines containing monounsaturated fatty acyl chains of lengths between C14 and C24. Phase transition temperatures for all these lipids are below 25 °C (Koynova & Caffrey, 1998) so that all the lipids are in the liquid crystalline phase at the assay temperature. DGK activity was assayed at 5 mM MgATP and 20 mol % DHG. Highest activity was observed in di(C18:1)PC with lower activities for phosphatidylcholines with shorter or longer chains (Figure 5.3). Activities were measured as a function of DHG concentration, at a MgATP concentration of 5 mM (Figure 5.4). The data fit well to a simple Michaelis-Menten scheme with the K_m and v_{max} values shown in Table 5.3 and plotted in Figure 5.5A. As shown, in di(C14:1)PC the K_m value for DHG is high but the value for v_{max} is the same as in di(C18:1)PC, whereas in long chain phosphatidylcholines K_m values for DHG are comparable to those in di(C18:1)PC but values for v_{max} are low. Activities as a function of ATP concentration at a fixed DHG concentration of 20 mol % also fit well to Michaelis-Menten kinetics (Figure 5.6) with the K_m and v_{max} values shown in Table 5.3 and plotted in Figure 5.5B. The K_m value for ATP is higher in di(C14:1)PC than in di(C18:1)PC but is little changed on increasing the phosphatidylcholine chain length from C16 to C24. The low value for v_{max} seen in di(C14:1)PC in Figure 5.5B follows because activity was assayed at 20 mol % DHG and the K_m value for DHG is high in di(C14:1)PC (Figure 5.5A). Thus the inverted U-shape profile for activity as a function of chain length shown in Figure 5.3 for activity measured with 20 mol % DHG and 5 mM ATP follows largely from a high K_m value for DHG in di(C14:1)PC and a low value for v_{max} in long chain phosphatidylcholines.

5.3.1.3 Effects of mixtures of phosphatidylcholines on DGK activity

The effects of mixtures of phosphatidylcholines are shown in Figure 5.7. Addition of increasing proportions of di(C14:1)PC or di(C24:1)PC to DGK reconstituted in di(C18:1)PC leads to a gradual decrease in activity (Figure 5.7). However, addition of di(C24:1)PC to DGK reconstituted in di(C14:1)PC results in an initial increase in activity so that at a mol fraction of di(C24:1)PC of 0.2, activity is almost equal to that in di(C18:1)PC. Further increases in the mole fraction of di(C24:1)PC up to 0.6 lead to only a small decrease in activity but activity decreases significantly beyond this (Figure 5.7). These results suggest that the thickness of the bilayer is an important parameter determining enzyme activity.

5.3.1.4 Effects of decane and cholesterol

In studies of the Ca^{2+}-ATPase it was observed that the effects of di(C14:1)PC on the ATPase could be reversed by addition of decane whereas the effects of di(C24:1)PC could not be reversed (Johannson et al., 1981). This is not seen with DGK (Figure 5.8). For DGK in di(C14:1)PC or di(C16:1)PC, addition of decane led to only a 10 % increase in activity. The small change observed in steady state activity is not due to fortuitous, opposing changes in K_m and v_{max}; for example, activities measured at a 0.63:1 molar ratio of decane:di(C14:1)PC as a function of mol % DHG fitted to K_m and v_{max} values equal to those in the absence of decane (Figure 5.9). Addition of decane to DGK in di(C18:1)PC had no significant effect on activity and in both di(C14:1)PC and di(C22:1)PC the addition of decane led to a 10 % decrease in activity at a molar ratio of decane:phospholipid of 2:1 (Figure 5.8).

In contrast to the lack of effect of decane, the presence of cholesterol has marked effects on enzyme activity (Figure 5.10). In di(C14:1)PC addition of cholesterol to a molar ratio of cholesterol:di(C14:1)PC of 0.5:1 led to a 2.5-fold increase in activity with higher concentrations of cholesterol resulting in slightly lower activities. In contrast, addition of cholesterol to DGK in di(C18:1)PC or di(C24:1)PC led to a 40 % or 75 % decrease in activity respectively, at a molar ratio of cholesterol:phospholipid of 1:1. The effect of cholesterol on DGK in di(C14:1)PC is an effect on the K_m for DHG rather than an effect on v_{max} (Figure 5.11). At a 0.5:1 molar ratio of cholesterol:di(C14:1)PC, a plot of activity against mol % DHG fits to a K_m of 31.9 ± 3.6 mol % with a v_{max} of 87.8 ± 6.7 IU/mg, compared to values of 64.5 ± 6.7 mol % and 74.9 ±6.3 IU/mg for K_m and v_{max} respectively in the absence of cholesterol (Figure 5.4).

5.3.2 Relative lipid binding constants

DGK contains five tryptophan (Trp) residues; transmembrane helices 1 and 3 are thought to contain 1 and 2 Trps respectively, whilst the remaining two are located in amphipathic helix 1. In both transmembrane regions the Trp residues are located near the bilayer surface. Quenching of Trp fluorescence was used to determine relative lipid binding constants. DGK was reconstituted with phosphatidylcholines, ranging in fatty acyl chain length from C14 to C24, and their brominated counterparts to calculate a value for n, the number of sites on DGK from which a Trp can be quenched. The initial fluorescence of DGK in all the non-brominated phospholipid species was identical within ± 2.5 %, indicating there was no major structural protein change when the chain length is varied from C14 to C24. The fluorescence intensity is

plotted as a function of the mole fraction of brominated phospholipid in the mixture in Figure 5.12. The data were fitted to Equation 5.10 to obtain a value for f_{min} and n. The values of n were all very similar, giving an average value of n = 2.53. As expected the values obtained for f_{min}, were very close to the experimental f_{min} values determined in the brominated phospholipid (Table 5.4). The f_{min} values for DGK in di(C14:1)PC, di(C16:1)PC, and di(C18:1)PC were virtually identical indicating that no major structural protein change has occurred. However, the f_{min} value for DGK in di(C24:1)PC is very different to that in di(C18:1)PC, which could be due to an increased distance between the Br atoms and the Trp residues, resulting in less efficient quenching.

Fluorescence quenching by brominated phospholipids can be used to study the possibility of specific binding of phospholipids to DGK. DGK was reconstituted into mixtures of di(Br_2C18:0)PC and phosphatidylcholines with fatty acyl chain lengths between C14 and C24. The quenching data is presented in Figures 5.13 to 5.17. The data for mixtures of di(C14:1)PC, di(C18:1)PC, or di(C24:1)PC and di(Br_2C18:0)PC are compared in Figure 5.18. As shown in Figure 5.18 the fluorescence intensities of DGK in mixtures of di(Br2C18:0)PC and di(C18:1)PC or di(C14:1)PC are identical, whilst fluorescence intensity is lower in mixtures with di(C24:1)PC. This indicates that longer chain length phosphatidylcholines are more easily displaced from DGK by di(Br_2C18:0)PC than shorter chain length phosphatidylcholines. The data for each phosphatidylcholine was fitted to Equation 5.12 using n = 2.53, providing a relative binding constant (K) for each phospholipid. The binding constants for each fatty acyl chain length are shown in Table 5.5 and plotted in Figure 5.19 where they are compared to those for the Ca^{2+}-ATPase (East & Lee, 1982). The results show that DGK has little preference for lipids with fatty acyl chain lengths from C14 to C20,

and that lipids with fatty acyl chains greater than C20 bind more weakly. In contrast, the Ca^{2+}-ATPase displays little selectivity for any particular fatty acyl chain length.

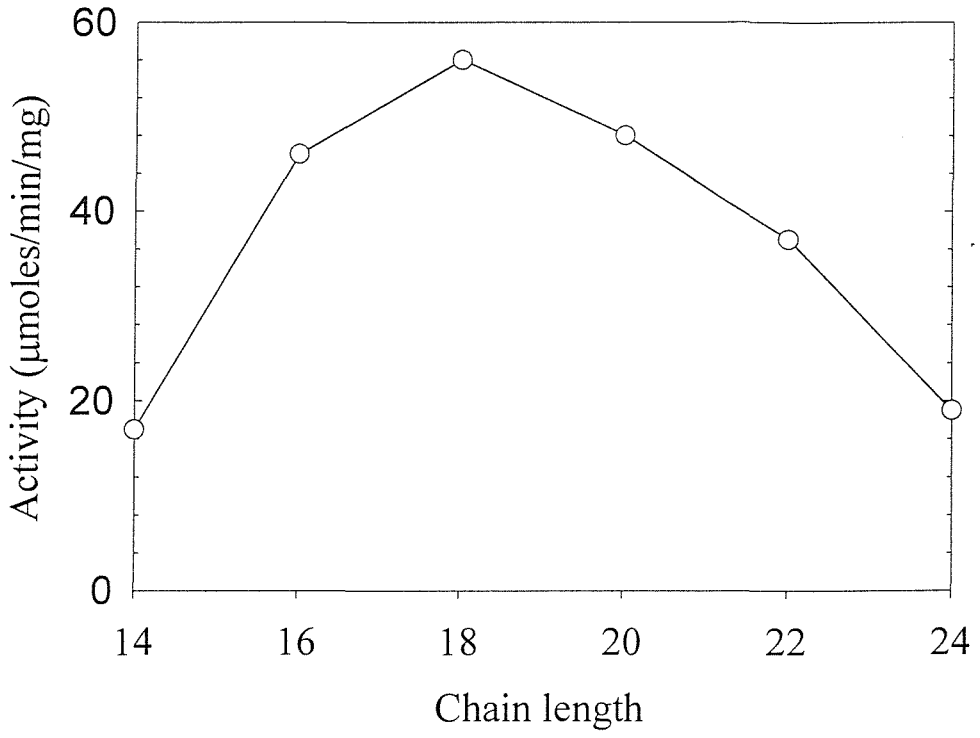

Figure 5.3 Effect of phosphatidylcholine fatty acyl chain length on DGK activity

The figure shows DGK activity when reconstituted with phosphatidylcholines with two mono-unsaturated fatty acyl chains of the given length, all being in the liquid crystalline phase. The reaction was initiated by addition of DGK (1.5 μg) dissolved in cholate with phospholipid and DHG to 1 ml of the assay medium. Activities were measured at 25 ^{o}C with 5 mM ATP, 15 mM Mg^{2+}, and 20 mol % DHG.

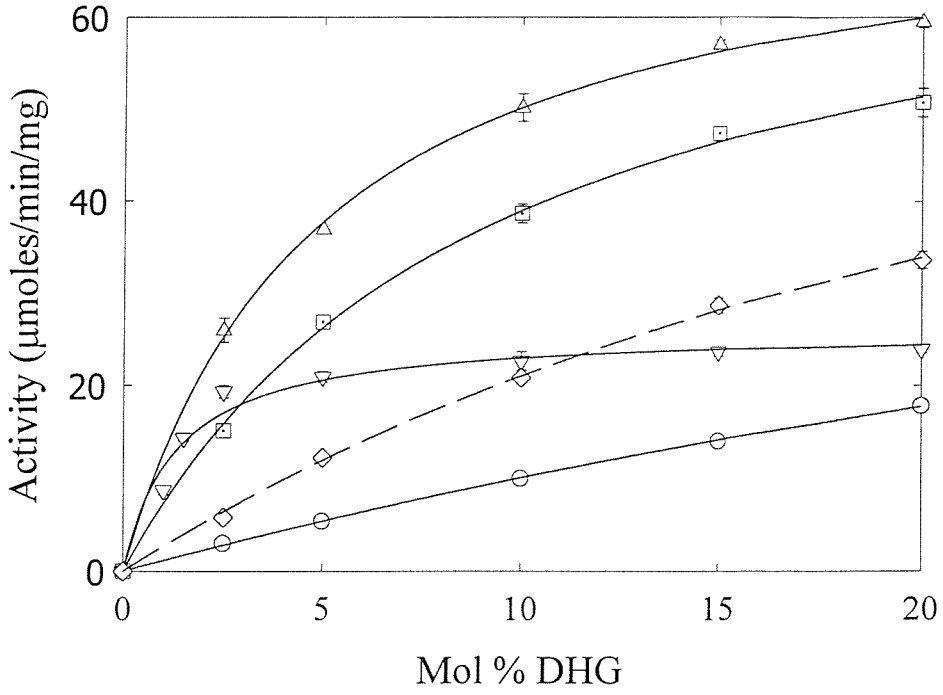

Figure 5.4 Effect of phosphatidylcholine fatty acyl chain length on DGK activity as a function of DHG concentration

The figure shows DGK activity when reconstituted with phosphatidylcholines of the given chain length, at a constant molar ratio of 6000:1 phospholipid:DGK and the given mol % DHG. Phospholipids were as follows: (○), di(C14:1)PC; (□), di(C16:1)PC; (Δ), di(C18:1)PC; (▽), and di(C24:1)PC. The solid lines show fits to the Michaelis-Menten equation with the values for K_m and v_{max} plotted in Figure 5.5A. Also shown is the activity for DGK reconstituted into a 1:0.5 molar ratio of di(C14:1)PC:cholesterol (◊). Activities were measured at 25 ^{o}C with 5 mM ATP, 15 mM Mg^{2+}, and the appropriate mol % DHG.

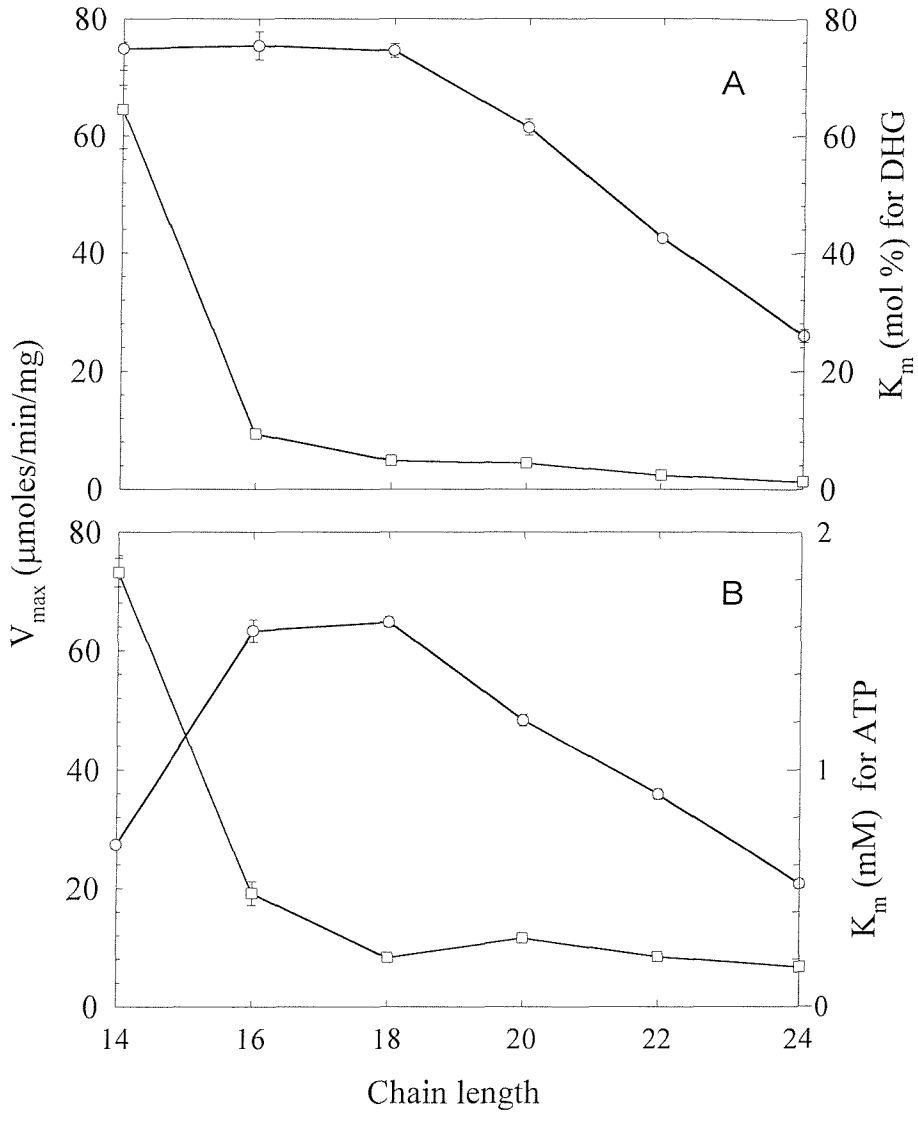

Figure 5.5 Effects of phosphatidylcholine chain length on K_m and v_{max} values of DGK for DHG (A) and ATP (B).

The figure shows K_m (□) and v_{max} (○) values obtained from fits of rates against mol % DHG at a fixed ATP concentration of 5 mM (A) or from fits of rates against ATP concentration at a fixed DHG concentration of 20 mol % (B) plotted against chain length.

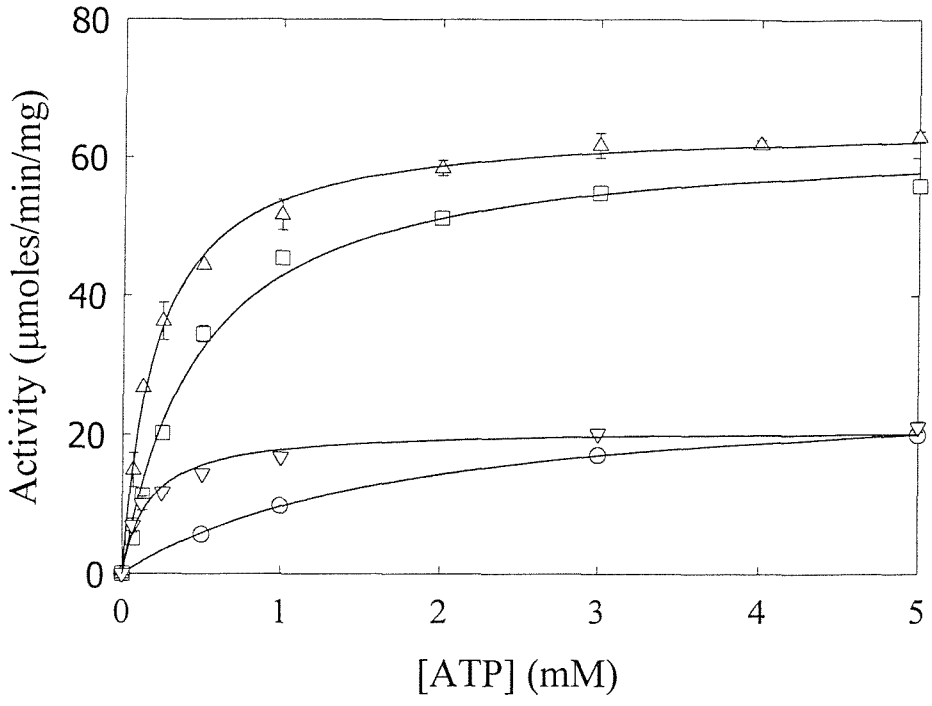

Figure 5.6 Effects of phosphatidylcholine fatty acyl chain length on DGK activity as a function of ATP concentration.

The figure shows DGK activity when reconstituted with phosphatidylcholines of the given chain length, at a constant molar ratio of 6000:1 of phospholipid:DGK and 20 mol % DHG. Phospholipids were as follows: (○), di(C14:1)PC; (□), di(C16:1)PC; (Δ), di(C18:1)PC; (▽), di(C24:1)PC. The solid lines show fits to the Michaelis-Menten equation with the values for K_m and v_{max} plotted in Figure 5.5B. Activities were measured at 25 ^{o}C with 15 mM Mg^{2+}, and 20 mol % DHG as a function of the concentration of ATP.

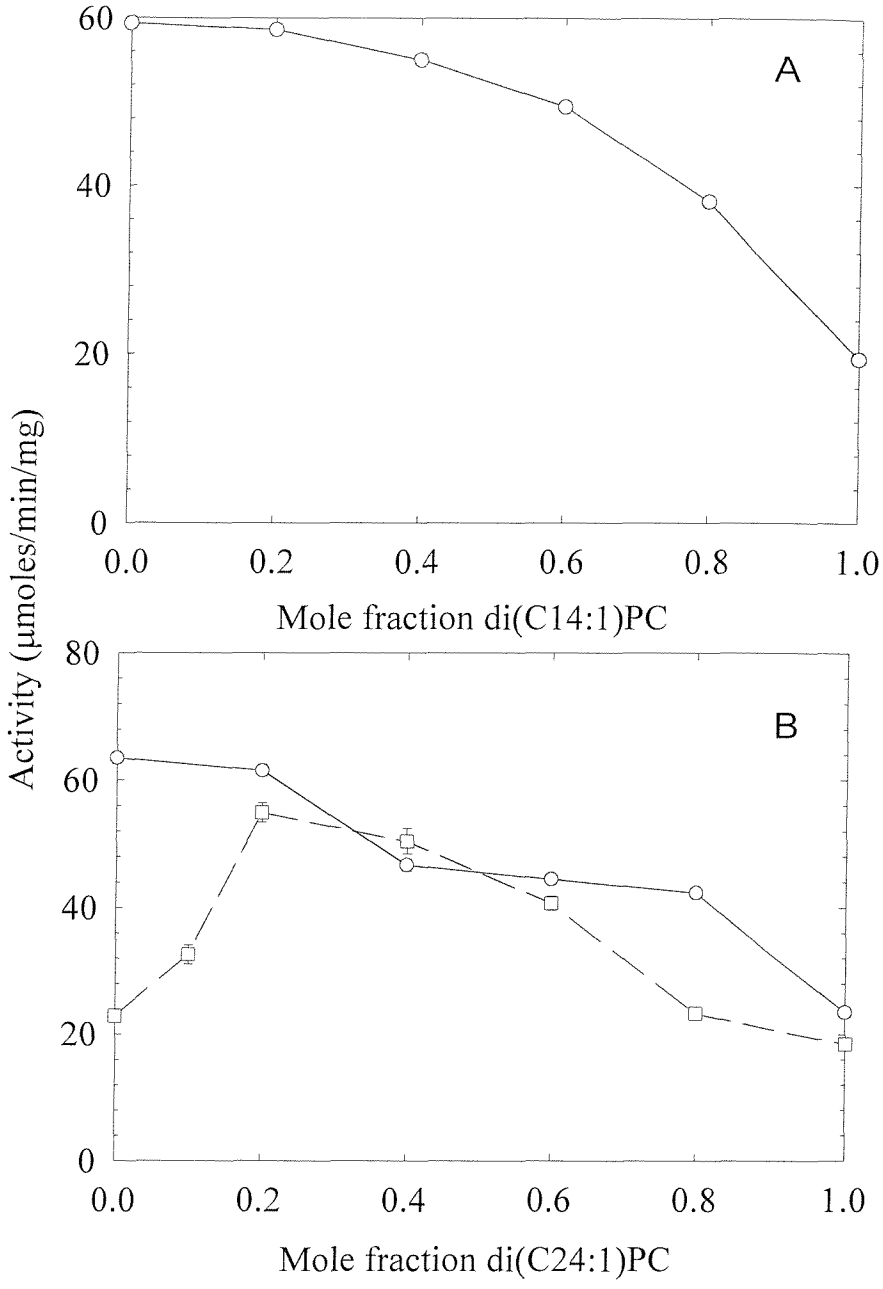

Figure 5.7 Effects of mixtures of phosphatidylcholines on DGK activity

The figure shows DGK activity when reconstituted with mixtures of: (A) di(C18:1)PC and di(C14:1)PC; (B) di(C18:1)PC and di(C24:1)PC (○) or di(C14:1)PC and di(C24:1)PC (□). Activities were measured at 25 ^{o}C with 5 mM ATP, 15 mM Mg^{2+}, and 20 mol % DHG.

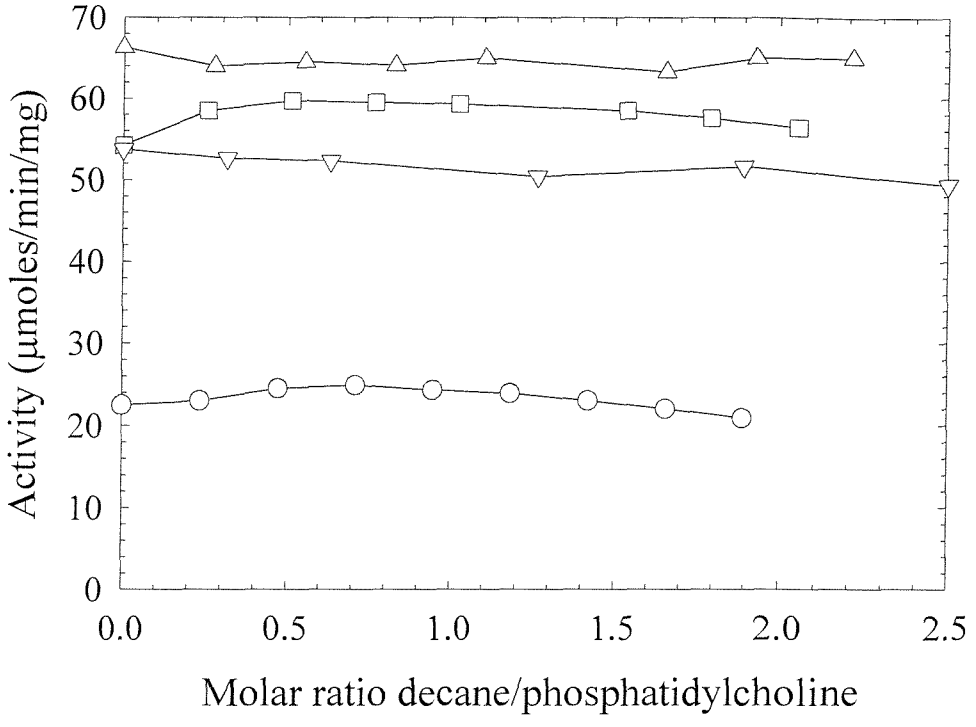

Figure 5.8 Effects of decane on the activity of DGK

The figure shows DGK activity when reconstituted into bilayers of phospholipid and decane at the given molar ratios of decane:phospholipid. Phospholipids were as follows: (○), di(C14:1)PC; (□), di(C16:1)PC; (Δ), di(C18:1)PC; (▽), di(C22:1)PC. Activities were measured at 25 ^{o}C with 5 mM ATP, 15 mM Mg^{2+}, and 20 mol % DHG.

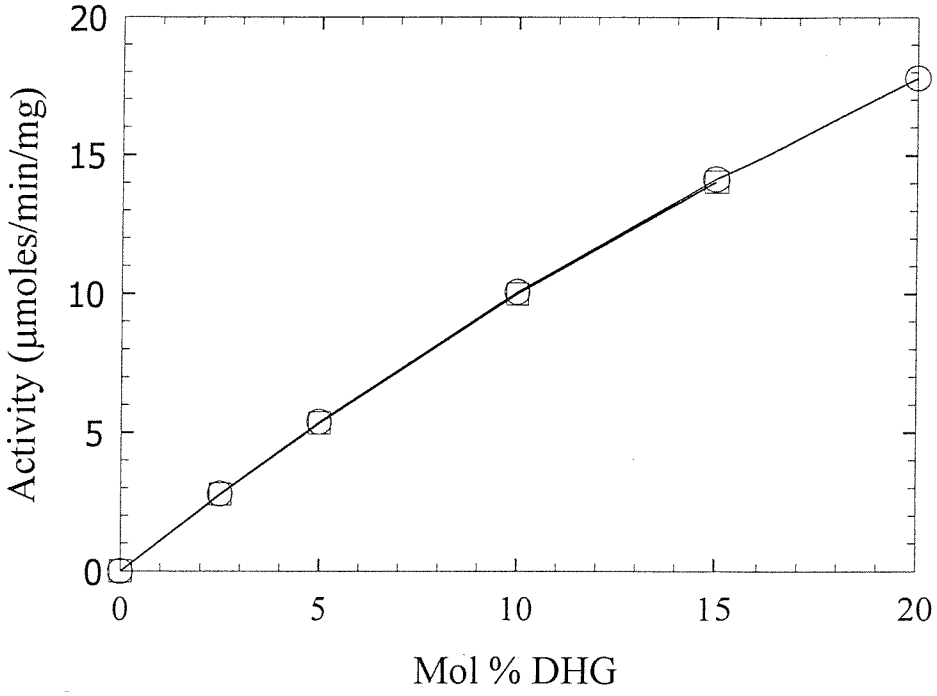

Figure 5.9 Effect of decane in di(C14:1)PC bilayers as a function of DHG concentration

The figure shows DGK activity when reconstituted with di(C14:1)PC (○) and di(C14:1)PC with decane (□) at a 0.63:1 molar ratio of decane:di(C14:1)PC, at a constant molar ratio of 6000:1 phospholipid:DGK and the given mol % DHG. Activities were measured at 25 °C with 5 mM ATP, 15 mM Mg^{2+}, and the appropriate mol % DHG. The solid lines show fits to the Michaelis-Menten equation.

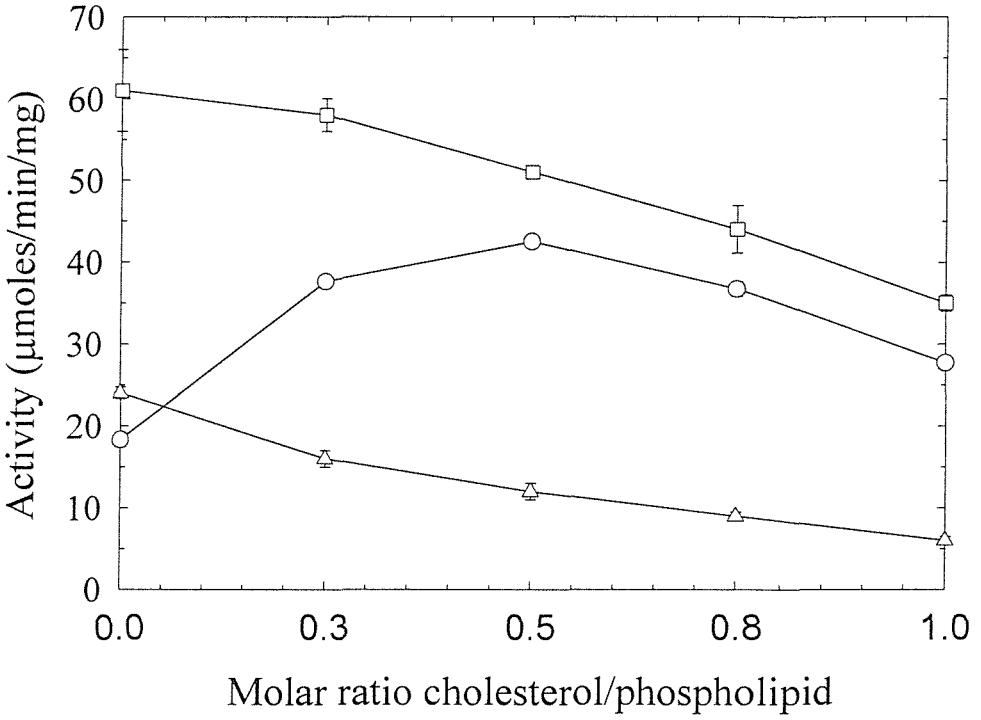

Figure 5.10 Effects of cholesterol on the activity of DGK

The figure shows DGK activity when reconstituted into bilayers of phospholipid and cholesterol at the given molar ratios of cholesterol to phospholipid. Phospholipids were as follows: (○), di(C14:1)PC; (□), di(C18:1)PC; (Δ), di(C24:1)PC. Activities were measured at 25 ^{o}C with 5 mM ATP, 15 mM Mg^{2+}, and 20 mol % DHG.

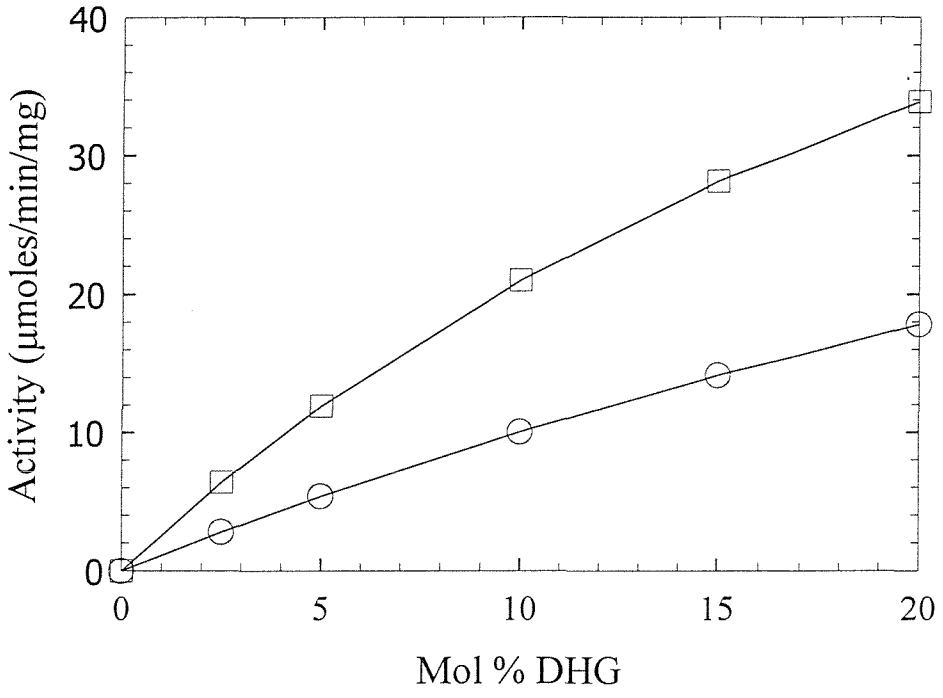

Figure 5.11 Effect of cholesterol in di(C14:1)PC bilayers as a function of DHG concentration

The figure shows DGK activity when reconstituted with di(C14:1)PC (○) and di(C14:1)PC with cholesterol (□) at a 0.5:1 molar ratio of cholesterol:di(C14:1)PC, at a constant molar ratio of 6000:1 phospholipid:DGK and the given mol % DHG. Activities were measured at 25 ^{o}C with 5 mM ATP, 15 mM Mg^{2+}, and the appropriate mol % DHG. The solid lines show fits to the Michaelis-Menten equation.

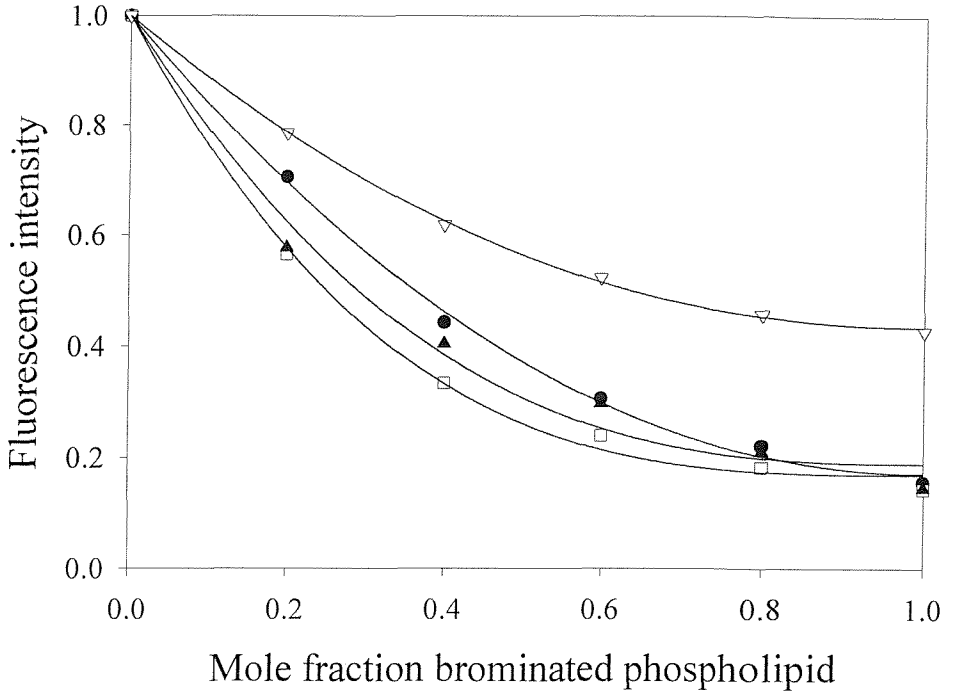

Figure 5.12 Relative fluorescence intensities for DGK in mixtures of brominated and non-brominated phosphatidylcholines

DGK was reconstituted into mixtures of brominated and non-brominated phosphatidylcholines, ranging in chain length from C14 to C24, at the given mole fraction of brominated lipid. The fluorescence intensities are scaled to those in non-brominated lipid. In all cases the fluorescence of 0.66 nmoles DGK was excited at 290 nm in 60 mM Pipes, pH 6.85. Shown are intensities for DGK in (●), di(C18:1)PC and di(Br_2C18:0)PC; (□), di(C14:1)PC and di(Br_2C14:0)PC; (▲), di(C16:1)PC and di(Br_2C16:0)PC; (▽) di(C24:1)PC and di(Br_2C24:0)PC.

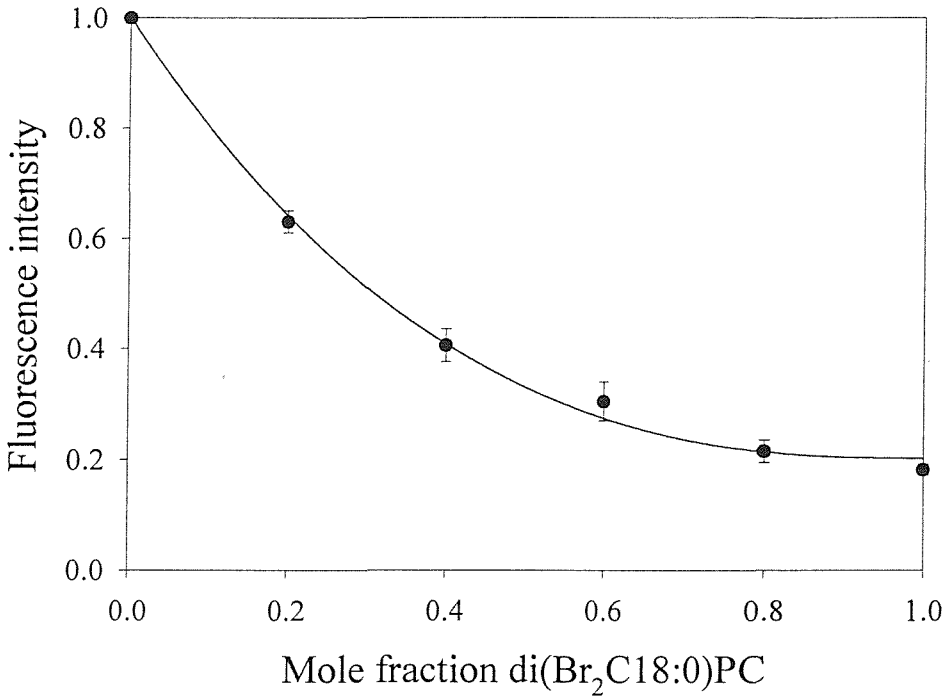

Figure 5.13 Relative fluorescence intensities for DGK in mixtures of di(C14:1)PC and di(Br_2C18:0)PC

DGK was reconstituted into mixtures of di(C14:1)PC and di(Br_2C18:0)PC at the given mole fraction of brominated lipid. The solid line is a fit to Equation 5.12 using an n value of 2.53 to give a relative binding constant of 0.94 ± 0.07. In all cases the fluorescence of 0.66 nmoles DGK was excited at 290 nm in 60 mM Pipes, pH 6.85.

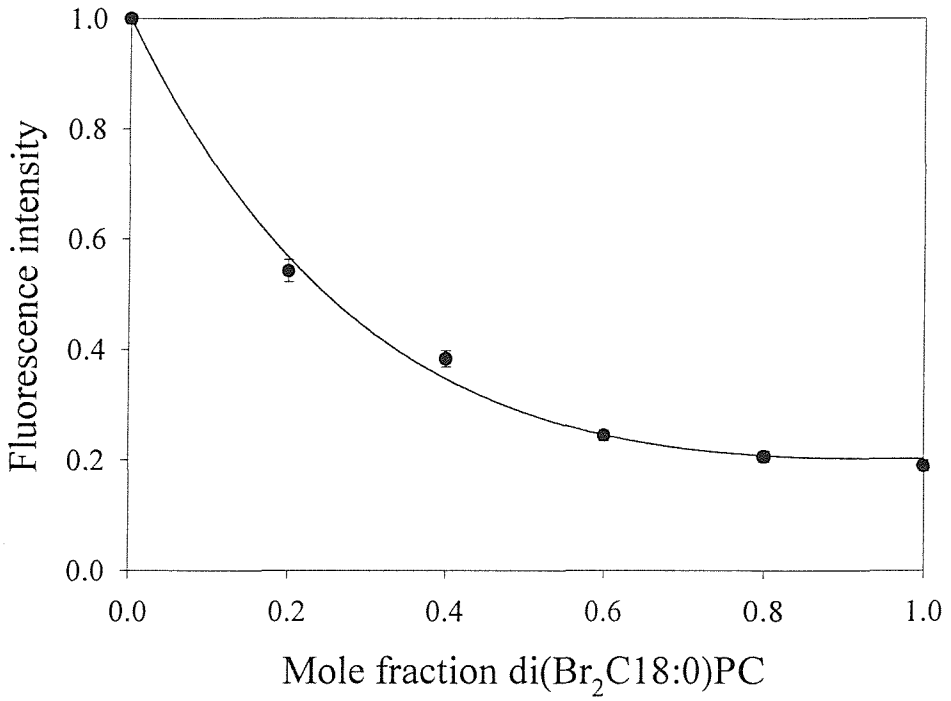

Figure 5.14 Relative fluorescence intensities for DGK in mixtures of di(C16:1)PC and di(Br_2C18:0)PC

DGK was reconstituted into mixtures of di(C16:1)PC and di(Br_2C18:0)PC at the given mole fraction of brominated lipid. The solid line is a fit to Equation 5.12 using an n value of 2.53 to give a relative binding constant of 0.69 ± 0.06. In all cases the fluorescence of 0.66 nmoles DGK was excited at 290 nm in 60 mM Pipes, pH 6.85.

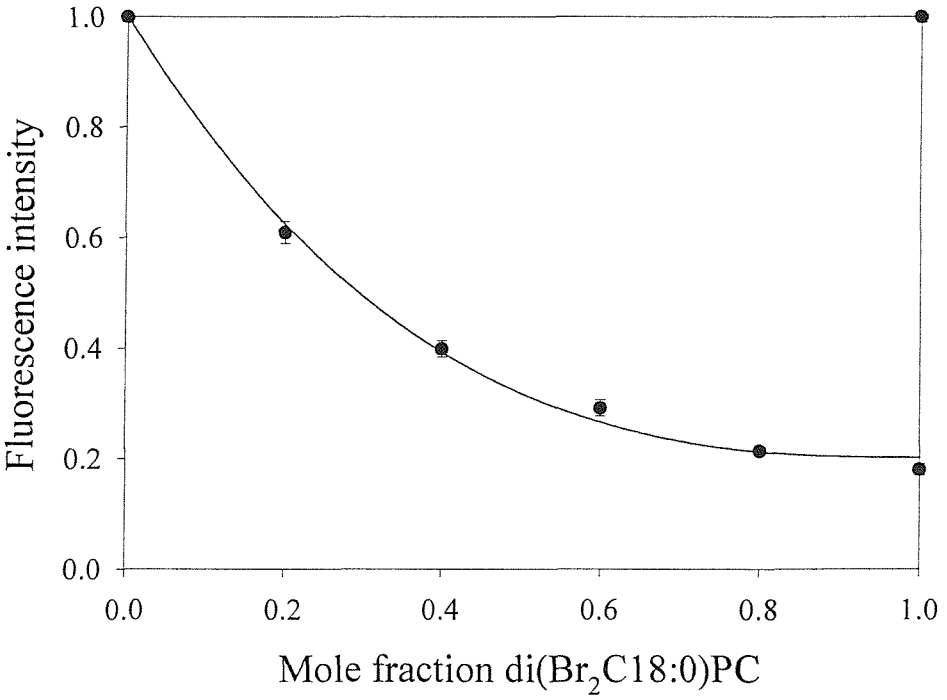

Figure 5.15 Relative fluorescence intensities for DGK in mixtures of di(C18:1)PC and di(Br_2C18:0)PC

DGK was reconstituted into mixtures of di(C18:1)PC and di(Br_2C18:0)PC at the given mole fraction of brominated lipid. The solid line is a fit to Equation 5.12 using an n value of 2.53 to give a relative binding constant of 0.88 ± 0.06. In all cases the fluorescence of 0.66 nmoles DGK was excited at 290 nm in 60 mM Pipes, pH 6.85.

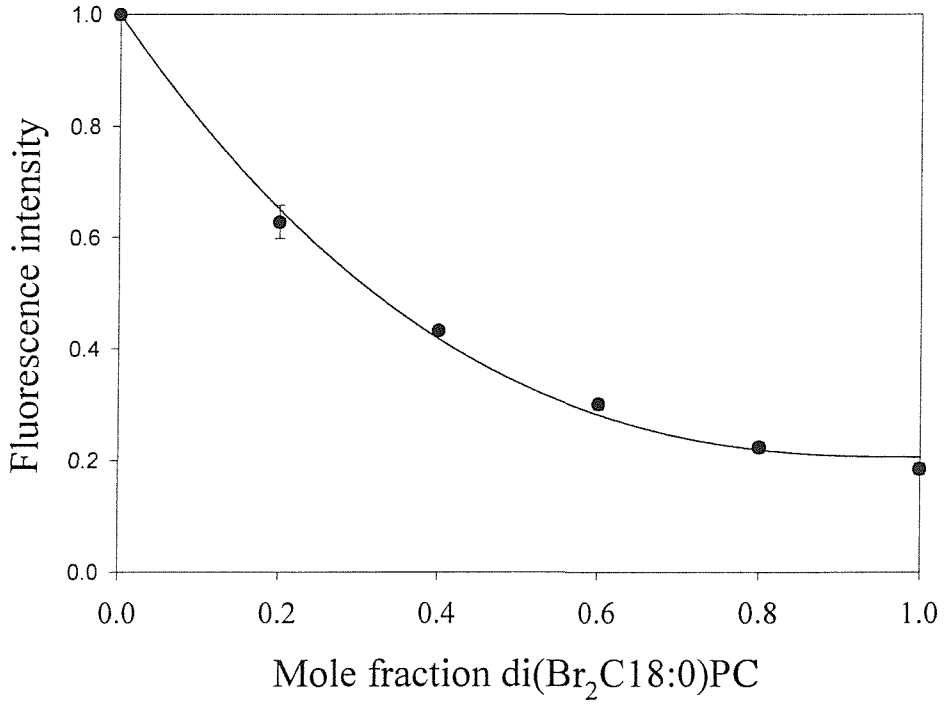

Figure 5.16 Relative fluorescence intensities for DGK in mixtures of di(C20:1)PC and di(Br_2C18:0)PC

DGK was reconstituted into mixtures of di(C20:1)PC and di(Br_2C18:0)PC at the given mole fraction of brominated lipid. The solid line is a fit to Equation 5.12 using an n value of 2.53 to give a relative binding constant of 0.97 ± 0.07. In all cases the fluorescence of 0.66 nmoles DGK was excited at 290 nm in 60 mM Pipes, pH 6.85.

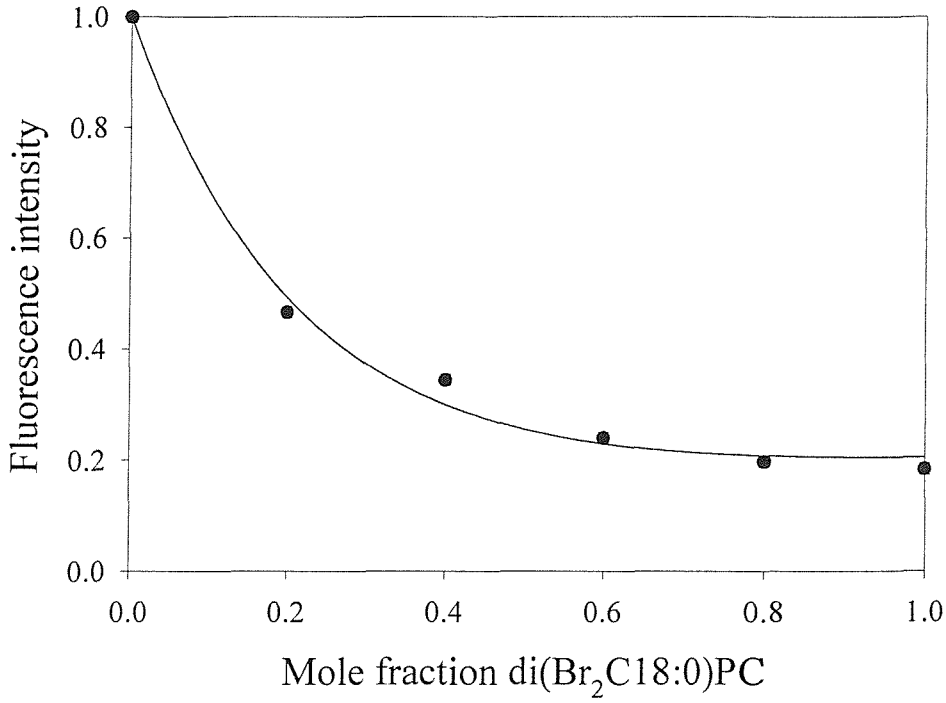

Figure 5.17 Relative fluorescence intensities for DGK in mixtures of di(C24:1)PC and di(Br_2C18:0)PC

DGK was reconstituted into mixtures of di(C24:1)PC and di(Br_2C18:0)PC at the given mole fraction of brominated lipid. The solid line is a fit to Equation 5.12 using an n value of 2.53 to give a relative binding constant of 0.51 ± 0.06. In all cases the fluorescence of 0.66 nmoles DGK was excited at 290 nm in 60 mM Pipes, pH 6.85.

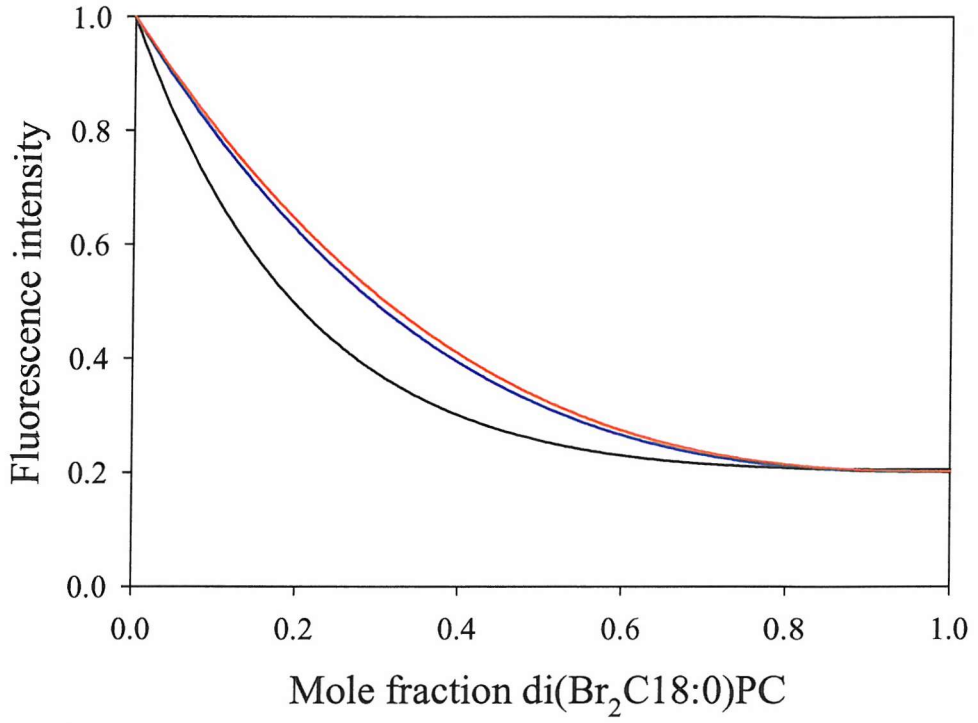

Figure 5.18 Comparison of the relative fluorescence intensities for DGK in mixtures of di(C14:1)PC, di(C18:1)PC, or di(C24:1)PC and di(Br_2C18:0)PC

DGK was reconstituted into mixtures of di(C14:1)PC (red trace), di(C18:1)PC (blue trace), or di(C24:1)PC (black trace) and di(Br_2C18:0)PC at the given mole fraction of brominated lipid. The solid lines are a fit to Equation 5.12 using an n value of 2.53. In all cases the fluorescence of 0.66 nmoles DGK was excited at 290 nm in 60 mM Pipes, pH 6.85. In all cases the fluorescence of 0.66 nmoles DGK was excited at 290 nm in 60 mM Pipes, pH 6.85.

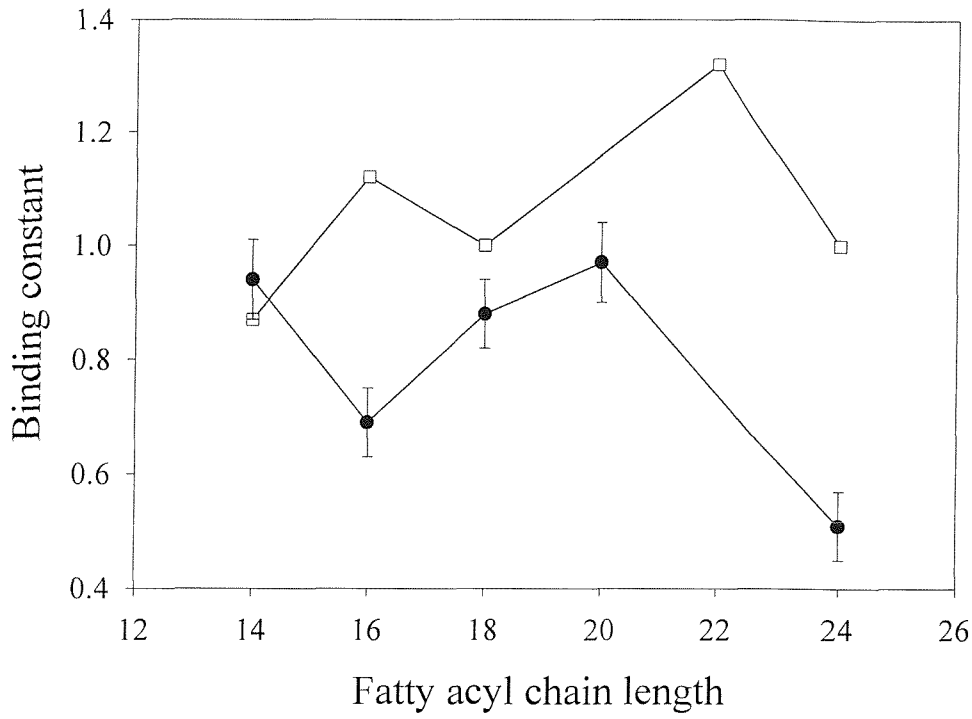

Figure 5.19 Binding constants of DGK for different chain length phosphatidylcholines compared to those obtained for the Ca^{2+}-ATPase (East & Lee, 1982)

The binding constants of DGK for phosphatidylcholines with different chain lengths were measured in fluorescence quenching studies with di(Br_2C18:0)PC. The values obtained for DGK (□) were compared to those obtained for the Ca^{2+}-ATPase (●) in previous studies (East & Lee, 1982).

Phospholipid	Activity against DOG (μmoles/min/mg protein)	Activity against DHG (μmoles/min/mg protein)
Di(C18:1)PC	63.3	1.5
Di(C14:0)PC	58.3	-
Di(C22:1)PC	66.2	-
Di(C18:1)PE	65.1	1.8
Di(C18:1)PS	67.1	1.2
Di(C18:1)PA	70.3	6.8
Cardiolipin	72.6	24.2
No added phospholipid	65.3	1.0

Table 5.1 Steady-state activities of DGK in 1,2-dioleoylglycerol mixed micelles of OG

The activity of DGK was measured according to the experimental conditions described in the methods section, in 1.5 % (w/v) octylglucoside (OG) at 25°C. In all assays the concentration of 1,2-dioleoyl-sn-glycerol (DOG) was 5.1 mol %, except when no cofactor was present, when the concentration was 4.6 mol %. All concentrations are expressed as a mol % of the mixture of OG, phospholipid and diacylglycerol.

Lipid	Time for reconstitution	Activity in di(C14:1)PC against DHG μmoles/min/mg protein	Activity in OG micelles against DOG μmoles/min/mg protein
di(C14:1)PC	5 min	21.1	53
	3 h	20.6	52.4
di(C18:1)PC	5 min	63.3	56.7
	1 h	63.0	58.1

Table 5.2 Effects of reconstitution are reversible

DGK was incubated in cholate with a 20 mol % mixture of DHG and the given phospholipid for the given period of time. A sample was then reconstituted by dilution, and the activity determined. A second sample was diluted into an assay cuvette containing OG and DOG and the activity determined.

Phospholipid	v_{max} (μmoles/min/mg) of DGK for DHG	K_d (mM) of DGK for DHG	v_{max} (μmoles/min/mg) of DGK for ATP	K_d (mM) of DGK for ATP
Di(C14:1)PC	74.9 ± 6.27	64.5 ± 6.71	27.4 ± 0.36	1.8 ± 0.06
Di(C16:1)PC	75.4 ± 2.39	9.4 ± 0.68	63.3 ± 1.88	0.5 ± 0.05
Di(C18:1)PC	74.5 ± 1.22	4.9 ± 0.24	64.8 ± 0.84	0.2 ± 0.01
Di(C20:1)PE	61.4 ± 1.39	4.4 ± 0.32	48.3 ± 0.92	0.3 ± 0.02
Di(C22:1)PS	42.5 ± 0.63	2.4 ± 0.15	35.9 ± 0.91	0.2 ± 0.02
Di(C24:1)PA	24.1 ± 1.13	0.5 ± 0.25	20.8 ± 0.77	0.2 ± 0.03

Table 5.3 Effects of phosphatidylcholine chain length on K_m and v_{max} values for DHG and ATP

DGK was incubated with the appropriate mol % of phospholipid and DHG. The activity of DGK was measured according to the experimental conditions described in the methods section.

Phospholipid	Fitted f_{min} (where n=2.53)	Experimental f_{min}
Di(C18:1)PC	0.20 ± 0.02	0.16
Di(C14:1)PC	0.14 ± 0.02	0.14
Di(C16:1)PC	0.18 ± 0.02	0.15
Di(C24:1)PC	0.46 ± 0.01	0.43

Table 5.4 Fitted and experimental f_{min} values for DGK reconstituted with phosphatidylcholines, ranging in chain length from C14 to C24, and their brominated counterparts

The experimental f_{min} values were determined relative to a factor of 1 using the initial fluorescence in the appropriate chain length non-brominated phospholipid. The fitted f_{min} values were calculated using Equation 5.12 and an n value of 2.53 ± 0.47.

Phospholipid	Relative binding constant (K)
Di(C14:1)PC	0.94 ± 0.07
Di(C16:1)PC	0.69 ± 0.06
Di(C18:1)PC	0.88 ± 0.06
Di(C20:1)PC	0.97 ± 0.07
Di(C24:1)PC	0.51 ± 0.06

Table 5.5 Relative binding constants for DGK in phosphatidylcholines of different chain lengths

The binding constants of DGK for phosphatidylcholines of different chain lengths were determined using an n value of 2.53 from data presented in Figures 5.13 to 5.17.

5.4 Discussion

Many physical features of a lipid bilayer have been suggested to be important in determining the activity of a membrane protein embedded within the bilayer, including bilayer fluidity, bilayer thickness, the free volume available within the bilayer, the charge on the bilayer surface, and any bilayer 'frustration' arising from the presence within the bilayer of lipids that prefer non-bilayer structures (Brown, 1997). In addition to these non-specific effects, specific phospholipids may bind strongly to a small number of sites on a membrane protein, acting as co-factors, the classic example being provided by cardiolipin, essential for the activity of many proteins important in bioenergetics (McAuley et al., 1999).

The simplicity of both the structure and the kinetics of DGK make DGK an ideal protein with which to define the important features of the surrounding lipid bilayer. Using the reconstitution protocol, using DHG as substrate, we have shown that bilayer thickness has a marked effect on the activity of DGK with a maximum activity at a chain length of C18 (Figure 5.3). DGK is predicted to contain three transmembrane α-helices (Smith et al., 1994). Wen et al. (1996) have suggested that transmembrane α-helix M1 is relatively short containing just 14 residues, running from Glu-34 to Asp-49, whereas M2 running from Asp-51 to Glu-69 contains 17 residues and M3, from Met-96 to Trp-117, contains 22 residues. In the family of bacterial DGKs, the residue equivalent to Glu-34 in *E. coli* DGK is not conserved, whereas Glu-28 is conserved in all but the DGK from the cyanobacterium *Synechocystis sp.* (de Boeck & Zidovetski, 1992) where it is replaced by a Gln. If it is assumed that M1 starts at Glu-28 rather than Glu-34, the length of M1 becomes 21 residues. This would imply that Glu-34 is embedded within the lipid bilayer. There

are precedents for suggesting that an acidic residue might be located within the hydrocarbon core of the bilayer. For example, in the Ca^{2+}-ATPase Asp-59 is buried within the bilayer and faces out into the bilayer, forming an ion pair with Arg-63 (Toyoshima et al., 2000). It is possible that in *E. coli* DGK Glu-34 forms an ion pair with Arg-32. Cross-linking experiments have suggested that M2 is at the trimer interface of DGK (Nagy et al., 2000) suggesting that M1 and M3 will be exposed to lipid. If helices M1 and M3 contain 21-22 residues, the length of the helices will be about 32 Å, assuming an ideal α-helix with a helix translation of 1.5 Å per residue. The hydrophobic thickness of a bilayer of di(C18:1)PC is about 29.8 Å (Lewis & Engelman, 1983; Sperotto & Mouritsen, 1988). The best hydrophobic match for DGK will therefore be with a bilayer of di(C18:1)PC, consistent with the observation that the highest activity is seen in a bilayer of this lipid (Figure 5.3).

The low activity observed in di(C14:1)PC measured at 20 mol % DHG and 5 mM ATP (Figure 5.3) follows from an increase in K_m value for DHG (Figure 5.5); the K_m value for DHG increases from 4.9 ± 0.7 mol % in di(C18:1)PC to 64.5 ± 6.7 mol % in di(C14:1)PC whereas v_{max} in di(C18:1)PC (74.5 ± 1.2 μmoles/min/mg) is the same as in di(C14:1)PC (74.9 ± 6.3 μmoles/min/mg). The K_m value for ATP also increases from 0.21 ± 0.01 mM in di(C18:1)PC to 1.83 ± 0.06 mM in di(C14:1)PC. The observation that the low activity in di(C14:1)PC follows from changes in K_m values and not from changes in v_{max} shows that any changes in the dynamic properties of the lipid bilayer (such as changes in fluidity or viscosity) are unimportant since changes in a dynamic property of the system cannot result in changes in an equilibrium property such as a K_m value (Lee & East, 1993). Since DGK catalyses direct phosphoryl transfer from ATP to diacylglycerol it is likely that ATP binds to DGK with its γ-phosphate close to the –OH group of the diacylglycerol (Badola &

Sanders, 1997). The binding sites for ATP have been located at the subunit-subunit interfaces in the DGK trimer (Lau et al., 1999) suggesting that the diacylglycerol binding site could also be located at the subunit-subunit interfaces. The observed increases in K_m for both ATP and DHG in di(C14:1)PC therefore suggest that packing at the subunit-subunit interface has changed as the transmembrane α-helices tilt to match the thin bilayer.

Effects of long chain phosphatidylcholines are very different to those of short chain phosphatidylcholines. For phosphatidylcholines with chain lengths greater than C18 the observed decreases in activity with increasing chain length do not follow from any changes in K_m for ATP or DHG but, rather, from a decrease in v_{max} (Figure 5.5). Such a change might occur, for example, if the binding sites for ATP and diacylglycerol on DGK became misaligned so that the rate of phosphoryl transfer is decreased.

Phosphatidylcholines in the liquid crystalline phase show close to ideal mixing even when there is a marked difference in chain length for the component phospholipids (Lee, 1978). The lipid environment experienced by DGK reconstituted into a mixture of two phosphatidylcholines with different chain lengths will therefore correspond to an averaged environment. In fact, effects of mixtures of phosphatidylcholines with different chain lengths are consistent with the idea that an important feature of the bilayer is its average thickness. For example, addition of di(C14:1)PC or di(C24:1)PC to a bilayer of di(C18:1)PC will result respectively in a decrease or increase in average bilayer thickness, resulting in a decrease in activity, as observed (Figure 5.7). Particularly striking is the observation that suitable mixtures of di(C14:1)PC and di(C24:1)PC support high activities even though each lipid supports only a low activity on its own (Figure 5.7). In these mixtures the average chain length

determines the activity. For example, the average chain length for a 0.8:0.2 mixture of di(C14:1)PC:di(C24:1)PC is C16, a chain length giving close to maximum activity (Figure 5.3), consistent with the high activity observed in the mixture. At a molar ratio of di(C14:1)PC:di(C24:1)PC of 0.4:0.6 the average chain length has become C20 and in di(C20:1)PC activities are still close to that seen in di(C18:1)PC (Figure 5.3). However, further increases in the proportion of di(C24:1)PC lead to average chain lengths corresponding to regions of the chain-length dependency curve where low activities are observed (Figure 5.3), explaining the decrease in activity observed in mixtures containing a mol fraction of more than 0.6 di(C24:1)PC. Similar observations have been made for the Ca^{2+}-ATPase although for the Ca^{2+}-ATPase activity changes more steeply with changes in lipid composition, suggesting that effects of chain length on the Ca^{2+}-ATPase are more cooperative than those on DGK (Starling et al., 1993).

The binding constants of DGK for phosphatidylcholines of different fatty acyl chain lengths suggest that DGK has little preference for lipids of fatty acyl chain length C14 to C20, whilst lipids with fatty acyl chains longer than this bind weakly (Figure 5.19). This is in contrast to binding studies of the Ca^{2+}-ATPase, which reveal no preference for fatty acyl chain length (East & Lee, 1982). This is probably attributable to differences in the secondary structures of these proteins. The fact that DGK fluorescence in non-brominated phosphatidylcholines is identical for chain lengths C14 to C24 and that the F_{min} values are nearly identical for DGK in di(Br_2C14:0)PC and di(Br_2C18:0)PC but different in di(Br_2C24:0)PC suggests that changing the fatty acyl chain length does not result in any significant change in protein structure, but that the difference seen in di(Br_2C24:0)PC is probably due to the position of the bromine in the bilayer being too far away from the Trp residues to

quench the fluorescence. The level of quenching of about 80 % observed with di(Br_2C18:0)PC is more than was expected with the predicted location of 3 of the 5 Trp residues (66 %) in the transmembrane regions of DGK (Nagy et al., 2000). This suggests that in addition to the three transmembrane Trp residues being quenched, at least one Trp residue in amphipathic helix 2 is also quenched indicating that it is in contact with the membrane or close enough to a membrane Trp residue for energy transfer to take place.

Effects of short chain phosphatidylcholines on the activity of the Ca^{2+}-ATPase can be reversed by addition of an alkane such as decane (Johannson et al., 1981; Lee et al., 1991; Jones et al., 1985). Since the effects of long chain phosphatidylcholines cannot be reversed in the same way it was suggested that decane partitioned into the centre of the lipid bilayer, thickened the bilayer and so increased the activity for the ATPase in di(C14:1)PC, but not in di(C24:1)PC (Johannsson et al., 1981). However, partitioning of hexane into bilayers of di(C18:1)PC has been shown to result in no increase in volume for the hydrocarbon core of the bilayer; that is, neither the thickness of the bilayer nor the area occupied per lipid molecule in the bilayer surface increases (Pope & Dubro, 1986; King et al., 1985). Hexane simply fills voids in the bilayer, believed to be concentrated in the most disordered region of the bilayer, the bilayer centre. This is consistent with neutron diffraction studies which show that hexane, in a phosphatidylcholine bilayer in the liquid crystalline state, is located mainly in a zone 10 Å wide in the centre of the bilayer (White et al., 1981). NMR studies of deuterated hexane show that the long axis of the hexane molecule is orientated parallel to the bilayer normal (that is, parallel to the lipid fatty acyl chains) (Jacobs & White, 1984). NMR studies show that longer chain alkanes such as dodecane are also oriented with their long axes parallel to the lipid fatty acyl chains (Pope et al., 1984).

Since long chain alkanes, long chain fatty acids and long chain fatty alcohols all have the same effect as decane on the Ca^{2+}-ATPase, it was also suggested that effects of all these molecules could follow from direct binding to the Ca^{2+}-ATPase rather than from any effect on bilayer thickness (Lee et al., 1991; Jones et al., 1985). As shown in Figure 5.8, decane had no significant effect on the activity of DGK in any of the lipid bilayers. This suggests that decane is unable to bind to DGK in the same way that it does to the Ca^{2+}-ATPase.

In contrast to the lack of effect of decane, addition of cholesterol to DGK in di(C14:1)PC roughly doubles activity whereas addition of cholesterol to DGK in di(C18:1)PC or di(C24:1)PC causes a slight decrease in activity (Figure 5.10). It has been estimated from the NMR order parameter data that, in the liquid crystalline phase, the effective length of the fatty acyl chains of di(C14:0)PC and di(C18:0)PC increase by 2.1 – 2.5 Å on incorporation of 50 mol % cholesterol (Sankaram & Thompson, 1990). The bilayer hydrophobic thickness d is related to chain length n by (Lewis & Engelman, 1983; Sperotto & Mouritsen, 1988)

$d = 1.75(n\text{-}1)$

The effect of 50 mol % cholesterol is therefore to increase the effective chain length by the equivalent of about 1 to 1.5 carbons, consistent with the observed increase in activity seen on addition of cholesterol to DGK in di(C14:1)PC to give an activity somewhat less than that observed in di(C16:1)PC (Figure 5.3). An increase in effective chain length on addition of cholesterol would be expected to reduce activity in the longer chain phosphatidylcholines, as observed experimentally (Figure 5.10). Also consistent with the proposal that cholesterol increases the activity of DGK in di(C14:1)PC through an effect on bilayer thickness is the observation that cholesterol

decreases the K_m value for DHG in di(C14:1)PC with no significant effect on v_{max} (Figure 5.4).

Cholesterol and other sterols have also been shown to increase the activity of the Ca^{2+}-ATPase in di(C14:1)PC but with no effect on the activity in di(C24:1)PC (Starling et al., 1993). The activity in di(C14:1)PC at a 1:1 molar ratio of sterol to phospholipid was equal to that in the optimum phospholipid, di(C18:1)PC; this is significantly different to the observations made here with DGK, where activities in mixtures of di(C14:1)PC and cholesterol were always less than those in di(C18:1)PC (Figure 5.10). This suggests that effects of cholesterol on the Ca^{2+}-ATPase could be more complex than those on DGK and, indeed, it has been suggested that the effects of cholesterol on the Ca^{2+}-ATPase could follow from direct binding to the ATPase (Starling et al., 1993; Ding et al., 1994).

In conclusion, *E. coli* DGK shows its highest activity in di(C18:1)PC the lipid which most closely matches the expected length of the DGK transmembrane α-helices. These effects can be compared with the effects of phospholipid chain length on the function of *E. coli* melibose permease where the highest rates of transport were seen in di(C16:1)PC (Dumas et al., 2000). Since membrane proteins seem to have little ability to select between lipids on the basis of chain length (Lee, 1998) it appears that either DGK or the melibose permease (or both) must be functioning in the *E. coli* membrane at less than their maximal rates.

CHAPTER 6: Effects of phospholipid headgroup and phase on the activity of diacylglycerol kinase of *Escherichea coli*

6.1 Introduction

Biological membranes contain a complex mixture of lipids, differing in their polar headgroups and fatty acyl chains. All membranes contain both anionic and zwitterionic lipids. The presence of anionic lipids is obviously important for the binding of peripheral membrane proteins to the surface of the membrane. Some peripheral proteins bind through domains specific for a particular class of lipid headgroup such as the PH domain that recognises phosphoinositides such as PtdIns(4,5)P_2 (Bottomley et al., 1998). Other peripheral proteins contain extended patches of positively charged residues that interact electrostically with any anionic lipids in the membrane (Murray et al., 1998). The presence of these anionic phospholipids has to be compatible with the proper function of the intrinsic membrane proteins present in the membrane. In fact, some intrinsic membrane proteins actually show a specific requirement for the presence of a particular class of anionic lipid. For example, there is considerable evidence that the presence of cardiolipin is required for the proper function of a number of enzymes involved in oxidative phosphorylation, such as cytochrome oxidase (Robinson, 1982; Robinson et al., 1990). Surprisingly although a tightly bound lipid molecule has been identified in the crystal structure of cytochrome oxidase from *P. dentrificans* this is a phosphatidylcholine rather than cardiolipin (Iwata et al., 1995). However, the crystal structure of the photosynthetic reaction centre from *Rhodobacter sphaeroides* does show the presence of a tightly bound cardiolipin molecule (McAuley et al., 2000).

The headgroup of the lipid is also important in determining the phase preference of the lipid. Whilst phospholipids such as the phosphatidylcholines adopt a lamellar, bilayer structure at normal temperatures, others, such as the phosphatidylethanolamines, can also adopt a curved hexagonal H_{II} structure (Marsh, 1990). Although this hexagonal structure is not compatible with the formation of a bilayer membrane, lipids favouring the hexagonal H_{II} phase are often the major lipids in a membrane. For example, in the cell membrane of *E. coli*, 72 % by weight of the lipid is phosphatidylethanolamine, 24 % is phosphatidylglycerol and 4 % is cardiolipin (Harwood & Russell, 1984; de Kruijff et al., 1998). The presence of relatively small amounts of a bilayer-favouring phospholipid (typically about 10 % or more) will force the phosphatidylethanolamine to adopt a bilayer structure, but the phosphatidylethanolamine is said to be in a state of frustration (Gruner, 1985). It has been suggested that the presence of lipids in a state of frustration could be important for the proper function of intrinsic membrane proteins (Gruner, 1985). For example, the presence of lipids able to form a hexagonal H_{II} phase seems to be required to produce the metarhodopsin II to metarhodopsin I ratio found for rhodopsin in the retinal rod membrane (Brown, 1994). Whilst the activity of the Ca^{2+}-ATPase in di(C18:1)PE has been shown to be about half that in di(C18:1)PC (East & Lee, 1982), the reconstitution of the ATPase into vesicles containing mixtures of di(C18:1)PE and di(C18:1)PC results in increasing Ca^{2+} accumulation levels with increasing di(C18:1)PE content up to 80 % (Navarro et al., 1984; Gould et al., 1987a). The effects of di(C18:1)PE on activity are observed only at temperatures at which the lipid adopts a hexagonal H_{II} phase, and is a result of a 60-70 % decrease in the rate of dephosphorylation of the phosphorylated ATPase (Starling et al., 1996), whilst the lipid headgroup structure itself has no effect (Starling et al., 1996). The presence of

di(C18:1)PE has been shown to decrease the rate of passive Ca^{2+} leakage from the reconstituted vesicles, thus increasing levels of Ca^{2+} accumulation (Gould et al.,1987a,b).

As demonstrated in Chapter 5 the thickness of the hydrophobic core of the lipid bilayer, largely determined by the length of the fatty acyl chains in the lipid, is also important for the proper function of intrinsic membrane proteins. Studies of the Ca^{2+}-ATPase of sarcoplasmic reticulum have shown that bilayers of dioleoylphosphatidylcholine (di(C18:1)PC support the highest rate of ATP hydrolysis for the Ca^{2+}-ATPase and that activities are lower in phosphatidylcholines with either longer or shorter fatty acyl chains (Lee, 1998). However, as shown in Chapter 3, rather low levels of Ca^{2+} transport were observed when the Ca^{2+}-ATPase was reconstituted into sealed vesicles of di(C18:1)PC alone. Much higher levels of accumulation of Ca^{2+} were observed when the Ca^{2+}-ATPase was reconstituted into bilayers containing 10 % of an anionic phospholipid such as phosphatidic acid, phosphatidylserine or cardiolipin. It was suggested that anionic phospholipids affected the rate of slippage on the ATPase, as described in Chapter 3.

6.1.1 Anionic phospholipids

In studies of the effects of negatively charged phospholipids on membrane protein activity, special attention needs to be paid to interactions between the phospholipid headgroups and divalent metal ions such as Ca^{2+} and Mg^{2+}. Dioleoylphosphatidic acid (diC18:1)PA) adopts a bilayer structure at room temperature in the pH range 4-9 in the absence of divalent metal ions. However, in the presence of Ca^{2+} or Mg^{2+}, structures are very pH dependent, rather ill defined, and

different for saturated and unsaturated lipids (Farren et al., 1983; Miner & Prestegard, 1984). At pH 8.0 di(C18:1)PA is present as a mixture of the singly and doubly charged forms and the addition of Ca^{2+} or Mg^{2+} to vesicles of di(C18:1)PA causes flocculation due to vesicle aggregation; the lipid, however, remains in a bilayer structure. At pH 7.4 or pH 6.0 when di(C18:1)PA is present largely in the singly ionised form, addition of Ca^{2+} or Mg^{2+} results in the formation of a unique phase that is neither lamellar nor hexagonal but with the fatty acyl chains being highly ordered (Caffrey & Feigenson, 1984). In the liquid crystalline phase phosphatidylcholine and phosphatidic acid mix almost ideally in the absence of divalent metal ions (Kouaouci et al., 1985; Graham et al., 1985), but addition of Ca^{2+} leads to the formation of clusters enriched in phosphatidic acid; Mg^{2+} is much less effective than Ca^{2+} in inducing cluster formation (Caffrey & Feigenson, 1984; Graham et al., 1985; Galla & Sackmann, 1975; Ito & Ohnishi, 1974; Haverstick & Glaser, 1987). Vesicles of phosphatidic acid undergo fusion upon the addition of 0.2 mM Ca^{2+} or 0.4 mM Mg^{2+} at pH 7.4. The threshold of cation necessary for fusion of phosphatidic acid to occur is dependent upon pH; fusion at low pH values requires higher concentrations of cation (Sundler & Papahadjopoulos, 1981; Ohki & Zschornig, 1993). The affinity of phosphatidic acid for Ca^{2+} and Mg^{2+} is almost identical. The presence of phosphatidylcholine in a vesicle with phosphatidic acid raises the threshold concentration of Ca^{2+} required for fusion, abolishes the Mg^{2+}-induced fusion, although aggregation still takes place, and reduces the rate of fusion (Sundler et al., 1981). The presence of phosphatidylethanolamine causes a slight increase in the Ca^{2+} threshold concentration for fusion even at 80 % phosphatidylethanolamine; in mixtures of phosphatidic acid and phosphatidylethanolamine Mg^{2+} can also induce fusion (Sundler et al., 1981).

Unsaturated phosphatidylserines also adopt a liquid crystalline, bilayer structure in the absence of divalent metal ions over the pH range 4-8 (Hope & Cullis, 1980; de Kroon et al., 1990; Browning & Seelig, 1980). Addition of Ca^{2+} to vesicles composed of phosphatidylserine results in precipitation of the lipid with the formation of cochleate cylinders (Portis et al., 1979); in these structures the bilayer is maintained but the temperature of the gel to liquid crystalline phase-transition is much increased so that the fatty acyl chains become rigidly packed (Hauser & Shipley, 1984; Dluhy et al., 1983). Addition of Mg^{2+} also precipitates vesicles composed of phosphatidylserine, but at higher concentrations than Ca^{2+}, and no change in chain packing is seen with dioleoylphosphatidylserine (di(C18:1)PS) (Hope & Cullis, 1980; Casal et al., 1989). Dioleoylphosphatidylcholine (di(C18:1)PC) and di(C18:1)PS mix almost ideally at high mole fractions of phosphatidylserine but non-ideally at low phosphatidylserine, the non-ideality being such as to favour interactions between unlike molecules (Feigenson, 1989). Addition of Ca^{2+} to mixtures of phosphatidylserine and phosphatidylcholine has been shown to result in phase separation of solid aggregates of phosphatidylserine, but again with Mg^{2+} having little effect (Haverstick & Glaser, 1987; Ohnishi & Ito, 1974). The reported changes in the phase of the anionic lipids on binding divalent metal ions could be important, since the activity of other membrane proteins, such as the Ca^{2+}-ATPase, are known to be sensitive to the physical phase of the lipid surrounding it in the membrane (Dalton et al., 1998).

6.1.2 Gel-phase phospholipids and chain length

Phosphatidylcholines undergo a phase transition between gel and liquid-crystalline phases at a temperature defined by the fatty acyl chain length and the

degree of unsaturation. For dimyristoylphosphatidylcholine (di(C14:0)PC) and dipalmitoylphosphatidylcholine (di(C16:0)PC), the transition temperatures are 24 and 42 °C respectively (Lee, 1983). The phase transition results in a marked change in the physical properties of the bilayer, with the fatty acyl chains being packed in a rigid crystalline array in the gel phase, but having considerable freedom of motion in the liquid-crystalline phase (Lee, 1983). It has been shown that phospholipids must be in the liquid-crystalline phase to support activity of the Ca^{2+}-ATPase; in the gel phase, the rate of hydrolysis of ATP becomes very slow (Warren et al., 1974a,b; Nakamura et al., 1976; Hidalgo et al., 1978; Gomez-Fernandez et al., 1985). Studies of the kinetics of the ATPase in di(C16:0)PC in the gel phase have shown that the low steady-state activity of the ATPase follows from a very slow rate of transfer of the γ-phosphate from ATP to the ATPase in the $E1Ca_2MgATP$ complex (Starling et al., 1994).

6.2 Methods

The purification, reconstitution, activity and fluorescence measurements of DGK are as described in Section 5.2.

6.3 Results

6.3.1 Effects of anionic phospholipids

The activity of DGK reconstituted into bilayers of di(C18:1)PA, di(C18:1)PS or cardiolipin is low, 10 % or less of that in di(C18:1)PC (Table 6.1). In mixtures of di(C18:1)PC and di(C18:1)PS or cardiolipin activity decreases fairly smoothly with increasing content of anionic phospholipid whereas in mixtures with di(C18:1)PA activity is very low even at 20 mol % di(C18:1)PA (Figure 6.1).

DGK shows simple Michaelis-Menten kinetics with respect to both ATP and diacylglycerol. Reconstitution of DGK into lipid bilayers containing different proportions of DHG allows activity to be measured as a function of DHG concentration, expressed as mol % in the lipid bilayer. Activities were measured at a MgATP concentration of 5 mM for DGK reconstituted into bilayers of di(C18:1)PC containing 20 mol % of the anionic phospholipid (Figure 6.2). The data fit well to a simple Michaelis-Menten scheme with the K_m and v_{max} values listed in Table 6.2. As shown, the presence of 20 mol % di(C18:1)PG had little effect on activity. The presence of 20 mol % di(C18:1)PS or di(C18:1)PI had little effect on v_{max} but caused a significant increase in K_m. In contrast, the presence of 20 mol % cardiolipin decreased activity through a decrease in v_{max} with little effect on the K_m for DHG. Finally, the presence of di(C18:1)PA, the most inhibitory of the anionic phospholipids, resulted in both a decrease in v_{max} and an increase in K_m for DHG.

Activities as a function of ATP concentration at a fixed DHG concentration of 20 mol % also fitted well to Michaelis-Menten kinetics (Figure 6.3) with the K_m and v_{max} values in Table 6.3. Effects on K_m for ATP were rather small, with the K_m decreasing somewhat in cardiolipin.

The true substrate of DGK is MgATP, but it has been shown that free Mg^{2+} is an activator of DGK activity with a K_a value of 3.4 mM (Walsh & Bell, 1986a). The activity of DGK in the reconstituted systems as a function of free Mg^{2+} concentration again fitted to simple Michaelis-Menten kinetics (Figure 6.4) with the K_a values listed in Table 6.4. The presence of 20 mol % cardiolipin had little effect on the K_a value but the presence of 20 mol % di(C18:1)PS or di(C18:1)PA increased the K_a value approximately 3 fold.

6.3.2 Effects of phospholipid phase

The activity of DGK in mixtures of di(C18:1)PC and di(C18:1)PE decreases linearly with increasing di(C18:1)PE content up to 80 mol % di(C18:1)PE (Figure 6.5). Samples of DGK reconstituted into di(C18:1)PE as the only phospholipid were very turbid, probably due to the formation of non-bilayer phases; measurements of activity in these turbid samples were considered to be unreliable, but activities appear to be very low. Activities for DGK in mixtures of 80 % phosphatidylethanolamine, 20 % di(C18:1)PC were determined as a function of temperature (Figure 6.6A). At temperatures above about 18 °C, di(C18:1)PE transforms from a bilayer to a hexagonal H_{II} phase (Marsh, 1990). Activities of DGK in bilayers of 80 mol % di(C18:1)PE at temperatures below 20 °C are less than those in bilayers of di(C18:1)PC at the same temperature (Figure 6.6A). Above 20 °C, the difference in activity for DGK in 80 mol % di(C18:1)PE and di(C18:1)PC increases with increasing temperature. The temperature for the bilayer/hexagonal H_{II} phase transition for egg yolk phosphatidylethanolamine (28 °C) is higher than that for di(C18:1)PE (Cullis & de Kruijff, 1978). Activities of DGK in 80 mol % egg yolk

phosphatidylethanolamine are equal to those in 80 mol % di(C18:1)PE up to about 20 °C, beyond which activities become higher. Above about 30 °C activities in 80 mol % egg yolk phosphatidylethanolamine relative to those in di(C18:1)PC decrease with increasing temperature (Figure 6.6A). These experiments suggest that phosphatidylethanolamines in the bilayer phase support lower activities than those in di(C18:1)PC and that the differences between phosphatidylethanolamines and phosphatidylcholines become more marked at temperatures where the phosphatidylethanolamine could be expected to adopt a hexagonal H_{II} phase. Activities in 80 mol % di(C18:1)PE as a function of DHG concentration fitted well to simple Michaelis-Menten kinetics with the v_{max} and K_m values listed in Table 6.5.

Phosphatidylcholines with saturated fatty acyl chains undergo phase transitions between the fluid, liquid crystalline and solid, gel phases at temperatures that depend on fatty acyl chain length. Phase transition temperatures for di(C14:0)PC and di(C16:0)PC are 24 and 42 °C, respectively (Marsh, 1990). The activity for DGK in di(C16:0)PC is lower than in di(C16:1)PC at all temperatures in the range 15 to 45 °C (Figure 6.6B). The differences in activity decrease with increasing temperature; at 20°C the activity in di(C16:1)PC is 3 times that in di(C16:0)PC, whereas at 40 °C the difference in activity is only 1.2 fold. Activities in di(C14:0)PC are less than in di(C14:1)PC at temperatures below about 30 °C although the differences are rather small (Figure 6.6B). Above about 35 °C activities in di(C14:0)PC no longer increase with increasing temperature and in di(C14:1)PC activities actually decrease with increasing temperature beyond about 35 °C (Figure 6.6B). Effects of low temperature on v_{max} and K_m values for DHG and ATP in di(C14:0)PC and di(C16:0)PC are given in Table 6.6.

Effects of temperature were fully reversible. For example, when DGK was reconstituted in di(C14:1)PC and incubated at 42 °C, followed by addition to micelles of OG containing dioleoylglycerol as substrate, the measured activity was the same as that for a sample of DGK that had not been reconstituted (data not shown).

6.3.3 Effects of phospholipid headgroup on phospholipid binding to DGK

DGK was reconstituted into mixtures of di(Br_2C18:0)PC and di(C18:1)PA, di(C18:1)PS, or cardiolipin. The fluorescence intensity observed for DGK in all of the anionic lipids was 66 % of that in di(C18:1)PC, indicating quenching of DGK fluorescence in anionic lipids. A similar observation has been made for the Ca^{2+}-ATPase where the fluorescence intensity in di(C18:1)PA is 70 % of that in di(C18:1)PC (Dalton et al., 1998). Fluorescence quenching in mixtures with di(Br_2C18:0)PC is shown in Figure 6.7. As shown the fluorescence quenching plots for DGK in mixtures with di(C18:1)PA, di(C18:1)PS and cardiolipin are virtually identical to those in di(C18:1)PC. Thus di(C18:1)PC, di(C18:1)PA, di(C18:1)PS, and cardiolipin all bind with similar affinity to DGK. The data for each phosphatidylcholine was fitted to Equation 5.12 using an n value of 2.53, providing a relative binding constant (K) for each anionic phospholipid. The relative binding constants for each anionic phospholipid are shown in Table 6.7. The results show that DGK has no preference for anionic phospholipids over di(C18:1)PC.

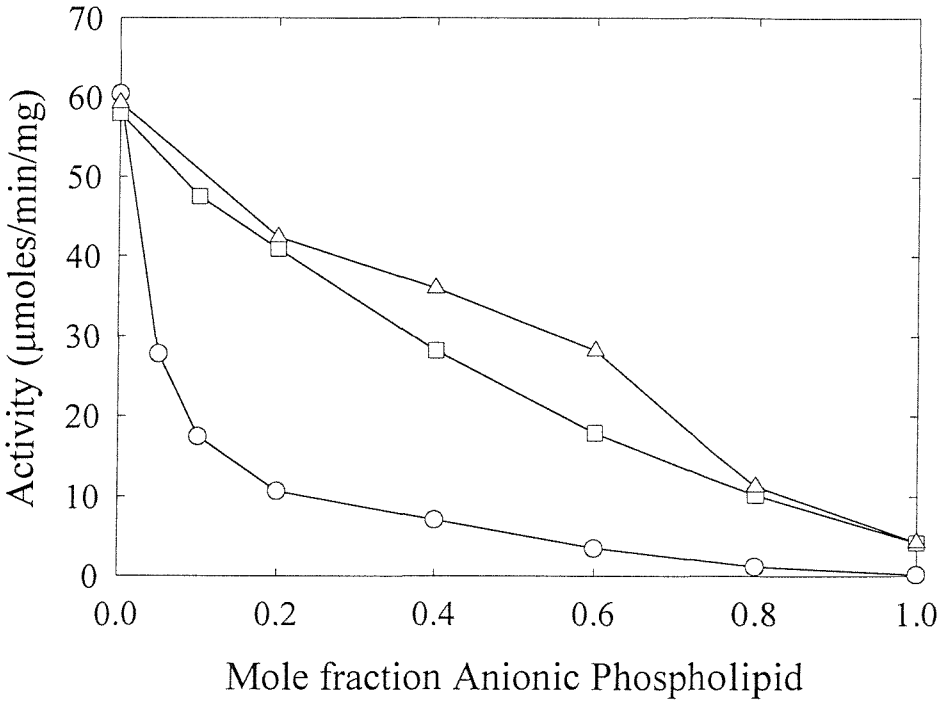

Figure 6.1 DGK activity in mixtures of di(C18:1)PC and anionic phospholipids

The figure shows DGK activity when reconstituted into mixtures of di(C18:1)PC and anionic phospholipids all being in the liquid crystalline phase. DGK was reconstituted with mixtures of di(C18:1)PC and: di(C18:1)PA (○); di(C18:1)PS (□); cardiolipin (Δ). The reaction was initiated by addition of DGK (1.5 μg) dissolved in cholate with phospholipid and DHG to 1 ml of the assay medium. Activities were measured at 25 ^{o}C with 5 mM ATP, 15 mM Mg^{2+}, and 20 mol % DHG.

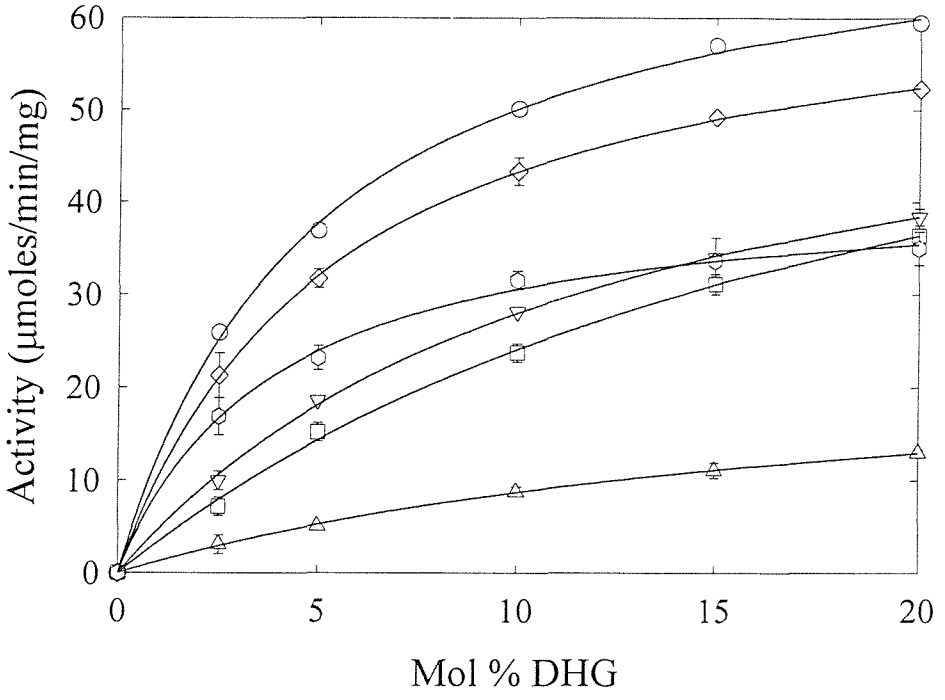

Figure 6.2 Effects of anionic phospholipids on DGK activity as a function of DHG concentration

The figure shows DGK activity when reconstituted into mixtures of di(C18:1)PC containing 20 mol % anionic phospholipid at a constant molar ratio of 6000:1 phospholipid:DGK and the given mol % DHG. Activities were measured at 25 ^{o}C with 5 mM ATP, 15 mM Mg^{2+}. DGK was reconstituted with di(C18:1)PC (○) of mixtures of di(C18:1)PC containing 20 mol % of the following anionic phospholipids; (◊), di(C18:1)PG; (▽), di(C18:1)PI; (□), di(C18:1)PS; (△), di(C18:1)PA; (▢) cardiolipin. The solid lines show fits to the Michaelis-Menten equation with the values for K_m and v_{max} listed in Table 6.2.

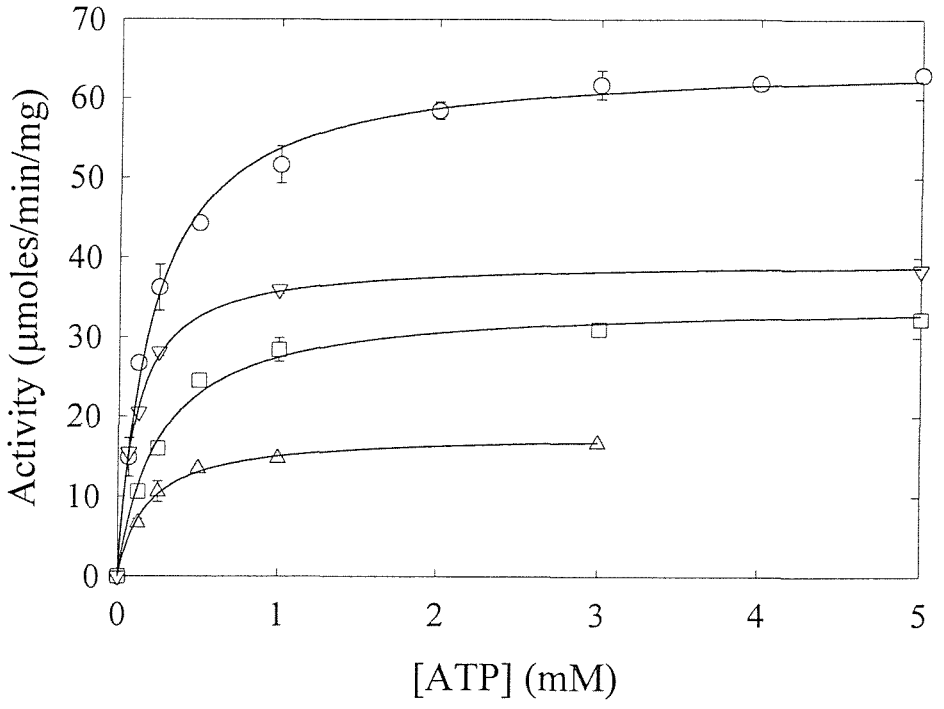

Figure 6.3 Effects of anionic phospholipids on DGK activity as a function of ATP concentration

The figure shows DGK activity when reconstituted into mixtures of di(C18:1)PC containing 20 mol % anionic phospholipid at a constant molar ratio of 6000:1 of phospholipid:DGK and 20 mol % DHG. Activities were measured at 25 ^{o}C with 15 mM Mg^{2+} and the given concentration of ATP. DGK was reconstituted with di(C18:1)PC (○) and with mixtures of di(C18:1)PC containing 20 mol % of the following anionic phospholipids; (□), di(C18:1)PS; (Δ), di(C18:1)PA; (▽) cardiolipin. The solid lines show fits to the Michaelis-Menten equation with the values for K_m and v_{max} listed in Table 6.3.

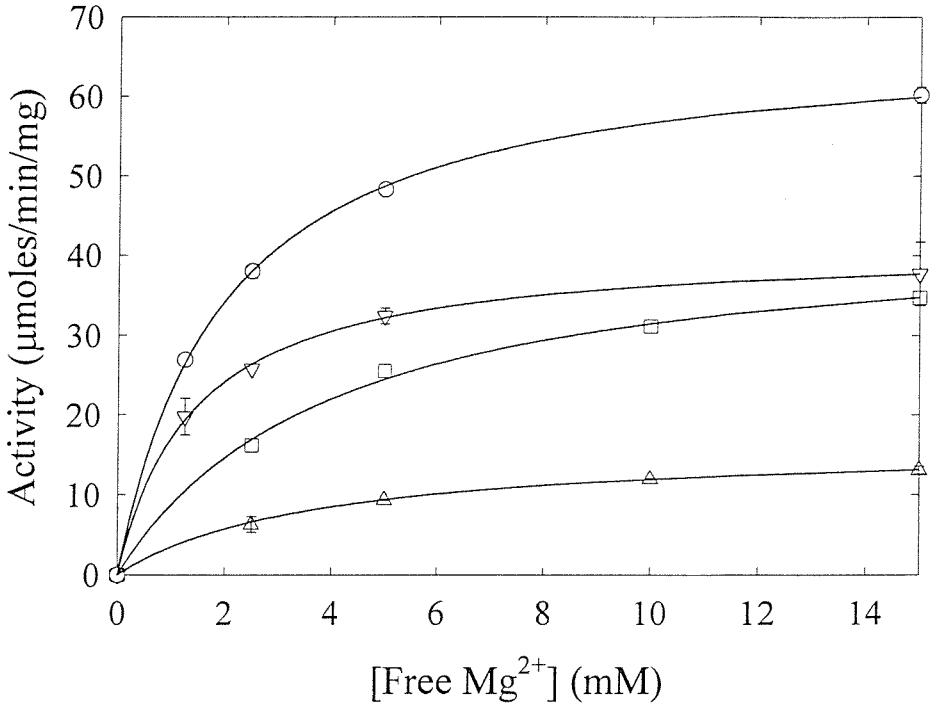

Figure 6.4 Effects of anionic phospholipids on DGK activity as a function of free Mg^{2+} concentration

The figure shows DGK activity when reconstituted into mixtures of di(C18:1)PC containing 20 mol % anionic phospholipid at a constant molar ratio of 6000:1 of phospholipid:DGK and 20 mol % DHG. Activities were measured at 25 °C with 5 mM ATP and the given concentrations of free Mg^{2+}. DGK was reconstituted with di(C18:1)PC (○) of mixtures of di(C18:1)PC containing 20 mol % of the following anionic phospholipids; (□), di(C18:1)PS; (Δ), di(C18:1)PA; (▽) cardiolipin. The solid lines show fits to the Michaelis-Menten equation with the values for K_m and v_{max} listed in Table 6.4.

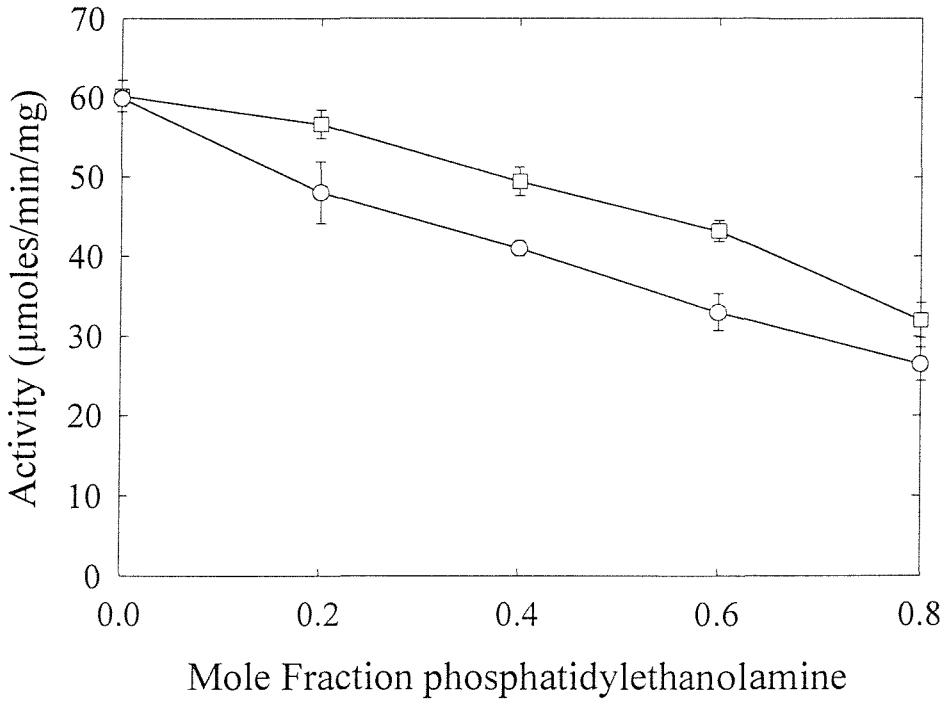

Figure 6.5 DGK activity in mixtures of di(C18:1)PC and phosphatidylethanolamines

The figure shows DGK activity when reconstituted into mixtures of di(C18:1)PC and: di(C18:1)PE (○) or egg yolk phosphatidylethanolamine (□). Activities were measured at 25 ^{o}C at 5 mM ATP, 15 mM Mg^{2+}, and 20 mol % DHG. The reaction was initiated by addition of DGK (1.5 μg) dissolved in cholate with phospholipid and DHG to 1 ml of the assay medium.

Figure 6.6 Effect of temperature on DGK activity in phosphatidylethanolamines and phosphatidylcholines

The figure shows DGK activity when: (A) DGK was reconstituted into di(C18:1)PC (○) or mixtures of 20 mol % di(C18:1)PC and 80 mol % di(C18:1)PE (Δ) or egg yolk phosphatidylethanolamine (□). (B) DGK was reconstituted into: di(C18:1)PC, (○), di(C16:0)PC, (▽); di(C16:1)PC, (□); di(C14:0)PC (Δ); di(C14:1)PC (◊). Activities were measured at 5 mM ATP, 15 mM Mg^{2+}, and 20 mol % DHG. The reaction was initiated by addition of DGK (1.5 μg) dissolved in cholate with phospholipid and DHG to 1 ml of the assay medium.

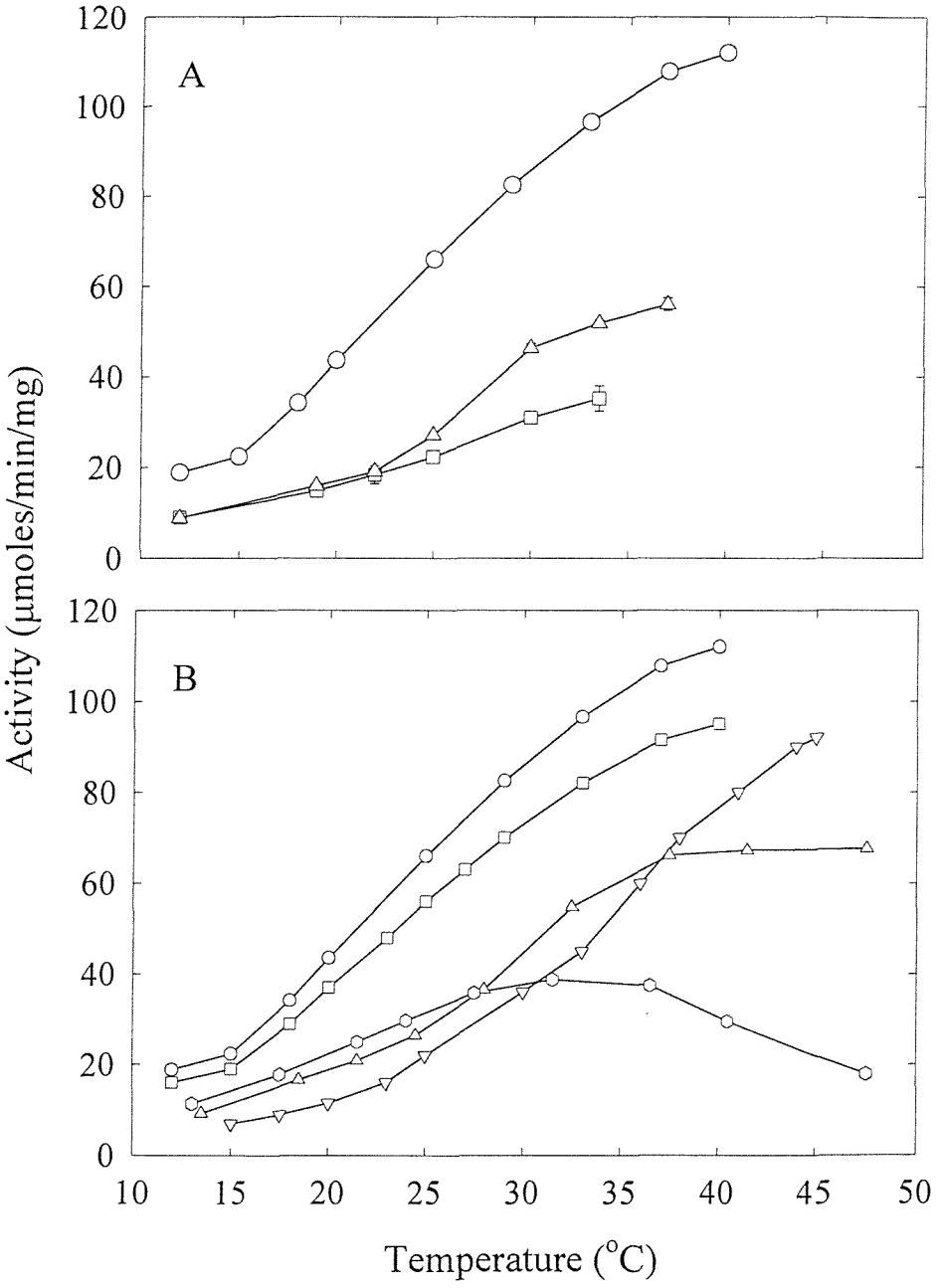
A
B
120
100
80
60
40
20
0
10
15
20
25
30
35
40
45
50
Activity (µmoles/min/mg)
Temperature (°C)

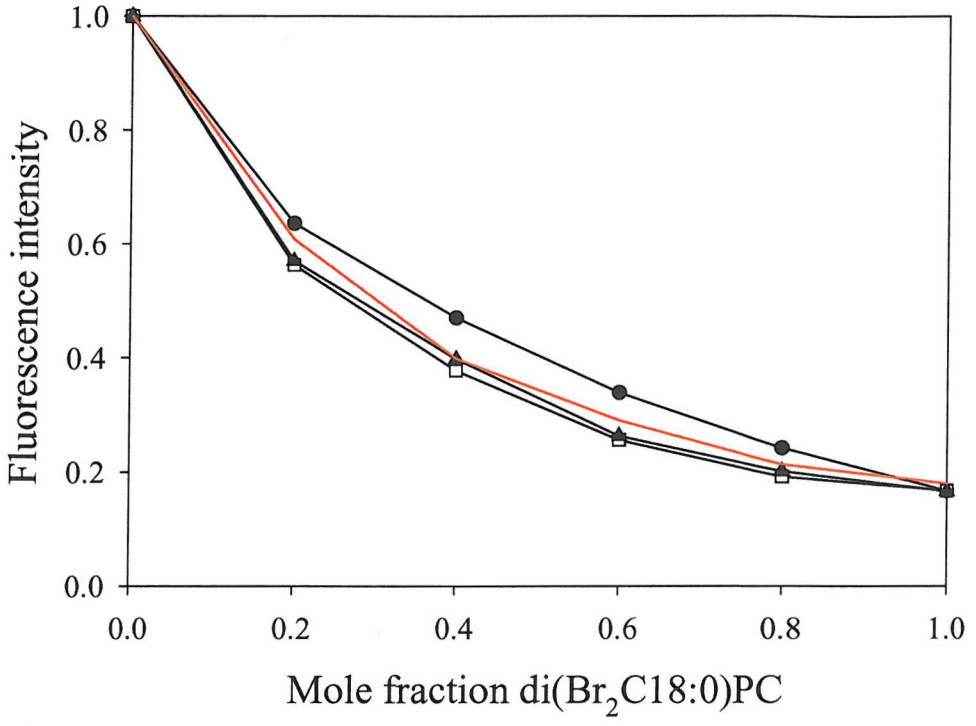

Figure 6.7 Relative fluorescence intensities for DGK in mixtures of di(C18:1)PA, di(C18:1)PS, or cardiolipin and di(Br_2C18:0)PC compared to di(C18:1)PC and di(Br_2C18:0)PC

DGK was reconstituted into mixtures of di(C18:1)PC (red line), di(C18:1)PA (□), di(C18:1)PS (▲), or cardiolipin (●) and di(Br_2C18:0)PC at the given mole fraction of brominated lipid. Fluorescence intensities are expressed relative to those in non-brominated lipid. The solid lines are a fit to Equation 5.12 using an n value of 2.53. In all cases the fluorescence of 0.66 nmoles DGK was excited at 290 nm in 60 mM Pipes, pH 6.85.

System	Activity (IU/mg)
Di(C18:1)PC	60.5
Di(C18:1)PA	0.2
Di(C18:1)PS	4.2
Di(C18:1)PG	25.0
Cardiolipin	4.3
80 % di(C18:1)PE + 20 % di(C18:1)PC	26.5
75 % di(C18:1)PE + 20 % di(C18:1)PG + 5 % cardiolipin	29.5
75 % di(C18:1)PE + 15 % di(C18:1)PG + 10 % cardiolipin	26.5

Table 6.1 Effects of anionic phospholipids on DGK activity

DGK was incubated with the above phospholipids containing 20 mol % DHG. The activity of DGK was measured according to the experimental conditions described in the methods section; activities were measured at 5 mM ATP, 15 mM Mg^{2+}, 20 mol % DHG, 25 °C.

Anionic phospholipid	V_{max} (μmoles/min/mg)	K_m (mol % DHG)
-	74.5 ± 1.2	4.9 ± 0.2
Di(C18:1)PG	66.6 ± 0.5	5.4 ± 0.1
Cardiolipin	42.1 ± 1.0	3.8 ± 0.3
Di(C18:1)PS	74.4 ± 4.9	20.9 ± 2.3
Di(C18:1)PI	61.2 ± 1.7	11.9 ± 0.7
Di(C18:1)PA	25.3 ± 0.9	19.1 ± 1.2

Table 6.2 Effects of anionic phospholipids on v_{max} and K_m values for DHG

DGK was reconstituted into bilayers containing di(C18:1)PC with 20 mol % of the anionic phospholipid. Activities were measured at 5 mM ATP, 15 mM Mg^{2+}, 25 ^{o}C.

Anionic phospholipid	V_{max} (μmoles/min/mg)	K_m (μM ATP)
-	64.8 ± 0.8	0.21 ±0.01
Cardiolipin	39.5 ± 0.4	0.11 ± 0.01
Di(C18:1)PS	34.3 ± 0.9	0.25 ± 0.03
Di(C18:1)PA	17.8 ± 0.4	0.18 ± 0.02

Table 6.3 Effects of anionic phospholipids on v_{max} and K_m values for ATP

DGK was reconstituted into bilayers containing di(C18:1)PC with 20 mol % of the anionic phospholipid. Activities were measured at 20 mol % DHG, 15 mM Mg^{2+}, 25 ^{o}C.

Anionic phospholipid[a]	V_{max} (IU/mg)	K_a (mM Mg^{2+})
-	67.7 ± 0.6	1.9 ± 0.1
Cardiolipin	41.2 ± 0.6	1.4 ± 0.1
Di(C18:1)PS	44.0 ± 1.6	4.0 ± 0.4
Di(C18:1)PA	16.3 ± 0.1	3. 7 ± 0.1

Table 6.4 Effects of anionic phospholipids on v_{max} and K_a values for Mg^{2+}

DGK was reconstituted into bilayers containing di(C18:1)PC with 20 mol % of the anionic phospholipid. Activities were measured at 20 mol % DHG, 5 mM ATP, 25 °C.

Phospholipid	Temperature (^{o}C)	V_{max} (μmoles/min/mg)	K_m (mol % DHG)
Di(C18: 1)PC	25	74.5 ± 1.2	4.9 ± 0.2
	30	108.6 ± 1.7	4.5 ± 0.2
80 mol % di(C18:1)PE	25	25.5 ± 0.6	2.4 ± 0.2
	30	50.8 ± 0.9	13.2 ± 0.5

Table 6.5 Effects of temperature on v_{max} and K_m values for DHG

DGK was reconstituted into bilayers containing 100 mol % di(C18:1)PC and 80 mol % di(C18:1)PE with 20 mol % di(C18:1)PC. Activities were measured at 20 mol % DHG, 5 mM ATP, 15 mM Mg^{2+}, 25 ^{o}C.

Phospholipid	Temp (^{o}C)	DHG (A)		ATP (B)	
		V_{max}	K_m	V_{max}	K_m
		(μmoles/min/mg)	(mol %)	(μmoles/min/mg)	(mM)
Di(C14:0)PC	16	47.9 ± 4.2	27.9 ± 3.7	16.7 ± 0.4	0.24 ± 0.02
Di(C16:0)PC	20	14.9 ± 0.3	3.1 ± 0.2		
	21			17.6 ± 0.4	0.38 ± 0.03

Table 6.6 Effects of temperature on v_{max} and K_m values for DHG in saturated phosphatidylcholines

DGK was reconstituted into bilayers containing di(C14:0)PC and di(C16:0)PC. Activities were measured at: (A) 5 mM ATP, 15 mM Mg^{2+} and (**B**) 20 mol % DHG, 15 mM Mg^{2+}.

Phospholipid	Relative binding constant (K)
Di(C18:1)PC	0.88 ± 0.06
Di(C18:1)PA	0.77 ± 0.06
Di(C18:1)PS	0.81 ± 0.08
Cardiolipin	1.11 ± 0.16

Table 6.7 Relative binding constants for DGK in phosphatidylcholines of different head groups

The binding constants of DGK for phosphatidylcholines of different head groups were determined using n = 2.53 from data presented in Figure 6.7.

6.4 Discussion

DGK in micelles of the detergent OG showed very low activity with dioleoylglycerol as substrate in the absence of added phospholipid (Walsh & Bell, 1986a). Addition of cardiolipin, di(C18:1)PC or di(C18:1)PG led to a large increase in activity. Although at high concentrations of added phospholipid the activities were the same for all three lipids, less cardiolipin was required to reach the maximum activity. It was therefore suggested that cardiolipin could bind to a small number of sites on DGK with high affinity, whereas interaction with the other lipids was less specific (Walsh & Bell, 1986a). Di(C18:1)PS was somewhat less effective at activating DGK than the other phospholipids, and the effect of di(C18:1)PA on activity was much smaller (Walsh & Bell, 1986a). Bohnenberger and Sandermann (1983) obtained somewhat different results assaying DGK activity in micelles of Triton X-100 with dipalmitoylglycerol as substrate. Again cardiolipin was found to be the most efficient phospholipid at activating DGK but activation at low concentrations of cardiolipin was followed by inhibition at higher concentrations whereas little inhibition was observed at high concentrations of phosphatidylglycerol or phosphatidylcholine. The maximal activity measured in the presence of phosphatidylethanolamine was about half that observed in cardiolipin (Bohnenberger & Sandermann, 1983).

Here we have studied the effects of lipid headgroup structure on the function of DGK in lipid bilayers. Although anionic phospholipids activate DGK in detergent micelles, in lipid bilayers cardiolipin, di(C18:1)PA and di(C18:1)PS support very low activities compared to those supported by di(C18:1)PC (Figure 6.1; Table 6.1). Even at 20 mol %, a level of anionic phospholipid typical of that in a biological membrane, the effects of these anionic phospholipids are inhibitory. The reason for the lower activities in the presence of anionic phospholipid is, however, different for the

different phospholipids. For di(C18:1)PS and di(C18:1)PI low activities follow largely from an increase in K_m for DHG with little effect on v_{max} (Table 6.2). The low activity in cardiolipin follows largely from a decrease in v_{max} with a slight decrease in the K_m for DHG. The low activity in di(C18:1)PA follows from an increase in both v_{max} and K_m for DHG. Finally, di(C18:1)PG at 20 mol % has little effect on activity; this is potentially important since phosphatidylglycerol is the major anionic phospholipid in the *E. coli* membrane.

Since the product of the DGK reaction is phosphatidic acid it is possible that the large effect of di(C18:1)PA on the K_m for DHG follows from binding of di(C18:1)PA at the active site in competition with DHG. The increase in K_m for DHG observed with di(C18:1)PS and di(C18:1)PI would then suggest that these could also bind to the active site. The lack of effect of cardiolipin on the K_m for DHG would suggest that cardiolipin is excluded from the active site, presumably because it is a lot bulkier than the other phospholipids containing as it contains four fatty acyl chains.

Only cardiolipin and phosphatidic acid have a significant effect on v_{max} (Table 6.2). Cardiolipin increases the affinity for MgATP by about a factor of 2 and for Mg^{2+} by a factor of three, whilst di(C18:1)PS and di(C18:1)PA have little effect on the affinities for either MgATP or Mg^{2+} (Tables 6.3 and 6.4). Since DGK catalyses the direct transfer of the γ-phosphate of ATP to the –OH group of the bound diacylglycerol it is likely that the two substrates are bound closely together at the subunit-subunit interface in the DGK trimer where the active site is located (Lau et al., 1999). It is possible therefore that binding of di(C18:1)PA or cardiolipin to DGK results in a conformation change on the enzyme, changing the relative locations of the ATP and diacylglycerol binding sites at the interface.

The Ca^{2+}-ATPase of sarcoplasmic reticulum was also inhibited by anionic phospholipids, the level of inhibition increasing markedly with increasing Mg^{2+} concentration (Dalton et al., 1998). The low activity for the Ca^{2+}-ATPase in di(C18:1)PA in the presence of high concentrations of Mg^{2+} was attributed to strong interaction between Mg^{2+} and di(C18:1)PA. It has been shown that binding of Mg^{2+} to di(C18:1)PA results in the formation of a non-lamellar structure in which the lipid fatty acyl chains are highly ordered (Caffrey & Feigenson, 1984). In contrast, addition of Mg^{2+} to di(C18:1)PS results in no change in chain packing (Hope & Cullis, 1980; Casal et al., 1989). The lower activities observed for DGK in di(C18:1)PA than in di(C18:1)PS (Table 6.1) could follow from formation of ordered structures of di(C18:1)PA in the presence of high concentrations of Mg^{2+}. However, Mg^{2+} has little effect on anionic phospholipids when they are present in a mixture with a zwitterionic phospholipid (Hope & Cullis, 1980; Haverstick & Glaser, 1987) and so the inhibitory effects observed for mixtures of di(C18:1)PC containing 20 mol % anionic phospholipid are unlikely to be Mg^{2+} dependent. Indeed, measurement of DGK activity as a function of Mg^{2+} concentration in these systems shows activity increasing with increasing Mg^{2+} concentration (Figure 6.4; Table 6.4), attributed to the activator role for Mg^{2+} previously reported in detergent micelles (Walsh & Bell, 1986a).

Fluorescence quenching experiments measuring the binding constant of anionic phospholipids at the lipid-protein interface of DGK suggest that the inhibitory effects of anionic phospholipids are likely to follow from binding to sites of low specificity, or in the case of di(C18:1)PA at the active site. The binding constants (Table 6.7) show that di(C18:1)PC, di(C18:1)PA, di(C18:1)PS and cardiolipin all bind to DGK with very similar affinities. Thus DGK has little preference for anionic phospholipids. The quenching of 33 % of the Trp fluorescence by the anionic

phospholipids has also been seen with the Ca^{2+}-ATPase (Dalton et al., 1998). It has been shown that anionic molecules such as oleic acid quench the fluorescence of a simple hydrophobic analogue of Trp incorporated into a lipid bilayer; it was suggested that quenching followed from close contact between an excited Trp residue and the carboxyl group (Froud et al., 1986b). Addition of oleic acid to the Ca^{2+}-ATPase also results in 35 % quenching of the Trp fluorescence (Froud et al., 1986b). In DGK, at least 1 or maybe 2 Trp residues (33 %) are predicted to be located close to the ends of transmembrane α-helices, whilst a Trp in amphipathic helix 1 is also thought to be close to the bilayer surface (Nagy et al., 2000). Therefore, the observed quenching of 33 % of Trp fluorescence with di(C18:1)PA, di(C18:1)PS or cardiolipin is consistent with a location for the lipid headgroups around the protein in a region close to the ends of the transmembrane α-helices and at the lipid-water interface.

All biological membranes contain lipids which, when isolated from the membrane, prefer to adopt a curved hexagonal H_{II} structure rather than a planar bilayer structure. In mixtures with lipids preferring a bilayer phase these non-bilayer preferring lipids are forced to adopt a bilayer structure and therefore exist in a state that has been referred to as one of curvature frustration; it has been suggested that the presence of bilayer frustration is important for the proper function of membrane proteins (Gruner, 1985).

The presence of long chain diacylglycerols lowers the temperature of the phase transition for phosphatidylethanolamine from the bilayer to the hexagonal H_{II} phase (Epand, 1985; Das & Rand, 1986). Effects of short chain diacylglycerols on phosphatidylethanolamines do not appear to have been reported in the literature but since we observed that mixtures of di(C18:1)PE containing 20 mol % DHG gave very cloudy samples typical of formation of a hexagonal H_{II} phase it is likely that the

presence of DHG also favours hexagonal H_{II} phase formation. However, mixtures of a 1:4 molar ratio of di(C18:1)PC to di(C18:1)PE containing 20 mol % DHG did not form cloudy suspensions in water, consistent with the well established ability of phosphatidylcholine to favour a bilayer structure (de Kruijff et al., 1985).

In mixtures of di(C18:1)PC and di(C18:1)PE up to 80 mol % di(C18:1)PE at 25 °C, DGK activity decreases almost linearly with increasing content of di(C18:1)PE (Figure 6.5). Egg yolk phosphatidylethanolamine (predominantly 1-palmitoyl 2-oleoylphosphatidylethanolamine) which has a higher liquid crystalline to hexagonal H_{II} phase transition temperature, has a slightly less inhibitory effect on DGK than di(C18:1)PE (Figure 6.5). It also seems that phosphatidylethanolamines support lower activities for DGK at temperatures that favour formation of the hexagonal H_{II} phase than at temperatures that favour the bilayer phase. Thus activities in di(C18:1)PE and egg yolk phosphatidylethanolamine are the same at temperatures up to about 25 °C but then activities become less in di(C18:1)PE than in egg yolk phosphatidylethanolamine (Figure 6.6). These results show that phosphatidylethanolamines support lower activities than phosphatidylcholines even at temperatures where both favour the liquid crystalline bilayer phase. In the bilayer phase, low activities in di(C18:1)PE follow from a low v_{max}, the K_m value for DHG being slightly less than in di(C18:1)PC (Table 6.5). However, at higher temperatures where di(C18:1)PE favours the hexagonal H_{II} phase the low activity follows from both a low v_{max} and a high K_m value (Table 6.5).

Many membrane proteins show low activities when the surrounding lipid is in the gel phase. For example, the Ca^{2+}-ATPase of sarcoplasmic reticulum reconstituted into bilayers of di(C14:0)PC is inactive below 24 °C, the temperature of the gel to liquid crystalline phase transition for this lipid (Warren et al., 1974a). Similarly, the

Ca^{2+}-ATPase is inactive in di(C16:0)PC at low temperatures but in this case activity appears above about 32 °C even though the phase transition temperature for di(C16:0)PC is 42 °C. The glucose transporter from red blood cells also shows no activity in gel phase di(C14:0)PC although there is activity in di(C18:0)PC in the gel phase (Carruthers & Melchior, 1984).

The activity of DGK in bilayers of di(C16:0)PC at temperatures below about 45 °C is less than in di(C16:1)PC, suggesting that gel phase lipid supports low activity (Figure 6.6). The decrease in activity with decreasing temperature in di(C16:0)PC is gradual with no sharp change at 42 °C, suggesting that the phase transition for the lipid around DGK is broad, as has been suggested previously for the Ca^{2+}-ATPase and other membrane proteins (Lee, 1977). At low temperatures in di(C16:0)PC K_m values for DHG and ATP are normal, the major effect of temperature being a large decrease in v_{max} (Table 6.6). Effects of gel phase lipid are much less clear for DGK in di(C14:0)PC (Figure 6.6). Differences in activity for DGK in di(C14:1)PC and di(C14:0)PC at temperatures below 24 °C are very small. It was shown in Chapter 5 that the low activity in di(C14:1)PC followed from a high K_m value for DHG with a value for v_{max} similar to that in di(C18:1)PC. The low activity in di(C14:0)PC also follows from a high K_m value, with a value for v_{max} in gel phase di(C14:0)PC considerably higher than that in di(C16:0)PC in the gel phase.

In the native *E. coli* cytoplasmic membrane about 72 % by weight of the lipid is phosphatidylethanolamine, 24 % is phosphatidylglycerol and 4 % is cardiolipin (Harwood & Russell, 1984; de Kruijff et al., 1998). Activities for DGK in bilayers of this composition are about half that observed in a bilayer of di(C18:1)PC when measured at 20 mol % DHG and 5 mM ATP (Table 6.1). The activity in mixtures containing high proportions of di(C18:1)PE are the same whether the other lipid(s) are

di(C18:1)PC or a mixture of di(C18:1)PG and cardiolipin, showing that the dominant effect is that of di(C18:1)PE. Low activities in di(C18:1)PE follow largely from a high K_m value for DHG. The importance of the effect on K_m could be less in the native membrane where the substrate for DGK will be a longer chain diacylglycerol, which will have a lower K_m value than that for DHG. Nevertheless, the value for v_{max} is also less in di(C18:1)PE than di(C18:1)PC and v_{max} values are expected to be independent of the chain length of the diacylglycerol (Walsh et al., 1990). Thus it seems that the lipid environment of DGK in the *E. coli* membrane is less than optimal as far as the rate of reaction is concerned.

Summary

The activities of many membrane proteins are determined by the physical features of their surrounding lipid bilayers, including bilayer thickness, fluidity, curvature frustration, surface charge and the presence of specific phospholipids, such as cardiolipin, acting as co-factors (McAuley et al., 1999). In many cases, it is unclear why this diversity is required for the correct functioning of the membrane and the proteins embedded in it. The simplicity of both the structure and the kinetics of DGK make DGK an ideal protein with which to define the important features of the surrounding lipid bilayer. A reconstitution protocol has been established by which DGK can be inserted into lipid bilayers, containing DHG as substrate, to define the important features of the surrounding membrane. Using this procedure bilayer thickness has been shown to have a marked effect on the activity of DGK with a maximum activity at a chain length of C18 (Figure 5.3). With an expected length of about 32 Å for transmembrane α-helices M1 and M3 of DGK, which are thought to be exposed to the lipid (Nagy et al., 2000), a bilayer of di(C18:1)PC with a hydrophobic thickness about 29.8 Å (Lewis & Engelman, 1983; Sperotto & Mouritsen, 1988) is the expected best hydrophobic match for DGK. Since DGK catalyses direct phosphoryl transfer from ATP to diacylglycerol, it is likely that ATP binds to DGK with its γ-phosphate close to the –OH group of the diacylglycerol (Badola & Sanders, 1997). The binding sites for ATP have been located at the subunit-subunit interfaces in the DGK trimer (Lau et al., 1999) suggesting that the diacylglycerol binding site could also be located at the subunit-subunit interfaces. The observed increases in K_m for both ATP and DHG in di(C14:1)PC therefore suggest that packing at the subunit-subunit interface has changed as the transmembrane α-helices tilt to match the thin

bilayer. The effects of long chain phosphatidylcholines with chain lengths greater than C18, do not follow from any changes in K_m for ATP or DHG but, rather, from a decrease in v_{max} (Figure 5.5). Such a change might occur, for example, if the binding sites for ATP and diacylglycerol on DGK became misaligned so that the rate of phosphoryl transfer is decreased.

Reconstitution of DGK into mixtures of phosphatidylcholines of different chain lengths has shown that an important feature of the bilayer is its average thickness. Similar observations have been made for the Ca^{2+}-ATPase although for the Ca^{2+}-ATPase activity changes more steeply with changes in lipid composition (Starling et al., 1993), suggesting that effects of chain length on the Ca^{2+}-ATPase are more cooperative than those on DGK. There are also other differences between DGK and the Ca^{2+}-ATPase. Thus effects of short chain phosphatidylcholines on the activity of the Ca^{2+}-ATPase can be reversed by addition of an alkane such as decane (Johannsson et al., 1981; Lee et al., 1991; Jones et al., 1985). It has been suggested that effects of decane on the Ca^{2+}-ATPase could follow from direct binding to the Ca^{2+}-ATPase rather than from any effect on bilayer thickness (Lee et al., 1991; Jones et al., 1985). As shown in Figure 5.8, decane had no significant effect on the activity of DGK in any of the lipid bilayers. This would be consistent with the results with DGK if decane were unable to bind to DGK in the same way that it does to the Ca^{2+}-ATPase. Similarly, effects of cholesterol are different between DGK and the Ca^{2+}-ATPase. For the Ca^{2+}-ATPase cholesterol has been shown to increase the activity in di(C14:1)PC but with no effect on the activity in di(C24:1)PC (Starling et al., 1993). Addition of cholesterol to DGK in di(C14:1)PC roughly doubles activity whereas addition of cholesterol to DGK in di(C18:1)PC or di(C24:1)PC causes a slight decrease in activity (Figure 5.10). Thus effects on the Ca^{2+}-ATPase could follow from

changes in bilayer thickness and from direct binding to the ATPase whereas effects on DGK could follow only from effects of bilayer thickness.

We have shown that DGK has an absolute requirement for a lipid cofactor in detergent micelles when DHG is used as substrate. Although anionic phospholipids activate DGK in detergent micelles, in lipid bilayers cardiolipin, di(C18:1)PA and di(C18:1)PS support very low activities compared to those supported by di(C18:1)PC (Figure 6.1; Table 6.1). Since the product of the DGK reaction is phosphatidic acid it is possible that the large effect of di(C18:1)PA on the K_m for DHG follows from binding of di(C18:1)PA at the active site in competition with DHG, whilst the lack of effect of cardiolipin on the K_m for DHG would suggest that cardiolipin is excluded from the active site, presumably because it is a lot bulkier than the other phospholipids. Both cardiolipin and phosphatidic acid have a significant effect on v_{max} for DHG (Table 6.2). Cardiolipin increases the affinity for MgATP by about a factor of 2 and for Mg^{2+} by a factor of three, whilst di(C18:1)PS and di(C18:1)PA have little effect on the affinities for either MgATP or Mg^{2+} (Tables 6.3 and 6.4). It is possible therefore that binding of di(C18:1)PA or cardiolipin to DGK results in a conformation change on the enzyme, changing the relative locations of the ATP and diacylglycerol binding sites at the interface.

The activity of the Ca^{2+}-ATPase of sarcoplasmic reticulum was also inhibited by anionic phospholipids, the level of inhibition increasing markedly with increasing Mg^{2+} concentration (Dalton et al., 1998). In fact the probable role of anionic phospholipids in the SR membrane is to increase Ca^{2+} accumulation levels, rather than maximise the rate of ATP hydrolysis. The presence of small quantities of negatively charged lipid in vesicles reconstituted with the Ca^{2+}-ATPase led to higher levels of Ca^{2+} accumulation than in purely di(C18:1)PC vesicles, with the effect of

cardiolipin being greater than that of di(C18:1)PA or di(C18:1)PS (Figure 3.7). The effect of the negatively charged lipid reaches an optimum at about 10 mol %, approximately the same as the mole fraction of negatively charged phospholipid in the native SR membrane (Lau et al., 1979; Milting et al., 1994), higher concentrations leading to lower levels of accumulation (Figures 3.8 and 3.9). The presence of anionic phospholipid results in increased levels of accumulation of Ca^{2+} as the rate of slippage on the Ca^{2+}-ATPase decreases. Slippage occurs when the phosphorylated intermediate of the Ca^{2+}-ATPase releases Ca^{2+} on the cytoplasmic side of the SR membrane, rather than the lumenal side (Scheme 3.1). We can conclude that the rate of slippage on the Ca^{2+}-ATPase is relatively high in the absence of negatively charged phospholipids, suggesting that reducing the slippage may be important for the physiological function of the Ca^{2+}-ATPase. The SR may be able to control levels of Ca^{2+} accumulation through the actions of di(C18:1)PI(4)*P*, which decreases the rate of slippage much more than the equivalent percentage of di(C18:1)PI.

The low activity for the Ca^{2+}-ATPase in di(C18:1)PA in the presence of high concentrations of Mg^{2+} was attributed to strong interaction between Mg^{2+} and di(C18:1)PA, resulting in the formation of a non-lamellar structure in which the lipid fatty acyl chains are highly ordered (Caffrey & Feigenson, 1984). This is not expected to be the cause for low activities of DGK in di(C18:1)PC containing 20 mol % di(C18:1)PA as Mg^{2+} has little effect on anionic phospholipids when they are present in a mixture with a zwitterionic phospholipid (Hope & Cullis, 1980; Haverstick & Glaser, 1987). Indeed, measurement of DGK activity as a function of Mg^{2+} concentration in these systems shows activity increasing with increasing Mg^{2+} concentration (Figure 6.4; Table 6.4), attributed to the activator role for Mg^{2+} previously reported in detergent micelles (Walsh & Bell, 1986a).

The measurement of relative binding constants for phospholipids to DGK suggest that DGK shows little preference for lipids of fatty acyl chain length between C14 to C20, whilst lipids with fatty acyl chains longer than this bind less well. Measurement of phospholipid binding constants show that DGK has no preference for anionic phospholipids.

The presence of phosphatidylethanolamine, a non-bilayer preferring lipid, introduces curvature frustration into the bilayer, which is suggested to be an important for the proper function of some membrane proteins (Gruner, 1985). However, it seems that phosphatidylethanolamines support lower activities of DGK than phosphatidylcholines even at temperatures where both favour the liquid crystalline bilayer phase. In the bilayer phase, low activities in di(C18:1)PE follow from a low v_{max}, the K_m value for DHG being slightly less than in di(C18:1)PC (Table 6.5). However, at higher temperatures where di(C18:1)PE favours the hexagonal H_{II} phase the low activity follows from both a low v_{max} and a high K_m value (Table 6.5).

Many membrane proteins show low activity when the surrounding lipid is in the gel phase. For example, the Ca^{2+}-ATPase of sarcoplasmic reticulum reconstituted into bilayers of di(C14:0)PC is inactive below 24 °C, the temperature of the gel to liquid crystalline phase transition for this lipid (Warren et al., 1974a). The activity of DGK in bilayers of di(C16:0)PC at temperatures below about 45 °C is less than in di(C16:1)PC, suggesting that gel phase lipid supports low activity (Figure 6.6). The decrease in activity with decreasing temperature in di(C16:0)PC is gradual with no sharp change at 42 °C, suggesting that the phase transition for the lipid around DGK is broad, as has been suggested previously for the Ca^{2+}-ATPase and other membrane proteins (Lee, 1977). At low temperatures in di(C16:0)PC K_m values for DHG and

ATP are normal, the major effect of temperature being a large decrease in v_{max} (Table 6.6).

In the native *E. coli* cytoplasmic membrane about 72 % by weight of the lipid is phosphatidylethanolamine, 24 % is phosphatidylglycerol and 4 % is cardiolipin (Harwood & Russell, 1984; de Kruijff et al., 1998). Activities for DGK in bilayers of this composition are about half that observed in a bilayer of di(C18:1)PC when measured at 20 mol % DHG and 5 mM ATP (Table 6.1).

In conclusion, *E. coli* DGK shows its highest activity in di(C18:1)PC the lipid which most closely matches the expected length of the DGK transmembrane α-helices. DGK has no binding preference for anionic phospholipids, whilst activity is lowered in the presence of anionic phospholipids, non-bilayer preferring lipids and gel-phase lipids. It appears that the lipid environment of DGK in the *E. coli* membrane is less than optimal as far as the rate of reaction is concerned.

Appendix: The sub-routine necessary for simulation of Ca^{2+} accumulation using FACSIMILE (UKEA)

```
VARIABLE E1 E2 E1Ca E1Ca2 Ca atp E1Ca2atp E2PCa2 Cai E2PCa E2P;
PARAMETER k1f k1b k2f k2b k3f k3b k4f k4b k5f k5b k6f k6b k7f k7b k8f
k8b k9f k9b k10f k10b intconc caup v;
EXEC OPEN 8 "dump.res";


COMPILE INITIAL;
E1Ca2=0.045e-6;
Ca=120.0e-6;
Cai=1.0e-12;
Atp=0.8e-3;
k1f=13.0;
k1b=47.0;
k2f=1.0e8;
k2b=1.0e2;
k3f=1.0e8;
k3b=1.0e2;
k4f=1.0e8;
k4b=1.0e3;
k5f=1.0e2;
k5b=1.0e-6;
k6f=60.0;
k6b=1.8e4;
k7f=30.0;
k7b=0.9e4;
k8f=100.0;
k8b=1.0e-6;
* k9f and k10f define the rates of slippage and simple leak respectively;
* to introduce slippage vary k9f and put k10f=1.0e-10;
* to introduce simple leak vary k10f and put k9f=1.0e-10;
k9f=1.0e-6;
k9b=1.0e-6;
k10f=1.0e-10;
k10b=1.0e-10;
v=382.6;
**;
```

```
COMPILE EQUATIONS;
%k1f%k1b: E2=E1;
%k2f%k2b: E1+Ca=E1Ca;
%k3f%k3b: E1Ca+Ca=E1Ca2;
%k4f%k4b: E1Ca2+atp=E1Ca2atp;
%k5f%k5b: E1Ca2atp=E2PCa2;
%k6f%k6b: E2PCa2=E2PCa+Cai+v;
%k7f%k7b: E2PCa=E2P+Cai+v;
%k8f%k8b: E2P=E2;
%k9f%k9b: E2PCa2=E2+Ca+Ca;
%k10f%k10b: Cai+v=Ca;
**;

COMPILE PRINT;
Caup=((120.0e-6)-ca)*1.0e9/20.0;
PSTREAM 2;
**;

PSTREAM 2 8 5;
time caup;
**;

WHEN TIME = 0 + 10.0 *100%CALL PRINT;
**;

BEGIN;
STOP;
```

Andersen, J.P., (1995) *Bioscience Reports* **15**, 243-261

Andersen, J.P., Skriver, E., Mahrous, T.S., & Moller, J.V. (1983) *Biochim. Biophys. Acta* **728**, 1-10

Andrews, D.M., Manev, E.D., & Haydon, D.A. (1970) *Spec. Disc. Faraday Soc.* **1**, 46-56

Ansell, G.B., hawthorne, J.N., and Dawson, R.M.C. (1973) *Form and function of phospholipids*, Elsevier, Amsterdam

Badola, P. & Sanders, C.R. (1997) *J. Biol. Chem.* **272**, 24176-24182

Barton, P.G. and Gunstone, F.D. (1975) *J. Biol. Chem* **250**, 4470-4476

Bennett, J.P. Smith, G.A., Houslay, M.D., Hesketh, T.R., Metcalfe, J.C. and Warren, G.B. (1978) *Biochim. Biophys. Acta* **513**, 310-320

Benz, R., Frolich, O., Lauger, P., & Montal, M. (1975) *Biochim. Biophys. Acta* **394**, 323-334

Bigelow, C.C. (1967) *J. Theoret. Biol.* **16**, 187-211

Boden, N., Jones, S.A., & Sixl, F. (1991) *Biochemistry* **30**, 2146-2155

Bohnenberger, E., & Sandermann, H., Jr. (1983) *Eur. J. Biochem.* **152**, 645-650

Bottomley, M.J., Salim, K., & Panayotou, G. (1998) *Biochim. Biophys. Acta* **1436**, 165-183

Brown, M.F. (1994) *Chem. Phys. Lipids* **73**, 159-180

Brown, M.F. (1997) *Curr. Top. Memb.* **44**, 285-356

Browning, J.L. & Seelig, J. (1980) *Biochemistry* **19**, 1262-1270

Caffrey, M. & Feigenson, G.W. (1981) *Biochemistry* **20**, 1949-1961

Caffrey, M. & Feigenson, G.W. (1984) *Biochemistry* **23**, 323-331

Campbell, K.P. and MacLennan, D.H. (1981) *J. Biol. Chem.* **256**, 4626-4632

Campbell, K.P. and MacLennan, D.H. (1983) *J. Biol. Chem.* **258**, 1391-1394

Carruthers, A. & Melchior, D.L. (1984) *Biochemistry* **23**, 6901-6911

Casal, H.L., Mantsch, H.H., & Hauser, H. (1989) *Biochim. Biophys. Acta* **982**, 228-236

Cheng, K.H., Lepock, J.R., Hui, S.W., & Yeagle (1986) *J. Biol. Chem.* **261**, 5081-5087

Copeland, R.A. (1994) *Methods for Protein Analysis*, Chapman & Hall, New York and London

Cornea, R.L. & Thomas, D.D. (1994) *Biochemistry* **33**, 2912-2920

Cronan, J.E., Jr., & Rock, C.O. (1996) *Neidhart, F.C., ed.* **Vol. 1**, 2nd Ed, 612-636

Cullen, J., Phillips, M.C., & Shipley, G.G. (1971) *Biochem. J.* **125**, 733-742

Cullis, P.R. and de Kruijff, B. (1978) *Biochem. Biophys. Acta* **513**, 31-42

Cullis, P.R., Hope, M.J. and Tilcock, C.P.S. (1986) *Chem. Phys. Lipids* **40**, 127-144

Dalton, K.A., East, J..M., Mall, S., Oliver, S., Starling, A.P. and Lee, A.G. (1998) *Biochem. J.* **329**, 637-646

Dalton, K.A., Pilot, J.D., Mall, S., East, J.M. & Lee, A.G. (1999) *Biochem. J.* **342**, 431-438

Das, S. & Rand, R.P. (1986) *Biochemistry* **25**, 2882-2889

Dawidowicz, E.A. & Rothman, J.E. (1976) *Biochim. Biophys. Acta* **455**, 621-630

de Boeck, H. & Zidovetski, R. (1992) *Biochemistry* **31**, 623-630

de Foresta, B., le Maire, M, Orlowski, S., Champeil P., Lund, S., Moller J.V., Michelangeli, F. and Lau, Y.H., Caswell, A.H., Brunschwig, J., Baerwald, R.J. and Garcia, M. (1979) *J. Biol. Chem.* **254**, 540-546

de Kroon, A.I.P.M., Timmermans, J.W., Killias, J.A., & de Kruijff, B. (1990) *Chem. Phys. Lipids* **54**, 33-42

de Kruijff, B., Cullis, P.R., Verkleij, A.J., Hope, M.J., Van Echteld, C.J.A., Taraschi, T.F., Van Hoogevest, P., Killian, J.A., Rietveld, A., & Van der Steen, A.T.M. (1985) in *Progress in Protein-Lipid Interactions* (Watts, A. & De Pont, J.J.H.H.M., eds) pp. 89-142, Elsevier, Amsterdam

de kruijff, B., Killian, J.A., Rietveld, A.G., & Kusters, R. (1998) *Current Topics in Membranes* **44**, 477-515

de Meis , L. (1981) The Sarcoplasmic Reticulum, Wiley, New York

Devaux, P.F (1991) *Biochemistry* **30**, 1163-1173

Dibble, A.R.G., Hinderliter, A.K., Sando, J.J. and Biltonen, R.L. (1996) *Biophys. J.* **71**, 1877-1890

Ding, J., Starling, A.P., East, J.M., & Lee (1994) *Biochemistry* **33**, 4974-4979

Dluhy, R.A., Cameron, D.G., Mantsch, H.H., & Mendelsohn, R. (1983) *Biochemistry* **22**, 6318-6325

Dumas, F., Tocanne, J.F., Leblanc, G., & Lebrun, M.C. (2000) *Biochemistry* **39**, 4846-4854

East, J.M. & Lee, A.G. (1982) *Biochemistry* **21**, 4144-4151

Epand, R.M. (1985) *Biochemistry* **24**, 7092-7095

Eytan, G.D. (1982) *Biochim. Biophys. Acta* **694**, 185-202

Farren, S.B., Hope, M.J., & Cullis, P.R. (1983) *Biochem. Biophys. Res. Commun.* **111**, 675-682

Feigenson, G.W. (1989) *Biochemistry* **28**, 1270-1278

Froud, R.J. & Lee, A.G. (1986) *Biochem. J.* **237**, 207-215

Froud, R.J., Earl, C.R.A., East, J.M. and Lee, A.G. (1986a) *Biochem. Biophys. Acta* **860**, 354-360

Froud, R.J., East, J.M., Rooney, E.K., & Lee, A.G. (1986b) *Biochemistry* **25**, 7535-7544

Gafnia, A. & Boyer, P.D. (1984) *Biochemistry* **23**, 4362-4367

Galla, H.J. & Sackmann, E. (1975) *Biochim. Biophys. Acta* **401**, 509-529

Gomez-Fernandez, J.C., Baena, M.D., Teruel, J.A., Villalain, J., & Vidal, C.J. (1985) *J. Biol. Chem.* **260**, 7168-7170

Gorzelle, B.M., Nagy, J.K., Oxenoid, K., Lonzer, W.L., Cafiso, D.S. & Sanders, C.R. (1999) *Biochemistry* **38**, 16373-16382

Gould, G.W., East, J.M., Froud, R.J., McWhirter, J.M., Stefanova, H.I., and Lee, A.G. (1986) *Biochem. J.* **237**, 217-227

Gould, G.W., McWhirter, J.M., East, J.M., and Lee, A.G. (1987a) *Biochem. Biophys. Acta* **904**, 36-44

Gould, G.W., McWhirter, J.M., East, J.M., and Lee, A.G. (1987b) *Biochem. Biophys. Acta* **904**, 45-54

Gould, G.W., Coyler, J., East, J.M., and Lee, A.G. (1987c) *J. Biol. Chem.* **262**, 7676-7679

Graham, I., Gagne, J. & Silvius, J.R. (1985) *Biochemistry* **24**, 7123-7131

Green, N.M. and Stokes, D.L. (1992) *Acta Physiol. Scand.* **146**, 59-68

Gruner, S.M. (1985) *Proc. Natl. Acad. Sci. USA* **82**, 3665-3669

Hamilton, J.A., Bhamidipati, S.P., Kodali, D.R., & Small, D.M. (1991) *J. Biol. Chem.* **266**, 1177-1186

Hardwicke, P.M.D. & Green, N.M. (1974) *Eur. J. Biochem.* **42**, 183-193

Harwood, J.L. & Russell, N.J. (1984) *Lipids in Plants and Microbes*, George Allen & Unwin, London

Haverstick, D.M. & Glaser, M. (1987) *Proc. Natl. Acad. Sci. U.S.A.* **84**, 4475-4479

Hauser, H., Pascher, I., Pearson, R.H. and Sundell, S. (1981) *Biochem. Biophys. Acta* **650**, 21-51

Hauser, H. & Shipley, G.G. (1984) *Biochemistry* **23**, 34-41

Hauser, H. (1991) *Chem. Phys. Lipids* **57**, 309-325

Haydon, D.A., Hendry, B.M., Levinson, S.R., & Requena, J. (1977) *Nature* **268**, 356-358

Heegaard, C.W., le Maire, M., Gulik Krzywicki, T., & Moller, J.V. (1990) *J. Biol. Chem.* **265**, 12020-12028

Heimburg, T., Wurz, U. and Marsh, D. (1992) *Biophys. J.* **63**, 1369-1378

Henderson, R and Unwin, P.N.T. (1975) Nature **257**, 28-32

Henderson, I.M.J., Khan, Y.M., East, J.M., & Lee, A.G. (1994) *Biochem. J.* **297**, 615-624

Hidalgo, C., Thomas, D.D., & Ikemoto, N. (1978) *J. Biol. Chem.* **253**, 6879-6887

Holloway, P.W. (1973) *Analytical Biochemistry* **53**, 304-308

Hope, M.J. & Cullis, P.R. (1980) *Biochem. Biophys. Res. Commun.* **92**, 846-852

Hope, M.J., Bally, M.B., Webb, G. & Cullis, P.R. (1985) *Biochim. Biophys. Acta.* **812**, 55-65

Inesi, G. & de Meis, L. (1989) *J. Biol. Chem.* **264**, 5929-5936

Ito, T. & Ohnishi, S.L. (1974) *Biochim. Biophys. Acta* **352**, 29-37

Iwata, S., Ostermeier, C., Ludwig, B., & Michel, H. (1995) *Nature* **376**, 660-669

Jacobs, R.E. & White, S.H. (1984) J. *Amer. Chem. Soc.* **106**, 915-920

Jain, M.K. & Zakim, D. (1987) *Biochim. Biophys. Acta* **906**, 33-68

Johannson, A., Keightley, C.A., Smith, G.A., Richards, C.D., Hesketh, T.R., & Metcalfe, J.C. (1981) *J. Biol. Chem.* **256**, 1643-1650

Jones, O.T., Froud, R.J., & Lee, A.G. (1985) *Biochim. Biophys. Acta* **812**, 740-751

Kaneko, T., Tanaka, A., Sato, S., Kotani, H., Sazuka, T., Miyajima, N., Sugiura, M., & Tabata, S. (1995) *DNA Res* **2**, 153-166

Kasahara, M. & Hinkle, P.C. (1977) *J. Biol. Chem.* **252**, 7384-7390

King, G.I., Jacobs, R.E., & White, S.H. (1985) *Biochemistry* **24**, 4637-4645

Knowles, A.F. & Racker, E. (1975) *J. Biol. Chem.* **250**, 3538-3544

Knowles, A.F., Eytan, E., & Racker, E. (1976) *J. Biol. Chem.* **251**, 5161-5165

Kobilka, B. (1992) *Annu. Rev. Neurosci.* **15**, 87-114

Kouaouci, R., Silvius, J.R., Graham, I. & Pezolet, M. (1985) *Biochemistry* **24**, 7132-7140

Koynova, R. & Caffrey, M. (1995) *Biochim. Biophys. Acta.* **1255**, 213-236

Koynova, R. & Caffrey, M. (1998) *Biochim. Biophys. Acta.* **1376**, 91-145

Lacapere, J.J., Bennett, N., Dupont, Y. & Guillain, F. (1990) *J. Biol. Chem.* **265**, 348-353

Laemmli, U.K. (1970) *Nature* **227**, 680-682

Lakowicz, J.R. (1983) Principles of Fluorescence Spectroscopy, Plenum Press, new York & London

Landbolt-Marticorena, C., Williams, K.A., Deber, C.M., and Reithmeier, R.A.F. (1993) *J. Mol. Biol.* **229**, 602-608

Lau, Y.H., Caswell, A.H., Brunschwig, J., Baerwald, R.J. and Garcia, M. (1979) *J. Biol. Chem.* **254**, 540-546

Lau, F.W. and Bowie, J.U. (1997) *Biochemistry* **36**, 5884-5892

Lau, F.W., Chen, X. and Bowie, J.U. (1999) *Biochemistry* **38**, 5521-5527

Lee, A.G. (1977) *Trends.in. Biochemical.Sciences.* **2**, 231-233

Lee, A.G. (1978) *Biochim. Biophys. Acta* **507**, 433-444

Lee, A.G. (1983) Membrane Fluidity in Biology Vol. 2 (Aloia, R.C., Ed.) pp 43-88, Academic Press, New York

Lee, A.G., East, J.M., & Balgavy, P. (1991) *Pestic. Sci.* **32**, 317-327

Lee, A.G. & East, J.M. (1993) in *Protein-Lipid Interactions* (Watts, A., ed) pp. 259-299, Elsevier, Amsterdam

Lee, A.G., Starling, A.P., Ding, J., East, J.M., & Witcome, M. (1994) *Biochem. Soc. Trans.* **22**, 821-826

Lee, A.G., Dalton, K.A., Duggleby, R.C., East, J.M. and Starling, A.P. (1995a) *Biosci. Rep.* **15**, 289-298

Lee, A.G., Baker, K., Khan, Y.M., & East, J.M. (1995b) *Biochem. J.* **305**, 225-231

Lee, A.G. (1998) *Biochim. Biophys. Acta.* **1376**, 381-390

Lee, A.G. (2000) in *Membrane Transport* (Baldwin, S.A., ed) pp. 21-46, OUP, Oxford

Lee, A.G. & East, J.M. (2001) *Biochem. J.* (In press)

Levy, D., Seigneuret, M., Bluzat, A. and Rigaud, J.K. (1990a) *J. Biol. Chem.* **265**, 19524-19534

Levy, D., Bluzat, A., Seigneuret, M. and Rigaud, J.K. (1990b) *Biochim. Biophys. Acta* **1025**, 179-190

Levy, D., Gulik, A., Seigneuret, M. and Rigaud, J.K. (1990c) *Biochemistry* **29**, 9480-9488

Levy, D., Gulik A., Bluzat, A. and Rigaud, J.L. (1992) *Biochem. Biophy. Acta* **1107**, 283-298

Lewis, B.A. & Engelman, D.M. (1983) *J. Mol. Biol.* **166**, 211-217

Lichtenberg, D., Robson, R.J., and Dennis, E.A. (1983) *Biochim. Biophys. Acta* **737**, 285-304

Lindblom, G. and Rilfors, L. (1989) *Biochem. Biophys. Acta* **988**, 221-256

Loomis, C.R., Walsh, J.P., and Bell, R.M. (1985) *J. Biol. Chem.* **260**, 4091-4097

Lopez-Garcia, F., Villalain, J. and Gomez-Fernandez, J.C. (1994a) *Biochim. Biophys. Acta* **1190**, 264-272

Lopez-Garcia, F., Villalain, J., Gomez-Fernandez, J.C. and Quinn, P.J. (1994b) *Biophys. J.* **66**, 1991-2004

MacDonald, R.C., MacDonald, R.I., Menco, B.P.M., Takeshita, K., Subbaro, N.K. & Hu, L. (1991) *Biochim. Biophys. Acta* **1061** 297-303

MacLennan, D.H., Seeman, P., Iles, G.H. and Yip, C.C. (1971) *J. Biol. Chem.* **246**, 2702-2710

MacLennan, D.H., Brandl, C.J., Korczak, B., & Green, N.M. (1985) *Nature* **316**, 696-700

MacLennan, D.H., Rice, W.J. & Green, N.M., (1997) *J. Biol. Chem.* **272**, 28815-28818

Mall, S., Broadbridge, R., Sharma, R.P., Lee, A.G., & East, J.M. (2000) *Biochemistry* **39**, 2071-2078

Mall, S.M., East, M. & Lee, A.G. (2001) *Current topics in transport and biogenetics* (In press)

Maniatis, T., Fritsch, E.F., and Sambrook, J. / Molecular Cloning, Second Edition, Vol. 1-4, Cold Spring Harbor Laboratory Press (1989)

Marsh, D. (1990) *CRC Handbook of Lipid Bilayers*, CRC Press, Boca Raton

Martonosi, A.N., (1995) *Bioscience Reports* **15**, 263-281

McAuley, K.E., Fyfe, P.K., Ridge, J.P., Isaacs, N.W., Cogdell, R.J., and Jones, M.R. (1999) *Proc. Natl. Acad. Sci. U.S.A.* **96**, 14706-14711

McAuley, K.E., Fyfe, P.K., Ridge, J.P., Isaacs, N.W., Cogdell, R.J., and Jones, M.R. (2000) *FEBS Lett.* **467,** 285-290

McPherson, P.S. & Campbell, K.P. (1993) *J. Biol. Chem.* **268**, 13765-13768

McWhirter, J.M., Gould, G.W., East, J.M., & Lee, A.G. (1987) *Biochem. J.* **245**, 731-738

Michelangeli, F., Orlowski, S., Cahmpeil, P., Grimes, E.A., East, J.M. and Lee, A.G. (1990a) *Biochemistry* **29**, 8307-8312

Michelangeli, F., Coyler, J., East, J.M. and Lee, A.G. (1990b) *Biochem. J.* **267**, 423-429

Michelangeli, F., Grimes, E.S., East, J.M. and Lee, A.G. (1991) *Biochemistry* **30**, 342-351

Milting, H., Heilmeyer, L.M.G. and Thieleczek, R. (1994) *FEBS Lett.* **345**, 211-218

Miner, V.W. & Prestegard, J.H. (1984) *Biochim. Biophys. Acta* **774**, 227-236

Møller, J.V., Juul, B. and leMaire, M., (1996) *Biochimica et Biophysica Acta-Reviews on Biomembranes*, **1286**, 1-51

Murray, D., Matsumoto, L.H., Buser, C.A., Tsang, J., Sigal, C.T., Ben-Tal, N., Honig, B., Resh, M.D., & McLaughlin, S. (1998) *Biochemistry* **37**, 2145-2159

Myung, J. & Jencks, W.P. (1994) *Biochemistry* **33**, 8775-8785

Myung, J. & Jencks, W.P. (1995) *Biochemistry* **34**, 3077-3083

Nagy, J.K., Lau, F.W., Bowie, J.U., & Sanders, C.R. (2000) *Biochemistry* **39**, 4154-4164

Nakamura, H., Jilka, R.L., Boland, R., & Martinosi, A.N. (1976) *J. Biol. Chem.* **251**, 5414-5423

Navarro, J. & Essig, A. (1984) *Biophys. J.* **46**, 709-717

Navarro, J., Toivio-Kinnucan, M. and Racker, E. (1984) *Biochemistry* **23**, 130-135

Nayar, R., Schmid, S.L., Hope, M.J., & Cullis, P.R. (1982) *Biochim. Biophys. Acta* **688**, 169-176

Neidhart, F.C. et al. *Escherichea coli* and Salmonella – Cellular and Molecular Biology, Second Edition, Volume 1, American Society for Microbiology (1996)

Noda, M., Ikeda, T., Kayano, T., Suzuki, H., Takeshima, H., Kurasaki, M., Takahashi, H. and Numa, S. (1986) *Nature* **320**, 188-192

Ohki, S. & Zschornig, O. (1993) *Chem. Phys. Lipids* **65**, 193-204

Ohnishi, S.I. & Ito, T. (1974) *Biochemistry* **13**, 881-887

Orlowski, S. & Champeil, P. (1991) *Biochemistry* **30**, 11331-11342

Ortiz, A.O., Villalain, J. and Gomez-Fernandez, J.C. (1988) *Biochemistry* **27**, 9030-9036

Pascher, I. (1996) *Curr. Opin. Struct. Biol.* **6**, 439-448

Patternostre, M.T., Roux, M. & Rigaud, J.L. (1988) *Biochemistry* **27**, 2668-2677

Petithory, J.R. & Jencks, W.P. (1982) *biochemistry* **25**, 4493-4497

Pick, U. (1981) *Arch. Biochim. Biophys.* **212**, 186-194

Pickart, C.M. & Jencks, W.P. (1982) *J. Biol. Chem.* **257**, 5319-5322

Portis, A., Newton, C., Pangborn, W. & Papahadjopoulos, D. (1979) *Biochemistry* **18**, 780-790

Pope, J.M., Walker, L.W., & Dubro, D.W. (1984) *Chem. Phys. Lipids* **35**, 259-277

Pope, J.M., & Dubro, D.W. (1986) *Biochim. Biophys. Acta* **858**, 243-253

Racker, E. (1972) *J. Biol. Chem.* **247**, 8198-8200

Ren, J.H., Lew, S., Wang, Z.W., & London, E. (1997) *Biochemistry* **36**, 10213-10220

Ren, J.H., Lew, S., Wang, J.Y., & London, E. (1999) *Biochemistry* **38**, 5905-5912

Rigaud, J.L., Bluzat, A., & Buschlen, S. (1983) *Biochem. Biophys. Res. Commun.* **111**, 373-382

Rigaud, J.L., Paternoste, M.T., and Bluzat, A. (1988) *Biochemistry* **27**, 2677-2688

Rigaud, J.L., Pitard, B. and Levy, D. (1995) *Biochem. Biophys. Acta* **123**, 223-246

Robinson, N.C. (1982) *Biochemistry* **21**, 184-188

Robinson, N.C., Zborowski, J., & Talbert, L.H. (1990) *Biochemistry* **29**, 8962-8969

Roseman, M.A., 7 Thompson, T.E. (1980) *Biochemistry* **19**, 439-444

Russ, E., Kaiser, U., and Sandermann, H. (1988) *Eur. J. Biochim.* **171**, 335-342

Sanders, C.J. (1994) *Chem. Phys. Lipids* **72**, 41-57

Sanders, C.R., Czerski, L., Vinogradova, O., Badola, P., Song, D., & Smith, S.O. (1996) *Biochemistry* **35**, 8610-8618

Sankaram, M.B. & Thompson, T.E. (1990) *Biochemistry* **33**, 10676-10684

Schafer, M., Behle, G., Varsanyl, M. & Heilmeyer, L.M.G. (1987) *Biochem. J.* **247**, 579-587

Schorn, K. and Marsh, D. (1996a) *Biochemistry.* **35**, 3831-3836

Schorn, K. and Marsh, D. (1996b) *Biophys. J.* **71**, 3320-3329

Seddon, J.M. (1990) *Biochem. Biophys. Acta* **1031**, 1-69

Shirai, Y., Segawa, S., Kuriyama, M., Goto, K., Sakai, N., & Saito, N. (2000) *J. Biol. Chem.***275**, 24760-24766

Simmonds, A.C., East, J.M., Jones, O.T., Rooney, E.K., McWhirter, J. & Lee, A.G. (1982) *Biochim. Biophys. Acta* **693**, 398-406

Simmonds, A.C., Rooney, E.K., & Lee, A.G. (1984) *Biochemistry* **23**, 1432-1441

Simons, K. & Ikonen, E. (1997) *Nature* **387**, 569-572

Singer, S.J. & Nicholson, G.L. (1972) *Science* **175**

Smith, P.K., Krohn, R.I., Hermanson, G.T., Mallia, A.K., Gartner, F.H., Provenzano, M.D., Fujimato, E.K., Goeke, N.H., Olsen, B.J. and Klenk, D.C. (1985) *Analytical Biochem.* **150**, 76-85

Smith, R.L., O'Toole, J.F., Maguire, M.E. and Sanders, C.R. (1994) *J. Bacteriol.* **176**, 5459-5465

Sperotto, M.M. & Mouritsen, O.G. (1988) *Eur. Biophys. J.* **16**, 1-10

Stahl, N. & Jencks, W.P. (1987) *Biochemistry* **26**, 7654-7667

Starling, A.P., East, J.M. and Lee, A.G. (1993) *Biochemistry* **32**, 1593-1600

Starling, A.P., Khan, Y.M., East, J.M. and Lee, A.G. (1994) *Biochem. J.* **304**, 569-575

Starling, A.P., East, J.M. and Lee, A.G. (1995a) *Biochem. J.* **310**, 875-879

Starling, A.P., East, J.M., & Lee, A.G. (1995b) *Biochem. J.* **308**, 343-346

Starling, A.P., East, J.M., & Lee, A.G. (1995c) *Biochemistry.* **34**, 3084-3091

Starling, A.P., East, J.M., & Lee, A.G. (1995d) *J. Biol. Chem.* **270**, 14467-14470

Starling, A.P., Dalton, K.A., East, J.M., Oliver, S., & Lee, A.G. (1996) *Biochem. J.* **320**, 309-314

Stryer. L. Biochemistry, Fourth Edition, Chapter 12, W.H. Freeman and Company, New York, U.S.A. (1995)

Sundler, R. & Papahadjopoulos, D. (1981) *Biochim. Biophys. Acta* **649**, 743-750

Sundler, R., Duzgunes, N., & Papahadjopoulos, D. (1981) *Biochim. Biophys. Acta* **649**, 751-758

Szoka, F.J. & Papahadjopoulos, D. (1978) *Proc. Natl. Acad. Sci. USA* **75**, 4194-4198

Szoka, F.J. & Papahadjopoulos, D. (1980) *Ann. Rev. Biophys. Bioeng.* **9**, 467-508

Szymanska, G., Kim, H.W., & Kranias, E.G. (1991) *Biochim. Biophys. Acta.* **1091**, 127-134

Tanford, C. (1980) *The Hydrophobic Effect: Formation of Micelles and Biological Membranes*, John Wiley, New York

Tilcock , C.P.S. (1986) *Chem. Phys. Lipids* **40**, 109-125

Topham, M.K. and Prescott, S.M. (1999) *J. Biol. Chem.* **274**, 11447-11450

Toyoshima, C., Nakasako, N., Nomura, H. and Ogawa, H. (2000) *Nature* **405**, 647-655

Trauble, H. and Eibl , H. (1974) *PNAS* **71**, 214-219

Ueno, T. & Sekine, T. (1986) *Jap. J. Physiol.* **36**, 231-235

Varsanyl, M., Messer, M. & Brandt, N.R. (1989) *Eur. J. Biochem.* **179**, 473-479

Vinogradova, O., Badola, P., Czerski, L., Sonnichsen, F.D. and Sanders, C.R. (1997) *Biophys. J.* **72**, 2688-2701

Von Heijne, G. (1992) *J. Mol. Biol.* **225**, 487-494

Von Heijne, G. (1996) *Prog. Biophys. Mol. Biol.* **66**, 113-139

Wallin, E., Tsukihara, T., Yoshikawa, S., von Heijne, G., & Elofsson, A. (1997) *Protein. Sci.* **6**, 808-815

Walsh, J.P. and Bell, R.M. (1986a) *J. Biol. Chem.* **261**, 6239-6247

Walsh, J.P. and Bell, R.M. (1986b) *J. Biol. Chem.* **261**, 15062-15069

Walsh, J.P. and Bell, R.M. (1990) *J. Biol. Chem.* **265**, 4374-4381

Walsh, J.P., Fahrner, L., & Bell, R.M. (1990) *J. Biol. Chem* **265**, 4374-4381

Warren, G.B., Toon, P.A., Birdsall, N.J., Lee, A.G. & Metcalfe, J.C. (1974a) *Biochemistry* **13**, 5501-5507

Warren, G.B., Toon, P.A., Birdsall, N.J., Lee, A.G. & Metcalfe, J.C. (1974b) *Proc Natl. Acad. Sci. U.S.A.* **71**, 622-626

Warren, G.B., Metcalfe, J.C., Lee, A.G., & Birdsall, N.J. (1975) *FEBS Lett.* **50**, 261-264

Webb, R.J., East, J.M., Sharma, R.P., & Lee, A.G. (1998) *Biochemistry* **37**, 673-679

Wen, J.A., Chen, X. and Bowie, J.U. (1996) *Nature. Struct. Biology.* **3**, 141-148

White, S.H., King, G.I., & Cain, J.E. (1981) *Nature* **290**, 161-163

Wimley, W.C. & White, S.H. (1996) *Nature Struct. Biology.* **3**, 842-848

Witcome, M., Khan, Y.M., East, J.M., & Lee, A.G. (1995) *Biochem. J.* **310**, 859-868

Yanagita, Y & Kagawa, Y. (1986) Techniques for the Analysis of membrane Proteins (Ragan, C.I. & Cherry, R.J., eds) *Solubilisation and Purification of Membrane Proteins*. 61-76, Chapman and Hall, London, New York.

Yau, W.M., Wimley, W.C., Gawrish, K., & White, S.H. (1998) *Biochemistry* **37**, 14713-14718

Yu, X. and Inesi, G. (1995) *J. Biol. Chem.* **270**, 4361-4367

Zhang, P.J., Toyoshima, C., Yonekura, K., Green, N.M. & Stokes, D.L. (1998) *Nature* **392**, 835-839.

Zhou, Y., Wen, J. and Bowie, J.U. (1997) *Nature Struct. Biology* **4**, 986-990

Zimniak, P & Racker, E. (1978) *J. Biol. Chem.* **253**, 4631-4637